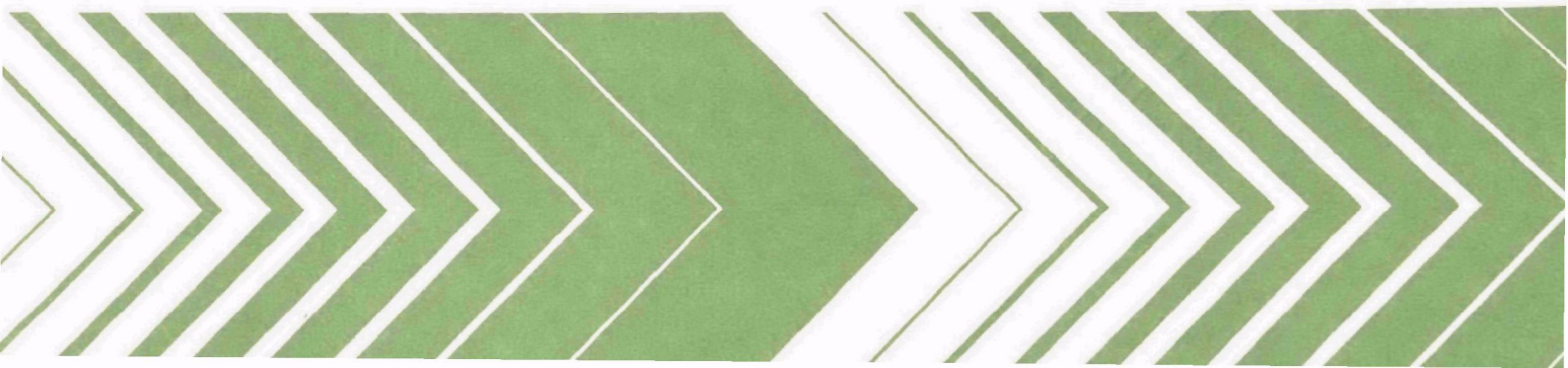


Research and Development



Proceedings of Stormwater and Water Quality Management Modeling Users Group Meeting, 25-26 March 1982



EPA 600/9-82-015
August 1982

PROCEEDINGS OF STORMWATER AND WATER QUALITY
MANAGEMENT MODELING USERS GROUP MEETING
25-26 MARCH 1982

Edited by

Thomas O. Barnwell, Jr.
Center for Water Quality Modeling
Environmental Research Laboratory
Athens, GA 30613

ENVIRONMENTAL RESEARCH LABORATORY
OFFICE OF RESEARCH AND DEVELOPMENT
U.S. ENVIRONMENTAL PROTECTION AGENCY
ATHENS, GA 30613

DISCLAIMER

Mention of trade names or commercial products does not constitute endorsement or recommendation for use by the U.S. Environmental Protection Agency. Similarly, publication of studies reporting better results from one model vis-a-vis others does not constitute endorsement.

FOREWORD

A major function of research and development programs is to effectively and expeditiously transfer technology developed by those programs to the user community. A corollary function is to provide for the continuing exchange of information and ideas between researchers and users, and between the users themselves. The Stormwater and Water Quality Modeling Users Group, sponsored jointly by the U.S. Environmental Protection Agency and Environment Canada/Ontario Ministry of the Environment, was established to provide such a forum. The group has recently widened its interest to include models other than the Stormwater Management Model, such as the Hydrologic Simulation Program-FORTRAN, and other aspects of modeling of water quality in urban and natural waters. This report, a compendium of papers presented at the March 1982 users group meeting, is published in the interest of disseminating to a wide audience the work of group members.

David W. Duttweiler
Director
Environmental Research Laboratory
Athens, Georgia

ABSTRACT

This report includes 16 papers on topics related to the development and application of computer-based mathematical models for water quantity and quality management presented at the semi-annual meeting of the Joint U.S.-Canadian Stormwater and Water Quality Modeling Users Group held 25-26 March 1982 in Washington, DC.

Topics covered include a study of selection, calibration and verification of water quality models in Louisiana and an assessment of measurement uncertainty in the estimation of stream reaeration rates for these models. Calibration of hydrology and sediment transport on small agricultural watersheds using the Hydrological Simulation Program-FORTRAN is described. Hydrologic modeling for studies of pollutant loads and transport in large river basins and the use of continuous simulation model calibration techniques to develop nonpoint pollution loading factors were described. A verification of a continuous dissolved oxygen model for a river in Missouri was presented. State-of-the-art data acquisition techniques in hydrometeorology were discussed. Mathematical analyses of turbulence in center-feed circular sedimentation basins and for dynamic model calibration are presented.

Preparing storm designs for urban drainage analysis was presented as well as studies of pollutant concentrations and loadings in highway runoff. An application of the EXTRAN model to off-site drainage is described. A desk-top calculator method for nonpoint source loads evaluation is described. Modifications to the QUAL-II model for continuous simulation of fecal coliforms is presented. A literature review was done of the relationship between atmospheric pollution and stormwater quality.

CONTENTS

	Page
FOREWORD.	iii
ABSTRACT	iv
A STUDY OF THE SELECTION, CALIBRATION AND VERIFICATION OF MATHEMATICAL WATER QUALITY MODELS	1
R.C. Whittemore, J.S. Hovis, and J.J. McKeown; National Council of the Paper Industry for Air and Stream Improvement	
AN ASSESSMENT OF THE MEASUREMENT UNCERTAINTY IN THE ESTIMATION OF STREAM REAERATION RATE COEFFICIENTS USING DIRECT TRACER TECHNIQUES	36
J.S. Hovis*, R.C. Whittemore*, L.C. Brown**, and J.J. McKeown*; *National Council of the Paper Industry for Air and Stream Improvement, **Tufts University	
CALIBRATION OF HYDROLOGY AND SEDIMENT TRANSPORT ON SMALL AGRICULTURAL WATERSHEDS USING HSPF	54
D.E. Schafer*, D.A. Woodruff*, R.J. Hughto*, and G.K. Young**; *Camp, Dresser & McKee, Inc., **GKY & Associates, Inc.	
HYDROLOGIC MODELING FOR STUDIES OF POLLUTANT LOADINGS AND TRANSPORT IN LARGE RIVER BASINS	69
A. Cavacas, J.P. Hartigan, E. Southerland, and J.A. Friedman; Northern Virginia Planning District Commission	
CONTINUOUS DO RESPONSE PREDICTED USING CSPSS IS VERIFIED FOR SPRING- FIELD, MISSOURI	90
J.E. Scholl and R.L. Wycoff; CH2M Hill	
USE OF CONTINUOUS SIMULATION MODEL CALIBRATION TECHNIQUES TO DEVELOP NONPOINT POLLUTION LOADING FACTORS	101
J.P. Hartigan, T.F. Quasebarth, and E. Southerland; Northern Virginia Planning District Commission	
HYDROMETEOROLOGICAL DATA ACQUISITION: INNOVATIVE, HIGH-RESOLUTION PROGRAMMABLE INSTRUMENTATION FOR STORMWATER MANAGEMENT	128
W. James, H. Haro, M.A. Robinson, D. Henry, and R. Kitai; McMaster University	
THE SEPARATION OF BOUNDARY LAYER AND FLOW TURBULENCE OF CENTER-FEED CIRCULAR SEDIMENTATION BASINS	152
T. Yin; National Capital Park and Planning Commission	

DYNAMIC MODEL ADJUSTMENT	162
D. Hoang; The City of Portland, Oregon	
AN IMPROVED SURCHARGE COMPUTATION IN EXTRAN	179
J.A. Aldrich and L.A. Roesner; Camp Dresser & McKee, Inc.	
PREPARING A DESIGN STORM	191
S.A. McKelvie; Gore & Storrie, Ltd.	
A PREDICTIVE MODEL FOR HIGHWAY RUNOFF POLLUTANT CONCENTRATIONS AND LOADINGS	210
B.W. Mar and R.G. Horner; University of Washington	
CHIMNEY HILL OFF-SITE DRAINAGE STUDY	229
J.M. Normann and E.R. Estes III; MMM DESIGN GROUP	
DESK-TOP METHODOLOGY FOR NONPOINT SOURCE LOAD EVALUATION	248
A.K. Deb; Roy F. Weston, Inc.	
CONTINUOUS SIMULATION OF INSTREAM FECAL COLIFORM BACTERIA	260
A.C. Rowney*, and L.A. Roesner**; *Proctor and Redfern Ltd. and **Camp Dresser and McKee, Inc.	
ATMOSPHERIC POLLUTION IN RELATION TO STORM WATER QUALITY MODELING: LITERATURE REVIEW FOR AN INDUSTRIAL CITY	274
B. Shivalingaiah and W. James; McMaster University	
LIST OF ATTENDEES	296

A STUDY OF THE SELECTION CALIBRATION AND VERIFICATION OF MATHEMATICAL WATER QUALITY MODELS

By: R.C. Whittemore, PhD, J.S. Hovis,
J.J. McKeown, National Council of the
Paper Industry for Air and Stream
Improvement, Inc., Tufts University,
Medford, Massachusetts 02155

I. INTRODUCTION

The general objective of this study was to examine the differences among various models when applied to a single watershed in order to illustrate the limitations inherent in mathematical water quality modeling. As an outgrowth of this examination, a procedure is presented for selection, calibration and verification of such models which uses definitive criteria to judge model validation. Although these criteria were developed for this particular study, the procedure is believed to have general application in cases where waste load must be allocated to achieve water quality standards for some steady state condition.

The study objectives may be more specifically stated as (a) testing the validity of four commonly used water quality models under increasingly strict calibration and verification criteria, (b) examining predictive capability of these models for conditions of varying complexity, and (c) elucidating the dominant issues with respect to model selection, calibration and verification which are believed to be of concern in most waste load allocation studies.

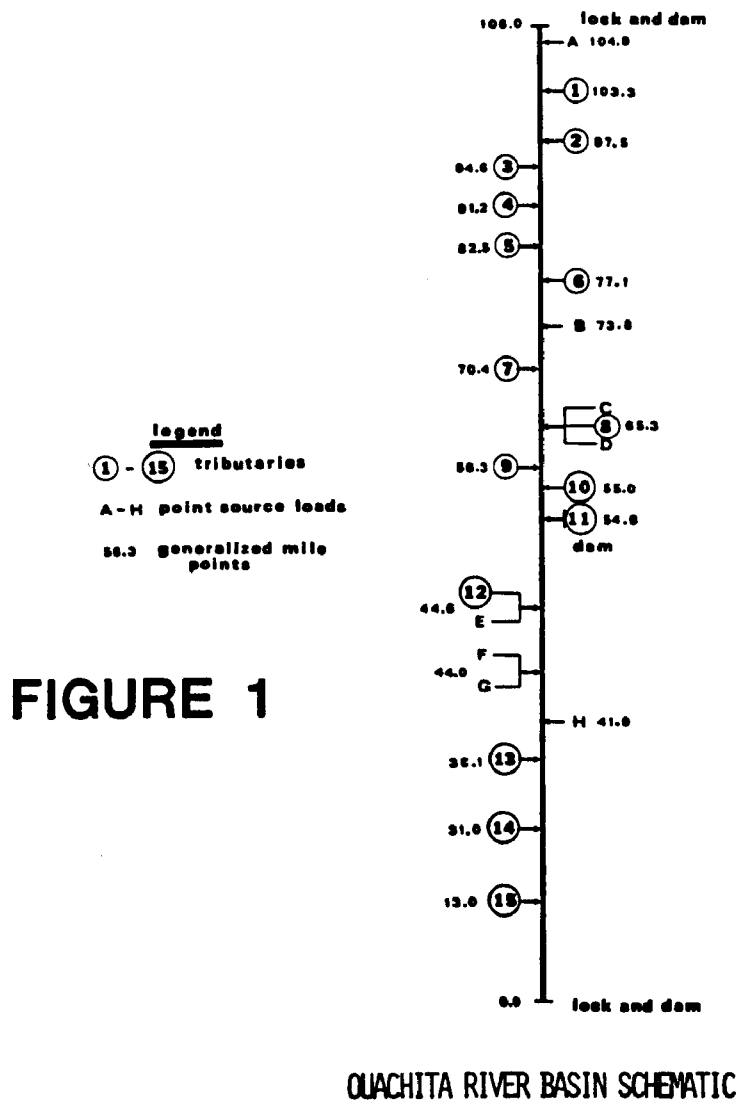
The work was conducted on the Ouachita River basin in southern Arkansas and north central Louisiana with special cooperation and assistance from the pulp and paper industry centered in the basin. It is important to note that this study was not designed to provide a verified model of the Ouachita River, but rather to fulfill the research objectives in calibration/verification noted earlier.

This paper will provide an overview of this study by outlining the field data collection program, a sensitivity study, the model selection, calibration, and verification criteria, and finally model validation. Readers are advised that NCASI Stream Improvement Technical Bulletins to be released during mid-1982 contain more thorough presentation and development of each of these topics.

II SITE DESCRIPTION

The Ouachita River has its source in the Ouachita Mountains in Central Arkansas next to the Oklahoma border. It flows southeasterly into central Louisiana where it joins the Tensas River to form the Black River. At the Arkansas/Louisiana state line, the Ouachita River has a drainage area of 10,835 square miles. At the confluence with the Tensas River, the Ouachita has a drainage area of 18,864 square miles.

That portion selected for this study included an approximate 100 mile stretch in north central Louisiana. A generalized basin map of the study area is presented in Figure 1. The river passes through the several communities whose total population approaches 200,000.



The hydrology of this segment is controlled by lock and dam structures which are operated by the U.S. Army Corps of Engineers. They are used exclusively for navigational purposes. Typical summer time dimensions of the Ouachita River are noted as follows:

(1) The average depth ranges from 13 feet at m.p. 106 to nearly 50 feet at m.p. 0.

(2) The average river width is approximately 460 feet with a range of 300 to 700.

III WATER QUALITY MODEL DESCRIPTIONS

Four water quality models were used in this work to simulate the hydraulic and water quality characteristics of the Ouachita River Basin. They include DOSAG (1), QUAL1E (2), QL2SMG (3), and SNSIM (4). Each has been extensively used by consultants, state, and federal regulatory groups for water quality assessment and wasteload allocation (5).

Three of these models have been tested and documented extensively by NCASI. This documentation included a thorough analysis of the computer code comprising the model and an extensive testing of model options. This work uncovered a number of problems and errors in the computer code which were ultimately corrected and further documented. The documented models are published in NCASI Technical Bulletins Nos. 327, 331, and 338 (1-3).

A comparison of the four models is presented in Table 1. This table includes both the hydraulic and water quality features available in each model. Readers are advised to review the referenced NCASI Technical Bulletins for further details concerning DOSAG, QUAL1E, and QL2SMG and the literature documentation for SNSIM (4).

TABLE 1 Model Comparison

Model	Solution Method	Hydraulics	Longitudinal Dispersion	CBOD	NBOD	Reaeration	SOD	Photo-synthesis	Temperature	Point Source Loads	Distributed Loads
DOSAG	Analytical	Steady State	No	1st order	1st order	options allowed	No	No	rate correction only	Steady State	No
QUAL1E	implicit finite difference	Steady State	Yes	1st order	1st order	options allowed	Yes	No	rate correction only	Steady State	Yes
QL2SMG	implicit finite difference	Steady State	Yes	1st order	Advanced Nutrient Cycle Coupled to Algae-Light	options allowed	Yes	Advanced Nutrient Algae Cycle Options	dynamic heat option	Steady State	Yes
SNSIM	Analytical	Steady State	No	1st order	1st order	options allowed	Yes	Gross P-R	rate connection	Steady State	Yes

IV MODEL CALIBRATION AND VERIFICATION SURVEY DATA

Four surveys were conducted on the lower Ouachita River Basin for the purpose of collecting data to calibrate and verify the four water quality models. The survey dates, locations, and approximate river flows are noted in Table 2. These surveys were planned following stable hydraulic and water quality conditions in the basin. No significant long term rain events preceded any survey.

The location of the sampling and measurement locations for these four surveys is further defined in Table 3 along with the kinds of measurements made at each. Table 4 presents the format for the spatial survey data collection at each station.

TABLE 2 SPATIAL SURVEY DATES ON
LOWER OUACHITA RIVER BASIN

<u>Date</u>	<u>River Locations</u>	<u>Approximate flow</u> <u>(CFS)</u>
7/21-22/80	m.p. 106 to 2.9	3,000
8/17/80	m.p. 106 to 0.0	1,200
9/23/80	m.p. 88.8 to 2.9	1,500
12/3-4/80	m.p. 106 to 2.9	17,000

The survey locations were chosen to coincide with a stream segmentation process established prior to the spatial surveys. The segmentation process was based upon the location of tributaries, point source discharges, significant velocity and depth changes in the stream, and observed changes in water quality. The velocity and depth data were taken from the Corps of Engineers HEC-II model output obtained for the anticipated flows, and the remaining factors were taken from the historical records and visual observations.

Measurements of stream velocity and depth were made throughout the basin at different flows for the purpose of verifying the HEC-II forecasts. The observed depth was approximately 20% lower than the predicted depth for some stream segments. No statistical differences between observed and forecasted velocity were observed.

TABLE 3 SUMMARY OF SPATIAL SURVEY SAMPLING LOCATIONS

River Mile/Location	7/21-22/80	Spatial Survey Date		
		8/17/80	9/23/80	12/3-4/80
106.0	XO	XO		XO
105.3	X	X		X
Load A	XO	XO		X
100.8	XO	X		X
96.8	XO	X		XO
Tributary 3	XO			
92.5	XO	X		
87.8	XO	X	XO	XO
82.8	XO	XO		
77.8	XO	X		
Tributary 6	XO	X		
74.8	X			XO
73.0	XO	X	X	
72.1	X			
Tributary 7	XO			
68.4	XO	X	X	XO
Tributary 4	X			
Tributary 8	XO	O		
64.8	X			
63.1	XO	XO	X	
57.5	XO	X	X	XO
Tributary 9	XO	X	XO	X
54.0	XO	X	X	XO
48.8	O	XO	XO	XO
44.8	X			
44.4	X			
Tributary 12	XO	XO		
42.4	X	X	X	XO
Load H	XO	XO		
37.4	XO	X	X	
Tributary 13	XO			
32.4	XO	X	XO	
27.6	X	X	X	XO
23.5	XO	XO	X	
16.9	XO	X	X	
12.8	X	X	X	X
8.0	XO	X	X	
2.9	X	X	X	XO

X DO, Temperature
O Ultimate BOD (BOD_u), NH₃-N, NO₃-N

TABLE 4 SPATIAL SURVEY DATA FORMAT

River Mile	Midstream Middepth
Width, Ft.	Temperature, C
Depth, Ft.	Dissolved Oxygen, mg/l
Headwater, Tributary, and Point Source Flow,	Conductivity, mho/cm
BOD ₅ , Temperature	Sample for BOD _u , NH ₃ -N, NO ₃ -N
Time of Day	
West Bank Middepth	Midstream Bottom
Temperature, C	Temperature, C
Dissolved Oxygen, mg/l	Dissolved Oxygen, mg/l
Midstream Surface	Eastbank Middepth
Temperature, C	Temperature, C
Dissolved Oxygen, mg/l	Dissolved Oxygen, mg/l
pH	Velocity, ft/sec (at selected stations)
	1/4 width middepth
	1/2 width middepth

V QUALITY ASSURANCE PROTOCOL

Model calibration and verification required laboratory and field measurement of a number of physical, chemical, and biological variables. They are outlined in Table 5 along with appropriate quality assurance protocol. Quality assurance was integrated into the field and laboratory measurements to (a) assure the integrity of the data base and (b) alert the field manager to analysis or instrumentation problems on a routine basis. The most frequent problems encountered were related to maintenance of DO electrode membranes and specific ion probes.

TABLE 5 SUMMARY OF QUALITY ASSURANCE PROGRAM

<u>Measurement</u>	<u>Source/Method</u>	<u>Location</u>	<u>Calibration Type</u>	<u>Calibration Frequency</u>
Location	Topographic Maps U.S. Army COE Navigation Charts	Field	-	-
Width	Rangefinder, Inc. Model 600	Field	Comparison to known	Monthly
Depth	Raytheon FR450W	Field	Comparison to known	Monthly
Temperature	YSI Model 56 DO Meter	Field/Lab	National Bureau of Standards Reference	Monthly
Conductivity	YSI Model S-C-T Meter	Field	-	-
pH	Orion Model 201	Lab	Single Reference Buffer	per use
Stream Velocity	Bendix Model B-10 Ducted Current Meter Gurley Current Meter	Field	Standard Plume	Monthly
Dissolved Oxygen	YSI Model 56, Model 57	Field/Lab	Air Calibration Winkler Wet Chemistry	Daily Weekly
Ammonia	Orion Electrode Model 95-10	Lab	Reference Solution, and spiked unknowns	Daily
Nitrate	Orion Electrode Model 92-07	Lab	Reference Solution, and spiked unknowns	Daily
Ultimate BOD	Single Bottle with Reaeration	Lab	Glucose-Glutamic Acid Control	Once during study
Point Source BOD ₅	Standard Methods, 14th ed.	Lab	EPA Quality Control Samples	Once during study

VI ESTIMATION OF MAJOR PARAMETERS

The following experimental procedures were used to estimate major parameter values and their uncertainty. They include carbonaceous and nitrogenous ultimate BOD's and their reaction rate coefficients, reaeration rates, sediment oxygen demands, and photosynthesis related parameters.

A. BIOCHEMICAL OXYGEN DEMAND STUDIES

Long term BOD studies were conducted to (a) estimate the magnitude of point source loads, and (b) estimate the rate of river deoxygenation. Both studies were conducted using a single dilution technique with sample reaeration (6).

The apparatus for these studies is shown in Figure 2. The strategy was to monitor the dissolved oxygen (DO) concentration changes and reaerate the contents of the container when the DO level approached 2 mg/l. Incubation was at 25C for all samples. Small (25 ml) samples were withdrawn for ammonia and nitrate ion concentration measurements which were used to define nitrification. A more detailed discussion of the theory and experience with this technique is discussed by McKeown, et al. (6).

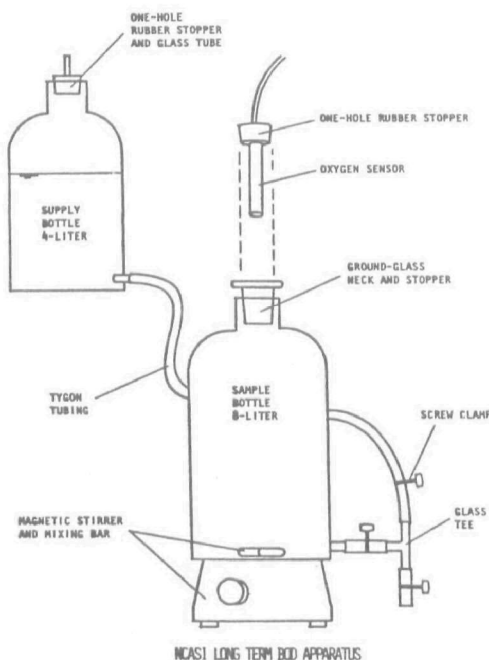


Figure 2

The reaction rates for the carbonaceous and nitrogenous BOD data are summarized in Table 6 along with an estimate of their 95 percent confidence limits. The reaction rates noted in Table 6 were used as needed in the four water quality models.

It is interesting to note that the average value for carbonaceous BOD of 0.02 per day (25C) is lower than has been traditionally measured in prior modeling studies. The low value, however, reflects the long term deoxygenation behavior of these river water samples. Short term experiments of 20-30 days would have resulted in estimates of lower ultimate BOD and higher rate coefficients. The k_{NH_3} and k_{NO_2} values were required only for QL2SMG and were obtained by non-linear regression of the ammonia, nitrate, and DO data.

TABLE 6 **SUMMARY OF BOD KINETICS FOR RIVER
WATER SAMPLES AT 25C**

Parameter	Description	Measured Value (1/day)	95% C.L. (1/day)
k_1	Carbonaceous BOD Decay	0.02	± 0.01
k_n	Nitrogenous BOD Decay	0.13	± 0.02
k_{NH_3}	Ammonia Oxidation to Nitrite	0.13	± 0.02
k_{NO_2}	Nitrite Oxidation to Nitrate	0.6	± 0.1

Each of the major point source loads were sampled at least once during the summer months for the purpose of determining their ultimate BOD value. NPDES reporting data which provided 5 day BOD values were also collected from each of the major sources. It was assumed that the ultimate values obtained from the long term experiments were constant and represented the point source for the entire simulation period. Consequently, a ratio of ultimate to 5 day BOD was established for each load.

It is important that recognition be given to the fact that ultimate to 5 day ratios are really a companion estimate of the oxidation rate constant. Because of this correlation, the values of the ratio and the reaction rate constant are not independent. If considered independent, selection of one without proper selection of the other will lead to erroneous application and will produce considerable bias in the allocation of waste loads.

B. RIVER REAERATION

The river reaeration rates on the lower Ouachita were estimated from radiotracer measurements made at two locations. These studies were performed by Law Engineering Co. of Marietta, Ga. with NCASI supervision and personnel and are further summarized in Table 7. The standard deviation values presented in this table are derived from the field data and are discussed in a companion paper to these proceedings.

TABLE 7 SUMMARY OF RADIOTRACER EXPERIMENTS
ON OUACHITA BASIN

Location	Segment Length, Miles	Approximate Flow, cfs	Average Velocity Ft/Sec.	Average Depth Ft	$k_{2,20C}$ (1/day)	95% Confidence Limits
m.p. 75	2	1200	0.09	30	0.02	± 1000
m.p. 195	18	850	0.40	15	0.17	± 18

A comparison was made between these values and several empirical equations. It was interesting to note that the O'Connor-Dobbins equation agreed to within 6% of the radiotracer measurement at both velocity conditions. This favorable comparison was used as the basis for concluding that the O'Connor-Dobbins equation was appropriate for estimating the reaeration coefficient of the Ouachita River for similar flow regimes. This equation, therefore, was used in all four models.

C. SEDIMENT OXYGEN DEMAND

Sediment oxygen demand (SOD) measurements were made on the Ouachita River Basin following procedures outlined in NCASI Technical Bulletins No. 317 and 321 (7, 8). The measurements were made in-situ using the respirometer shown in Figure 3. Prior research by NCASI has shown that SOD can be a function of the velocity at the sediment water interface. It was hypothesized that the rise in turbulence generated by increased velocity was responsible for increased transport of soluble organic material across the sediment interface, resulting in increased SOD.

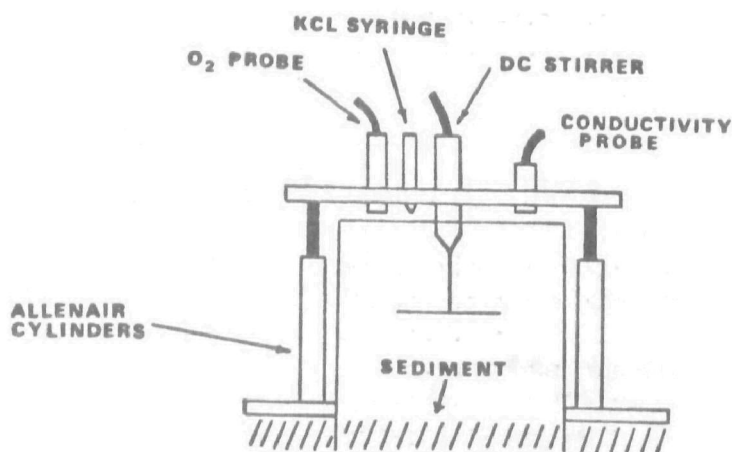


Figure 3

NCASI IN-SITU SOD APPARATUS

The variability in the measured SOD values was assessed with repeated measurements. The average and standard deviation were 1.6 gm/m²/day and 1.0 gm/m²/day ($\pm 62\%$) respectively. Other NCASI experience has shown that in-situ SOD measurements exhibit variability of the order of $\pm 44\%$ (8).

D. PHOTOSYNTHESIS

Previous water quality studies of the lower Ouachita River did not identify algal productivity as a major water quality process (9). NCASI field work in this area consisted of the following studies:

- (1) Light penetration at 4 locations.
- (2) Three diurnal DO profiles at location.
- (3) Light-dark bottle at 4 locations.

The light and dark bottle measurements were measured after a technique developed by NCASI. Standard BOD bottles filled with river water from a common well mixed sample were suspended from a triangle rack constructed of 2" x 4" lumber. The bottles were suspended at depths of 1/2, 1, 2, 4, and 8 feet as shown in Figure 4. The dark bottles were also standard BOD bottles but covered with 2 layers of black electrical tape. Six bottles were suspended at each depth, spaced randomly across the rack.

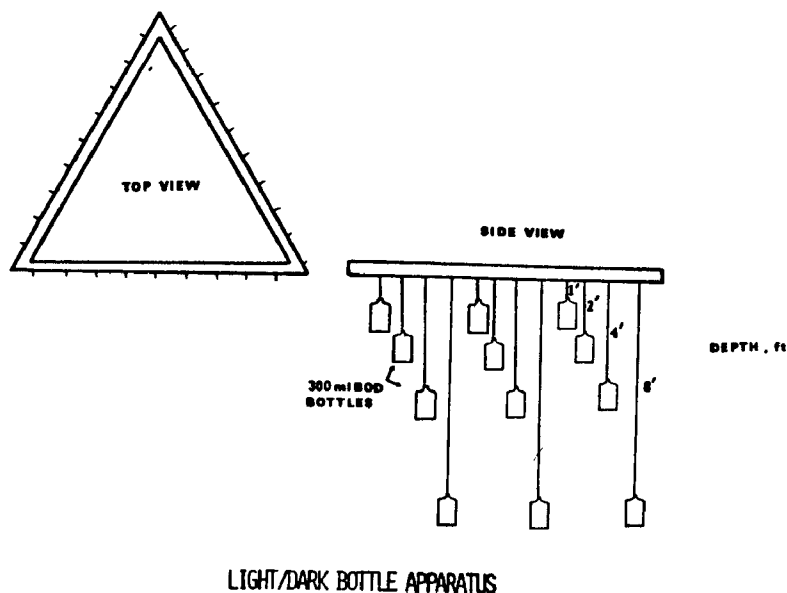


Figure 4

The results of these studies are presented in Table 8. It was noted that the depth at which the maximum photosynthesis occurs is approximately 1-2 feet. Net algal respiration occurred below a depth of 2 feet in all cases. The average daily p-r term in Table 8 of 1.8 mg/l/day applied strictly to the active photosynthetic zone which was approximately 1 to 4 feet in depth. This distance was approximately 15% of the basin's average depth of 25 feet. The average daily p-r term was, therefore, multiplied by 0.15 to obtain a cross sectional average of 0.3 mg/l/day + 0.1 (95% C.L.). This value was necessary for the SNSIM simulation which required a p-r term for the entire water column. The uncertainty in p-r of $\pm .1$ mg/l/day was later used in the sensitivity study.

Table 8

SUMMARY OF LIGHT-DARK
BOTTLE PHOTOSYNTHESIS EXPERIMENTS

Location	Date	Initial DO (mg/l)	Dark Bottle DO (mg/l)	Water Temperature	(1) Light Bottle DO at Stream Incubation Depth (mg/l)					Maximum Net p-r, mg/l	Maximum Net p-r per 14 hour sunlight day, mg/l/day
					6"	1'	2'	4'	8'		
m.p. 52	8/24	5.1	4.8	32C	5.7	5.5	5.4	4.8	4.7	0.6	2.6
m.p. 33	8/27	5.4	4.3	32C	5.1	5.6	5.2	4.7	4.7	0.2	0.9
m.p. 73	8/29	6.4	5.5	32C	6.8	6.8	6.0	6.2	6.0	0.4	1.7
m.p. 133	8/28	6.5	5.6	32C	7.0	7.0	6.1	6.0	6.0	0.5	2.2

Avg. = 1.8
Standard
Deviation =
0.7

(1) All values are an average of 3-6 bottles following 3 1/4 hours of instream incubation.

VII PARAMETER SENSITIVITY

A. Mathematical Expression of Sensitivity

Parameter sensitivity in water quality modeling is defined as the response of an output variable such as DO or BOD to a change in a single input model parameter. Sensitivity can be illustrated mathematically using the Streeter-Phelps DO model shown in Equation 1.

$$D = \frac{L}{k_2 - k_1} (e^{-k_1 t} - e^{-k_2 t}) \quad (\text{Eq. 1})$$

D = DO deficit, mg/l

L = Instream ultimate BOD, mg/l

t = Time, days

k_1 = Deoxygenation rate parameter, 1/day

k_2 = Reaeration rate parameter, 1/day

The sensitivity of the deficit to the parameters k_1 and k_2 is represented by Equations 2 and 3 respectively.

$$\frac{\partial D}{\partial k_1} = \frac{1}{k_2 - k_1} (D - tLe^{-k_1 t}) \quad (\text{Eq. 2})$$

$$\frac{\partial D}{\partial k_2} = \frac{1}{k_2 - k_1} (Lte^{-k_2 t} - D) \quad (\text{Eq. 3})$$

In the case of the model expressed by Equation 1, the sensitivity of the oxygen deficit to the parameters k_1 and k_2 is complex and a function of all variables and parameters in the model. The sensitivity equations (2 and 3) also illustrate that there are no apriori assumptions that can be made about one model parameter being more sensitive than another. The mathematical representatives of sensitivity preclude such assumptions.

B. Significance of Sensitivity Studies

Sensitivity is initially of importance in modeling to define those parameters that are most sensitive and logically require emphasis during field parameter estimation work. Consider the following example in which the importance of SOD is being considered during a wasteload allocation determination. Historical and literature sources indicate that the SOD should fall in the range 1-5 gm O_2/m^2 day for the basin in question. Further, the measurement of SOD with an in-situ respirometer would require 1/2 to 1 month for a two person team to complete. The question is, what would be the benefit in the wasteload allocation determination as a result of determining SOD?

A sensitivity study could be used to investigate the impact of SOD over the range 1-5 gm O₂/m² day on DO predictions. The study may reveal that SOD has relatively little impact on stream DO compared to other stream process and, therefore, should not be measured. On the other hand, the model may show extreme sensitivity to SOD and suggest that the work be completed. In this later case, the field work will become more precise and more fairly represent this oxygen sink in the model. Proper distribution of the DO sinks has definite implications on waste load allocation for if the oxygen sinks can be better defined during calibration, they won't be lumped together into the stream deoxygenation rate, k_1 .

C. Ouachita River Sensitivity Study

1. Sensitivity Study Conditions - In practice sensitivity is examined by perturbing one parameter from a given value by a constant amount (i.e. +50%) while the other are kept constant. The perturbation amount usually represents the amount of uncertainty or error associated with each parameter.

The sensitivity of each calibrated model is examined relative to a base case. In each model, the base case is the best calibration of the July survey conditions. These calibrations are presented in later sections on model selection, calibration and verification. DOSAG is calibrated for DO and CBOD. QUAL1E, SNSIM and QL2SMG are calibrated for DO, CBOD and NBOD. The base case DO varied slightly from model to model because of differences in individual model conceptualization and input parameters.

The sensitivity in each of the models was examined by perturbing the input value for each parameter, one at a time, around the input value for the base case. The perturbation for temperature is +1°C. The perturbation for reaction rates, algae parameters and loads is +50% of the base case value. The perturbation for hydraulic parameters is +20% of the base case value. The magnitude of these perturbations is standardized within each group of parameters in order to facilitate the comparison of the sensitivity of similar parameters. "No BOD" means that BOD was not simulated in the model. In addition, the magnitude of the perturbation used in each group of parameters represents the relative confidence in the estimation of each parameter type

2. Summary of Sensitivity Study Results - The results of this sensitivity study are presented graphically in Figures 5 to 8. These results are commented upon in a general sense in the following paragraphs. In summary, calibrations of the water quality models DOSAG, QUAL1E, SNSIM, and QL2SMG for the July survey conditions have been reviewed for the sensitivity of their dissolved oxygen predictions to the perturbation of input para-

meter values. In general the models showed an increase in sensitivity at the end of the basin over the midpoint, probably reflecting the increase of travel time in the basin and its affect on various reaction parameters. In the simplest model, DOSAG, the two major oxygen reaction rates, k_1 and k_2 , displayed the most sensitivity. As the complexity of the model increased (parameters were added) the dissolved oxygen sensitivities evened out somewhat, and were reduced in magnitude. In QL2SMG, additional complexity in the form of the algal growth cycle added greatly to the range of predicted dissolved oxygen values.

While the sensitivity of most reaction parameters remained roughly equivalent among QUAL1E, SNSIM and QL2SMG, the algae parameters made the prediction of dissolved oxygen value from zero to saturation and beyond possible. It should be noted that the p-r algae term in SNSIM, based on light and dark bottle experiments, showed nowhere near the sensitivity possible with the QL2SMG algae cycle.

The relationship in water quality models between hydraulic and water quality parameters was demonstrated. The sensitivity of the reaction rate and algae parameters was a complex function of other parameters in the model, particularly hydraulic parameters. The simple addition of an SOD term to the model calibrations reversed the relative sensitivities of velocity and depth. The addition of the QL2SMG algae cycle gave depth an extremely high sensitivity.

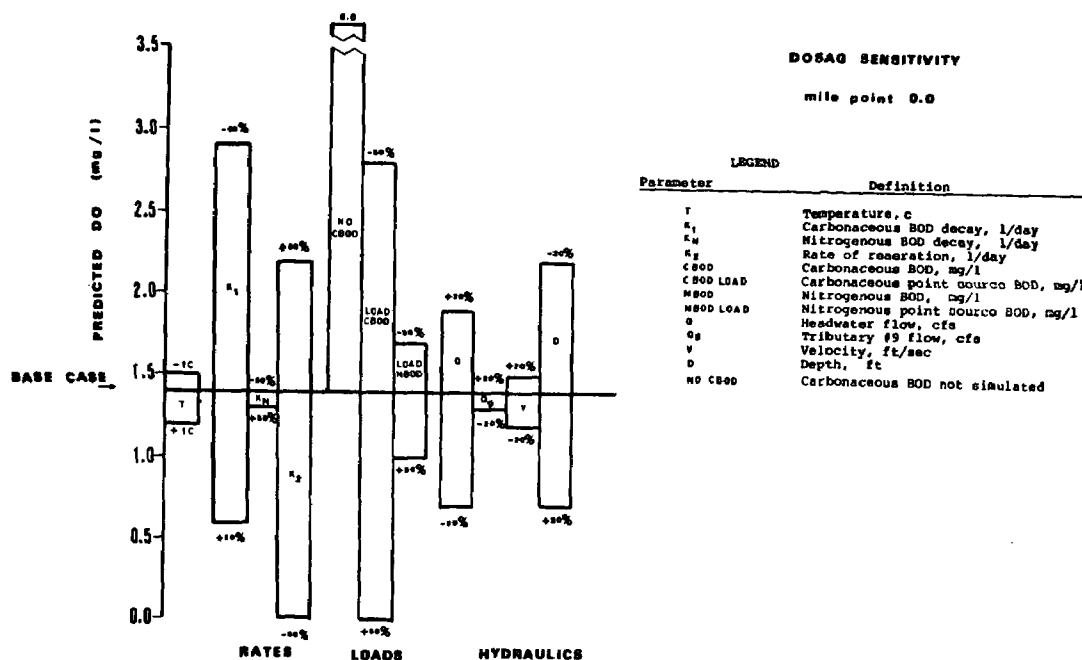
Viewing this sensitivity study from the standpoint of waste load allocation and model predictive capabilities, several interesting points emerged.

- 1) The relative sensitivity of point source loads to DO predictions was often minor when compared to the relative sensitivity obtained with some other model parameters.
- 2) The algae parameters, SOD, and k_2 displayed the highest sensitivity.
- 3) The hydraulic parameters of velocity and depth confounded the sensitivity of other model parameters such as k_2 and SOD because they were often related.

This sensitivity study also illustrated some current problems in the use of water quality models for waste load allocations. Simple models such as DOSAG show high sensitivity of the CBOD kinetics to the prediction of D.O. Yet, in complex situations (like the one modeled herein), the most sensitive parameters are not always included in simple models. More complex models such

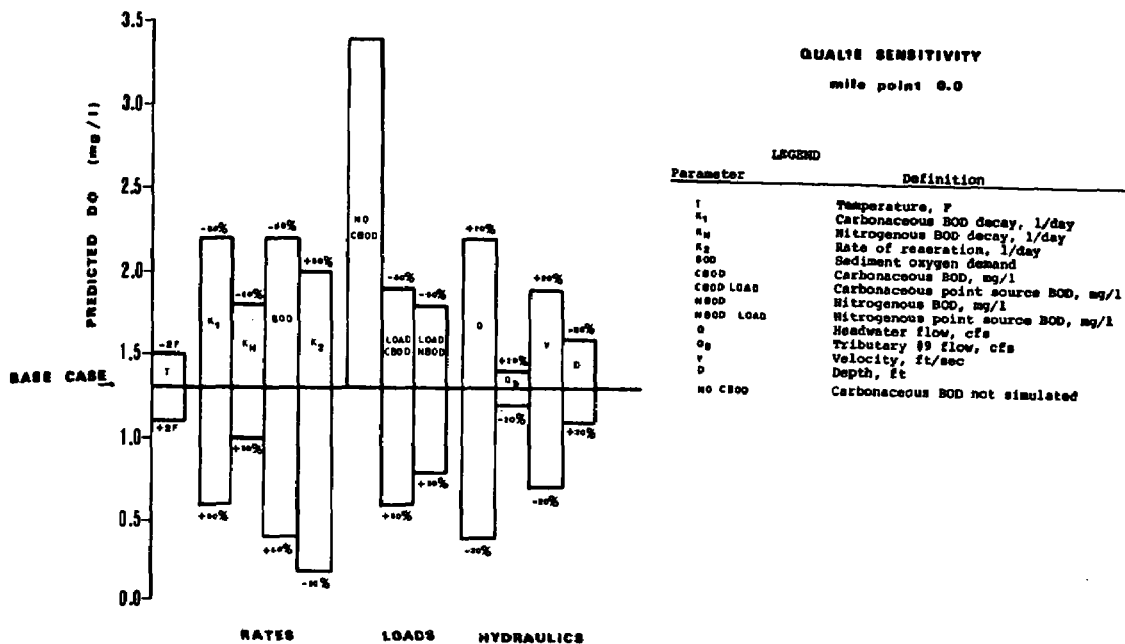
as QL2SMG, however, require the estimation or measurement of several algae-nutrient cycle parameters as well as SOD. These parameters which have exhibited high sensitivity are often not measured in the field when they are modeled. Additional error is introduced if inappropriate values for these sensitive parameters are selected.

In short, the most sensitive parameters in many models were also the least understood parameters. Because of this lack of understanding and the uncertainty in the parameter value, model calibration may be little more than a curve fitting exercise with little hope of achieving the correct balance between these sensitive parameters. There are many values for these parameters which may be used together such that one or two output variables may be calibrated. Yet, only one of these combinations could be a true mechanistic representation of the stream. Mechanistic representation and correct parameter balance can only be tested by model verification as discussed in the next section.



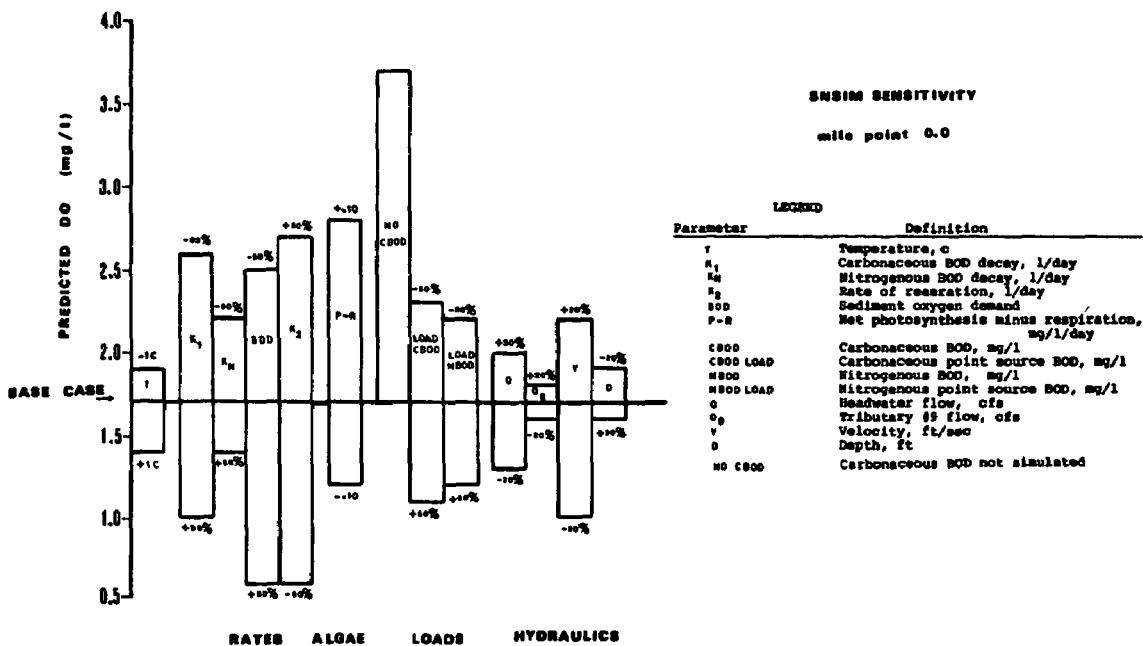
DOSAG SENSITIVITY - M.P. 0

Figure 5



QUALIE SENSITIVITY - M.P. 0

Figure 6



SNSIM SENSITIVITY - M.P. 0

Figure 7

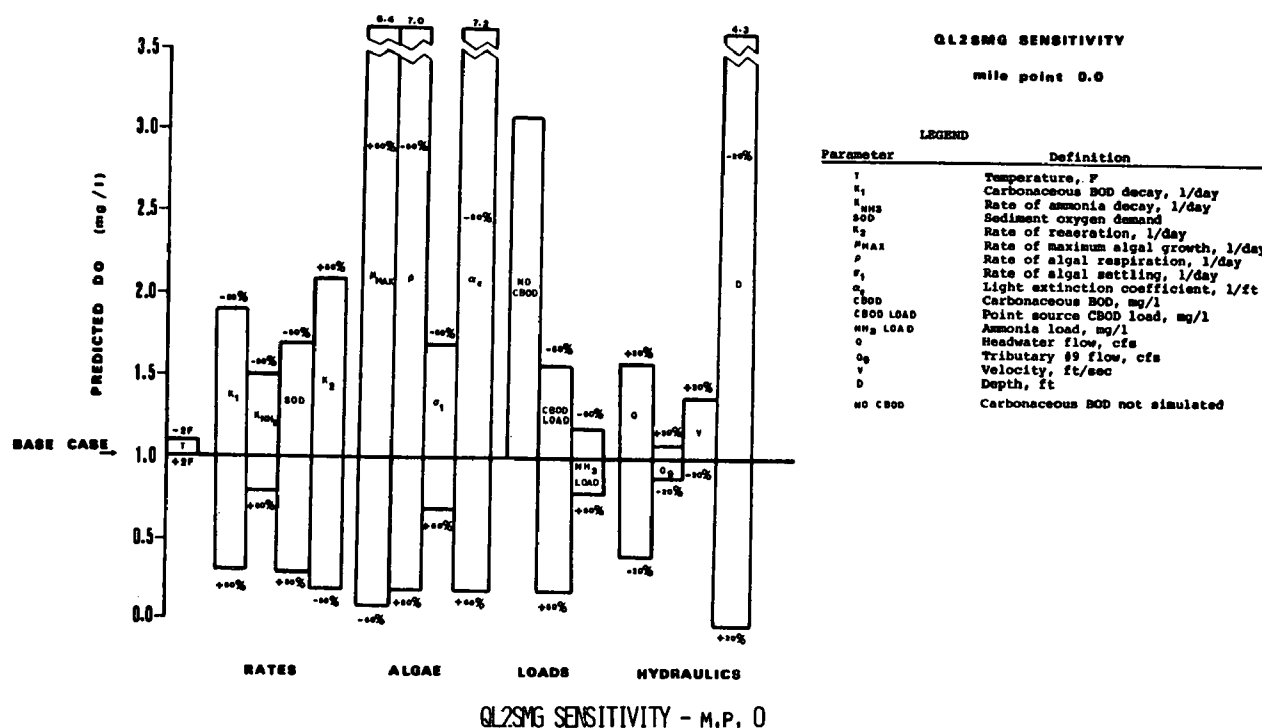


Figure 8

VIII MODEL SELECTION, CALIBRATION AND VERIFICATION

This section addresses the process of selection, calibration and verification of the four water quality models (DOSAG, QUAL1E, SNSIM, and QL2SMG). It must be stressed that this study presents this process for a single river basin using a particular methodology. The examples given demonstrate many of the problems commonly encountered in the validation of water quality models. As a result of examining these problems, a pattern of effective model selection, calibration, and verification emerges which should have application to most receiving water situations.

In order to make reasoned decisions as to whether or not a model is properly selected, calibrated and verified, it is necessary to establish criteria for the fulfillment of each modeling step. It is recognized that these criteria may be initially subjective because it is probable that no two modelers would view a receiving water situation in exactly the same way.

Nevertheless, establishing a clear set of criteria or adopting a structured approach to model selection, calibration and verification enhances the understanding of the role each of these steps plays in the development of model predictive capability, and allows a clearer comparison among models which is the objective of this study.

A. Model Selection Criteria

The primary basis for choosing criteria which would be used to select a model was that the criteria must result in a model that is a "reasonable" representation of the river basin. A "reasonable" representation is one which models the most important physical, biological and chemical processes to allow the prediction of water quality for specific conditions.

Table 9 summarizes the evolution of the model selection criteria used by NCASI in this study. The first column lists the various topics explored above. The second column lists the criteria that would have resulted if only the data collected prior to the NCASI spatial surveys had been used. The third column lists the criteria which were compatible with NCASI spatial survey data and the four water quality models selected for comparison. The fourth column lists the few conditions observed in the basin which were not included in the selection criteria. For the most part they represent minor conditions in the basin, and their exclusion did not affect the predictive capability of the selected models. However, a few of the conditions (notably the N and algae cycles) are discussed further in subsequent sections of this report, as they may play a role in developing model predictive capability.

B. Model Calibration/Verification Criteria

1. General Criteria The first step toward calibration was described earlier in this report as one in which both model parameters and input loads had been measured by appropriate experiments or assigned by sound engineering judgment. The model is considered calibrated when the resulting model output, such as stream DO or BOD, matches observed data. The model is considered verified, on the other hand, when the calibrated model produces some water quality condition perturbed from the calibration case. Generally, the perturbed case involves different flow, temperature, and/or load conditions.

TABLE 9

EVOLUTION OF THE MODEL SELECTION CRITERIA

	Validation Topic	Initial Criteria Based On Data Prior to NCASI Spatial Surveys	Final Criteria Used in this Study, Based on NCASI Survey Data Spatial	Observed Conditions Excluded from this Selection Criteria*
19	Hydraulics	One-dimensional steady state rectangular channel	One-dimensional steady state rectangular channel	Two-dimensional vertically stratified dynamic trapezoidal channel
	Loads	8 point sources 15 tributaries non-point sources	6 point sources 7 tributaries no non-point sources	2 point sources 8 tributaries non-point sources
	Physical, Chemical and Biological Processes	CBOD NBOD Reaeration SOD	CBOD NBOD Reaeration SOD (Algae (p-r))	N-Cycle Algae-Cycle
	Temperature	Direct T Input T Correction of Rates	Direct T Input T Correction of Rates	Heat Balance

* See text for the significance of these conditions.

This notion of model calibration/verification, which has been cited in numerous water quality studies during the past two decades, contains several subjective and arbitrary features. The first of these was the manner in which parameters were adjusted during calibration which called upon the modelers recognition that parameter estimation procedures were subject to error. The second of these related to the comparison of model output with observed conditions. The modeler was simply faced with making a judgment as to when the comparison was "acceptable". This judgment was necessary for both model calibration and verification.

A review of state-of-the-art modeling practice has revealed an interesting dichotomy amongst modelers in their approach to obtaining an "acceptable" verification. One approach simply relied upon a visual inspection of the predicted vs observed model variable and made a subjective judgment about goodness of fit. A vast majority of current modeling studies fall in this category. Examples of this approach are presented below:

(1) "The goodness of fit reached for the predicted variables during calibration of each of the stream models is illustrated by graph plots of computed and observed data vs stream distance" (10).

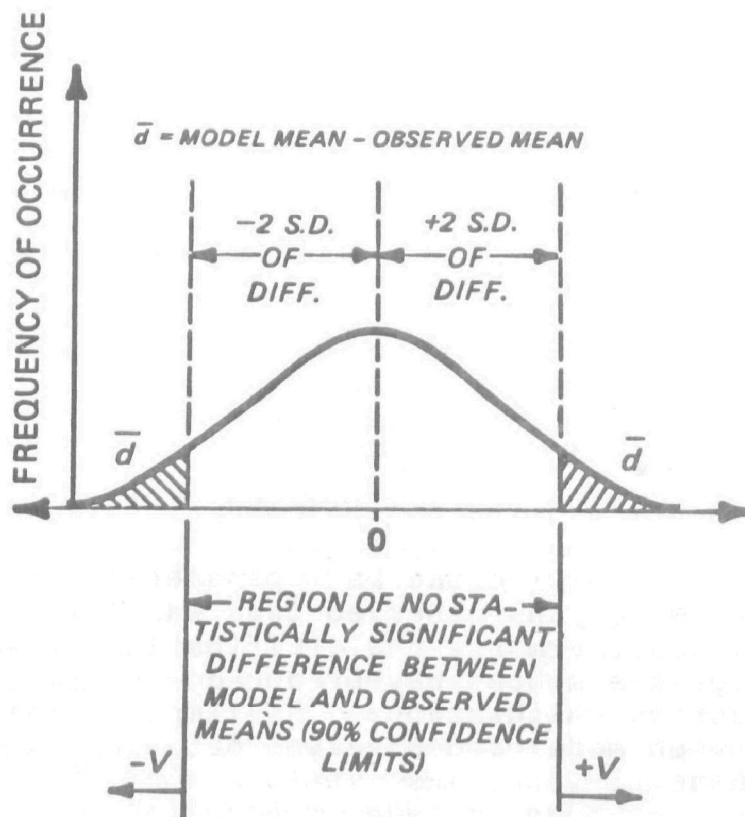
(2) "As shown in the upper panels of Figure X good agreement is shown between observed and calculated BOD and DO" (11).

(3) "Verification (calibration) of the DO and the BOD mathematical models presented elsewhere in this report has been made for various conditions of flow and water temperature. Verification (calibration) of the mathematical models is obtained when good correlation is evident between the calculated profiles and the observed data for various conditions of flow, temperature, and loading, using consistent parameters" (12).

(4) "Inspection of these figures shows that the calibration on DO and BOD is quite accurate. Even though the variation in the values measured at each sampling location was relatively high for both DO and BOD, the averaged values match reasonably well. Greater agreement with the averaged data points could be obtained by adjusting certain parameters. However, given the variation in the measured data and the fact that certain parameters such as reaeration, sedimentation rate, and benthic demand were unknown, it was felt that a closer fit could not be justified. The calculated profiles indicate that the proper mechanisms have been accounted for in the model" (13).

The second approach relied upon statistical tests for interpreting goodness of fit. O'Connor, et al. (14) examples of such analyses for a three dimensional eutrophication model of Lake Ontario.

The verification statistic discussed involved the use of Student's t distribution to compare model output to observed data. The results of such analyses were plotted for a general case in Figure 9. The physical interpretation of the plot in Figure 9 was that the observed and predicted means were statistically indistinguishable at the 90% confidence level. Inversely, the modeler was accepting a risk of one chance in ten that the model mean was statistically different than the observed mean. It is important to note that another modeler might have chosen another confidence level where the differences might be significant.



(After Reference 14)

COMPARISON OF MODEL TO OBSERVED DATA

Figure 9

A crude statistical measure of goodness of fit was referenced in a proprietary modeling study reviewed by NCASI. The modelers sought to minimize the statistic noted below for DO.

$$\text{Goodness of fit} = \frac{\sum_{i=1}^N (\text{Observed} - \text{Predicted})^2}{N}$$

A summary of the use of this statistic during model calibration and verification is presented in Table 10. Three data sets (A, B, C) were available for use. The technique was illustrated for two different model parameter sets.

Table 10 Summary of Goodness
of Fit (Variance) Statistics
(Proprietary Model Study)

	Calibration		Verification
	Phase		Phase
	Data Set A	Data Set B	Data Set C
Parameter Set I	1.4561	1.9546	1.5086
Parameter Set II	1.1797	1.7729	1.5382

Parameter Set II was called the best parameter set because the variance between model and observed data was lower than other parameter sets. Furthermore, the verification attempts were considered acceptable since they produced a variance less than that obtained during calibration. This implies that the residual differences between model and observed data were smaller for the verification phase.

The problem with this methodology lies in the fact that the goodness of fit or variance for both model calibration and verification was relatively high. A DO variance (S^2) of 1.1797 (Table 10) implied that the mean deviation of the model from the observed data ($\sqrt{S^2}$) was 1.08 mg/l DO. This measure of model predictive capability may not be acceptable for certain model applications.

2. Specific Criteria for NCASI Study - The calibration/verification criteria used by NCASI for the Ouachita River Basin modeling work was based upon a structured format. For a model to be calibrated, its prediction of an output variable (DO, CBOD, NBOD, etc) had to fall within the 95% confidence range of the corresponding spatial survey data for 95% of the measured data points. This was analogous to assuming a risk of 1 time in 20 that the predicted output would not match the observed data within the confidence range specified.

The verification criteria required that the model prediction of an output variable had to fall within the 95% confidence limits for 60% of the measured data points. This less stringent criteria for model verification was based upon the fact that the 95% confidence limits for some of the measured data points was small (approximately ± 0.12 mg/l) for DO. Hence, in some cases the predicted output variable came close to the measured 95% confidence range without falling inside. A second and more important point deals with the uncertainty associated with the algal mechanisms inherent in the models SNSIM and QL2SMG. SNSIM utilized a gross photosynthesis minus respiration mechanism whereas QL2SMG used a complex algal growth cycle dependent upon both light and nutrients. None of the parameters in this latter mechanism were measured and therefore required estimation.

The NCASI criteria also required that the model output match all significant trends in the measured data. The assessment of significant trends was made with statistical tests, thereby avoiding the use of visual observations of trends when comparing observed data and/or model output.

The three criteria adopted for calibration and verification were applied to all model outputs, not just DO. Also, these criteria were selected following an analysis of the field data and several attempts to calibrate and verify the various models. Although their format was based on experience, the actual numbers (i.e. 60% of the values) were selected for this particular study. If the data had shown 90% of the values to fall within the 95% confidence level, then the criterion for verification would have been raised to 90%. As already mentioned, the important point is that definitive criteria be used to encourage proper consideration of the uncertainty surrounding eventual use of the model to make water quality forecasts.

C. Model Calibration Strategy

A systematic approach to model calibration was applied to the four water quality models in order to test several aspects of the model's predictive capabilities. Central to this systematic approach was the calibration criteria developed in a previous section. Calibration of the models was attempted using the spatial survey data from 7/21-22/80 (DO, CBOD, and NBOD) as a reference, even for the models which did not match the selection criteria. The systematic approach was designed to test the following aspects of model predictive capability. First, the ability of a properly selected model (i.e. SNSIM or QL2SMG) to be calibrated was tested versus an improperly selected model (i.e. DOSAG or QUAL1E). Here the models were tested to see if it was possible to arrive at an acceptable representation of the calibration survey data, even when all of the significant processes in the river were not modeled. To some degree, this was a function of the confidence range of the parameter estimates and the survey data being modeled. The effect of model selection on predictive capability was further examined during verification.

Second, the ability of various state-of-the-art parameter estimation procedures to define input parameters, and hence lead to calibration, was examined. The examination focused on four types of parameters from a previous 208 modeling study which were largely "textbook" in nature; 2) NCASI "best parameter estimates" based on field surveys and laboratory data; 3) parameter estimates calibrated by the perturbation of the "best parameter estimates" within their 95% confidence ranges; 4) parameter estimates calibrated by the perturbation of the "best parameter estimates" outside their 95% confidence ranges, but with engineering judgment. The predictive capability of each type of parameter estimate was further investigated in the verification section.

Third, the importance of the order and number of survey data calibrated was investigated. This was done by first calibrating the models to the spatial survey DO data. DO data had the smallest confidence range when compared to CBOD and NBOD data. Calibration then proceeded with further spatial survey data (DO and CBOD; DO, CBOD and NBOD). Then, the process was reversed and calibration was started with the spatial survey data with the lowest confidence (largest confidence range), NBOD. The models were further calibrated with increasing spatial survey data (NBOD and CBOD; NBOD, CBOD and DO) as will be explained in the discussion that follows. The effect of these various approaches to calibration (various orders and numbers of spatial survey data calibrated) on model predictive capability was further examined during verification.

The effect of these various aspects of model calibration on model predictive capability was examined via the four calibration phases outlined below.

Calibration Phase 1 used the reaction parameters (k_1 , k_2 , k_d , SOD, algae) from a 208 modeling study of this river basin to model the physical and biological processes. The models were otherwise setup with geometry, hydraulics, and loads as determined during the NCASI spatial surveys.

Phase 2 was the attempted calibration of the models using the "best parameter estimates" for all inputs as established by NCASI field and laboratory studies. The procedures used to estimate these parameters were reviewed earlier in this report.

Calibration Phase 3 involved the perturbation of the "best parameter estimates" in order to calibrate with an increasing amount of spatial survey data. First, the models are calibrated for the most confident survey data, DO. Then the calibration proceeded to DO and CBOD; and finally to DO, CBOD and NBOD. In Phase 3a the perturbations were restricted to the 95% confidence ranges of all of the input parameters. Phase 3b allowed these perturbations to fall outside the 95% confidence range, but within a range which could be justified through engineering practice. If parameter estimates outside the accepted engineering judgment range were required to meet the calibration criteria for any particular survey data (DO, CBOD, or NBOD), then the model was deemed as uncalibrated for that data.

Phase 4 involved essentially the same procedure as Phase 3 except calibration was started with the least confident survey data, NBOD. From there it proceeded to NBOD and CBOD, and finally to NBOD, CBOD and DO. Phase 4a allowed perturbations within the 95% confidence limits of the input parameters, analogous to Phase 3a. Phase 4b permitted perturbations within the range of engineering judgment, analogous to Phase 3b. Once again, any model which could not meet the calibration criteria for a particular survey data within the constraints of Phase 4b was deemed uncalibrated for that data.

Table 11 presents a synopsis of these four calibration phases. Reference to this table will be useful in interpreting the calibration/verification summary figures (Figures 10 to 13). These four figures are a condensation of many individual calibration/verification attempts.

Table 11

Summary of Calibration Phases

PHASE 1	208 modeling study parameters
PHASE 2	NCASI "best parameter estimates" based on field and laboratory data.
PHASE 3	Calibrated parameter sets, starting with DO, then DO and CBOD, then DO, CBOD and NBOD (NH_3). a. Parameters held to within 95% confidence range based on field and laboratory data. b. Parameters held to an accepted "engineering judgment" range, outside the 95% confidence range.
PHASE 4	As in Phase 3 except calibrated first with NBOD (NH_3), then NBOD (NH_3) and CBOD, then NBOD (NH_3), CBOD, and DO. a. As in 3a. b. As in 3b.

D. Model Calibration/Verification Summary

Model selection had several effects upon model calibration and verification. A comparison of DOSAG's calibration (Figure 10) to QL2SMG's calibration (Figure 13) demonstrated this effect. DOSAG, an improperly selected model, had poor calibration potential, while QL2SMG, a properly selected model, could be calibrated in many different ways. The models QUAL1E and SNSIM, on the other hand, showed similar calibration potentials. This fact raised an important point about model calibration and its relationship to model selection. SNSIM allows simulation of algal productivity and QUAL1E does not. However, the 7/21-22/80 survey data used for calibration did not show much algal productivity. Thus, the failure of the calibration process to distinguish between QUAL1E and SNSIM was not surprising. It was found to be important, therefore, to define model selection criteria such that all major physical, chemical, and biological processes active during the temporal and spatial regimes of interest are considered. A single spatial survey was not sufficient in this study to define these processes.

The effect of the parameter estimation procedure on model predictive capability was also illustrated in Figures 10 to 13. Several important effects were noted. First, Phase 1 (parameters used in Phase 1 were largely textbook values) provided the least exact predictions of the observed conditions.

Second, the effect of parameter uncertainty on model calibration and verification was explored. Both Phase 1 and Phase 2 failed to calibrate and verify because in both cases, the input parameter values were treated as absolute numbers. This rigidity in input parameter specification did not recognize that every measurement had an inherent uncertainty. Failure to recognize, and quantify this uncertainty was partly responsible for the poor model predictions shown in Phase 1 and 2 of this study.

On the other side of this issue was the use of parameter values outside their established confidence ranges. A comparison of the "a" and "b" type calibrations and verifications of Phase 3 and 4 demonstrated this effect. Parameter values in Phase 3a and 4a calibrations and verifications adhered to their 95% confidence limits, while Phase 3b and 4b allowed values outside that range where they could be justified. In general, it was possible to calibrate more survey data with "b" type input data, but predictive capability was not enhanced. In examining Figures 10 to 13, the only place where significant predictive capability was gained using "b" parameter values was with QL2SMG. In that case, it was not a calibration parameter that was outside its 95% confidence range, but rather the verification flow for the 8/17/80 survey. The use of a flow outside the 95% confidence range was actually a compensation for a known violation of the basic steady-state modeling assumption (during the 8/17/80 survey). Incidentally, in the case of SNSIM and QUAL1E, the use of "b" parameter values during calibration actually reduced the predictive capability of the model.

It was found that parameter uncertainty must be applied in moderation during the perturbation of parameter values for calibration and verification. Mathematical water quality modeling parameters are neither single values nor excessively broad ranges. State-of-the-art parameter estimation procedures must involve field and laboratory measurements of important environmental processes to establish the uncertainty estimates in parameter values. If the model is appropriate for the natural system being represented, then parameter values outside the experimentally or theoretically determined confidence range should never be needed.

In order to verify if an output variable was correctly modeled, it was first necessary to calibrate the model to predict the specific variable. In other words, a model which was calibrated for only NBOD was not expected to predict DO for some future condition. Several of the model calibrations demonstrated this point

(See Figures 10, 11 and 12). For example, the calibration of QL2SMG for all outputs (DO, CBOD, and NH_3) enhanced the predictive capability over partial calibrations (NH_3 and CBOD only) as shown in Figure 13.

Finally, the order of calibration of output variables did not have any measurable effect on predictive capability. If the calibration of complex water quality models is an iterative process, as was the case in this study, the order of calibration has little meaning. However, if calibration and verification are kept independent, as is the traditional case, then the order of calibration may be important in certain cases.

An additional point was that calibration and a verification of a model was not the final test of model predictive capability. For example, both SNSIM and QL2SMG were calibrated and verified, yet QL2SMG possessed predictive capabilities that SNSIM lacked. This was due to the different style of modeling the algal processes in these two models. SNSIM modeled algae (p-r) and nitrogen (NBOD) as gross, unrelated processes. QL2SMG, on the other hand, modeled algae and nitrogen as a mechanistic nutrient-algal growth cycle. This cycle was complete with interdependencies between the processes. Although the QL2SMG nutrient-algal growth cycle was not a thorough representation of algae and nitrogen in the aquatic environment, the cycle did establish the important relationships between the natural processes. This allowed various model outputs to vary as the input environmental conditions changed. This mechanistic interrelationship between the processes in QL2SMG gave this model more predictive capability when compared with the gross modeling processes used in SNSIM. In summary, QL2SMG could be used to predict conditions that SNSIM could not.

This suggested that selection criteria may need to incorporate factors beyond a "simple" representation of all the processes important to the river basin. In this case, in order to ensure maximum predictive capability, the selection criteria should have included a requirement for a mechanistic representation of the important processes occurring in the river.

An important process can be considered as one which may change significantly over the range of conditions to be predicted. In this study, such mechanistic representations would have required a host of additional parameters to be measured or estimated. As shown in the sensitivity study, QL2SMG was extremely sensitive to many of these parameters (notably maximum growth rate, respiration rate, light extinction coefficient, and depth). Thus the selection requirement of mechanistic representations for processes like algae adds to the complexity of the modeling process.

DOSAG SUMMARY

CALIBRATION PHASE	<u>CALIBRATION</u>			<u>VERIFICATION</u>			
	7/21-22/80			8/17/80	8/23/80	12/3-4/80	
	DO	CBOD	NBOD	DO	DO	DO	BOD
phase 1							
phase 2							
phase 3a							
phase 3b							
phase 4a							
phase 4b							

CALIBRATION LEGEND

- Matches 95% or more of calibration data, Calibration criteria is met.
- Matches > 50% but < 95% of calibration data
- Matches < 50% of calibration data

VERIFICATION LEGEND

- Matches 60% or more of verification data, Verification criteria is met.
- Matches > 30% but < 60% of verification data.
- Matches < 30% of verification data.

DOSAG CALIBRATION/VERIFICATION SUMMARY

Figure 10

QUAL1E SUMMARY

CALIBRATION PHASE	<u>CALIBRATION</u>			<u>VERIFICATION</u>			
	7/21-22/80			8/17/80	9/23/80	12/3-4/80	
	<u>DO</u>	<u>CBOD</u>	<u>NBOD</u>	<u>DO</u>	<u>DO</u>	<u>DO</u>	<u>BOD</u>
phase 1							
phase 2							
phase 3a							
phase 3b							
phase 4a							
phase 4b							

CALIBRATION LEGEND

- Matches 95% or more of calibration data, Calibration criteria is met.
- Matches > 50% but < 95% of calibration data
- Matches < 50% of calibration data











































VERIFICATION LEGEND

- Matches 60% or more of verification data, Verification criteria is met.
- Matches > 30% but < 60% of verification data.
- Matches < 30% of verification data.


QUAL1E CALIBRATION/VERIFICATION


Figure 11


SNSIM SUMMARY

CALIBRATION PHASE	<u>CALIBRATION</u>			<u>VERIFICATION</u>			
	7/21-22/80			8/17/80	9/23/80	12/3-4/80	
	<u>DO</u>	<u>CBOD</u>	<u>NBOD</u>	<u>DO</u>	<u>DO</u>	<u>DO</u>	<u>BOD</u>
phase 1							
phase 2							
phase 3a							
phase 3b							
phase 4a							
phase 4b							


CALIBRATION LEGEND


 Matches 95% or more of calibration data, Calibration criteria is met.


 Matches > 50% but < 95% of calibration data

 Matches < 50% of calibration data

VERIFICATION LEGEND

 Matches 60% or more of verification data, Verification criteria is met.

 Matches > 30% but < 60% of verification data.

 Matches < 30% of verification data.

SNSIM CALIBRATION/VERIFICATION SUMMARY

Figure 12

QL2SMG SUMMARY

CALIBRATION PHASE	<u>CALIBRATION</u>			<u>VERIFICATION</u>			
	7/21-22/80			8/17/80	9/23/80	12/3-4/80	
	DO	CBOD	NBOD	DO	DO	DO	BOD
phase 1							
phase 2							
phase 3a							
phase 3b							
phase 4a							
phase 4b							

CALIBRATION LEGEND

Matches 95% or more of calibration data, Calibration criteria is met.

Matches > 50% but < 95% of calibration data

Matches < 50% of calibration data

VERIFICATION LEGEND

Matches 60% or more of verification data, Verification criteria is met.

Matches > 30% but < 60% of verification data.

Matches < 30% of verification data.

QL2SMG CALIBRATION/VERIFICATION SUMMARY

Figure 13

IX CONCLUSIONS

The following conclusions have been divided into the topical areas of selection, parameter estimation, and model calibration-verification technique.

MODEL SELECTION ISSUES

(1) Model documentation is an important precursor to the development of a specific water quality model, and can be a most significant issue.

(2) It is important to define model selection criteria such that all major physical, chemical, and biological processes active during the temporal and spatial regimes of interest are considered. It is possible, for example, that a specific stream process may not be significant during model calibration but become dominant in a verification attempt based upon a later stream survey. This problem was encountered in this model study with algal productivity becoming more significant in the verification surveys of August 17 and September 23 than in the July 21-22 calibration survey.

(2a) Model development should emphasize a selection phase which should precede the calibration-verification phase.

(2b) Model selection should not be based upon a single temporal or spatial survey of stream water quality.

(3) The selection of an applicable water quality model is enhanced by a careful mechanistic representation of stream processes. The model DOSAG, for example, could not be verified because it did not include sediment oxygen demand or photosynthetic oxygen production effects. QL2SMG which included these stream processes was verified and, therefore, had greater predictive accuracy.

PARAMETER ESTIMATION ISSUES

(4) It was not possible to calibrate and verify a water quality model in this study that contained lumped parameters. A lumped parameter was defined as one which jointly represented more than one stream process such as instream BOD and sediment oxygen demand.

(5) It was important to measure all major model parameters to establish measurement uncertainty.

(6) Water quality models based upon measured parameters are more readily verified and, hence, provide more predictive capability.

(7) The model calibration phase should serve to refine measured parameter estimates within their range of uncertainty and not be solely used to assess their magnitude.

(8) The state-of-the-art procedures used in this study for estimating stream deoxygenation, reaeration, and SOD were extremely useful in model calibration.

(9) The measurement of the parameters associated with nutrient interactions and algal productivity limited the extent to which these processes could be modeled and, therefore, limited the predictive capability of the resultant model.

(10) It was possible to calibrate and in certain cases verify the models SNSIM and QL2SMG with parameter values within the measured 95% confidence limits for the lower Ouachita.

(11) The use of textbook parameter values for stream deoxygenation, reaeration, and SOD did not result in calibrated models.

MODEL CALIBRATION-VERIFICATION ISSUES

(12) It is important to establish calibration and verification criteria in model development. The following were defined for this study:

(a) Model calibration was achieved when the model output predicted within the 95% confidence range of 95% or more of the variables' measured output values.

(b) Model verification was achieved when the model output predicted within the 95% confidence range of 60% or more of the variables' measured output values.

(13) It is important to calibrate and verify as many output variables as possible. DO, BOD, and a nitrogen species were examples used in this study.

(14) Model calibration and verification based upon only one variable such as DO did not result in verification for other variables. It was necessary to calibrate and verify based upon DO, BOD, and a nitrogen species. Predictive capability was enhanced when all three variables were verified simultaneously.

(15) The order of model calibration-verification was not important in this study. Those models calibrated in the order (1) DO, (2) DO and BOD, and (3) DO, BOD, and nitrogen species provided the same predictive capability as those calibrated in the reverse order (1) nitrogen species, (2) nitrogen species and BOD, and (3) nitrogen species, BOD, and DO.

(16) A procedure for model calibration is likely to be situation dependent. Sensitivity analysis is a useful approach to illustrate which measured parameters to refine.

(17) Sensitivity was observed to be situation and model dependent and a function of stream location, point source loads, temperature, and the magnitude of individual parameter values.

(18) The most sensitive parameters in the four models investigated were those which were often estimated through calibration and not measurement in past studies. SOD, reaeration, and algal productivity are three examples.

X. REFERENCES

1. "A Review of the Mathematical Water Quality Model DOSAG and Guidance for Its Use," NCASI Stream Improvement Bulletin No. 327, NY, NY, Oct., 1979.
2. "A Review of the Mathematical Water Quality QUALIE and Guidance for Its Use," NCASI Stream Improvement Bulletin No. 331, NY, NY, April, 1980.
3. "A Review of the Mathematical Model Qual-II and Guidance for Its Use," NCASI Stream Improvement Bulletin No. 338, NY, NY, Oct., 1980.
4. Braster, R.E., et al., "Documentation for SNSIM," US EPA, Region II, 26 Federal Plaza, NY, NY, March, 1978.
5. "Use of Mathematical Models in the Development of Area-wide 208 Plans," NCASI Stream Improvement Bulletin No. 326, NY, NY, Sept., 1979.
6. McKeown, J., et al., "Ultimate BOD Estimation in Receiving Water Quality Modeling," NCASI Central Lakes States Regional Meeting, Chicago, Ill., June, 1980.
7. "Interfacial Velocity Effects on the Measurement of SOD," NCASI Stream Improvement Bulletin No. 317, NY, NY, November, 1978.
8. "Further Studies of SOD and Its Measurement Variability," NCASI Stream Improvement Bulletin No. 321, NY, NY, March, 1979.
9. "Ouachita River Basin Water Quality Management Plan," by Hydrosience, Arlington, Tx. (Draft Final Report), Nov. 2, 1979.
10. Bryant, C.E., et al., "Water Quality Model of the Illinois River Basin," USGS, Little Rock, Arkansas, March, 1980.
11. "Upper Mississippi River 208 Grant Water Quality Modeling Study" Hydrosience, Inc. Jan., 1979.
12. O'Connor, D.J., "Water Quality Analysis of The Mohawk River Bridge Canal," NY State Dept. of Health, July, 1968.
13. Waddel, W.W., et al., "A Water Quality Model for the South Platte River Basin," Pacific Northwest Lab. Batelle, Richland, Wash., April, 1974.
14. O'Connor, D.J., "Verification Analysis of Lake Ontario and Rochester Embayment 3D Eutrophication Models," EPA-600/3-79-094, Aug. 1979.

The work described in this paper was not funded by the U.S. Environmental Protection Agency. The contents do not necessarily reflect the views of the Agency and no official endorsement should be inferred.

An Assessment of the Measurement Uncertainty in
the Estimation of Stream Reaeration Rate Coefficients
Using Direct Tracer Techniques

By: J.S. Hovis¹, R.C. Whittemore, PhD¹,
L.C. Brown, PhD², J.J. McKeown³

I. INTRODUCTION

All experimental measurements have an inherent uncertainty associated with the measurement technique. The purpose of this paper is to elucidate the major sources of error in the direct tracer methods of reaeration rate coefficient (k_2) measurement. The magnitude of several of the component errors² is estimated for direct tracer measurements by both the hydrocarbon and radiotracer methods. Examples from the literature and measurements made on the Ouachita River Basin by NCASI, Law Engineering Testing Co. of Marietta, Georgia, and the USGS are used. Estimates of total measurement error are made, and related to the component sources of error.

The utility and necessity of error quantification becomes clear when the role of k_2 in water quality management is examined. The reaeration rate is one of the most important parameters in the dissolved oxygen budget; it has a significant impact in most water quality management decisions, particularly waste load allocation.

Experimental measurements do not always advance the state of knowledge about the process under study. When the measurement error is greater than the bounds which could be placed on the quantity in question prior to the experiment, then the measurement may be of little use. For example, it is possible, particularly in low rate situations, to obtain a measured k_2 value that has greater error than would result from the use of an appropriate empirical equation. This situation will be demonstrated in this

-
1. Research Engineer, National Council of the Paper Industry for Air and Stream Improvement, Inc. (NCASI), Northeast Regional Center, Tufts University, Medford, Massachusetts 02155
 2. Professor, Department of Civil Engineering, Tufts University
 3. Regional Manager, NCASI, Northeast Regional Center

report. The impact of this finding is that the use of the direct tracer methodologies for k_2 measurement is probably not justified in some situations. Some guidelines for conducting direct tracer measurements such that measured rates will have sufficient precision to justify the expense of the measurements are given.

II. BACKGROUND, TRACER TECHNIQUES AND STATISTICS

It is assumed that the reader is familiar with the radiotracer and the hydrocarbon tracer techniques. As it is beyond the scope of this paper to review those techniques, the reader is directed to the work of Tsivoglou (1) and Tsivoglou, et al. (2) for a description of the radiotracer technique, and to the work of Rathbun, et al. (3, 4) for a description of the hydrocarbon technique. In addition, it is assumed that the reader will possess a general knowledge of statistical principles, particularly those related to error structure, experimental measurement uncertainty, precision, accuracy, and their contributions to total error. Reference to a general statistics text such as Mandel (5) should provide sufficient background.

One statistical concept that will be introduced in detail here is the concept of propagation of error. Serth, et al. (6) presented an excellent discussion of the propagation of experimental error through mathematical relationships. Random error, experimental precision, may be propagated through a generalized mathematical relationship using Equation 1.

$$f(A,B) \pm \sqrt{\left[\frac{\partial f[A,B]}{\partial x_1}\right]^2 a^2 + \left[\frac{\partial f[A,B]}{\partial x_2}\right]^2 b^2} \quad (\text{Eq. 1})$$

$A \pm a$ and $B \pm b$ are error bounds
for x_1 and x_2

Systematic error, experimental accuracy, may be propagated through a generalized mathematical relationship using Equation 2.

$$\text{sgn}[AB] ab \pm [a|B| + b|A|] \quad (\text{Eq. 2})$$

$\text{sgn}(AB)$ denotes the algebraic
sign of the product AB

The propagation of component random and systematic errors results in an assessment of total error.

The concept of error propagation is important to reaeration measurement for two reasons. First, the calculation of the reaeration rate from gas tracer data involves several mathematical relationships. In order to completely assess the measurement uncertainty of the technique, any experimental error, either random or systematic, must be properly propagated through these calculations. Second, it is important to recognize that mathematical water quality models are equations. In a mathematical water quality model with an analytical solution it is possible to apply Equations 1 and 2 to the entire set of parameters and thus determine the impact of parameter uncertainty on the water quality model output. Although such an exercise is beyond the scope of this paper, the recognition of the possibility of such a calculation will help one understand the significance of the results presented herein.

III. THE ERROR COMPONENTS OF REAERATION RATES AS MEASURED BY DIRECT TRACER METHODS

A. General Discussion

Contributions to the error of measured reaeration rates come from many parts of the measurement method. It is the purpose of this section to enumerate the various error sources in the two techniques. Then several examples quantifying some of these component errors are given. These component errors will be related to the overall measurement uncertainty examined later in this paper (Section IV.).

The total error of direct tracer reaeration is broken down into three separate areas for examination. First are errors generated by the selection of a particular protocol. Second are errors generated within the data analysis, particularly those related to the reaeration model which is fit to the data, and to the parameter estimation technique employed. Third are the random experimental errors inherent in any measurement methodology. Each of these areas is examined in detail below.

B. Protocol Selection Errors

Protocol selection errors are errors which are generated by the selection of a particular measurement protocol. These errors are related to the accuracy of the methodology. Among the accuracy questions which arise are those concerning sampling, the nature of the gas tracer, the nature of the conservative tracer, the hydraulics of the test site, the gas tracer to oxygen transfer ratio, and the temperature correction coefficient, θ .

The sampling methodology employed by both techniques is recognized not to be state-of-the-art dissolved gas sampling (1, 2, 3). It is possible with either technique to inaccurately represent the instream gas transfer through either improper tracer release or sampling location. Velten (7) demonstrated that even "proper" sample handling and shipping resulted in some loss of tracer gas in transit. Such a loss could affect the measured rate.

The nature of Kr-85 appears to make it an ideal gas tracer because it is inert and easily detected by liquid scintillation counting. Ethylene and propane are not ideal gas tracers. Abeles (8) has reviewed the biological activity of ethylene. Dissolved ethylene gas may be consumed by microorganisms. In addition Swimmerton and Lamontague (9) have measured very small natural concentrations of the hydrocarbon tracers in ocean waters.

Among the conservative tracers, tritiated water is an ideal dispersion tracer for water. It behaves identically to the water in which it is mixed. Rhodamine WT and other fluorescent dyes, however, are not ideal conservative tracers. Smart and Laidlaw (10) in their review of fluorescent dye tracers quantified many of the potential losses of such tracers in natural systems including photochemical decay, bleaching, pH effects, adsorption. An example of the effect of loss of conservative tracer on the measured reaeration coefficient is presented below.

The hydraulics of the test site enter the accuracy considerations from two perspectives. First, there is a concern over whether or not the path taken by the tracer slug is an accurate representation of the entire stream cross section. Second, there is the question of the accuracy of the hydraulic steady state. As will be explained in Section III. D., in low reaeration situations the tracer must be followed for quite a length of time in order to ensure a precise measurement. Over the time lengths in question (often multiple days), the accuracy of the hydraulic steady state could limit the measurement accuracy.

The accuracy of the ratio between the gas tracers and oxygen transfer rates is well established both experimentally and theoretically (1, 11, 12). However, it should be noted that no experimental measurements of this critical ratio have been made at low transfer rates (<1.0 , 1/day, base e).

The accuracy of the temperature correction coefficient, θ , has not been established. The multitude of values currently in use demonstrates this fact (13). Indeed, the values used in the two techniques are different; $\theta = 1.022$ for the radiotracer technique (1), $\theta = 1.024$ for the hydrocarbon technique (14).

Consider this example of the effect of protocol selection errors on reaeration rate measurement accuracy. The results of a hypothetical hydrocarbon tracer study are presented in Table 1. A single reach with three sampling stations, and triplicate determinations of the tracer materials for each station were assumed. The reaeration rate was calculated from these data using the two parameter log transformation model, with a linear least-squares parameter estimation scheme (discussed in Section III. C.). In addition to the original data, the reaeration rate was then recalculated from modified data representing a 10% and 20% loss of the conservative tracer relative to the original hypothetical data. This conservative tracer loss was calculated by assuming that the total loss had occurred by Station 3 (See Table 1). The conservative tracer data for Station 3 was reduced by the total percent dye loss. The conservative tracer data for Stations 1 and 2 were reduced by a fraction of the percent dye loss based on the relative time to the peak as compared to Station 3. The resulting calculated reaeration rates, with 95% confidence limits (95% C.L.) are presented in Table 2. The 95% confidence limits presented in this example reflect only the error associated with the linear regression of the log transformed data. Error sources in the calculation of k_2 from k_e (ethylene) were not considered. As can be seen from Table 2, non-conservative characteristics of the conservative tracer can seriously affect the accuracy of the reaeration rate calculation.

C. Parameter Estimation and Reaeration Model Errors

Errors associated with the reaeration model and parameter estimation raise some complex questions concerning the correct way to fit the models to experimental data. The details of these issues are beyond the scope of this paper, however references presented in the discussion below should provide ample detail for the interested reader.

There are many models for the desorption of the tracer gas with time (and hence the absorption of oxygen with time). All of the models used to estimate the reaeration rate are based on the basic form given by Camp (15) in Equation 3.

$$\frac{dC}{dt} = k (C_{\infty} - C) \quad (\text{Eq. 3})$$

k = transfer rate

t = time

C = concentration of gas at time, t

C_{∞} = concentration of gas at infinite time

The integrated form of Equation 3 is presented in Equation 4:

$$C_{\infty} - C = (C_{\infty} - C_0) e^{-kt} \quad (\text{Eq. 4})$$

C_0 = concentration of gas at zero time

A common, logarithmic transformation of Equation 4 is shown in Equation 5:

$$\ln (C_{\infty} - C) = \ln (C_{\infty} - C_0) - kt \quad (\text{Eq. 5})$$

TABLE 1

Hypothetical Hydrocarbon Tracer Study Data

<u>Station</u>	<u>Peak Concentration ($\mu\text{g/l}$)</u>		<u>Ratio Ethylene/Dye</u>	<u>ln Ratio</u>	<u>Time to Peak (days)</u>
	<u>Ethylene</u>	<u>Dye</u>			
1	50.4	12.7	3.97	1.379	0.125
	49.5	12.6	3.93	1.369	
	51.6	12.6	4.10	1.411	
2	26.7	9.5	2.81	1.033	0.194
	26.9	9.2	2.92	1.072	
	26.3	9.3	2.83	1.037	
3	17.5	7.6	2.30	0.833	0.292
	17.3	7.3	2.37	0.863	
	17.2	7.3	2.23	0.802	

TABLE 2

Calculated Reaeration Rates from Hypothetical
Hydrocarbon Tracer Study With Loss of
Conservative Tracer During the Study

<u>Amount of Conservative Tracer (Dye) Lost</u>	<u>Calculated Reaeration Rate with 95% C.L., n = 9 (1/day, 20C, base e)</u>
None (1)	3.7 ± 0.8
10% (2)	3.1 ± 0.9
20% (2)	2.8 ± 0.9

(1) Data as in Table 1

(2) % loss relative to data
in Table 1, lost over
0.292 days.

Equations 4 and 5 are the models most commonly used to fit gas tracer data. Gas transfer parameters may be obtained from the data using Equation 4 via either a two or three parameter non-linear regression. A two parameter, linear regression analysis is used to obtain gas transfer parameters when Equation 5 is applied. The two parameter methods have assumed values at C_{∞} .

Both the hydrocarbon and the radiotracer technique often employ Equation 5 and fit the data from two sampling stations (upstream and downstream) to obtain two parameters (C_0 and k) (1, 3). This is a trivial case of the linear regression fit using Equation 5. Because two data values are used to fit a two parameter model, there are no degrees of freedom left from which to estimate the error in the parameters.

Rathbun et al. (12) discussed three separate estimation methods for extensive hydrocarbon tracer data. Attempts were made to use two and three parameter non-linear estimations with Equation 4 as well as a two parameter linear estimation with Equation 5. Rathbun's final choice for the analysis of hydrocarbon tracer data was a two parameter non-linear regression with Equation 4. The three parameter model was rejected because C_{∞} could not be precisely estimated from the data. The linear, two parameter model was not used because the non-linear, two parameter model appeared to give a better fit of the data.

There is a process analogous to the direct tracer measurement of k_2 for which parameter estimation techniques have been carefully studied. This process is the unsteady-state, clean water test for wastewater treatment system oxygen transfer. Because both oxygen transfer and tracer gas transfer are governed by Equation 3, the parameter estimation problems are similar. Reference to the extensive literature on parameter estimation for the oxygen transfer test sheds some light on the proper method of parameter estimation in direct tracer measurements.

Boyle, et al. (16), Brown (17) and Stenstrom, et al. (18) extensively discuss the parameter estimation issues for the oxygen transfer test. Stenstrom et al. state that it is the opinion of all the investigators cited, and of the ASCE sub-committee on Oxygen Transfer Standards that the three parameter, non-linear estimation is the preferred method of analysis. If non-linear estimation is not possible, then a two parameter, linear estimation with an iterative estimation of C_{∞} should be used. This iterative C_{∞} estimate involves multiple applications of the linear regression analysis with various estimates of C_{∞} until a minimum residual sum of squares is found.

The discussions by Boyle et al. (16), Brown (17) and Stenstrom et al. (18) concerning the choice among the various

parameter estimation possibilities primarily focus on an analysis of the residuals from the regression. As observed by Rathbun (12), the non-linear techniques (both two and three parameter) resulted in lower and more uniformly distributed residuals for the analysis of direct tracer data. However, the two parameter technique is inappropriate unless an iterative procedure is used to estimate C_{∞} , the third parameter. Because of the expense and difficulty in applying a non-linear regression analysis, the linear regression of log transformed data has been recommended as the technique of choice for the two parameter estimation. The complications of an iterative, non-linear regression analysis do not seem justified.

It should be noted that neither of the direct tracer methods currently employ the recommended parameter estimation procedures. When the linear, two parameter estimation is used, C_{∞} is assumed rather than estimated by iterative methods. When non-linear programming is applied, only a two parameter estimate is supported by the data. The probable reason in both cases for the inability to estimate C_{∞} is insufficient data collection in the vicinity of equilibrium.

The issue of the data requirements for proper parameter estimation is an important one. Guidelines have been proposed to the ASCE concerning the proper protocol for data collection to allow the estimation of K_L via the clean water unsteady-state test. These guidelines are presented here because they are also believed to be applicable to the direct tracer measurement of k_2 .

The tracer experiment should be followed for a time period not less than $4/k_2$ (98% gas transfer). In that period there are three critical regions for parameter estimation, the areas near zero time, around $1/k_2$, and approaching infinite time. In order to ensure that each of these regions is appropriately represented it is recommended that a minimum of 10 data points be collected during each tracer study. Those data points should be distributed with two-thirds between zero and $2/k_2$, evenly spaced; and one-third between $2/k_2$ and $4/k_2$, evenly spaced. An experimental protocol for the direct tracer measurement which includes this amount of data would certainly enhance one's ability to estimate the reaeration rate.

On the practical side, tracking the tracers to $4/k_2$ may be problematic. For a k_2 of 0.1 (1/day, base e), the recommended guidelines require the experiment to be conducted for a time of 40 days. Such a time period for testing is clearly not possible. Dilution of the tracers by dispersion can severely attenuate their concentrations. There are practical restrictions on the amount of tracer which can be "instantaneously" released (as well as legal restrictions in the radiotracer case). It is generally wise to make the appropriate dilution/dispersion calculation

prior to the tracer release. An insufficient tracer release, or tracking of the tracers for less than the recommended length of time, will result in an increase in the error of the estimated k_2 .

The level of error associated with the improper application of the parameter estimation techniques is difficult to quantify. Much of the error hinges on the quantity and quality of the direct tracer data collected. In the oxygen transfer work, however, the error has been quantified, and has often been found to be substantial (16, 17).

D. Random Experimental Error

Random experimental error is an inherent part of any measurement procedure. The component errors associated with random experimental error all contribute to the precision of a measurement technique. Often one or more of these errors will limit the applicability of a measurement technique due to the error's magnitude.

Random experimental errors enter the uncertainty calculations for reaeration measurements from several sources. Each of the analytical methods (liquid scintillation counting, gas chromatography, fluorometry) has an inherent measurement precision. Cohen, et al. (19) presented data from which the liquid scintillation counting precision has been ascertained. In the range of values commonly encountered in the radiotracer technique, the liquid scintillation counting has a precision of $\pm 1\%$ to $\pm 4\%$ per channel. Shultz, et al. (20) analyzed data from the gas chromatographic procedure used in the hydrocarbon technique to determine its precision. Schultz found that the gas chromatography technique had a coefficient of variation in the range of $\pm 1.3\%$ to $\pm 6.9\%$ of the measured tracer gas concentration.

The precision of several of the constants used in the calculation of k_2 from the tracer rate coefficient has been presented in the literature. Tsivoglou (1, 2) found the ratio between the krypton-85 transfer rate (k_{Kr}) and k_2 to be 0.83 ± 0.04 (s.d.). Rathbun, et al. (12) presented the precision of the ratio between the ethylene transfer rate (k_e) and k_2 , and the ratio between the propane transfer rate (k_p) and k_2 . $k_e : k_2$ was found to have a precision of 1.15 ± 0.025 (95% C.L.); $k_p : k_2$ was found to have a precision of 1.39 ± 0.028 (95% C.L.). Tsivoglou (1) also presented the precision of the temperature correction coefficient θ as 1.022 ± 0.004 (s.d.). Because there are many values for this coefficient presented in the literature, their precision may be of little consequence relative to the question of the accuracy of θ . In order to demonstrate how these various experimental precisions can limit the applicability of a measurement procedure, an example calculation using the radiotracer method is presented below.

As mentioned before, the liquid scintillation counting technique has a precision in the range of +1 to +4% (95% C.L.) for each counting channel (see Cohen, et al., 19). Applying the random error propagation formula, Equation 1, to the calculation method presented in Cohen et al. (19), this precision translates to a precision of about +7% (95% C.L.) in the precision of the krypton (Kr) to tritium (T) ratio at each sampling station. This results in a precision of +9% (95% C.L.) in the ratio between the Kr : T at the downstream sampling point and the Kr : T at the upstream sampling point. k_{Kr} is then calculated from the sampling point ratios via a regression analysis. However, because the model, Equation 3, is exponential, the precision from upstream to downstream does not directly translate to the precision of k_{Kr} . The precision of k_{Kr} is dependent on the magnitude of the ratio between (Kr : T) downstream and (Kr : T) upstream. This effect is demonstrated in Table 3.

Table 3 Theoretical Precision of k_{Kr}

<u>Kr : T downstream</u> <u>Kr : T upstream</u>	<u>% of Tracer Gas</u> <u>Lost</u>	<u>Precision of</u> <u>k_{Kr}</u>
0.1	90%	+ 4%
0.5	50%	+13%
0.9	10%	+90%

Since the ratio between the downstream and upstream (Kr : T) is directly related to the amount of tracer gas lost from the stream during the study, then the precision of k_{Kr} is also related to the amount of tracer gas lost. The amount of tracer gas lost from the stream is dependent on two things, the magnitude of k_{Kr} and the length of time between the upstream and downstream sampling points. Because k_{Kr} is related to k_2 via a constant of known precision (0.83 ± 0.04 , 95% C.L.), it is possible, from the theoretical precision of k_{Kr} , to determine the length of time a Kr-85 tracer study must be followed in order to achieve a desired precision, given an approximate knowledge of the oxygen transfer coefficient. Some results of this calculation are presented in Table 4 (21). Ultimately, the precision of the Kr-85 technique is limited by ones ability to follow the dye tracer to detect the tracer slug, and by the precision of the $0.83 k_{Kr} : k_2$ ratio.

Table 4 Length of Time a Kr-85 Tracer Study
Must Be Followed to Achieve a Desired
Precision Based on Theoretical Considerations

<u>Approximate k_2 to Be Measured (1/day, base e)</u>	<u>Time Necessary to Achieve Precision \pm 50%</u>	<u>Time Necessary to Achieve Precision \pm 10%</u>
1.0	3.9 hours	22. hours
0.5	7.8 hours	1.8 days
0.1	1.6 days	9.2 days
0.05	3.2 days	18. days

IV. ESTIMATION OF UNCERTAINTY IN ACTUAL TRACER MEASUREMENTS

A. General Discussion

The preceeding review of the error components of the direct tracer measurement of reaeration rates has raised some important questions concerning measurement uncertainty. Because of the questions which have been raised, an assessment of the measurement uncertainty of the entire direct tracer measurement process is warranted. To accomplish this assessment, tracer studies described in the literature as well as studies conducted on the Ouachita River Basin in Arkansas and Louisiana by NCASI, Law Engineering and the USGS will be reviewed.

There are several ways to assess the uncertainty of a measurement technique. If replicate measurements are available (preferably three or more) for controlled experimental conditions, then an examination of the variability among the replicates can lead to an understanding of the precision of the measurement. In order to isolate the sources of the random error, it is important to know all the conditions of the experiment, as well as how well they were controlled. Control of experimental conditions is particularly difficult in environmental measurements. Nevertheless, an estimate of the experimental precision of both the radiotracer and the hydrocarbon techniques at moderate to high transfer rates ($k_2 > 1.0$, 1/day, base e) can be made from published replication experiments. This analysis is presented in Section IV. B.

A second method of evaluating the uncertainty of a measurement technique is to start with the raw data and conduct the entire parameter estimation procedure, statistically analyzing the confidence limits during each calculation step. This procedure was followed for data collected from three radiotracer studies conducted by NCASI and Law Engineering on the Ouachita River Basin, as well as for one hydrocarbon study conducted by the USGS in the same basin. These studies involved reaeration rates in the range of 0.02 - 1.0 (1/day, base e). The results of the measurement uncertainty for these studies based in parameter estimation statistics and error propagation through the calculations are presented in Section IV. C.

The evaluation of the measurement uncertainty of the direct tracer methods from the literature and the Ouachita River Basin studies is primarily an analysis of precision. The accuracy of the direct tracer methods is more difficult to assess because the techniques represent the current state-of-the-art in k_2 measurement. Currently, by definition, they are accurate. This is not to say that there is no bias in the direct tracer measurement techniques. The sources of bias enumerated in Section III. B. illustrate that measurement bias should be a concern when these techniques are used. However, without a standard for comparison, the quantification of the accuracy of these techniques is not possible.

B. Replication Studies From the Literature

A major replication study was conducted early in the testing of the radiotracer technique on the Jackson River near Covington, Virginia (1). In that study a k_2 of the magnitude of 1.5 (1/day, base e) was measured for 14 subreaches from seven tracer releases spread out over 14 days. Between two and three replicate determinations were made for each subreach. During the course of the study, the hydraulic stability of the stream was rather good; the flow varied $\pm 10\%$ over the 14 days. Among the 14 sets of replicate determinations the coefficient of variation for the replicates ranged from $\pm 1.0\%$ to $\pm 25.8\%$. The mean coefficient of variation was $\pm 11.9\%$. It should be noted that these coefficients of variation represent uncertainty in both the measured value and in the hydraulic stability of the stream segment during the replication study.

There is limited data available for the assessment of uncertainty in the hydrocarbon technique literature. However, one study designed to compare the hydrocarbon technique and the radiotracer technique does provide some replicate information (14). This study was conducted on two small streams in Wisconsin. In each stream a double gas tracer dump (ethylene and propane) was made and the reaeration rate was computed via two different parameter estimation methods for each of the tracer gases. This

gave a total of four possible replicate k_2 determinations for each reach. A total of four reaches were studied. It should be noted that because the replicate determinations for each reach were calculated from a single tracer release the question of hydraulic stability is not as serious in this study as it was in the Jackson River study previously discussed. The coefficient of variation among the three or four replicates for each reach ranged from $\pm 4.3\%$ to $\pm 13.8\%$; the average coefficient of variation was about $+7.5\%$. The magnitude of k_2 measured in this study was about 7.5 (1/day, base e). The variability calculated from this hydrocarbon work can be attributed to random experimental error and the variability introduced by the two different parameter estimation techniques.

C. Ouachita River Basin Studies

Replication of direct tracer studies in order to determine the measurement uncertainty is rarely possible because of the cost of such studies. Reaeration rate uncertainty estimates must often be based on a single tracer study. Fortunately, statistical methods may be applied to the regression analyses used to estimate the gas transfer rate from direct tracer data allowing one to estimate the confidence range of estimated parameters. The uncertainty thus calculated may then be propagated through the calculation necessary to compute k_2 , giving an estimate of the error in k_2 . Such calculations have been made in radiotracer data collected by NCASI and Law Engineering and on hydrocarbon data collected by the USGS, on the Ouachita River Basin in the summer of 1980. All data were analyzed using the two parameter, linear regression model based on Equation 5. The results of this uncertainty analysis are discussed below.

As part of NCASI's MWQM program, three radiotracer studies were conducted in the Ouachita River Basin by NCASI and Law Engineering (21). The reaeration coefficients for a total of seven stream reaches were estimated from these tracer studies. Figure 1 presents an example of the data collected with the results of the linear, log transformation parameter estimates. The 95% confidence limits from the parameter estimation statistics for each of the seven reaeration coefficients were propagated through the conversion calculations from k_{Kr} (T, 1/day) to K_2 (20C, 1/day) (via the ratio = 0.83 ± 0.04 and $\theta = 1.022 \pm 0.01$). Table 5 presents the estimated reaeration coefficients for the Ouachita River Basin studies with their confidence limits. Also presented in Table 5 is the theoretical precision of the measured k_2 based on the propagation of the random error associated with liquid scintillation counting. A discussion of these theoretical calculations may be found in Section III. D. A comparison of the 95% confidence limits (95% C.L.) with the theoretical precision calculations implied that the precision of the liquid scintillation counting technique was a major component of the measurement uncertainty of

the reaeration coefficients estimated in this study. It also appears that the two reaeration coefficient measurements with low gas loss ($0.02 \pm 1000\%$ and $0.13 \pm 800\%$, 1/day, base e, 95% C.L.) are of limited utility because of the magnitude of their uncertainty. The five tracer measurements with greater than 25% gas loss all display acceptable error.

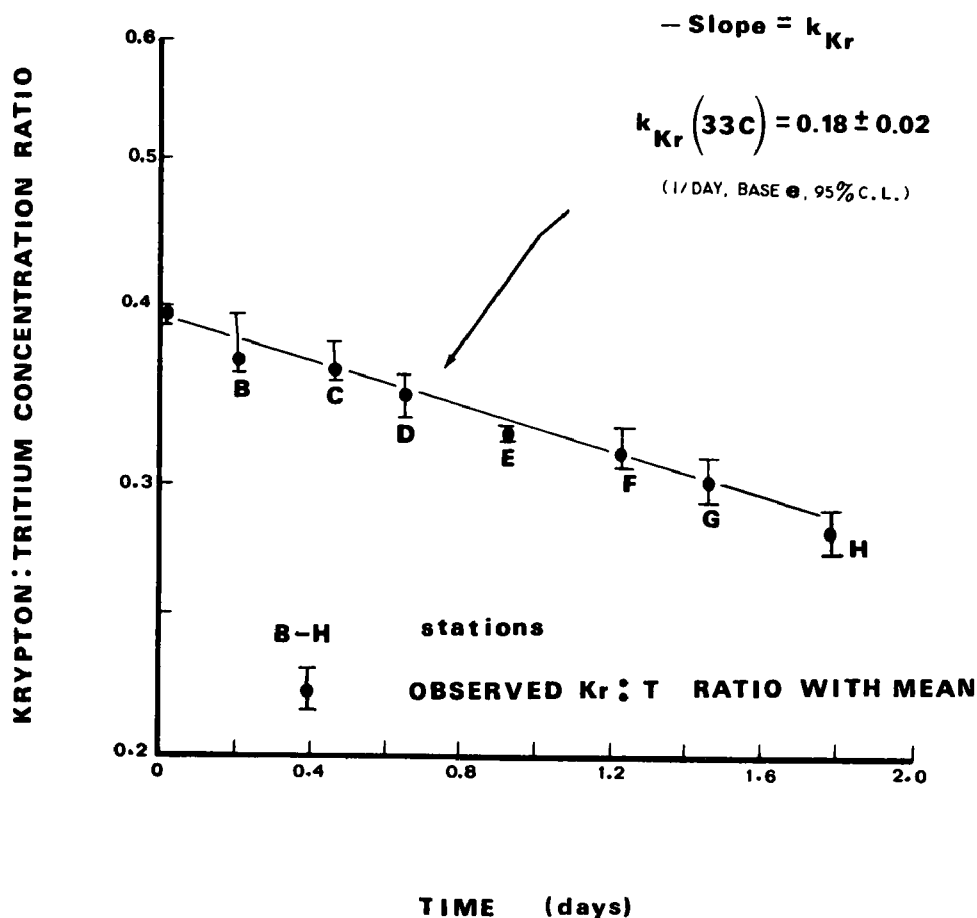


FIGURE 1

Table 5 Uncertainty of Reaeration Coefficient, k_2 , as Measured by
The Radiotracer Technique, and Comparison With Theoretical
Precision of The Radiotracer Technique Based on Gas Loss

Study Area	Measured k_2 , 20C (1/day, base e)	95% Confidence Range of k_2 (as a % of k_2)	% Tracer Gas Lost During Study	Theoretical Precision of k_2 Based on Tracer Gas Loss (as a % of k_2)(1)
OUACHITA RIVER Northeastern La.	0.02	$\pm 1000\%$ ⁽²⁾	4	$\pm 200\%$
TRIBUTARY	0.13	$\pm 800\%$	2.8	$\pm 300\%$
OUACHITA RIVER Southeastern Ark.	0.17	$\pm 18\%$	29	$\pm 27\%$
TRIBUTARY	0.34 to 0.37	$\pm 14\%$	28 to 30	$\pm 30\%$ to $\pm 25\%$
TRIBUTARY	0.91 to 1.06	$\pm 6\%$	54 to 89	$\pm 12\%$ to $\pm 4\%$

(1) See explanation in Section III. D.

(2) Technique may have had interference due to partial withdrawal of tracer material by power plant intake.

At the same time that NCASI and Law Engineering conducted the radiotracer study on the Ouachita River in Southeastern Arkansas, the USGS also conducted a hydrocarbon study on the same river reach. NCASI has attempted to quantify the uncertainty of this hydrocarbon measurement at the low transfer rate, and to compare the radiotracer and the hydrocarbon measurements of the reaeration coefficients for that river reach (22). Unfortunately, sampling problems and limited data collection severely restricted the information available to estimate the hydrocarbon transfer rate. The final value for k_2 , 20C computed by NCASI using several assumptions about the data was 0.44 ± 0.98 (1/day, base e, 95% C.L.). The error from this calculation did not compare favorably with the radiotracer error (0.17 ± 0.03 , 1/day, base e, 95% C.L.).

The primary reason for the discrepancy in error between the two techniques was probably the sampling and data collection differences. The radiotracer reaeration coefficient estimate was based on 24 data points distributed over 8 sampling locations. The hydrocarbon reaeration coefficient estimate was based on three data points from three sampling locations, one of which was highly suspect. This comparison between the two levels of sampling and data collection clearly illustrates the importance of the quantity and quality of data in reaeration coefficient parameter estimation (see Section III. C.). The eight sampling station data collection scheme (radiotracer work) with triplicate determinations at each station (24 data points) resulted in an estimate of k_2 to $\pm 18\%$ (95% C.L.). The three sampling station data (hydrocarbon work) with one highly suspect data point (3 data points) resulted in an estimate of k_2 to $\pm 230\%$ (95% C.L.).

V. SUMMARY

The quantification of the uncertainty of direct tracer measurements of reaeration coefficients is important for several reasons. Reaeration rates play an important role in dissolved oxygen budget calculations used in water quality management decisions. Because of the cost of direct tracer measurements, a cost/benefit analysis comparing the expected knowledge to be gained from the tracer study to the tracer study cost is usually in order.

The error components in the direct tracer measurements fall into three broad classes.

- 1) Protocol selection errors (accuracy considerations) include sampling methodology and location, the nature of the gas conservative tracers, the accuracy of θ and the tracer gas to oxygen transfer ratios, and consideration of the hydraulic state of the testing site.
- 2) Parameter estimation and reaeration model errors involve both the estimation technique and the data requirements. The preferred estimation technique is a three parameter, non-linear regression estimation k , C and C_{∞} . A second estimation method is a two parameter, linear estimation on log transformed data, where C and k are fit directly and C_{∞} is iteratively estimated. The data requirements for these estimations procedures is a minimum of 10 data points, two-thirds evenly spaced between 0 and $2/k_2$, one-third evenly spaced between $2/k_2$ and $4/k_2$.
- 3) Random experimental errors (precision considerations) include the precision of the analytical methodologies (liquid scintillation counting, gas chromatography, fluorometry), the precision of the transfer rate ratios and the precision of θ .

The significance of the propagation of random error through the reaeration coefficient calculation was demonstrated via an analysis of the effect of the amount of tracer gas lost on the reaeration coefficient's theoretical precision. In addition, theoretical calculations showing the length of time a radiotracer study must be followed in order to achieve a desired precision in the measured rate were presented.

Actual direct tracer reaeration measurements were analyzed for uncertainty. Errors in the radiotracer technique measurements ranged from $\pm 1.0\%$ to $\pm 1000\%$ (the former from replication studies at a moderate rate, the latter from a single low rate measurement on the Ouachita River). Errors in the hydrocarbon technique

measurements ranged from +4.3% to +230% (the former from the Wisconsin replication study, the latter from a single measurement on the Ouachita River). The relationship between the amount of tracer gas lost and the measurement uncertainty of the Ouachita River Basin radiotracer measurements was found to parallel the theoretical precision calculations.

The large uncertainty associated with several of the direct tracer measurements has raised serious questions about the utility of these measurements in low transfer environments. The uncertainty of the hydrocarbon tracer measurement from poor and insufficient sampling and of the radiotracer measurement from the inherent analytical precision demonstrates the need to calculate potential errors prior to conducting such studies. If it is impossible to improve the experimental protocol to reduce these errors to an acceptable range, then consideration should be given to not conducting the studies. In such situations empirical equations may produce reaeration coefficient estimates having comparable precision to those from the direct tracer measurements.

VI. REFERENCES

1. Tsivoglou, E.C., "Tracer Measurements of Stream Reaeration," FWPCA, Dept. of the Interior, Washington, D.C. (1967).
2. Tsivoglou, E.C., Cohen, J.B., Shaerer, S.D., and Godsil, P.J., "Tracer Measurements of Atmospheric Reaeration. II. Field Studies," JWPCF 40:285 (1968).
3. Rathbun, R.E., Shultz, D.J., and Stephens, D.W. "Preliminary Experiments With a Modified Tracer Technique for Measuring Stream Reaeration Coefficients," USGS Open File Report 75-256, Bay St. Louis, Miss. (1975).
4. Rathbun, R.E., Shultz, D.J., Stephens, D.W., and Tai, D.Y. "Experimental Modeling of the Oxygen Absorption Characteristics of Streams and Rivers," International Association for Hydraulic Research, 17th Congress, 1:A61 (1977).
5. Mandel, J., The Statistical Analysis of Experimental Data, Interscience Publishers, New York, N.Y. (1964).
6. Serth, R.W., Hughes, T.W., Opferkuch, R.E., and Eimutis, E.C. "Analysis of Uncertainty - Principles and Applications," USEPA - 600/2-78-004U (1978).
7. Velton, R.J., "Laboratory Procedures," Symposium on Direct Tracer Measurement of the Reaeration Capacity of Streams and Estuaries, Water Pollution Control Research Series, #16050, USEPA (1972).
8. Abeles, F.B., Ethylene in Plant Biology, Academic Press, New York, N.Y. : 302 (1973).

9. Swinnerton, J.W. and Lamoutague, R.A., "Oceanic Distribution of Low-molecular-weight Hydrocarbons; Baseline Measurements, EST 8,7:657 (1974).
10. Smart, P.L., and Laidlaw, I.M.S., "An Evaluation of Some Fluorescent Dyes for Water Tracing," Water Resources Research 13,1:15 (1977).
11. Tsivoglou, E.C., O'Connell, R.L., Walter, C.N., Godsil, P.J. and Logsdon, G.S., "Tracer Measurements of Atmospheric Reaeration - I. Laboratory Studies," JWPCF 37,10:1343 (1965).
12. Rathbun, R.E., Stephens, D.W., Shultz, D.J., and Tai, D.Y., "Laboratory Studies of Gas Tracers for Reaeration," JEED, ASCE 104,EE2:215 (1978).
13. Zison, S.W., Mills, W.B., Deimer, D., and Chou, C.W., "Rates, Constants, and Kinetic Formulations in Surface Water Quality Modeling," USEPA - 600/3-78-105 (1978).
14. Rathbun, R.E. and Grant, R.S., "Comparison of the Radiotracer and Modified Techniques for Measurement of Stream Reaeration Coefficients," USGS Water-Resources Investigations 78-68 (1978).
15. Camp, T.R., Water and Its Impurities, 4th Printing, Reinhold Publishing Co., New York, N.Y. (1968).
16. Boyle, W.C., Berthouex, P.M. and Rooney, T.C. "Pitfalls in Parameter Estimation for Oxygen Transfer Data," JEED, ASCE 100,EE2:391 (1974).
17. Brown, L.C., "Oxygen Transfer Parameter Estimation," Proceedings, Workshop Toward an Oxygen Transfer Standard, USEPA - 600/9-78-021 (1979).
18. Stenstrom, M.K., Brown, L.C., and Hwang, H.J., "Oxygen Transfer Parameter Estimation," JEED, ASCE 107,EE2, : 379 (1981).
19. Cohen, J.B., Setsen, J.L., Kelley, W.D., and Shearer, S.D., Jr. "Determination of ^3H and ^{85}Kr in Aqueous Samples by Liquid Scintillation Techniques," Talanta 15:233 (1968).
20. Schultz, D.J., Pankow, J.F., Tai, D.Y., Stephens, D.W., and Rathbun, R.E. "Determination, Storage, and Preservation of Low Molecular Weight Hydrocarbon Gases in Aqueous Solution," Jour. Research U.S. Geol. Survey 4,2:247 (1976).
21. Whittemore, R.C. and Hovis, J.S., "A Review of Reaeration Capacity Estimation and Its Measurement Uncertainty," NCASI Technical Bulletin, New York, N.Y. (pending, 1982).
22. Whittemore, R.C. and Hovis, J.S., "A Comparison of Reaeration Estimation Techniques for the Ouachita River Basin," NCASI Technical Bulletin, New York, N.Y. (pending, 1982).

The work described in this paper was not funded by the U.S. Environmental Protection Agency. The contents do not necessarily reflect the views of the Agency and no official endorsement should be inferred.

CALIBRATION OF HYDROLOGY AND SEDIMENT TRANSPORT ON SMALL AGRICULTURAL WATERSHEDS USING HSPF

By
David E. Schafer¹
David A. Woodruff¹
Richard J. Hughto²
G. K. Young³

INTRODUCTION

The ability to accurately predict the hydrologic response and sediment movement on agricultural watersheds through mathematical simulation modeling can play an active role in the development of sound agricultural management practices. Specifically, it provides the agricultural scientist with a valuable yet inexpensive means to assess non-point source runoff potential and its resulting sediment transport capacity. Coupling this with knowledge pertaining to the physio-chemical characteristics and transport mechanisms associated with agricultural chemicals provides a basis for evaluating receiving water quality impacts.

This paper discusses the capabilities of the Environmental Protection Agency's Hydrologic Simulation Program-Fortran (HSPF) for modeling runoff and sediment transport on three small agricultural watersheds: Mississippi 802; Oklahoma C-4, and; Oklahoma C-5. Following a brief description of each a general calibration methodology is outlined and simulation results are presented. Direct comparisons of hydrologic and sediment simulation results are made utilizing monthly and annual totals, double mass analyses, monthly standard deviations and coefficients of variation. Finally, relationships among physically based parameter value estimates are investigated.

WATERSHED DESCRIPTIONS

Watershed 802, located in the Mississippi Delta Region, covers 15.5 ha., and is comprised of a Sharkey Silty Clay. The land has been mechanically formed to a slope of 0.2 percent and planted with one meter row spacing. The drainage pattern, designed to direct runoff via turn-rows or shallow V-ditches, has been equipped with instrumentation for flow monitoring and sampling. During the 1974 and 1975 calibration period, cotton was the sole crop grown and harvested.

¹Water Resources Engineer, Camp, Dresser & McKee, Inc., Boston, MA

²Senior Water Resources Engineer, Camp, Dresser & McKee, Inc., Boston, MA

³President, GKY & Associates, Inc., Springfield, VA

Oklahoma Watersheds C-4 and C-5 are representative of cropland of the Central Great Plains. C-4 is 12.1 ha. in size and has also been planted with cotton. C-5, situated approximately one kilometer from C-4, covers an area of 5.2 ha., and has been continuously planted with winter wheat. Man-made ridges form the watershed boundaries and each has been graded and smoothed to a slope of 0.3 percent. Soil types are similar and are characteristic of those found in alluvial bottom land deposits of clay and silt loams. The two-year calibration period selected for these watersheds extends from January, 1973, through December, 1974.

Annual tillage operations performed on each watershed are considered typical with respect to crop type and location. For Watershed 802 these included shredding cotton stalks after harvest, disking and forming rows in late winter or early spring, followed by herbicide application, planting, cultivation, and application of pesticides during the growing season. In addition to the above, the cotton crop on C-4 was irrigated during the 1974 cropping season. On C-5, dryland wheat cultivational practices included disk harrowing in the summer, followed by planting in early winter and harvest in late spring.

Field Data

Climatological data, used as the driving force for model simulation, consisted of 15 minute precipitation volumes and daily evapotranspiration measurements. The rainfall data for Watershed C-4 were adjusted to include irrigation applications on appropriate dates. Model calibration data consisted of monthly total runoff volumes and sediment mass.

Annual precipitation totals for the calibration periods were 1732 mm and 1467 mm for Watershed 802 and 1023 mm and 714 mm for Watersheds C-4 and C-5. Compared with 30 year average annual values, Watershed 802 received 38% and 17% above normal rainfall; Watersheds C-4 and C-5 received 28% above normal rainfall in 1973 followed by 10% below normal rainfall in 1974. This is of particular interest with respect to the calibration of Watershed 802, since, significant deviations from average annual conditions during both hydrologic and sediment calibration can have significant impact, should the model be used for prediction. There is a general need, therefore, to verify the calibration variables using precipitation data that approach average conditions over the simulation period prior to utilization of calibrated parameter values in a predictive mode.

CALIBRATION PROCEDURE

Hydrologic and sediment simulation was conducted utilizing the PWATER and SEDMNT sections of the PERLND module of HSPF. The PWATER algorithms in HSPF are designed to continuously simulate the hydrologic processes occurring on a watershed. For the purposes of this calibration, the major component of interest is total overland flow. The SEDMNT algorithms in HSPF simulate the production and removal of detached fines. Since sediment simulation is

dependent upon the results of the hydrology simulation, model calibration was carried out in two stages, which involved calibration of PWATER parameters followed by the SEDMNT parameter calibration on each watershed.

For each stage of the calibration, an eight-step procedure was followed:

1. Identify and compile appropriate watershed and field measurement data;
2. Determine appropriate target values and time scales for calibration based on available field data;
3. Select initial values of section module parameters based on reported watershed characteristics;
4. Identify good results from previously calibrated modules;
5. Make an initial simulation run based on selected parameter values, compare model output to field measurements, and establish a base-case;
6. Identify the set of primary calibration variables;
7. Make a series of model simulations adjusting, as appropriate, the primary calibration parameter values from the base-case to minimize the error between simulated results and measured data, and;
8. Interpret the results of final calibration and sensitivity analyses to facilitate model verification and application.

Hydrologic Calibration

Initial estimates for values of the PWATER parameters for each site were developed from a review of available field data, the HSPF User's Manual (1), guidelines provided in the ARM User's Manual (2), previous algorithm calibration experience (3) and several site related publications (4,5,6,7,8,9,10,11). A preliminary screening of measured monthly precipitation and runoff data revealed that the hydrologic response of each watershed can be reasonably described on a monthly basis, however, no discernable trends were apparent from the data with respect to the annual cropping cycle.

Calibrated parameter estimates for the PWATER module are listed in Table 1. Simulation results for each watershed are presented graphically in Figures 1, 2, and 3. As shown by the dashed lines in the double mass analysis plots, overall model performance for the PWATER module was good in each case. Early periods of undersimulation resulted in underestimation of the period of record totals, however, monthly values generally follow a linear trend with a slope parallel to the line of one to one correspondence of measured versus simulated

TALBE 1

SUMMARY OF CALIBRATED PWATER PARAMETER ESTIMATES

<u>Parameter</u>	<u>802</u>		<u>C-4</u>		<u>C-5</u>	
NBLKS	1		1		1	
LZSN	2.0		2.5		2.5	
INFILT	0.005		0.15		0.15	
LSUR	500		650		300	
SLSUR	0.002		0.003		0.003	
KVARY	0	**	0	**	0	**
AGWRC	1.0	**	1.0	**	1.0	**
FOREST	0	**	0	**	0	**
PETMIN	35	**	35	**	35	**
PETMAX	40	**	40	**	40	**
INFEXP	2.0		2.0		2.0	
INFILD	1.0		2.0		2.0	
DEEPFR	1.0	**	1.0	**	1.0	**
BASETP	0	**	0	**	0	**
AGWETP	0	**	0	**	0	**
INTFW	0.7		0.6		0.6	
IRC	0.01		0.01		0.01	
CEPS	0.001	*	0.001	*	0.001	*
SURS	0.001	*	0.001	*	0.001	*
UZS	0.15		0.3		0.20	
IFWS	0.001	*	0.001	*	0.001	*
LZS	2.0		3.0		3.0	
AGWS	0.001	**	0.001	**	0.001	**
GWVS	0.001	**	0.001	**	0.001	**
UZSN	0.05-0.30		0.05-0.30		0.15-0.40	
CEPSC	0.05-0.25		0.10-0.25		0.10-0.20	
NSUR	0.20		0.15-0.25		0.15-0.20	
LZETP	0.05-0.40		0.10-0.25		0.10-0.20	

* Model default values required for program execution.

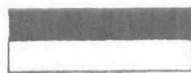
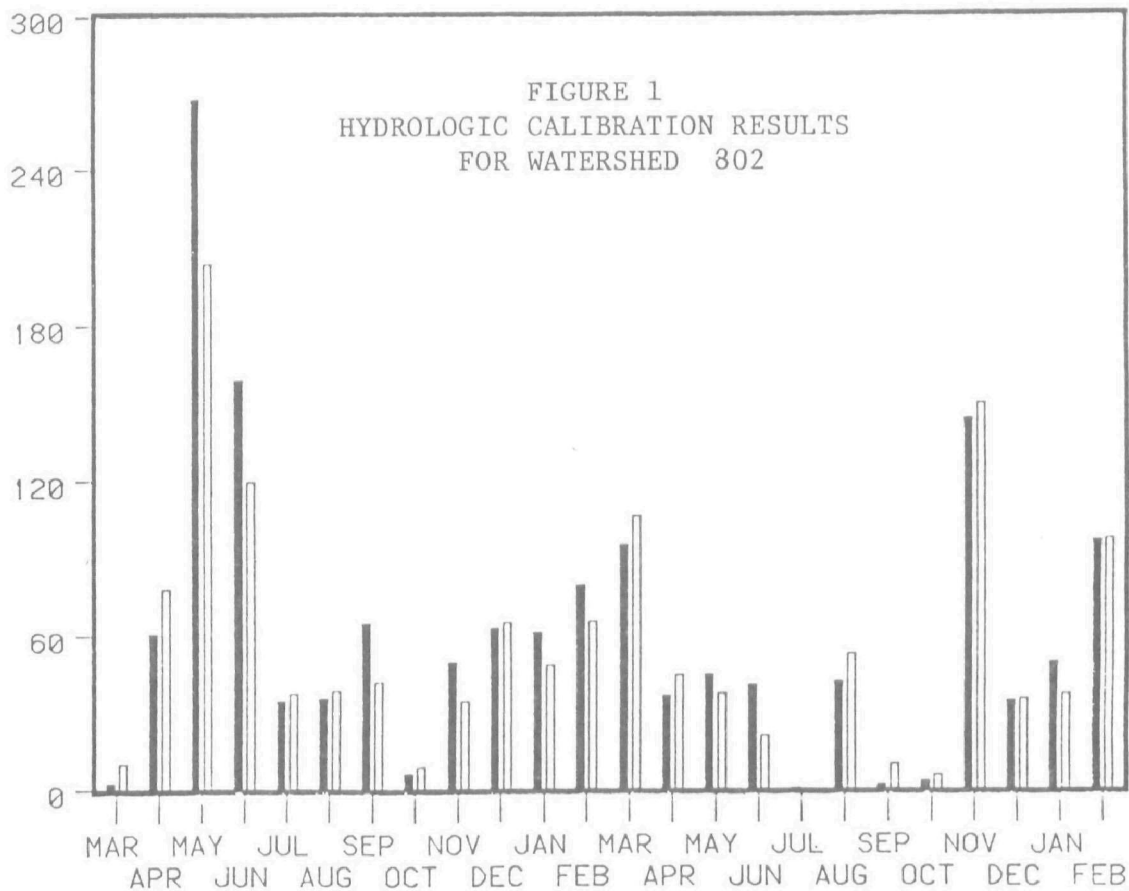
** Model-default values required for program execution but not applicable to the Oklahoma Watershed application of HSPF.

R
U
N
O
F
F

I
N

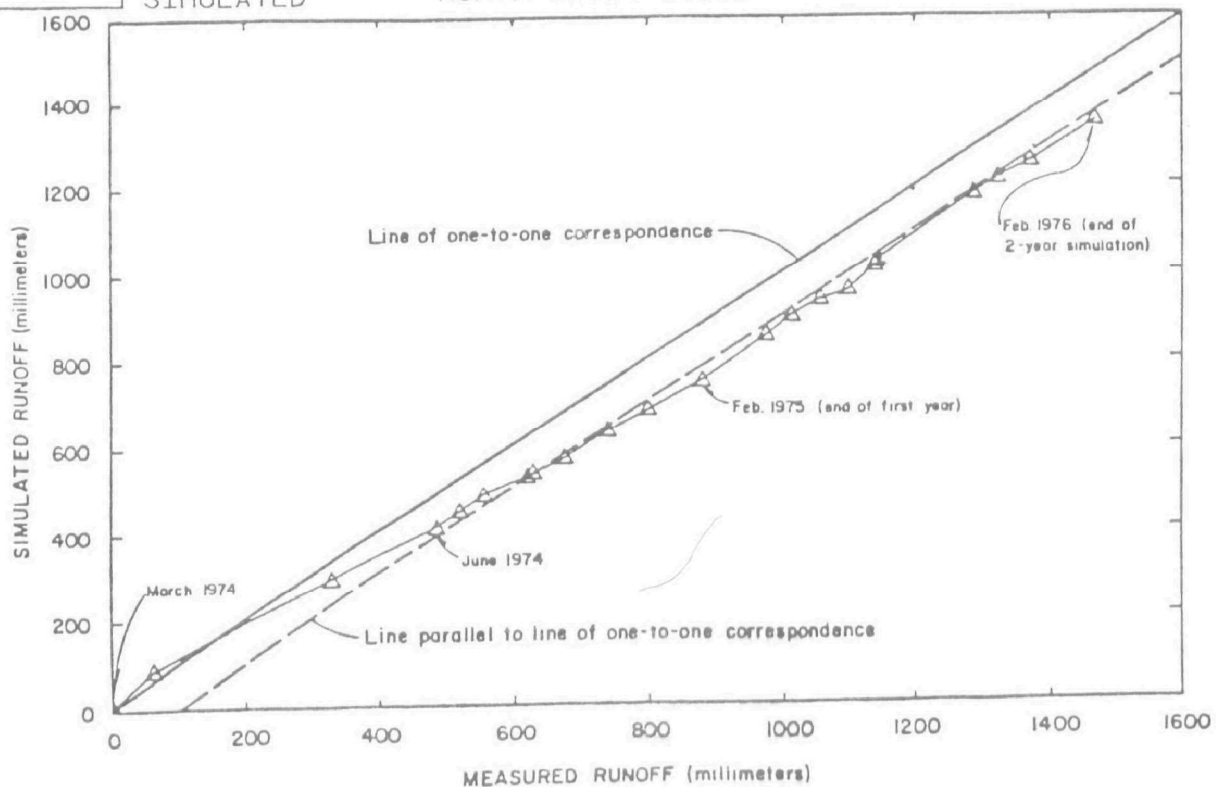
M
M

FIGURE 1
HYDROLOGIC CALIBRATION RESULTS
FOR WATERSHED 302



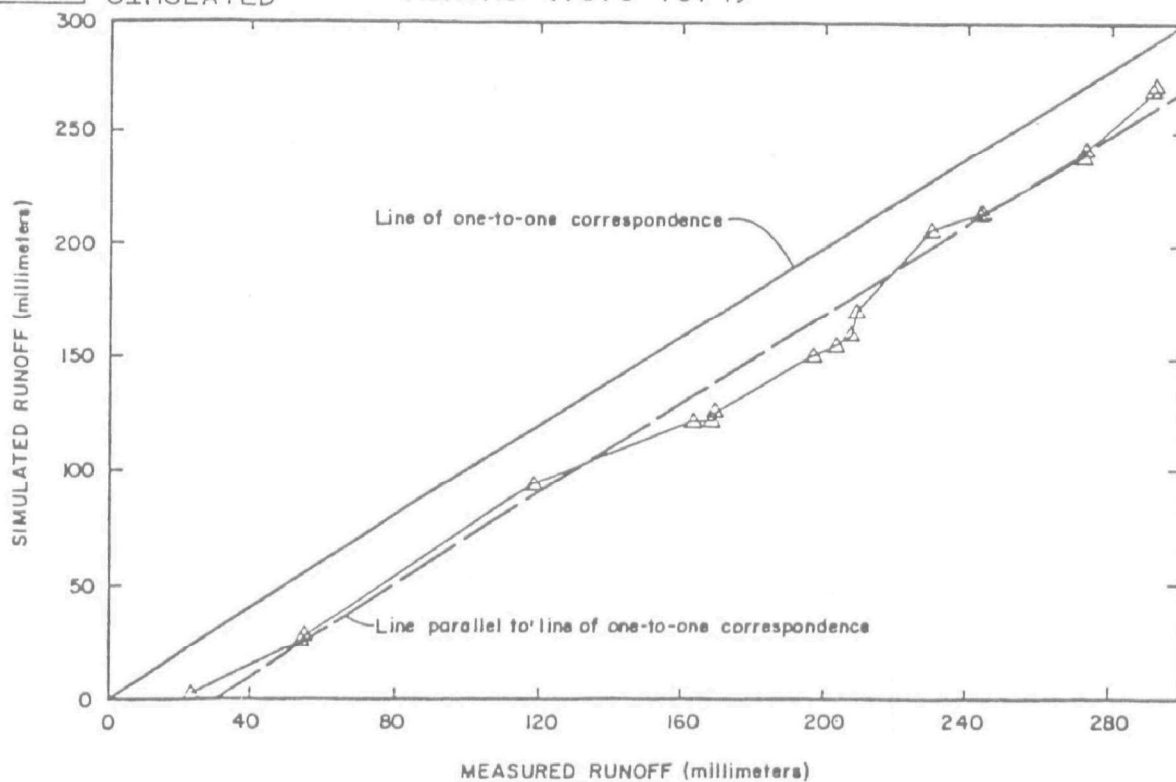
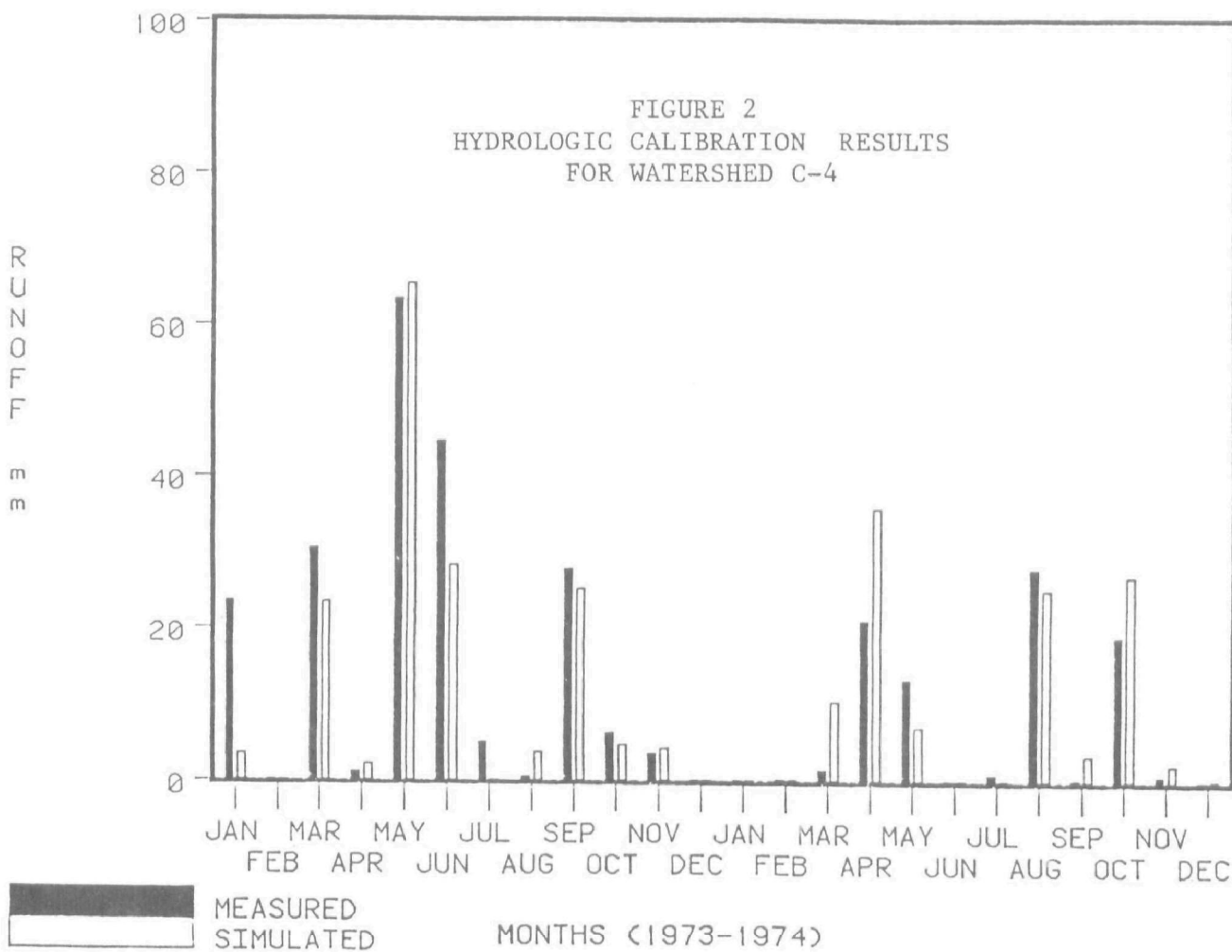
MEASURED
SIMULATED

MONTH (1974-1976)



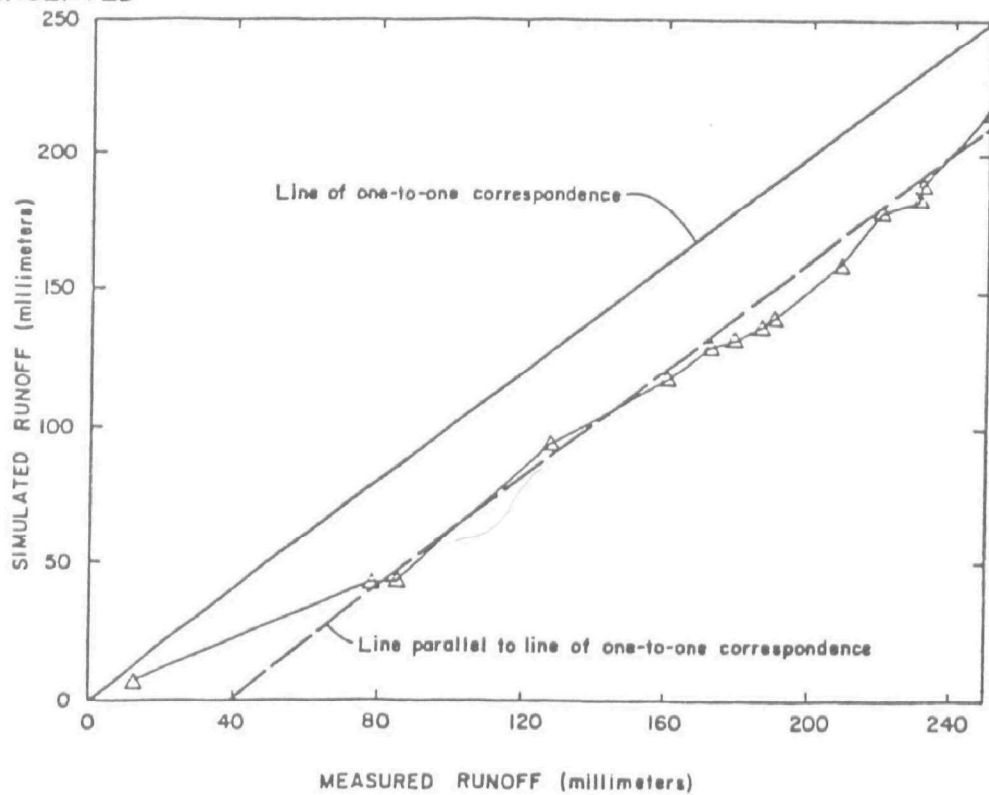
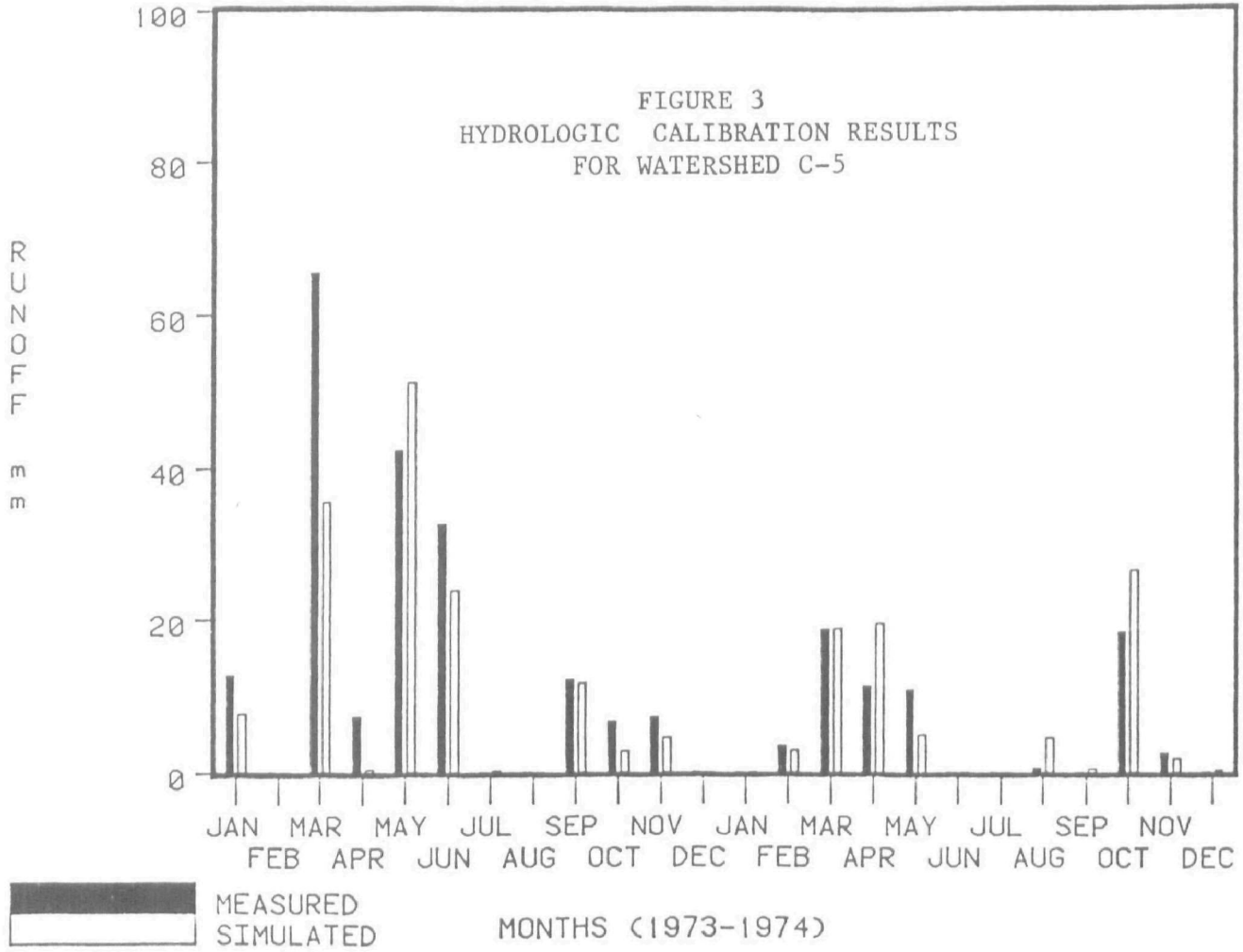
R
U
N
O
F
F
E

FIGURE 2
HYDROLOGIC CALIBRATION RESULTS
FOR WATERSHED C-4



337702020

FIGURE 3
HYDROLOGIC CALIBRATION RESULTS
FOR WATERSHED C-5



results.

For Watershed 802, poor simulation during May and June, 1974 is attributed to extreme hydrologic conditions occurring on the watershed. Precipitation measured 365 mm and 237 mm, respectively, compared with thirty year monthly mean values of 120 mm and 77 mm. Runoff for these months measured 266 mm (73% of rainfall) and 159 mm (67%) whereas simulation totals were 204 mm (56%) and 120 mm (51%). These discrepancies accounted for approximately 80% of the total annual error in 1974.

The slightly more erratic behavior of the model in simulating runoff for the Oklahoma watersheds is primarily attributed to the characteristics of major runoff producing storm events. Review of the precipitation data revealed that the Oklahoma sites were frequently subjected to storms of high intensity and short duration. Simulation of these events using HSPF, however, is extremely difficult due to the non-convergent nature of the model's algorithms for cases of intense precipitation. This was found to be particularly true for small agricultural watersheds where annual tillage practices can drastically impact hydrologic response on a storm level of detail.

For each calibration, parameter sensitivity runs indicated that annual results were most sensitive to the values of INFILT, the infiltration capacity coefficient, and UZSN, the upper zone nominal storage capacity parameter. More pronounced, however, was the impact that distributed monthly UZSN values had upon the annual distribution of runoff. Direct variation of UZSN on a monthly basis to reflect the effects that soil type, tillage practices and antecedent soil moisture conditions have on soil moisture field capacity allows for a better representation of annual variations in the physical system simulated. Parameters not found to significantly impact simulation results included: NBLKS, LSUR, SLSUR, INFEXP, INFILD, IRC, and NSUR.

Statistical comparison of simulation results can be made utilizing computed coefficients of variation, monthly runoff totals, and monthly standard deviations. For the six watershed years simulated, period of record coefficients of variation were 0.30, 0.58, and 0.71 for Watersheds 802, C-4, and C-5. Corresponding mean monthly runoff totals were 61 mm, 12 mm, and 10 mm, respectively. Average monthly standard deviations of simulated versus measured runoff were 18.3 mm for Watershed 802, 7.0 mm for C-4, and 7.1 mm for C-5. These results indicate that, although the best overall simulation was achieved on Watershed 802, simulation on the Oklahoma sites was also good.

Sediment Calibration

Calibration of parameters in the SEDMNT module of HSPF followed the general procedure previously outlined. From step four, since simulation results of PWATER serve as direct input to SEDMNT, particular attention was focused on the possibility of error transfer between modules. Testing this hypothesis involved an examination of the natural association between runoff and sediment yield for each watershed under cropped and fallow conditions. Through logarithmic linear regression, correlation coefficients were

calculated as 0.92 and 0.91 for Watershed 802, 0.84 and 0.94 for C-4 and 0.38 and 0.98 for C-5. These correlations imply that a good hydrologic simulation is an important pre-requisite to an accurate simulation of sediment removal. All analyses performed, however, indicated that PWATER results would not significantly limit SEDMNT parameter calibration.

The calibrated SEDMNT parameter estimates for each watershed are listed in Table 2. Since tillage operations during each cropping season were frequent, the models' "special actions" feature was utilized to reset the storage of detached fines (DETS) to an amount representative of newly tilled soil. All major activities occurring on each watershed were assumed to affect the supply of detached fines to the same degree, therefore, a single value for DETS was used at each soil disturbance. Adjustment of this parameter in an effort to simulate peak sediment production months facilitated calibration of remaining variables.

Following establishment of the value for DETS, sediment parameters KSER and JSER, the coefficient and exponent in the transport equation, were determined to be most sensitive during and immediately after months in which tillage operations occurred. During periods when tillage did not occur, simulation results were sensitive to the values of detachment algorithm parameters. Gully erosion was considered negligible in each watershed.

Sediment simulation results for each watershed are graphically illustrated in Figures 4, 5, and 6. The double mass analysis plots for sediment indicate, as did the hydrology plots, that undersimulation in the initial months resulted in underestimation of the two year totals. Overall simulation for months in which a substantial amount of sediment was measured appear to be good. This fact is shown by observing that those months for which the cumulative mass curves are increasing significantly, the trend is toward a line with a slope approximately equal to one. The erratic behavior exhibited during periods in which very little sediment was recorded reveals that equally distributed over and undersimulation of the data occurred. Given the relative magnitudes of these values, this erratic behavior is not considered significant.

Sediment simulation results for each watershed were, however, found to be closely related to hydrologic simulation results. This is best illustrated through review of the monthly totals in bar graph form. The correspondence between months in which over or undersimulation occurred for both hydrologic and sediment results existed in approximately 80% of the months in which there were measurable differences in their respective totals.

Coefficients of variation for the measured versus simulated sediment results were 0.69, 0.97, and 1.08 for Watersheds 802, C-4 and C-5. Corresponding mean monthly sediment yields were 1.65, 0.47 and 0.08 tonnes/ha., and monthly standard deviations were 1.14, 0.46, and 0.09 tonnes/ha., respectively.

The results of these calibrations indicate that parameter values in the sediment simulation algorithms of HSPF, although empirically derived, are related for watersheds having similar characteristics. For Watersheds C-4 and

TABLE 2
SUMMARY OF CALIBRATED SEDMNT PARAMETER ESTIMATES

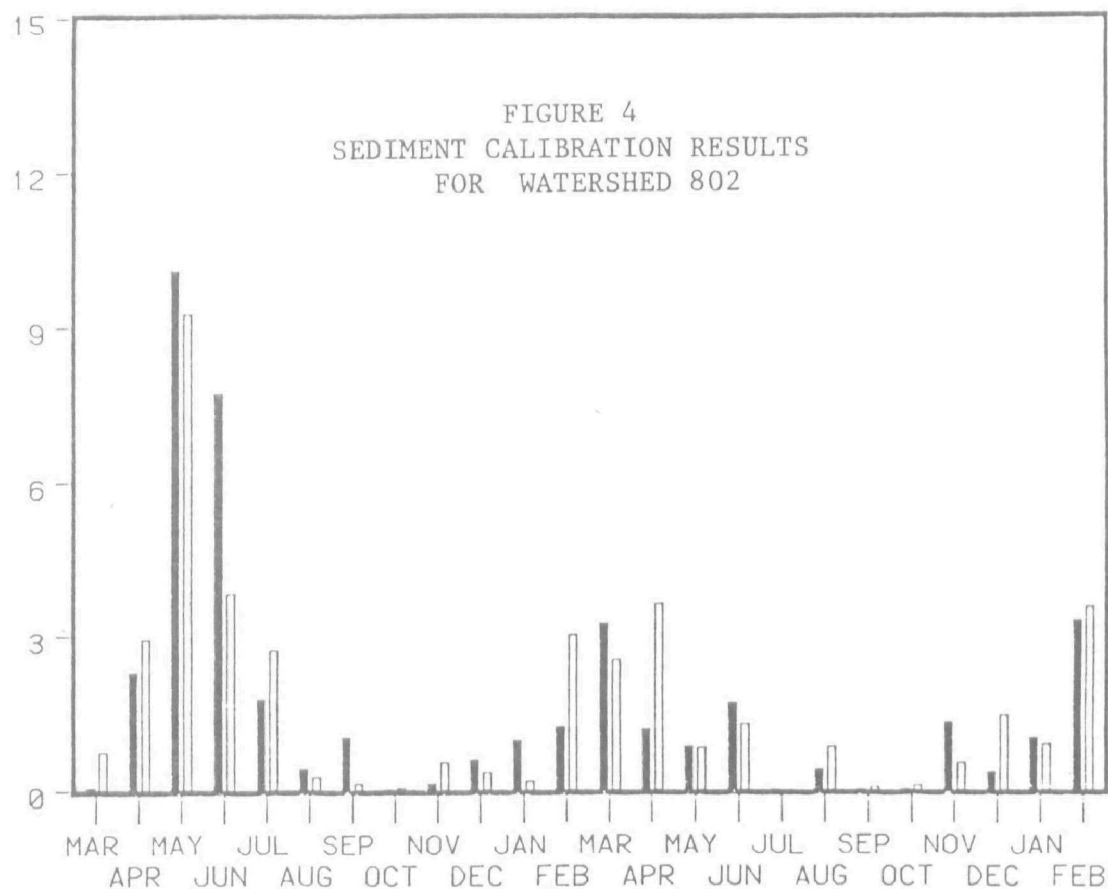
<u>Parameter</u>	<u>802</u>	<u>C-4</u>	<u>C-5</u>
KGER*	0	0	0
JGER*	0	0	0
KRER	0.1	0.05	0.05
JRER	2.5	2.0	2.0
KSER	1.0	0.5	1.0
JSER	1.8	1.6	3.0
COVERM:			
Jan	0.10	0.10	0.90
Feb	0.10	0.10	0.90
Mar	0.10	0.10	0.90
Apr	0.10	0.10	0.90
May	0.10	0.30	0.90
Jun	0.50	0.60	0.90
Jul	0.90	0.90	0.20
Aug	0.90	0.90	0.10
Sep	0.90	0.90	0.10
Oct	0.90	0.90	0.10
Nov	0.50	0.80	0.50
Dec	0.20	0.50	0.90
DETS**(ton/acre)	1.0	5.0	5.0
AFFIX (day ⁻¹)	0.05	0.05	0.05

* Gully erosion was assumed to be zero.

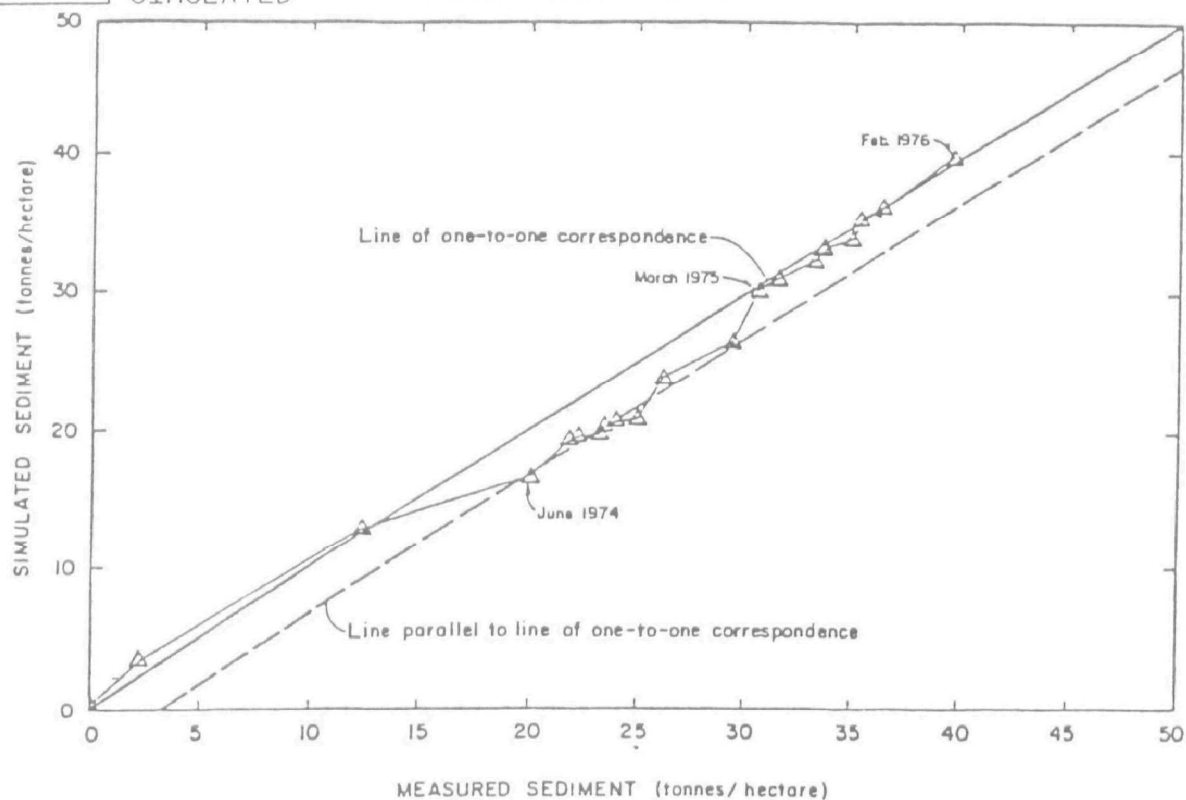
** The reset value for detached fines storage following tillage operations.

SEDIMENT
IN
TONNES/H A

FIGURE 4
SEDIMENT CALIBRATION RESULTS
FOR WATERSHED 802

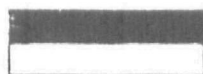
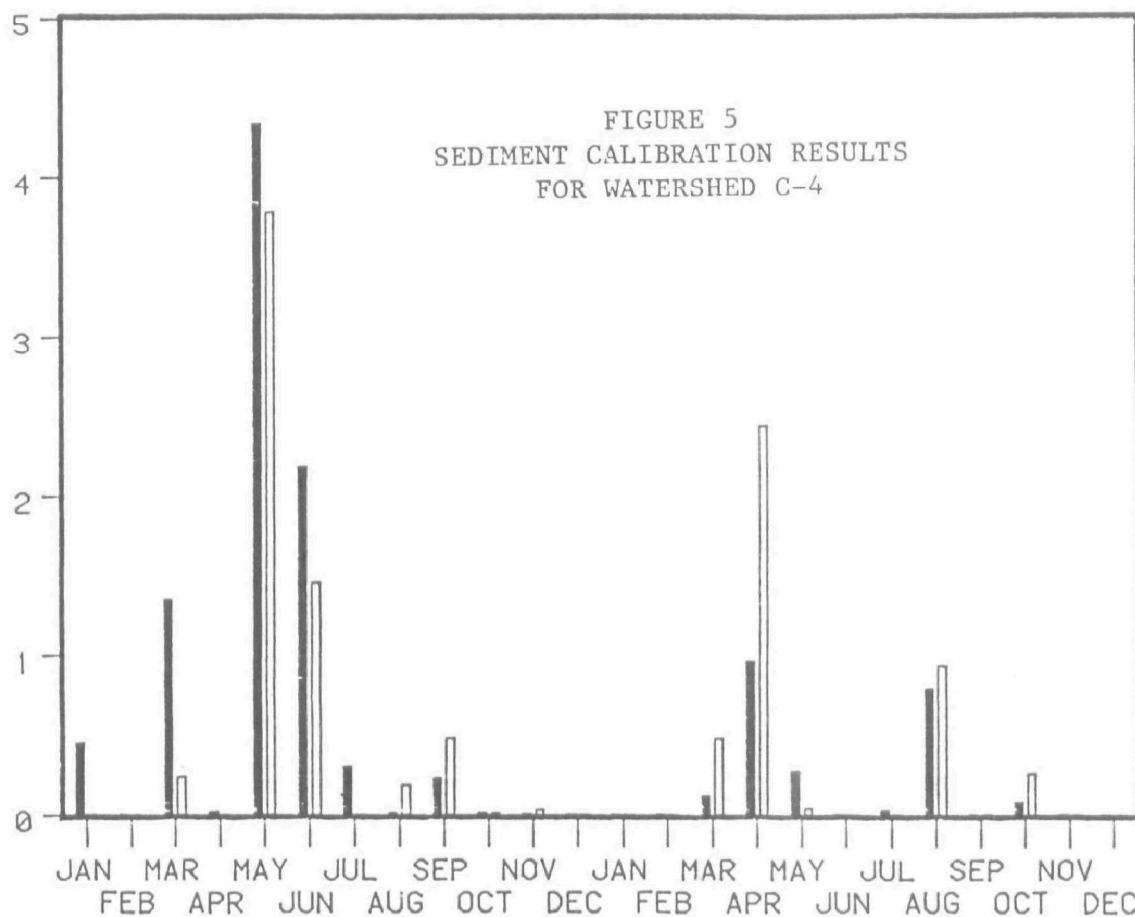


MONTH (1974-1976)



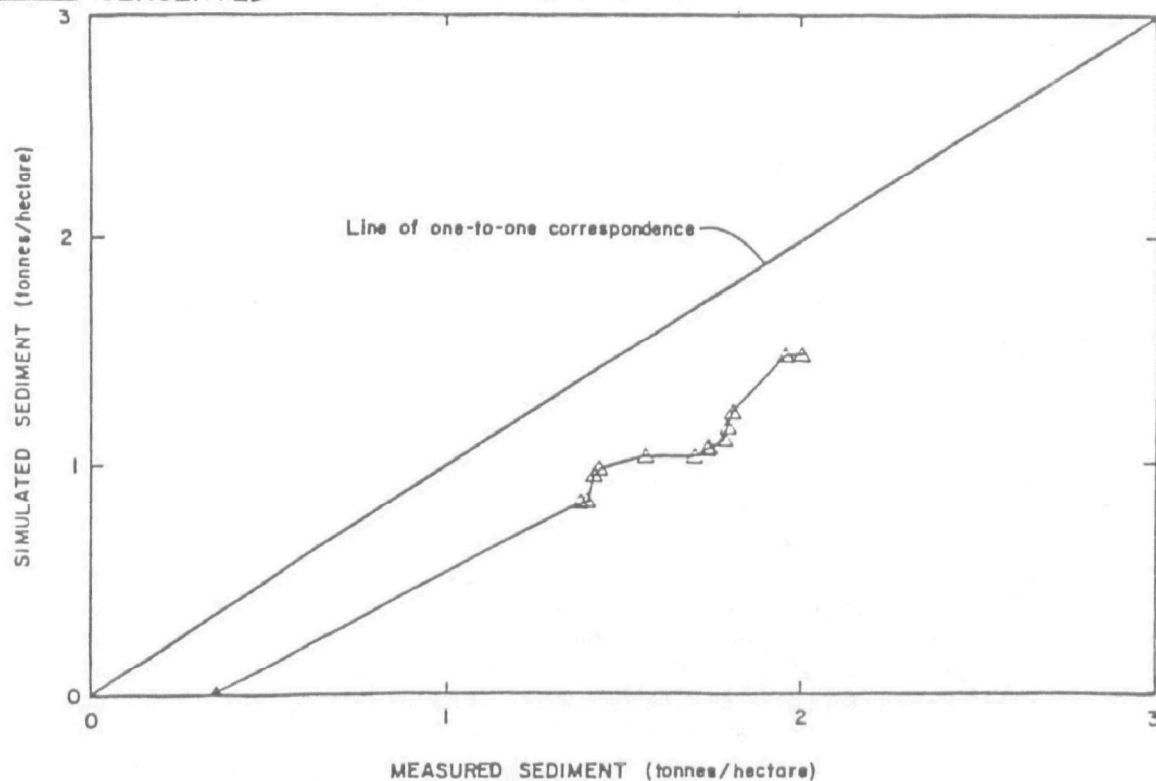
SEDIMENT IN TONNES/HA

FIGURE 5
SEDIMENT CALIBRATION RESULTS
FOR WATERSHED C-4



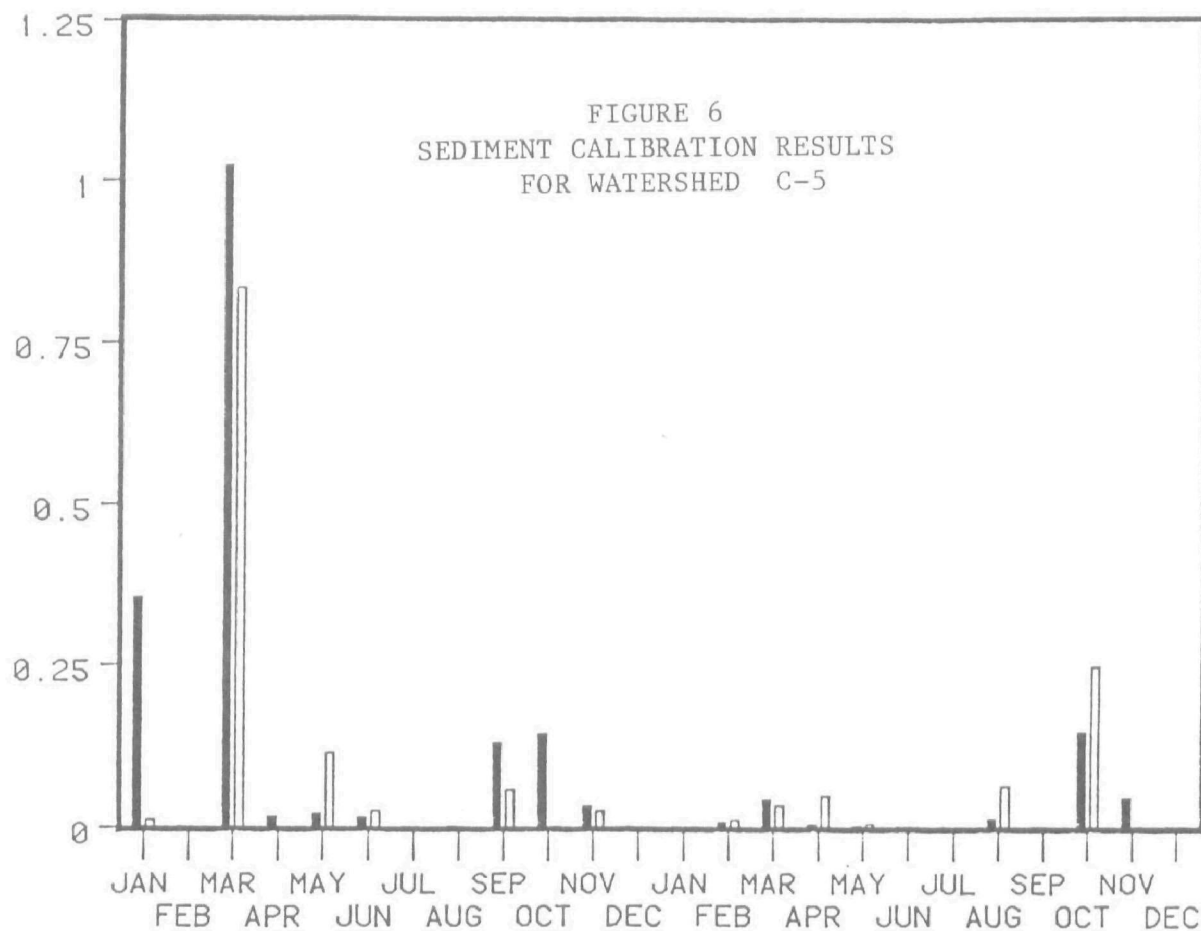
MEASURED
SIMULATED

MONTHS (1973-1974)



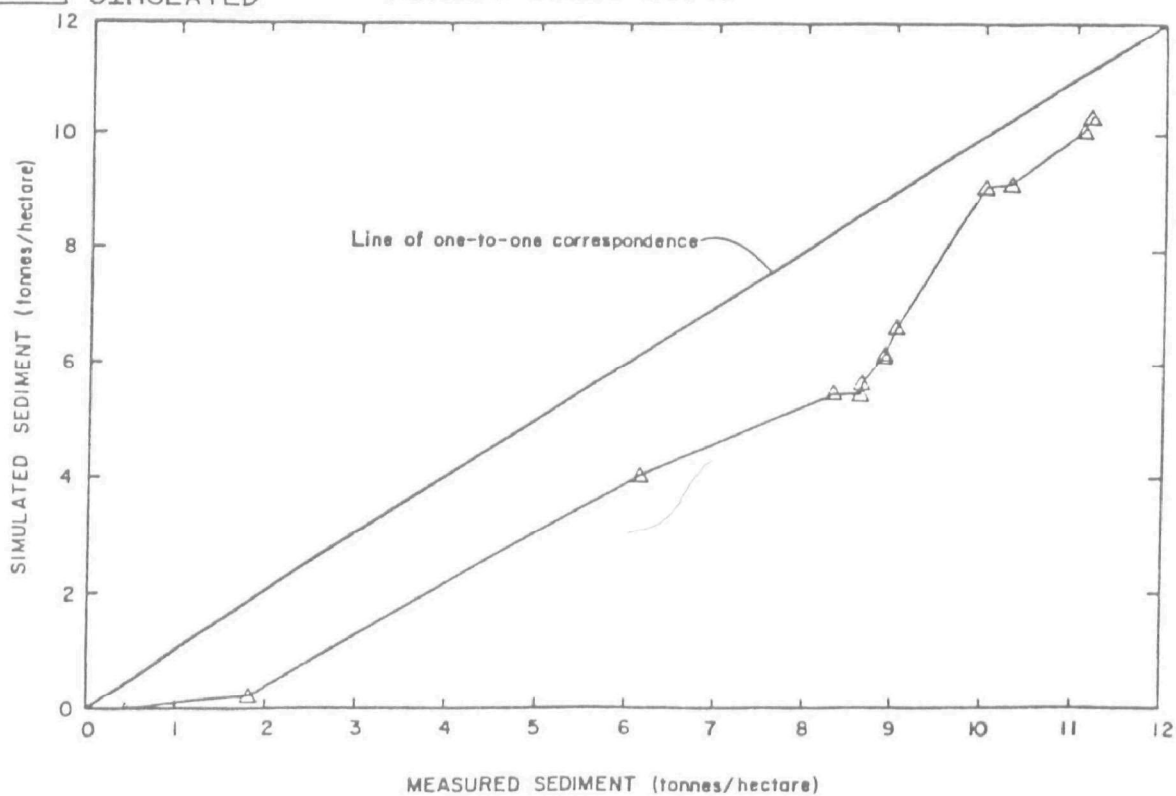
SEDIMENT
IN
TONNES/H A

FIGURE 6
SEDIMENT CALIBRATION RESULTS
FOR WATERSHED C-5



MEASURED
SIMULATED

MONTHS (1973-1974)



C-5 parameters KRER, JRER, DETS and AFFIX have identical values. This would be expected since the values of these parameters are primarily related to the erodibility and detachability of the specific soil type and land surface conditions, and soils in the two watersheds are nearly the same. Differences in the monthly distributions of COVERM are a function of the differences in the growing seasons.

Values for parameters KSER and JSER were expected to vary over the year, as these are transport capacity coefficients and exponents, and should vary as crop cover varies over the growing season. These parameters represent approximations as to the relationships between overland flow intensity and sediment transport capacity. Within year differences are expected, since the algorithms attempt to combine the effects of slope, overland flow length, sediment particle size, and alternative agricultural management practices into a single relationship. Since several watersheds and crop characteristics are incorporated into these parameter value estimates, numerical differences in parameter values cannot be attributed to a single factor.

CONCLUSIONS

The results of HSPF calibration on the Oklahoma watersheds were not as good as those obtained in the Mississippi watershed calibration. However, the ability of the model to simulate the hydrologic response and sediment removal from the watersheds is considered reasonably good. Large percent differences between measured and simulated annual totals resulted from poor simulation of relatively few months in which measured values were extremely high. This is particularly evident during the initial months of simulation in which initial conditions may be partially responsible for poor simulation. Overall good model performance is best illustrated by the double mass analysis plots. These show that, aside from undersimulation during model start up, parallel lines can be drawn to the lines of one-to-one correspondence of measured and simulated values.

Sediment simulation errors on Oklahoma Watersheds C-4 and C-5 were found to be significantly related to errors in their respective hydrology calibrations. Months during which sediment was oversimulated (or undersimulated) normally corresponded with similar results for hydrology. Difficulties in the hydrologic calibration on both watersheds is presumed to stem from the inability of the model to consistently simulate storms of high intensity and short duration. Calibrated parameter value estimates which physically should be transferable between these watersheds were found to provide good simulation results for each. In addition, correlation was found between calibrated parameter estimates for the Mississippi site for those parameters that are physically based, and have similar characteristics.

HSPF appears to be suitable for simulating runoff and sediment from agricultural watersheds. However, the model should be verified on each of these watersheds before being used as a predictive tool. An independent data set for verification would provide a test for the calibrated parameter values, and further analyze the model's applicability to these particular watersheds and to agricultural watersheds in general. For the Oklahoma sites calibration

over a two year period with one above average and one below average rainfall year provides a good first test for the model, but is not a substitute for independent verification.

REFERENCES

1. Johanson, R.C., Imhoff, J.C., and Davis, H.H. Jr., "User's Manual for Hydrological Simulation Program-Fortran (HSPF)," U.S. Environmental Research Laboratory, Publication No. EPA-600/9-80-015, Athens, Georgia, 1980
2. Hydrocomp, Inc., ARM User's Manual, Palo Alto, California, 1977.
3. GKY & Associates, Inc., "Calibration and Testing of Agricultural Runoff Management (ARM) Model and Non-Point Source Pollutant Loading Model," Alexandria, Virginia, 1979.
4. McDowell, L.L., Personal Communication and Correspondence, 1981.
5. McDowell, L.L., Willis, G.H., Murphree, C.E., Southwick, L.M., and Smith, S., "Toxaphene and Sediment Yields in Runoff from a Mississippi Delta Watershed." Journal of Environmental Quality, 10:120-125, 1981.
6. Murphree, C.E., Muchler, C.K., and McDowell, L.L., Sediment Yields from a Mississippi Delta Watershed," In Proc. 3rd Fed. Interagency Sediment Conference, Denver, CO, March 22-25, 1976.
7. Willis, G.H., McDowell, L.L., Parr, J.F., Murphree, C.E., "Pesticide Concentrations and Yields in Runoff and Sediment from a Mississippi Delta Watershed" In Proc. of the 3rd Fed. Interagency Sedimentation Conference, Denver, CO, March 22-25, 1976.
8. Menzel, R.G., Rhoades, E.D., Olness, A.E., and Smith, S.J., "Variability of Annual Nutrient and Sediment Discharges in Runoff from Oklahoma Cropland and Rangeland," Journal of Environmental Quality, Vol. 7, No. 3, 1978
9. Nicks, A.D., Gander, G.A., Frere, M.H., Menzel, R.G., "Evaluation of Chemical Transport Models on Range and Cropland Watersheds," Presented at the Summer Joint Meeting of the American Society of Agricultural Engineers and the Canadian Society of Agricultural Engineering, held at Winnipeg, Manitoba, June 24-27, 1979.
10. Olness, A., Smith, S.J., Rhoades, E.D., and Menzel, R.G., "Nutrient and Sediment Discharge from Agricultural Watersheds in Oklahoma," Journal of Environmental Quality, Vol. 4, No. 3, 1975.
11. Rhoades, E.D., Welch, N.H., and Coleman, G.A., "Sediment-Yield Characteristics from Unit Source Watersheds," In Present and Prospective Technology for Predicting Sediment Yield and Sources, U.S.D.A. ARS Southern Regional Bulletin, ARS-5-40, 1974.

The work described in this paper was not funded by the U.S. Environmental Protection Agency. The contents do not necessarily reflect the views of the Agency and no official endorsement should be inferred.

HYDROLOGIC MODELING FOR STUDIES OF POLLUTANT LOADINGS
AND TRANSPORT IN LARGE RIVER BASINS

By Alan Cavacas,¹ John P. Hartigan,² Elizabeth Southerland,³
and John A. Friedman⁴

Introduction

The Chesapeake Bay, located in eastern Maryland and Virginia, is one of the largest and most economically important of the 850 estuaries that ring the United States. The Bay is approximately 300 mi long with 13,000 mi of shoreline and a surface area of 4,300 sq mi. In order to determine the sources of eutrophication problems in the upper Bay and major tidal tributaries and to formulate appropriate control strategies, the U.S. Environmental Protection Agency (EPA) Chesapeake Bay Program funded the development of three computer models to represent the fluvial and estuarine sections of the Chesapeake Bay system. The River Basin Model, which is the subject of this paper, simulates streamflow and transport of point and nonpoint source pollution loadings in the 64,000 sq mi drainage area of the Bay (see Figure 1). The Major Tidal Tributary Model serves as the interface between the Basin Model and the Bay Model by simulating pollutant transport through the Potomac, James, Rappahannock, and York estuaries. These models are linked to the two-dimensional Main Bay Model which simulates vertically-averaged water quality impacts of pollutant loadings delivered to the Chesapeake Bay. A flow chart which outlines the relationships among the three models of the Chesapeake Bay system is shown in Figure 2. By operating the three computer models in series, management agencies can evaluate Baywide impacts of regional water quality management strategies in terms of the frequency of violations of water quality criteria/standards for various beneficial uses (i.e., fisheries habitat, recreation).

This paper describes the calibration/verification of the hydrology component of the River Basin Model. The continuous simulation hydrologic model was linked with a water quality model for studies of nonpoint pollution loadings and the transport of nutrient and organic loadings in tributary watersheds of Chesapeake Bay. The River Basin Model represents the Susquehanna, Potomac, and James river basins as well as 33 other river basins which contribute freshwater inflows, nonpoint pollution loadings, and wastewater discharges to the Bay. The Model was used by the EPA Chesapeake Bay Program for assessments of management strategies for nonpoint pollution and wastewater treatment. This paper focuses on the hydrology/hydraulics modeling requirements for the river basin water quality modeling studies.

¹Water Resources Engineer, Northern Virginia Planning District Commission (NVPDC), 7630 Little River Turnpike, Annandale, Virginia 22003.

²Director, Engineering-Planning Division, NVPDC

³Environmental Engineer, NVPDC

⁴Water Resources Engineer, NVPDC

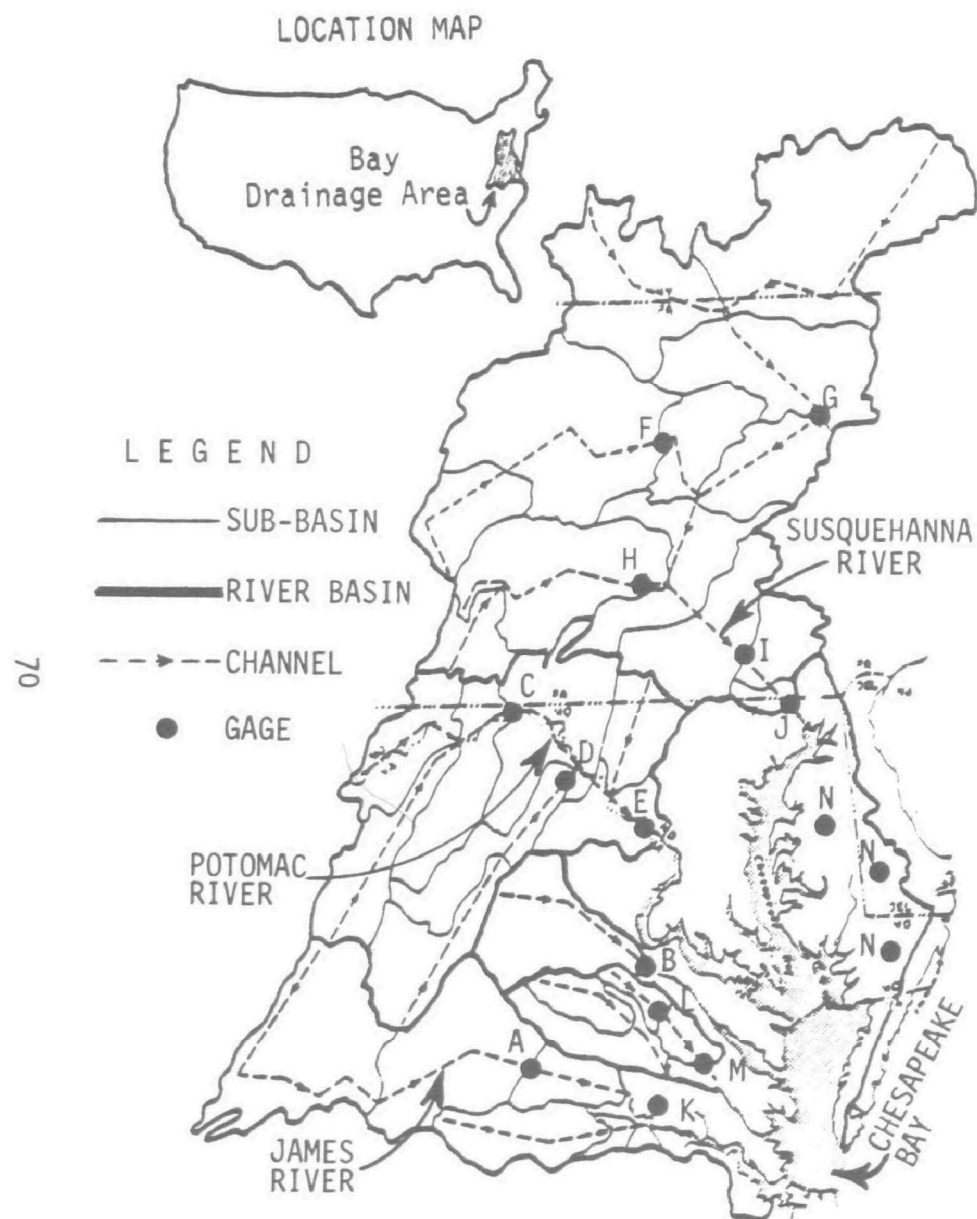


Figure 1. Map of Chesapeake Bay Basin Showing Calibration/Verification Gages and Sub-basin/Channel Network

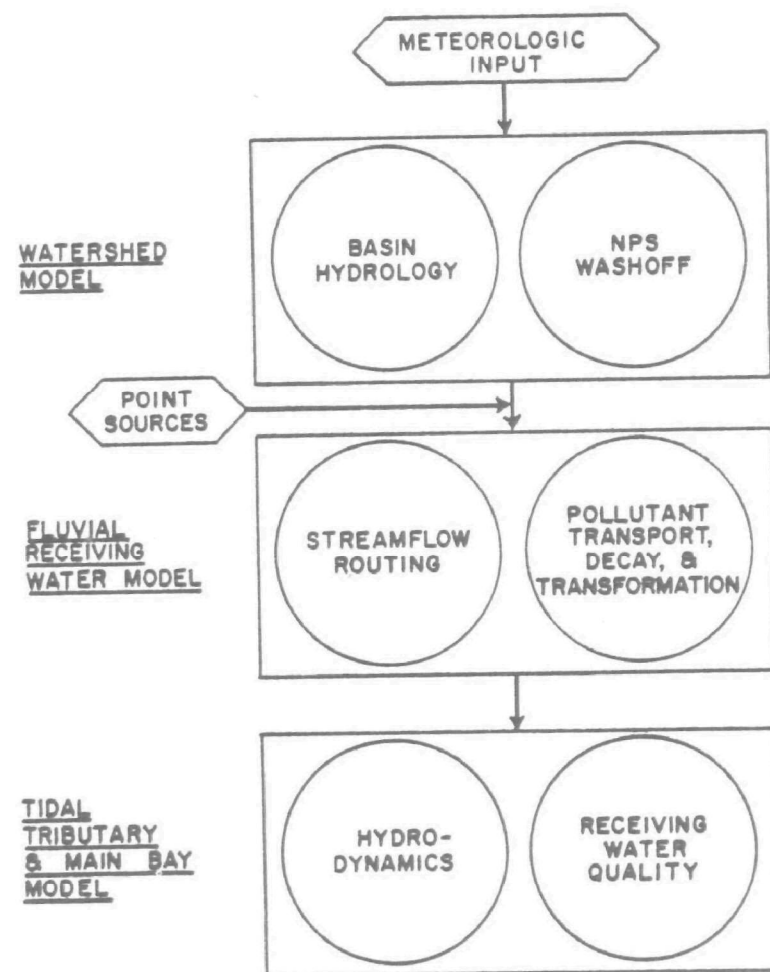


Figure 2. Flow Chart Showing Models Included in Chesapeake Bay Model Package

Modeling Framework

The principal functions of the River Basin Model are to use meteorologic records to calculate the streamflow and nonpoint pollution loadings in the Bay's 64,000 sq mi drainage area (see Figure 1) and to simulate the transport of point source and nonpoint pollution to the Bay's estuarine system. In other words, the water quality problem to be addressed is the transport of streamflow and pollutant loadings to the Bay and its tidal tributaries, rather than localized receiving water quality problems (e.g., dissolved oxygen sag) within the fluvial river system.

The temporal dimensions of the River Basin modeling framework are as follows: (a) simulations of weekly or monthly pollutant loadings delivered to the Bay's estuarine system are more important than simulations of hour-to-hour changes in water quality within the tributary rivers; (b) since one would not expect all point source and nonpoint pollution loadings to reach the Bay due to physical, chemical, and biological processes during channel transport, the River Basin Model must be capable of accounting for pollutant degradation enroute to the Bay; (c) simulations of long-term records of streamflow and pollutant loadings which reach the tidal tributaries and the Main Bay are necessary for analyses of the frequency of water quality criteria violations in the Bay system; (d) in order to simulate long-term records of streamflow and nonpoint pollution loadings, the River Basin Model should be capable of accounting for long-term changes in watershed state variables (e.g., soil moisture, vegetative cover, soil disturbance, and pollutant loading factors); (e) since most computer models require short-term rainfall intensity data in order to accurately calculate the amount of rainfall which does not infiltrate into the soil profile and soil erosion due to the kinetic energy of raindrops, precipitation records should be input at intervals of one hour or less; (f) since localized water quality impacts in the river basins are not the principal focus of the modeling study, idealized channel reaches with relatively high travel times (e.g., 1-3 days) and lengthy computation time-steps (e.g., 12 hrs) for flow routing and water quality processes can be used to ensure that computer costs for long-term simulations do not become prohibitive; and (g) April 1st through October 31st is the critical period for studies of eutrophication management in the Bay system.

The spatial dimensions of the River Basin modeling framework are as follows: (a) sub-basin size is limited by homogeneity of hydrologic characteristics (e.g., soils, geology) and by areal variations in rainfall; (b) since the Model is not intended for flooding simulations, accurate projections of flood elevations and hydrograph timing are not critical, thereby permitting a network consisting of relatively large sub-basins (e.g., 1,000-2,000 sq mi) and relatively long channel reaches (e.g., 30-50 mi) with idealized trapezoidal cross-sections; and (c) since localized receiving water quality problems are not addressed by the modeling study, a one-dimensional model assuming completely mixed conditions in each reach can be used.

Description of River Basin Model

Based upon the temporal and spatial dimensions of the required modeling framework, software which had previously been applied to portions of the Chesapeake Bay Basin was selected to serve as the River Basin Model. The selected software (1) is a predecessor of EPA's HSPF model (2) with a hydrologic submodel based upon a modified version of the Stanford Watershed Model (3).

The Model is executed with hourly rainfall and daily evaporation records to calculate the amount of rainfall converted to runoff and to provide a continuous accounting of the water balance on the land surface and within several idealized storage compartments in the soil profile. During storm periods, hourly rainfall is distributed between surface runoff and soil moisture storage compartments based upon adjusted infiltration rates and the nominal storage capacities assigned to different sections of the soil profile. Between rainstorms, water storage in soil moisture zones is depleted by mechanisms such as evapotranspiration and subsurface recharge of streams, thereby freeing up soil moisture storage capacity for rainfall inputs from the next storm. Streamflow transport is handled with a form of kinematic wave routing, while pollutant transport out of a given channel reach into a downstream channel reach is based upon advection. A twelve-hour routing interval was used for hydrologic simulations.

The selected software has been used for several modeling studies in the metropolitan Washington, D.C. region. It has been applied most extensively to the 580 sq mi Occoquan River Basin of Northern Virginia for studies ranging from nonpoint pollution management assessments (4,5) to evaluations of advanced wastewater treatment (AWT) needs (6).

Description of Model Networks and Input Datasets

Sub-basin Data. The delineation of the sub-basin network was based upon an analysis of geographic variations in the following characteristics listed in the order of consideration: (1) physiographic province; (2) topography; (3) hydrologic soil group; and (4) total water holding capacity of soil. Map overlays (1:500,000 scale) were developed for each dataset for purposes of hydrologic segment delineation. In the case of datasets 2, 3, and 4, the overlays display the predominant or average characteristic in a 100 sq mi grid cell network which is used to manage and aggregate basinwide physical features data (i.e., each cell has dimensions of 10 mi x 10 mi).

The 100 sq mi grid size was felt to provide a reasonable level of detail for a 64,000 sq mi basin. The authors' previous modeling experiences in the Northern Virginia region suggested that localized variations in physical features tend to have a relatively insignificant effect on the development of lumped parameter model datasets for sub-basins on the order of a few hundred square miles. Confidence in the representativeness of the 100 sq mi grid cell datasets for the Chesapeake Bay Basin was gained through sensitivity studies based upon county soils maps and 1:24,000 scale topographic maps.

Due to the size of the Chesapeake Bay Basin, assessment of soils characteristics were based upon soil association characterizations carried out on a state-by-state basis. The distribution of the Chesapeake Bay Basin's 135 soil associations among the five states in the drainage area is as follows: Virginia: 54; Maryland: 27; West Virginia: 12; Pennsylvania: 34; and New York: 8. Each soil association consists of one-to-four soil series listed in order of dominance. Composite characteristics for each association are typically developed by weighting the characteristics of individual soil series according to the fraction of the association that is typically attributed to a series. Unfortunately, statewide data on the fraction of each association that is attributed to each series is available only for Pennsylvania and Northern Virginia. The only source of such data in other sections of the basin are the soil surveys prepared by the individual counties in each state. Based on a review of typical soil series distributions attributed to Pennsylvania and Northern Virginia soil associations, the following relative distributions were assumed to analyze soil association characteristics throughout the Chesapeake Bay Basin:

<u>Soil Series Order</u>	<u>Total Number of Soil Series in Association</u>		
	<u>Two Soil Series</u>	<u>Three Soil Series</u>	<u>Four Soil Series</u>
1st Series	60%	60%	50%
2nd Series	40%	30%	30%
3rd Series		10%	10%
4th Series			10%

The "soil series order" refers to the hierarchy implicit in the soil association name. These assumed distributions were used to weight the hydrologic characteristics of each series to derive a composite characteristic for each soil association.

Average values of the following characteristics were derived for each soil association by applying the assumed distributions to the soil series data presented in State SCS-5 reports: permeability; hydrologic soil group; total water holding capacity; soil texture; soil depth; and erodibility factor (K). Using the 100 sq mi grid cell network, 1:500,000 scale map overlays showing the average value for the predominant soil association in each grid cell were developed for each of these characteristics.

The first step in the delineation of homogeneous hydrologic segments was to overlay the physiographic province map with the grid map of average slopes. Areas with relatively uniform slopes within physiographic provinces were selected as the first segment approximation. The next step was to overlay this intermediate segment network with the grid maps of hydrologic soil group and total water holding capacity. More detailed segments were derived from these last two overlays since they delineated areas with relatively similar infiltration rates and soil moisture storage capacities. Particular attention was given to defining more detailed segments in the Coastal Plain where surface runoff and nonpoint pollution loads have a greater chance of reaching the Bay's estuarine system due to the relatively short travel times. This analysis of basinwide physical features resulted

in the delineation of a preliminary hydrologic unit network consisting of 23 hydrologic segments.

This preliminary segment network was further refined by analyzing areal variations in rainfall patterns within each segment. National Weather Service (NWS) tapes with hourly/daily raingage records for the period 1966-1978 were used for the modeling study since this period included a good mix of wet, dry, and average years. A total of 93 raingages were included in this study (see Figure 3). Statistics such as mean annual volume, standard deviation, and coefficient of variation were calculated for each raingage and compared with surrounding gages to identify groupings with similar characteristics. Raingage groupings were further refined through intercorrelation analyses based upon daily rainfall totals. Basinwide isohyetal maps and Thiessen polygons constructed for the final raingage groupings were used to further subdivide seven hydrologic segments, resulting in the final network of 30 segments shown in Figure 3. In general, the hydrologic segment boundaries correspond to physiographic boundaries as might be expected for a generalized network representing a 64,000 sq mi basin. Segments 1-10 represent Coastal Plain province areas, segments 11-15 represent Piedmont province areas, segments 16 and 17 represent the Blue Ridge and Great Valley province, segments 18-24 represent Appalachian Ridge and Valley province areas, and segments 25-30 represent Appalachian Plateau province areas. Average soils characteristics and topography data used in the hydrologic submodel were tabulated for each segment by weighting the values stored in the grid cell dataset.

Since the hydrologic segments often overlapped river basin boundaries, a network of sub-basins was delineated to represent each river basin. In order to maximize homogeneity, the sub-basins were sized to ensure that the majority of the drainage area was located within a single hydrologic segment. In addition, an effort was made to maintain a bankfull channel travel time on the order of 24-72 hrs in establishing the outflow of each sub-basin. As shown in Figure 1, the resulting sub-basin network for the major river basins consists of 34 sub-basins on the order of 1,000-2,000 sq mi. In addition, 29 Coastal Plain watersheds are included in the Model network to provide detailed representations of direct inflows to the major tidal tributaries and embayments of the Main Bay. The hydrologic characteristics assigned to the segments traversed by each sub-basin were weighted for input to the hydrologic submodel.

In light of the size of the study area, sophisticated remote-sensing techniques offered the only feasible method for defining land cover data for each sub-basin. Existing land use summaries for each sub-basin are based upon interpretations of LANDSAT satellite images from the period 1977-1979 with state-of-the-art software available at the Goddard Space Flight Center in Greenbelt, Maryland. A total of 15 LANDSAT scenes were required to cover the entire Chesapeake Bay Basin.

Meteorologic Data. To produce a single hourly rainfall record for each hydrologic segment for the period 1966-1978, the Thiessen polygon method was used. Special software was designed to produce an hourly rainfall record which was based on a representative area-weighted daily rainfall

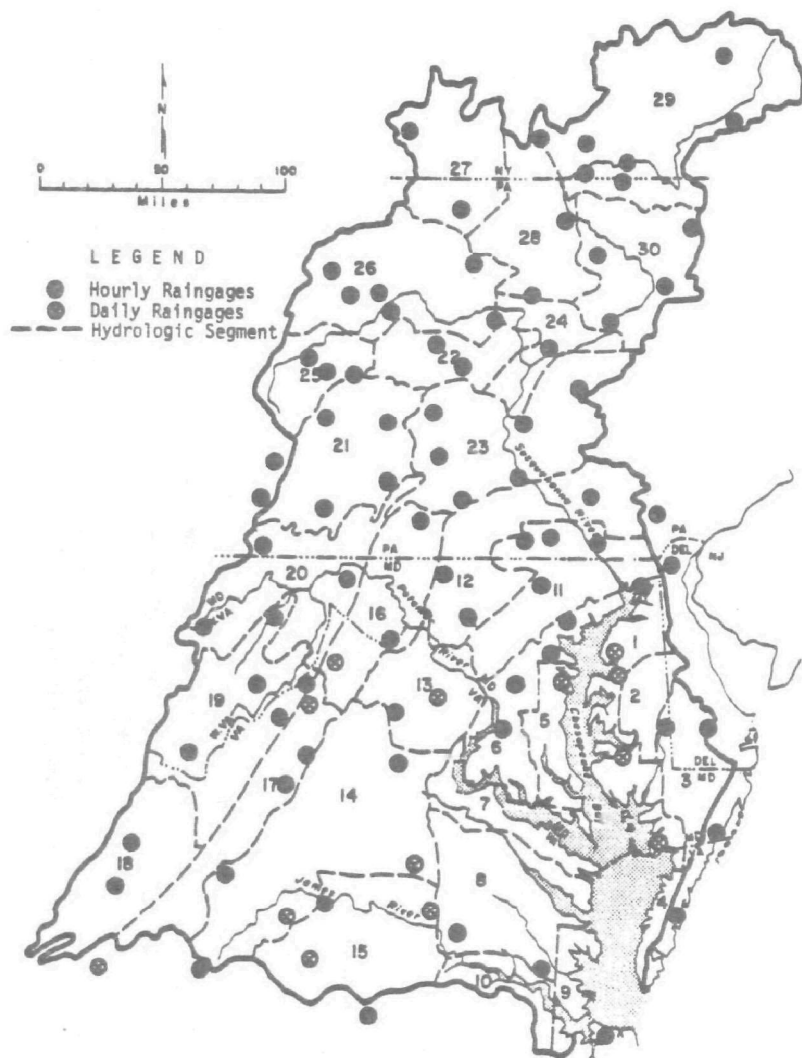


Figure 3. Map of Hydrologic Segments
Showing Distribution of
Hourly and Daily Raingages

Table 1
Listing of Streamgages Used for Calibration/Verification

MAP KEY ¹	NUMBER	U S G S NAME	G A G E	DRAINAGE AREA (SQ MI)
A	02035000	James River at Cartersville, VA		6,257
B	01668000	Rappahannock River near Fredericksburg, VA		1,596
C	01613000	Potomac River at Hancock, MD		4,073
D	01636500	Shenandoah River at Millville, WV		3,040
E	01646500	Potomac River near Washington, D.C.		11,560
F	01551500	West Branch Susquehanna River at Williamsport, PA		5,682
G	01536500	Susquehanna River at Wilkes-Barre, PA		9,960
H	01567000	Juniata River at Newport, PA		3,354
I	01576000	Susquehanna River at Marietta, PA		25,990
J	01578310	Susquehanna River at Conowingo, MD		27,100
K	02042500	Chickahominy River at Providence Forge, VA		248
L	01674000	Mattaponi River at Bowling Green, VA		257
M	01674500	Mattaponi River at Buelahville, VA		601
N	EASTERN SHORE GAGES (SUM OF FLOWS)			249
	01491000	Choptank River near Greensboro, MD		(113)
	01487000	Nanticoke River near Bridgeville, DE		(75)
	01485000	Pocomoke River near Willards, MD		(61)

¹Gage locations are shown in Figure 1

volume, preserved hourly rainfall intensities, and compensated for missing records. Other daily meteorologic datasets (e.g., evaporation, air temperature, solar radiation, wind speed) required for the hydrologic and water quality submodels were derived for eight meteorologic regions. Eight regions for non-precipitation data were felt to be adequate because the gages for these records are fewer in number than the rainfall gages, areal variations in these meteorologic indicators tend to be easier to characterize, and hydrologic responses in the river basins tend to be more sensitive to month-to-month fluctuations in these data in comparison with the day-to-day fluctuations in rainfall which are so important.

Channel Data. A single idealized trapezoidal channel with constant cross-sectional geometry is assigned to each sub-basin. To facilitate the development of idealized cross-sections, all channels are terminated at U.S.G.S. streamgaging stations where data on channel geometry is available from the table (Form 9-207) used to construct the stage-discharge relationship for the gage. As indicated above, idealized channel length was established in conjunction with the determination of sub-basin size in order to maintain bankfull travel times on the order of 1 to 3 days for each channel reach. Flood plain slopes for each idealized channel were determined from 1:24,000 scale topographic maps for the sub-basin. A sketch of the Basin Model's channel reach system is shown in Figure 1. It consists of 28 idealized channels with lengths ranging from 25 to 190 mi and seven reservoirs. The idealized channel system is restricted to the main stems of the major river basins, since the focus of Basin Model applications is the transport of pollutant loadings to the Chesapeake Bay rather than localized receiving water problems. For purposes of this pollutant transport study, it was assumed that the time lag and pollutant transformations achieved by channel storage in minor tributaries and small Coastal Plain watersheds is relatively insignificant.

Since the idealized channel reaches begin and end at U.S.G.S. streamgaging stations, the channel invert elevations reported for each streamgage were assigned to the respective channels for gradient calculations. Data on channel roughness coefficients was collected from state and regional agencies which had performed local flood insurance studies in the Chesapeake Bay Basin. An average value was derived for each idealized channel reach based upon the arithmetic means of roughness coefficient values at several representative cross-sections.

The following major reservoirs are represented by the Basin Model as single-layer lakes: Lake Anna (York River Basin); Lake Chesdin (Appomattox River Basin); Raystown Reservoir (Juniata River Basin); the two Patuxent River reservoirs; the Lake Aldred/Lake Clarke reservoir system (Susquehanna River Basin); and Conowingo Reservoir (Susquehanna River Basin). In the case of the two Patuxent reservoirs and the Lake Aldred/Lake Clarke system, the two reservoirs in series are combined into a single idealized impoundment with appropriate aggregate characteristics. For the Conowingo hydroelectric reservoir at the mouth of the Susquehanna River, a separate operating rule computer program (7) is used to calculate daily spills from simulated daily streamflows entering the reservoir.

Hydrology Calibration/Verification

Methodology. As indicated in Table 1 and Figure 1, a total of 14 streamgages were used for hydrology calibration/verification. The period April 1971 through October 1976 was used for model calibration, since this period included a good mixture of relatively wet, dry, and average years. Model verification was based upon the periods April 1966 through June 1970 and November 1976 through December 1978, which were generally somewhat drier than the calibration period. During calibration, the models were operated with meteorologic records for the entire 5.75-yr period and a single set of parameter values. Based on comparisons of simulated and observed streamflows, the most sensitive parameter values were iteratively adjusted to establish the final parameter sets. After acceptable agreement was achieved on a seasonal and annual basis, simulated and observed daily streamflows were compared for storm events to set hydrograph shape factors and for dry weather flow periods to set baseflow recession constants. Following calibration, the models were operated for the 6.4 year verification period without any adjustment to the calibrated parameter values to determine how well the models represented conditions different from the calibration period.

Since only a very small percentage of the Chesapeake Bay Basin is urbanized, calibration activities focused on soils parameters that determine an undeveloped area's hydrologic characteristics. Due to the distribution of raingages and streamgages, it was not possible to calibrate the Basin Model for every major watershed in the 64,000 sq mi basin. Therefore, one objective of hydrology calibration was to derive relationships between river basin physical features and model parameter values which could be applied to major watersheds that could not be calibrated separately. In other words, rather than indiscriminately adjusting the Model's parameter values to produce the best possible comparisons between simulated and observed streamflows at each streamgage, hydrology calibration focused on developing parameter estimation methods that could be applied to ungaged watersheds. This approach has previously been used to calibrate hydrologic models of several watersheds in the Northern Virginia portion of the Chesapeake Bay Basin (8,9,10).

LZSN (soil moisture storage capacity) and INFIL (infiltration rate) are the most important parameters for simulations of annual streamflow volumes. An increase in LZSN will increase the storage of water in the idealized lower zone of the soil, thereby lowering seasonal and annual streamflows by increasing the depletion of soil moisture through evapotranspiration and by reducing the frequency of saturated soil conditions. An increase in INFIL will likewise lower annual streamflows by reducing direct runoff due to higher infiltration and increasing soil moisture depletion through evapotranspiration. INFIL is most often used to modify seasonal streamflows after LZSN and a reasonable range of INFIL values which achieve acceptable annual streamflows have been identified. As has been the case in previous studies (8,9,10,11), LZSN in the Chesapeake Bay Basin was found to generally be directly related to average total water holding capacity and depth of soil above the restrictive layer. Calibrated LZSN values ranged from approximately 2-4 in. in the Appalachian Plateau and mountainous areas of

the Appalachian Ridge and Valley to approximately 6-8 in. in the Coastal Plain, lower Piedmont, and portions of the Appalachian Ridge and Valley. INFIL was found to be related to indicators of surface runoff potential such as hydrologic soil group, soil permeability, and soil texture. Calibrated INFIL values ranged from approximately 0.01 to 0.015 in/hr in the Appalachian Plateau and sections of the Coastal Plain and lower Piedmont with "D" hydrologic soil groups to 0.06 to 0.075 in/hr in sections of the Coastal Plain with "B" hydrologic soil groups. K3 is an evapotranspiration index that is generally set at reasonable levels to reflect vegetative cover, and then held constant while LZSN and INFIL are calibrated. K3 values on the order of 0.3-0.45 were used throughout the Chesapeake Bay Basin, with the higher values typically associated with areas characterized by high forest cover to account for the effect of vegetative cover on evapotranspiration. Although it is not as sensitive a parameter as either LZSN or INFIL, UZSN (i.e., moisture storage near the soil surface most closely related to depression storage) can have some effect on seasonal and annual streamflow volumes because of its impact on individual storm events. UZSN is most often related to the calibrated LZSN value and in the Chesapeake Bay Basin was typically found to be 5%-15% of LZSN. After acceptable agreement between simulated and observed streamflows was achieved on an annual and seasonal basis, the interflow coefficient INTER was adjusted to redistribute streamflows between surface runoff and subsurface flows in order to match the shapes of the recession limbs of observed hydrographs. Relatively low INTER values assign a higher percentage of streamflow to surface runoff, thereby resulting in higher peak flows and steep recession limbs. Like previous studies (8,9,10), Chesapeake Bay Basin calibration results indicated that INTER could be related to average land slopes, with values ranging from 1.0 in relatively flat Coastal Plain areas to 1.5 in mountainous areas. After INTER had been set, the baseflow recession coefficient (KK24) was fine tuned to improve the agreement between simulated and observed dry weather flows.

Results. Calibration runs were terminated for each streamgage when it was determined that: (a) the differences between simulated and observed streamflows could not be improved with further parameter adjustments, and (b) a sufficient number of model runs had been completed to develop reasonable regional parameter sets. The hydrology parameter sets produced by these calibration runs are quite reasonable based upon some previous continuous simulation modeling studies in the Chesapeake Basin (1,9,10,12) and other literature values (13,14,15).

Comparisons of simulated and observed streamflow data based upon streamflow volumes (annual and seasonal), daily streamflow time series, correlation coefficients, and daily flow-duration plots (period of record and seasonal) generally indicate very good calibration and verification results. Table 2 summarizes comparisons of simulated and observed annual streamflow volumes for 10 major streamgages. As may be seen, differences between simulated and observed annual volumes are typically within the range of observation errors associated with meteorologic and streamflow data collection activities. In general, the greatest differences between simulated and observed streamflow were associated with winter periods and drought periods. Winter periods, which were typically somewhat

Table 2

Mean Ratio of Simulated to Observed Water Year
Streamflow Volumes and Number of Years with
Ratio between 0.8 and 1.2
(i.e., No. of Yrs./Total No. of Yrs.)

STREAMGAGE	DRAINAGE AREA (SQ. MI.)	SIMULATED : OBSERVED WY VOLUMES			
		CALIBRATION PERIOD		VERIFICATION PERIOD	
		MEAN	0.8 ≤ RATIO ≤ 1.2	MEAN	0.8 ≤ RATIO ≤ 1.2
SUSQUEHANNA R. AT WILKES-BARRE, PA.	9,960	0.94 ±0.05	6/6	1.00 ±0.04	5/5
WEST BR. SUSQUEHANNA R. AT WILLIAMSPORT, PA.	5,682	0.93 ±0.03	6/6	1.01 ±0.07	5/5
JUNIATA R. AT NEWPORT, PA.	3,354	0.93 ±0.05	6/6	1.15 ±0.2	4/5
SUSQUEHANNA R. AT MARIETTA, PA.	25,990	0.90 ±0.04	6/6	0.99 ±0.04	5/5
SUSQUEHANNA R. AT CONOMINGO, MD.	27,100	0.91 ±0.04	6/6	0.97 ±0.05	4/4
JAMES R. AT CARTERSVILLE, VA.	6,257	0.96 ±0.17	5/6	0.96 ±0.2	4/5
RAPPAHANNOCK R. NEAR FREDERICKSBURG, VA.	1,596	1.00 ±0.22	5/6	0.93 ±0.15	4/5
POTOMAC R. AT MARCOCK, MD.	4,073	0.88 ±0.06	6/6	0.95 ±0.13	5/5
SHERMANDOAN R. AT MILLVILLE, W.VA.	3,040	1.10 ±0.13	5/6	1.07 ±0.27	3/5
POTOMAC R. NEAR WASH., D.C.	11,560	0.94 ±0.06	6/6	0.94 ±0.10	5/5

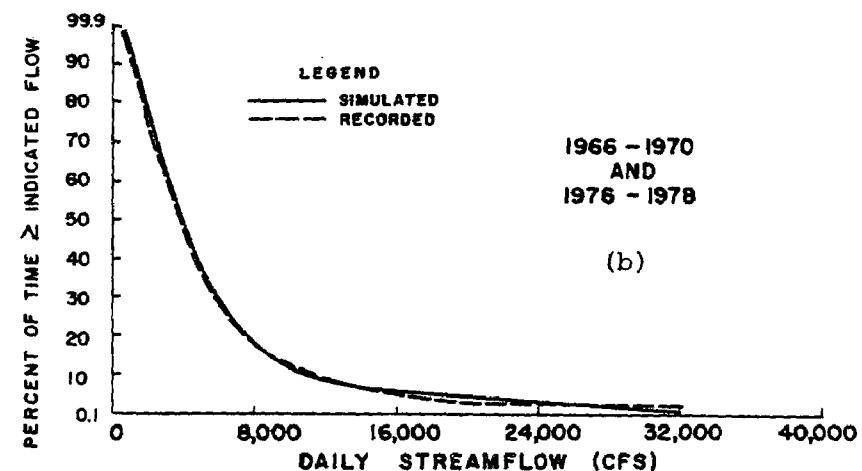
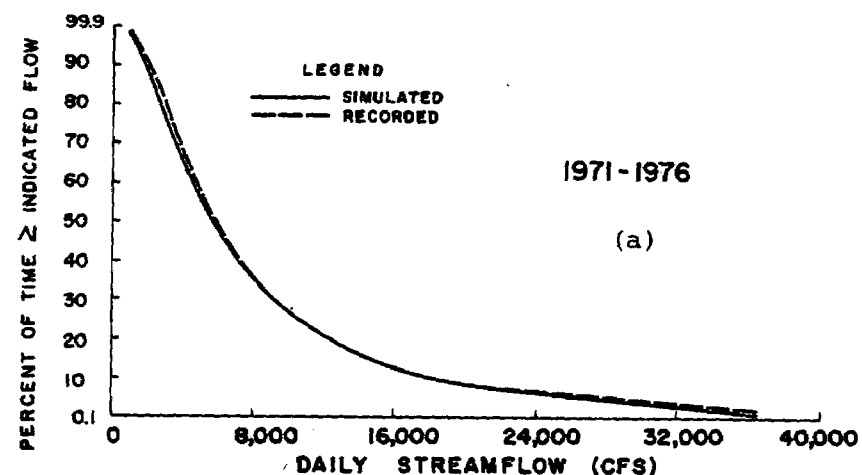


Figure 4. Flow-Duration Curves for
Calibration (a) and Verification (b)
Periods: James River at Cartersville,
VA (6,257 sq mi)

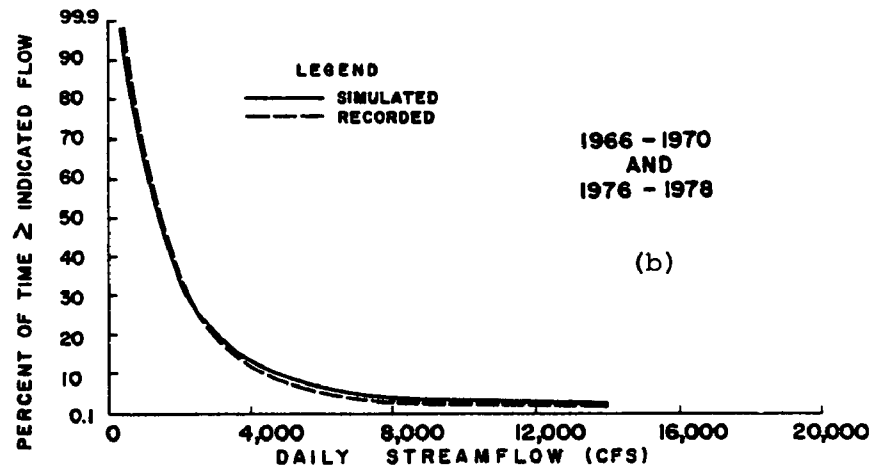
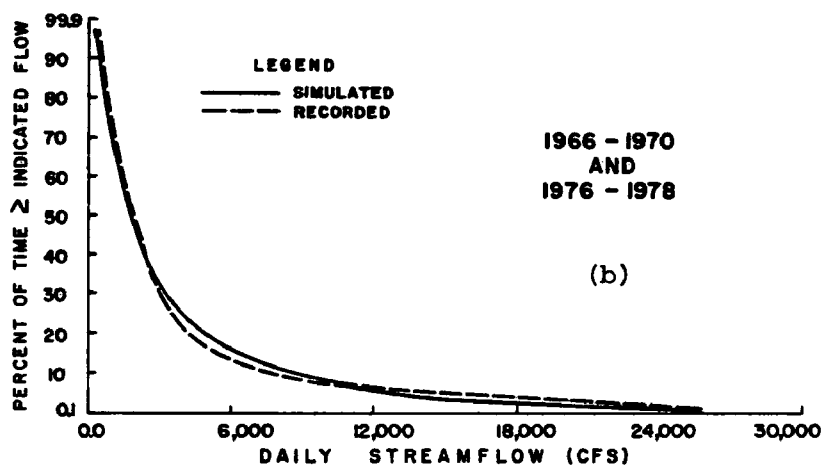
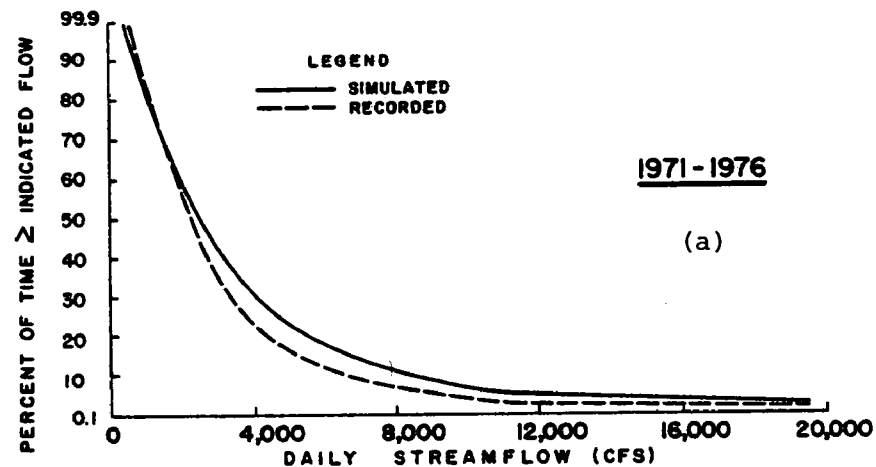
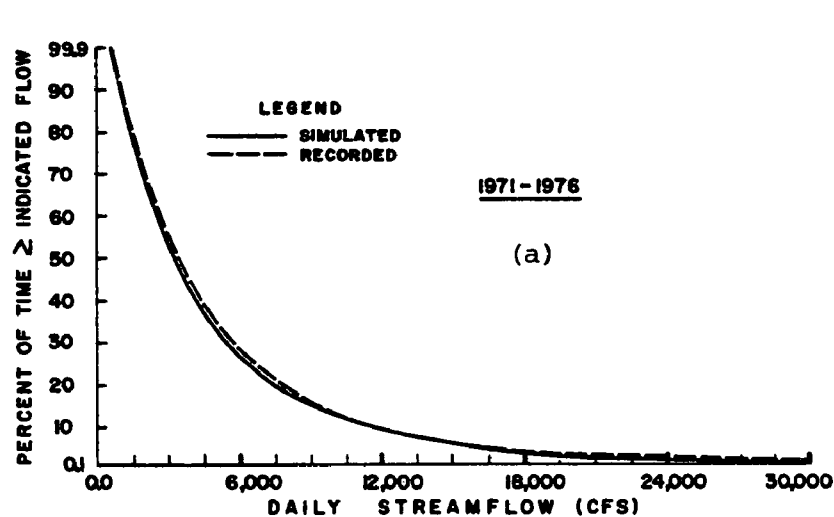


Figure 5. Flow-Duration Curves for Calibration (a) and Verification (b) Periods: Potomac River at Hancock, MD (4,073 sq mi)

Figure 6. Flow-Duration Curves for Calibration (a) and Verification (b) Periods: Shenandoah River at Millville, W.VA. (3,040 sq mi)

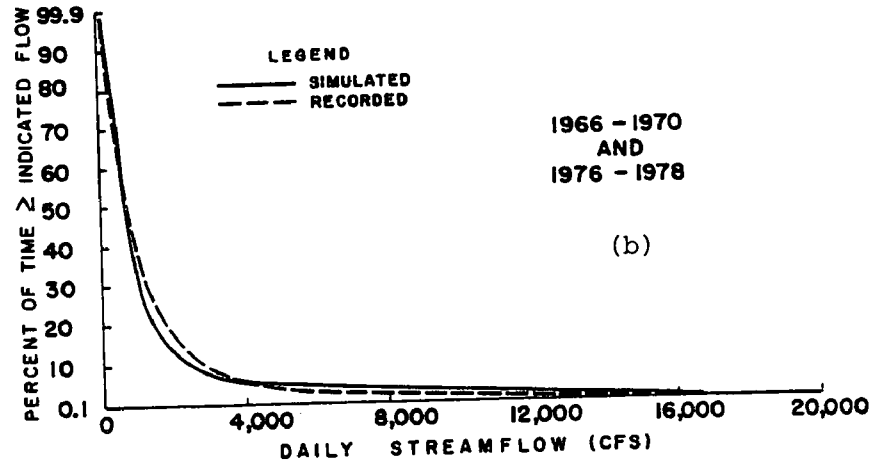
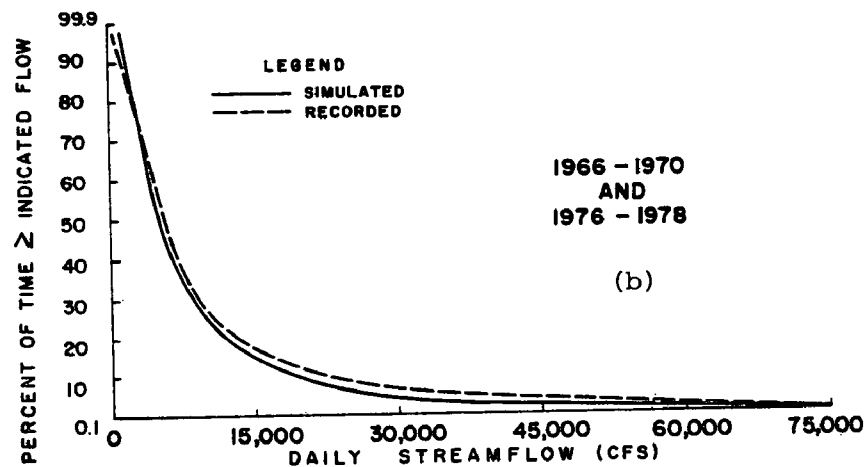
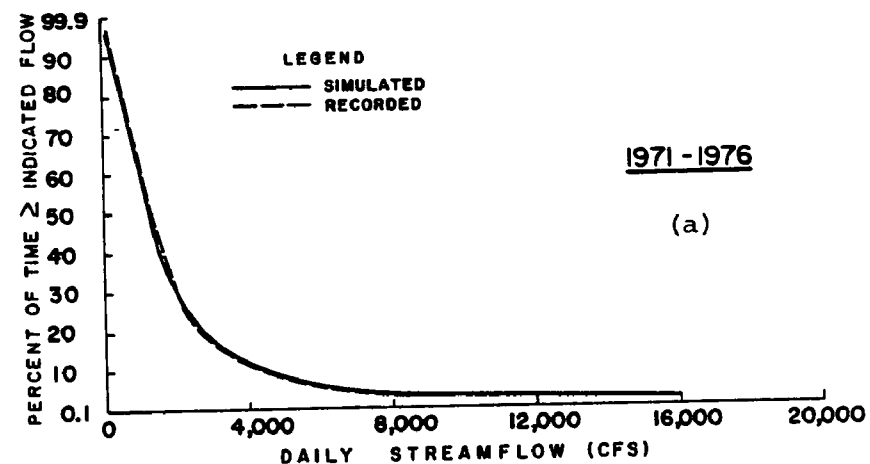
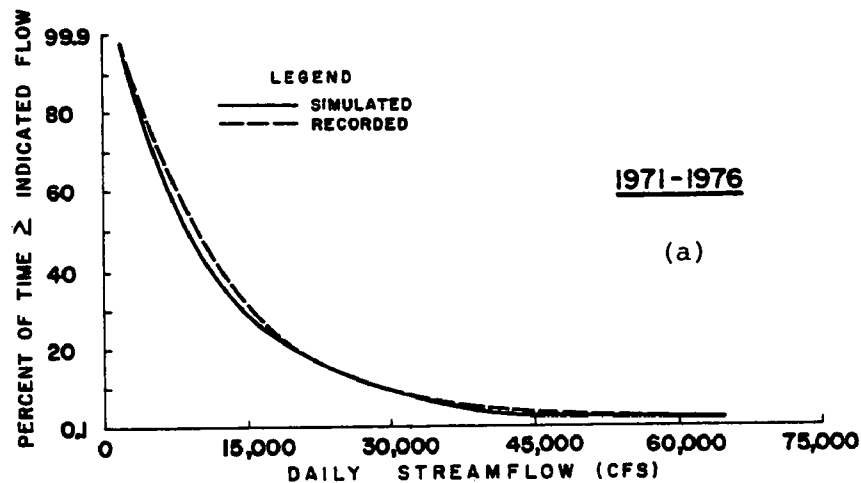


Figure 7. Flow-Duration Curves for Calibration (a) and Verification (b) Periods: Potomac River near Washington, D.C. (11,560 sq mi)

Figure 8. Flow-Duration Curves for Calibration (a) and Verification (b) Periods: Rappahannock River at Fredericksburg, VA (1,596 sq mi)

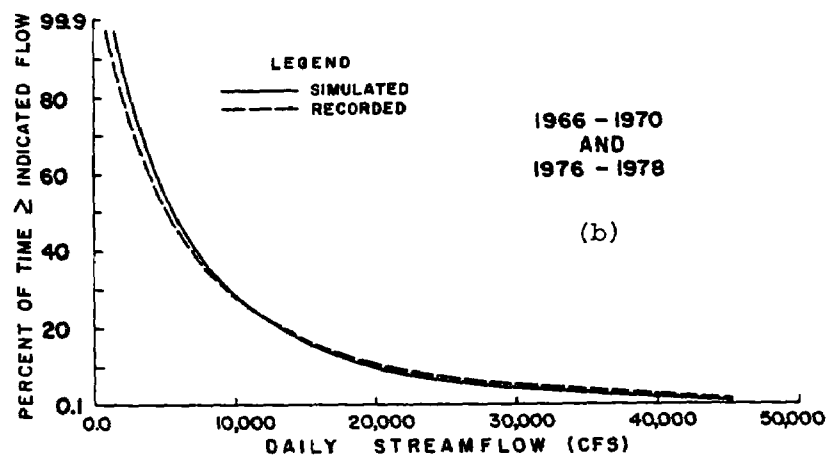
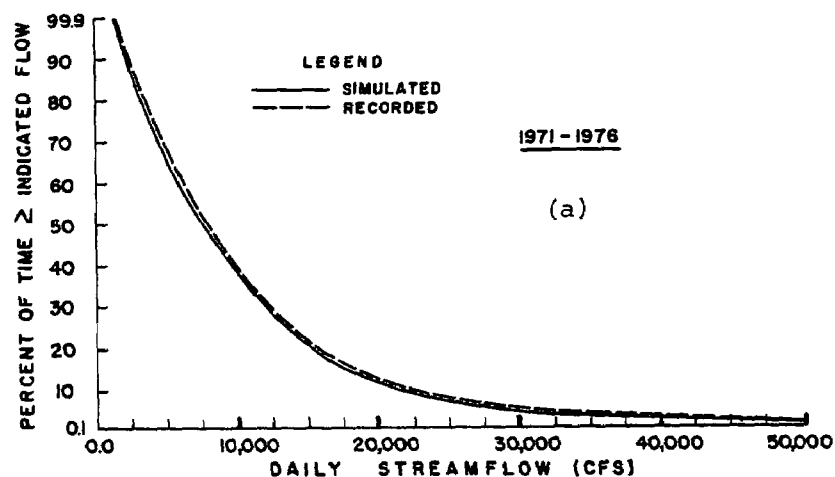


Figure 9. Flow-Duration Curves for Calibration (a) and Verification (b) Periods: West Branch Susquehanna River at Williamsport, PA (5,682 sq mi)

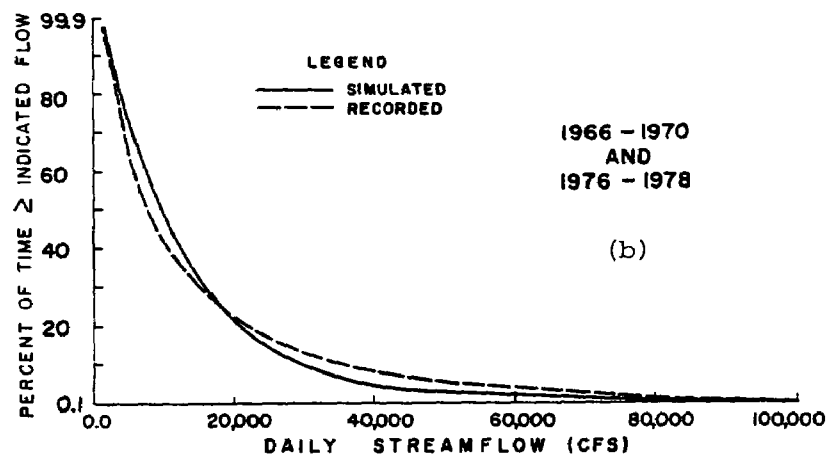
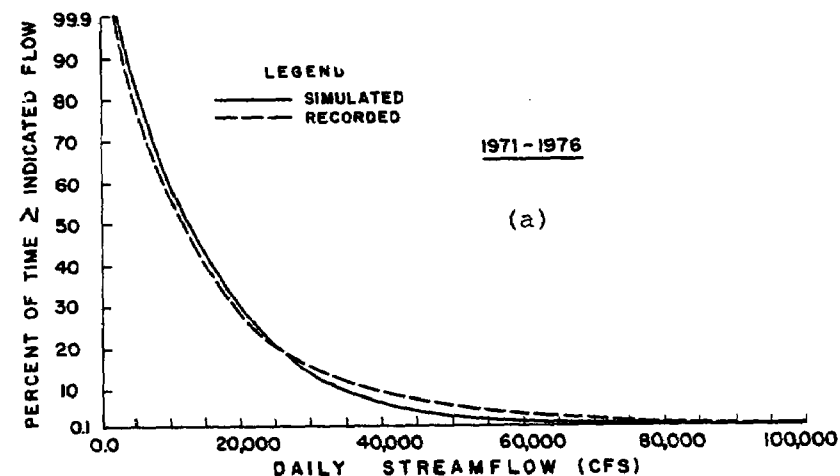


Figure 10. Flow-Duration Curves for Calibration (a) and Verification (b) Periods: Susquehanna River at Wilkes-Barre, PA (9,960 sq mi)

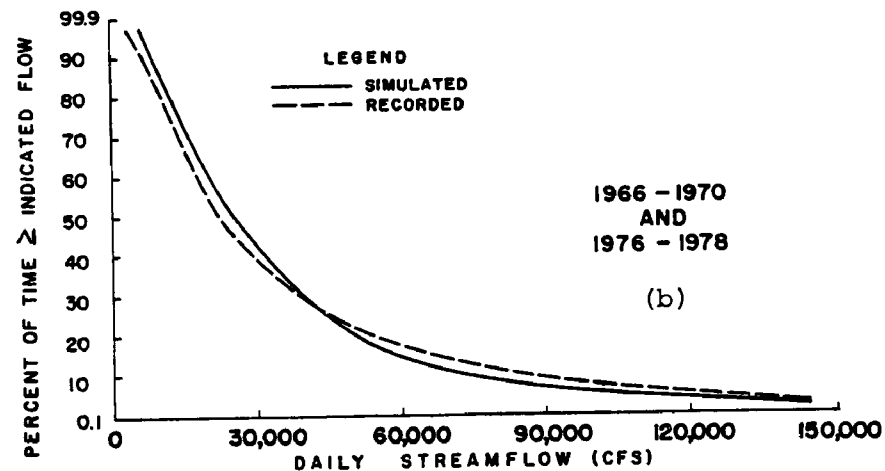
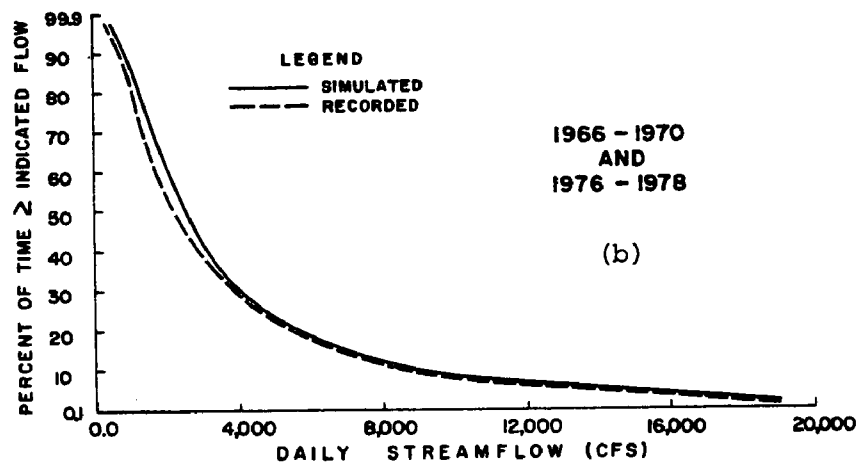
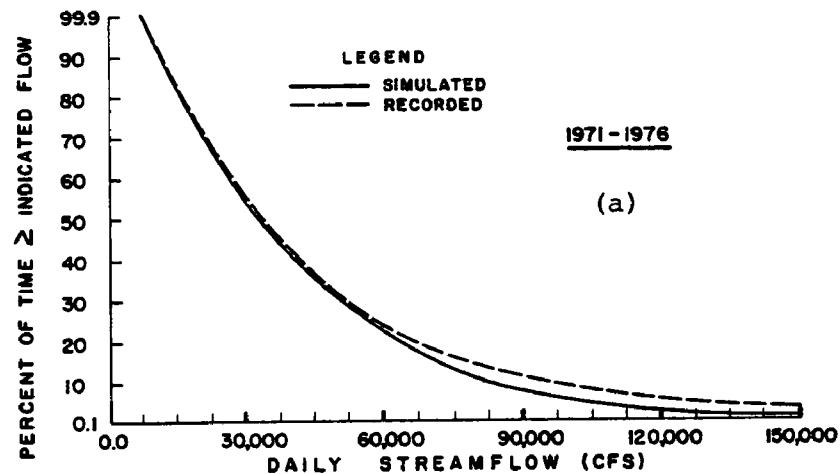
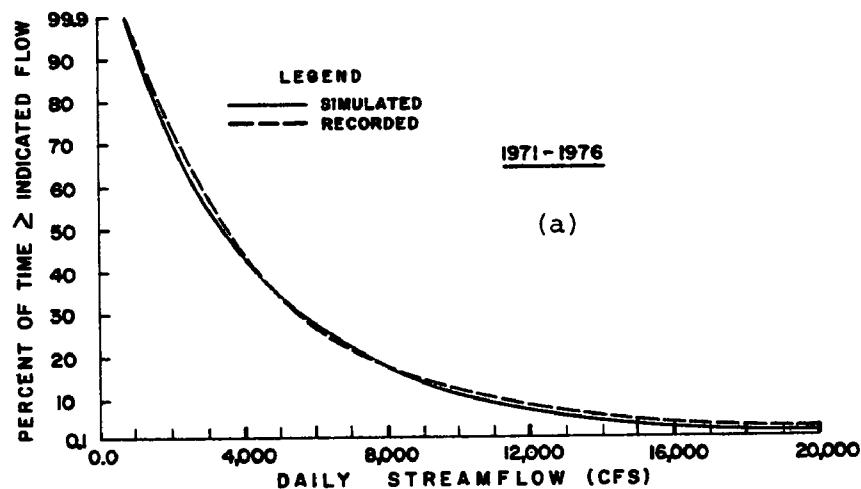


Figure 11. Flow-Duration Curves for Calibration (a) and Verification (b) Periods: Juniata River at Newport, PA (3,354 sq mi)

Figure 12. Flow-Duration Curves for Calibration (a) and Verification (b) Periods: Susquehanna River at Marietta, PA (25,990 sq mi)

undersimulated by the Model, tend to be characterized by frozen ground conditions which are not simulated by the River Basin Model as well as the highest raingage errors due to freezing conditions. Streamflow errors during drought periods, which were typically oversimulated by the River Basin Model, can be attributed in large part to the tendency of the Thiessen-weighting procedure to exaggerate the areal distribution of localized storms which tend to be more significant during droughts.

Comparisons of simulated and observed daily flow-duration curves are shown in Figures 4 through 12 for both calibration and verification periods at nine major streamgages. As may be seen, the agreement between simulated and observed curves is typically quite good, with goodness-of-fit for the verification period typically almost as good as for the calibration period. In general, the calibration period exhibits better agreement for low flow periods than does the verification period, which was characterized by drought periods that presented difficulties with the development of a representative mean segment rainfall record.

As another indication of goodness-of-fit, Table 3 summarizes statistics on the correlation between simulated and observed weekly streamflows. Correlation coefficients are based upon weekly streamflows because weekly-to-monthly flows were of greatest interest for the pollutant transport study. As may be seen in Table 3, correlation coefficients for the calibration period are somewhat higher than for the verification period, although coefficients for both periods are within acceptable ranges. The gages at the mouths of the three largest river basins are characterized by the highest correlation coefficients.

Comparisons of simulated and observed hydrographs for Hurricane Agnes (late June 1972) and Tropical Storm Eloise (late September 1975) reveal that the Model appears to handle these relatively infrequent events rather well at some gages. Sample comparisons are presented in Figure 13 for the gages on the West Branch Susquehanna River at Williamsport, Pennsylvania and on the Potomac River at Hancock, Maryland. It is felt that the River Basin Model handled infrequent storm events better than some earlier models (1,9,10) of smaller watersheds in large part because the rainfall during these storms tends to be rather uniformly distributed over sub-basins with areas on the order of 2,000 sq mi.

In summary, both calibration and verification results are very good particularly in light of the very large rainfall segments. Most of the remaining error can probably be attributed to factors such as frozen ground conditions which were not explicitly represented by the Model and to errors in the mean segment rainfall record due to localized rainstorms, low raingage densities in some areas, missing rainfall records, and freezing conditions.

Use of Hydrologic Model to Identify Production Run Periods

Introduction. In the case of low flow, high flow, and long-term assessments, model executions focus on impacts during the spring, summer, and fall when water temperatures are high enough to result in the most

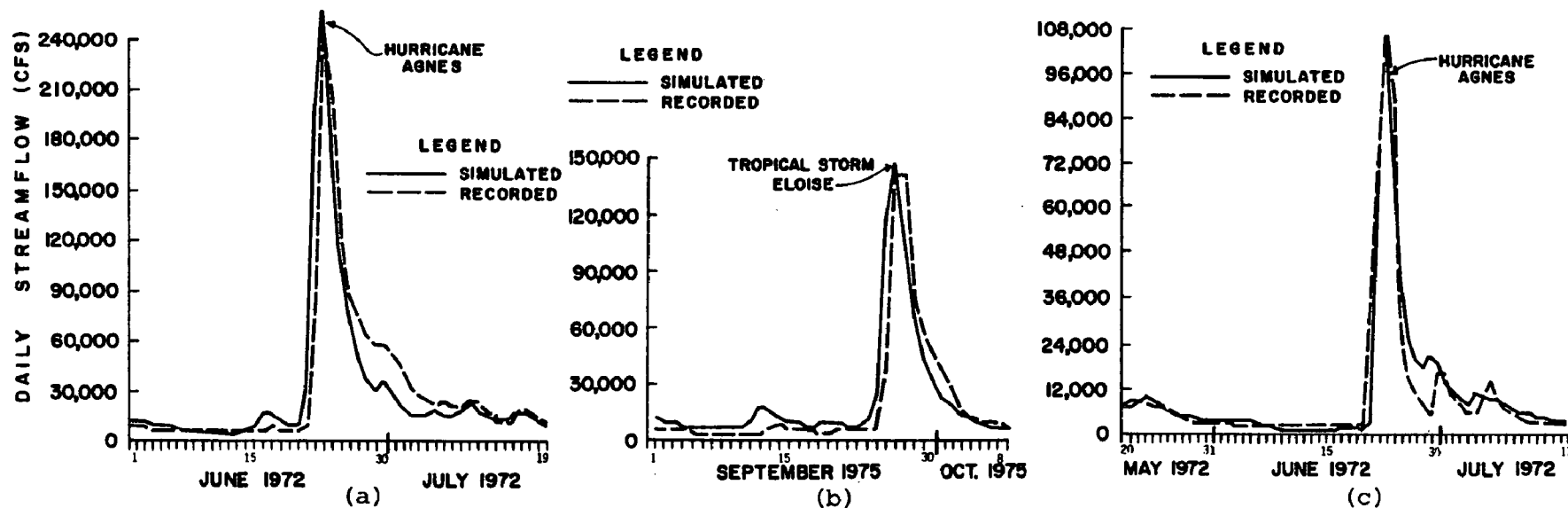
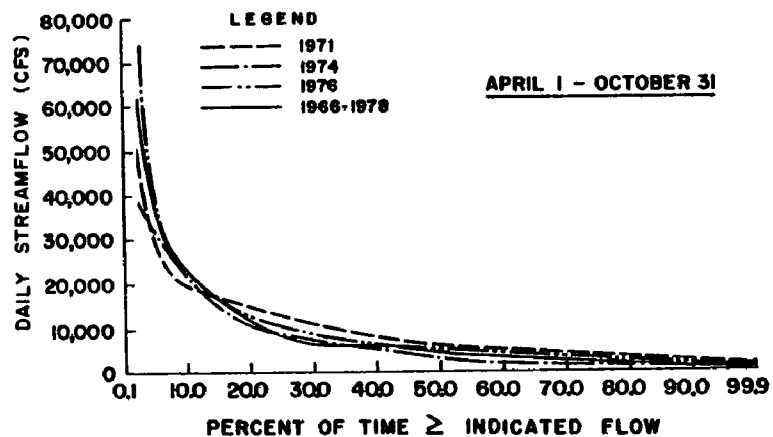


Figure 13. Comparison of Simulated and Recorded Hydrographs: (a) and (b) West Br. Susquehanna River at Williamsport, PA; and (c) Potomac River at Hancock, MD

POTOMAC RIVER NEAR WASHINGTON, D.C. (11,560 SQ. MI.)



SUMMATION OF RECORDED DAILY FLOWS: SUSQUEHANNA, POTOMAC, AND JAMES (43,807 SQ. MI.)

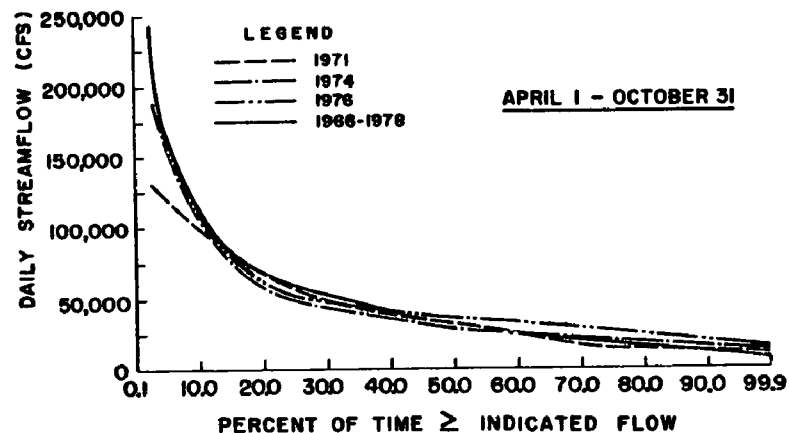


Figure 14. Sample Flow-Duration Curves for Recorded Daily Streamflow: Typical Year Analysis

Table 3

Correlation Coefficients for Weekly Streamflows at Major River Gages

STREAMGAGE	CORRELATION COEFFICIENT (WEEKLY STREAMFLOWS)	
	CALIBRATION PERIOD	VERIFICATION PERIOD
James River at Cartersville, VA	0.94	0.84
Potomac River at Hancock, MD	0.91	0.78
Shenandoah River at Millville, WV	0.92	0.74
Potomac River near Washington, D.C.	0.95	0.80
Rappahannock River near Fredericksburg, VA	0.85	0.81
West Branch Susquehanna River at Williamsport, PA	0.85	0.71
Susquehanna River at Wilkes-Barre, PA	0.88	0.74
Juniata River at Newport, PA	0.86	0.81
Susquehanna River at Marietta, PA	0.92	0.80

critical water quality problems within the Bay's estuarine system. Following calibration/verification, the hydrologic model was used to identify the periods to be used for production runs to evaluate water quality management strategies.

Analyses of Long-Term Water Quality Impacts. It is technically possible to execute the Bay Model package with many years of rainfall and streamflow records in order to assess long-term water quality impacts of a particular management strategy. However, since the computer costs for long-term continuous simulations can be very high, some investigations have relied upon a short period (e.g., a full year; several seasons) which can serve as a less expensive surrogate for the multi-year period of interest (1,4,16,17). This shorter "typical" period should be characterized by streamflow and water quality statistics that are reasonably close to the period of record for the meteorologic data which would be used for a long-term simulation. Production runs of the Model package with meteorologic records for the typical period are then assumed to produce streamflow and water quality statistics which approximate the statistics that would result from a model production run covering the entire period. In terms of streamflow statistics, this typical period can also be referred to as a period of "average wetness" since its flow-duration curve and total streamflow volumes will most closely approximate long-term conditions. Since the use of a typical period permits simulations of long-term water quality impacts at a reasonable cost, this approach was selected for management studies with the Bay Model package.

A fall-line monitoring study by the U.S. Geological Survey (18) had previously demonstrated a positive relationship between daily streamflow and pollutant loadings at the mouths of the Susquehanna, Potomac, and James rivers. The USGS study produced regression equations relating streamflow and pollutant loadings which can be used to produce loading-frequency relationships from a daily flow-duration curve. Therefore, a year characterized by a daily flow-duration curve that approximates the streamgage's long-term flow-duration curve is also characterized by

loading-frequency relationships which approximate long-term loading statistics. Daily flow-duration relationships for gages at the mouths of the Susquehanna, Potomac, and James rivers were screened to identify a typical year for water quality management studies. A composite flow-duration curve based upon the summation of daily flows at the three river mouth gages was also included in the screening study.

Because the available meteorologic record for River Basin Model studies covered the period 1966-1978, the selection of the typical period was based on analyses of the daily streamflow statistics associated with April through October of each year in this thirteen-year period. The year with April-October streamflow statistics which come closest to the statistics for the full thirteen-year period can be designated as a typical year for assessments of long-term impacts with the Bay Model package. Simulated flow-duration curves for individual years were plotted with the simulated flow-duration curve for 1966-1977 and the assessment of similarity in distribution was based upon visual inspection. Sample flow-duration curves are shown in Figure 14. Since 1974 exhibits better agreement with the 1966-1978 curves for the Susquehanna, Potomac, and "summation" gages, it was selected over 1976 as the most typical year.

Analyses of "Worst Case" Point Source Impacts. As suggested above, Model executions for a "dry year" with an extended low streamflow period can be expected to provide the greatest insights into the Baywide impacts of wastewater treatment strategies for the Chesapeake Bay Basin. Because it is characterized by the highest frequency of extreme low flows in the two largest river basins and the lowest overall volumes for the sum of Susquehanna, Potomac, and James basin streamflows, April-October 1966 was designated for dry year production runs of the Bay Model package.

Analyses of "Worst Case" Nonpoint Source Impacts. Model operations for a "wet year" characterized by relatively high streamflows will provide the greatest insights into "worst case" impacts of nonpoint pollution. A review of simulated flow-duration curves for the Susquehanna, Potomac, and James basins and the summation dataset indicates that 1972 is the wettest year for all four gages, with 1975 the second wettest. Since it was felt that a period which includes an event as rare as Hurricane Agnes (June 1972) may not be an appropriate "design condition" for basinwide assessments of nonpoint pollution controls, the second wettest year, 1975, was selected for wet year production runs.

Further Evaluations of Selected Periods. The decision to restrict the rainfall records to the period 1966-1978 was one based primarily on costs in an effort to keep the budget for the acquisition and analysis of NWS rainfall tapes from becoming prohibitive. Since NWS hourly rainfall records for the Chesapeake Bay Basin recording gages are currently available for 17 additional years (i.e., 1949-1965), it was necessary to screen observed April-October flow-duration curves for each year in the period 1949-1978 to demonstrate that the selected years were the most appropriate for Model production runs.

For the typical year comparisons, the flow-duration curves for the period 1966-1978 were found to adequately approximate the curves for the full 30-year period (1949-1978) covered by NWS hourly rainfall records, indicating that selections of a typical year based on comparisons with the shorter period were appropriate. Further, 1974 exhibited as good an agreement with the 1949-1978 period as did the only two years (1950 and 1961) in the earlier period which merited consideration as a typical year. Similar reevaluations reinforced the selections of 1966 and 1975 as the design dry year and wet year, respectively.

Acknowledgements

The work described herein was funded through a Cooperative Agreement with the U.S. Environmental Protection Agency's Chesapeake Bay Program (CPB). The assistance of James T. Smullen, EPA Project Officer, and Alan M. Lumb of the U.S. Geological Survey is gratefully acknowledged.

References

1. Hydrocomp, Inc., "The Occoquan Computer Model: Calibration, Verification, and User's Manual," prepared for Northern Virginia Planning District Commission, Falls Church, VA, May 1978.
2. Johanson, R.C., Imhoff, J.C., and Davis, H.H., "Users Manual for Hydrological Simulation Program - FORTRAN (HSPF)," EPA-600/9-80-015, U.S. Environmental Protection Agency, Athens, GA, April 1980.
3. Crawford, N.H., and Linsley, R.K., "Digital Simulation in Hydrology: Stanford Watershed Model IV," Dept. of Civil Engineering Technical Report 39, Stanford University, Stanford, CA, 1966.
4. Hartigan, J.P., et al., "Areawide and Local Framework for Urban Nonpoint Pollution Management in Northern Virginia," Stormwater Management Alternatives, Tourbier, J.T. and Westmacott, R., eds., University of Delaware, DE, April 1980, pp. 211-245.
5. Bonuccelli, H.A., Hartigan, J.P., and Biggers, D.J., "Computer Modeling for Watershed Management in Northern Virginia," Proceedings of Stormwater Management Model User's Group Conference: January 10-11, 1980, EPA 600/9-80-017, U.S. Environmental Protection Agency, Washington, D.C., March 1980, pp. 17-40.
6. Northern Virginia Planning District Commission (NVPDC), "Follow-up Assessments of Alternate AWT Operating Rules with Occoquan Basin Computer Model," prepared for Camp, Dresser, McKee, Inc., consultants to Virginia State Water Control Board, Richmond, VA, February 1980.
7. Arbruster, J.T., "Flow Routing in the Susquehanna River Basin: Part I - Effects of Raystown Lake on the Low-Flow Frequency Characteristics of the Juniata and Lower Susquehanna Rivers, Pa.," U.S. Geological Survey Water Resources Investigations 77-12, USGS, Harrisburg, PA, April 1977.

8. Hartigan, J.P., et al., "Calibration of Urban Nonpoint Pollution Loading Models," Proceedings of ASCE Hydraulics Division Specialty Conference on Verification of Mathematical and Physical Models in Hydraulic Engineering, ASCE, New York, NY, August 1978, pp. 363-372.
9. NVPDC, "Water Quality Modeling Study of Goose Creek, Broad Run, and Sugarland Run Watersheds," Falls Church, VA, June 1980.
10. NVPDC, "Modeling Study of Nonpoint Pollution Loadings from Potomac Embayment Watersheds," Final Report prepared for Virginia State Water Control Board, Richmond, VA, March 1981.
11. Lumb, A.M. and James, L.D., "Runoff Files for Flood Hydrograph Simulation," Journal of the Hydraulics Division, ASCE, Vol. 102, No. HY10, October 1976, pp. 1515-1531.
12. CH₂M-Hill, "Stormwater Management: A Comprehensive Study of the Muddy Branch and Seneca Creek Watersheds," prepared for Montgomery County (MD) Planning Board, Silver Spring, MD, April 1975.
13. Donigian, A.S. and Crawford, N.H., "Modeling Nonpoint Pollution from the Land Surface," EPA-600/3-76-083, U.S. Environmental Protection Agency, Environmental Research Laboratory, Athens, GA, July 1976.
14. Hydrocomp, Inc. Hydrocomp Simulation Programming: Hydrology Simulation Operations Manual, Palo Alto, CA, January 1976.
15. Lumb, A.M., "UROS04: Urban Flood Simulation Model, Part 1: Documentation and Users Manual," School of Civil Engineering, Georgia Institute of Technology, Atlanta, GA, March 1975.
16. Huber, W., "Discussion Remarks," Proceedings of Seminar on Design Storm Concept, Ecole Polytechnique de Montreal, Montreal, Quebec, 1979.
17. Southerland, E., "A Continuous Simulation Modeling Approach to Nonpoint Pollution Management," Dissertation presented to Virginia Polytechnic Institute & State University, Blacksburg, VA, in December 1981, in partial fulfillment of the requirements for the degree of Doctor of Philosophy in Environmental Sciences and Engineering.
18. U.S. Geological Survey, "Water Quality of the Three Major Tributaries to the Chesapeake Bay, January 1979-April 1981," prepared for USEPA Chesapeake Bay Program, November 1981.

The work described in this paper was not funded by the U.S. Environmental Protection Agency. The contents do not necessarily reflect the views of the Agency and no official endorsement should be inferred.

CONTINUOUS DO RESPONSE PREDICTED
USING CSPSS IS VERIFIED FOR
SPRINGFIELD, MISSOURI¹

By: James E. Scholl², P.E.
and
Ronald L. Wycoff², P.E.

ABSTRACT:

Springfield, Missouri was one of 15 receiving water sites studied for the 1978 Needs Survey to estimate the cost associated with controlling stormwater-induced pollution nationwide. Receiving water impacts on the James River near Springfield were evaluated using the Continuous Stormwater Pollution Simulation System (CSPSS), which is documented in a user's manual by Wycoff and Mara (1979). The simulation of James River DO concentrations was calibrated to match continuous in-stream DO measurements collected by the USGS between 1974 and 1977. This calibrated CSPSS model was then used to simulate the impact of the recently completed (November 1977) AWT facility in Springfield and to quantify the impact of alternatives to control pollution from urban stormwater runoff.

Since 1954, six major fishkills have occurred on the James River after storm events. At the outset of this project, the cause of those major fishkills was suspected to be urban stormwater pollution. However, as reported in a paper by Scholl and Wycoff (1981), the analysis, using CSPSS indicated that, the poor quality secondary effluent of the WWTP, rather than urban stormwater pollution, was probably the major cause of these fishkills. It is the purpose of this paper to present information which verifies the conclusions reported in the paper by Scholl and Wycoff (1981). The verification was obtained by developing a cumulative duration curve for DO concentrations observed at the calibration point on the James River between 1979 and 1980 (post-AWT conditions).

INTRODUCTION

In light of the significant costs associated with water pollution control projects, it is imperative that the potential for perceptible improvements in the use of a receiving water body be evaluated prior to committing public monies for such projects. The potential for perceptible improve-

¹Presented at the Stormwater and Water Quality Users Group Meeting, in Washington, D.C., March 25-26, 1982.

²Water Resources Engineer, CH2M HILL; P.O. Box 1647, Gainesville, Florida 32602. (904) 377-2442.

ments in receiving water use can be determined using water quality simulation if sufficient field data are available.

This paper summarizes the application of the Continuous Stormwater Pollution Simulation System (CSPSS) to the James River near Springfield, Missouri. The CSPSS is a water quality planning model developed for the Facilities Requirements Division of EPA. It was possible to calibrate CSPSS to observed dissolved oxygen (DO) concentrations in the James River using continuous water quality data collected by the U.S. Geological Survey (USGS). After the CSPSS was calibrated, the DO response was predicted for proposed AWT facilities and possible treatment of urban stormwater. Details related to DO calibration and prediction were published in a paper by Scholl and Wycoff (1981). Recent continuous DO data for the James River provide a unique opportunity to determine if the continuous DO responses predicted in 1978 using the CSPSS were in fact reasonable.

The discussion which follows includes brief descriptions of the Springfield study site, CSPSS, and results of the model calibration and verification for the James River.

SITE DESCRIPTION

The Springfield study area as shown on Figure 1 is located in the Missouri Ozark Plateau province of the White River basin. The City lies on an east-west ridge which divides two major watersheds in Missouri. Surface drainage north of this east-west divide flows into the Osage and Missouri River basins, and to the south of this divide drainage is into the James and White River basins. The James River is the major receiving water body of concern in this paper.

Incorporated in 1846, Springfield experienced little growth until westward railroad expansions occurred during the 1870's. In 1970, the population was estimated to be 145,000, with an incorporated area of 62.2 square miles. Improvements to storm drainage and wastewater collection facilities have not kept pace with recent urban growth, resulting in serious flooding and pollution problems. For example, six major fishfills have occurred in the James River downstream from Springfield since 1954. In November of 1977, construction of AWT facilities was completed at the City's Southwest Wastewater Treatment Plant (WWTP).

A review of water quality planning performed for Springfield's AWT facility, which cost approximately \$41.6 million (ENR approximately 2410), revealed shortfalls in the water quality planning process. The most apparent had to do with establishing a cause and effect relationship between pollutant loads from the Springfield urban area and observed fishkills on the James River. Since such a relationship was not clearly established, the potential for eliminating fishkills by constructing AWT facilities was not known. In fact, it was hypothesized by some investigators that only by capturing and treating urban stormwater would future fishkills be eliminated.

Five of the six USGS gauging stations within the study area are located as shown on Figure 1. The sixth station (No. 07050700) is located on the

James River upstream from Lake Springfield. The types of data collected at these stations are identified in Table 1. Continuous DO concentrations and temperature were monitored at three of these stations (No. 07052100, 07052160, and 07052250) beginning in 1972. Collection of this continuous data was terminated in 1980 at Station No. 07052250 (Frazier Bridge).

MODEL DESCRIPTION

The CSPSS was developed specifically for use in the receiving water impact portion of the 1978 and 1980 Needs Surveys. A User's Manual by Wycoff and Mara (1979) documents the model's theoretical basis and data requirements. The CSPSS is a computer-based probabilistic simulation model that generates long-term synthetic records of: (1) rainfall, (2) runoff, (3) runoff quality, (4) upstream receiving streamflow, (5) excess sewer system infiltration, (6) dry-weather WWTW discharges, and (7) receiving water quality response. In addition, the CSPSS accounts for storage and treatment of urban runoff. Pollutants considered are: (1) biochemical oxygen demand (BOD), (2) total kjeldahl nitrogen (TKN), (3) suspended solids (SS), (4) lead (Pb), and (5) fecal coliform. The recently added fecal coliform simulation capability is currently operational and will be documented in an updated version of the user's manual scheduled for completion in 1982. Receiving water responses can be simulated for DO concentrations, SS concentrations, total and dissolved lead concentrations, and fecal coliform organisms.

MODEL CALIBRATION

The continuous DO simulation for the James River was calibrated in 1978 for pre-AWT conditions (Scholl and Wycoff, 1981). This calibration was based primarily on continuous DO records collected by the USGS at Frazier Bridge Gauging Station No. 07052250 (see Figure 1) during water years 1974 through 1977. A summary of calibrated values for selected receiving water variables on the James River is provided in Table 2. The slope model as proposed by Tsivoglou and Neal (1976) was used to estimate a preliminary value of K_2 , the reaeration coefficient, for DO calibration. After reasonable values of all other input data were established, K_2 was adjusted until the predicted DO cumulative duration curve closely matched the duration curve observed at Frazier Bridge. The energy dissipation model, as proposed by Tsivoglou and Neal (1976) was then used to confirm that the calibrated K_2 value was in fact reasonable. The calibrated pre-AWT cumulative duration curve simulated by CSPSS and the observed pre-AWT (1974-1977) curve are shown on Figure 2. The agreement between these two curves is generally good, especially in the range of 0 to 6 mg/l. Statistical characteristics of the pre-AWT calibration are presented in Table 3.

To simulate the probable impact of AWT effluent on DO concentrations in the James River, the calibrated CSPSS data set was modified to include AWT effluent characteristics and a reduced benthic oxygen demand of 0.5 g O_2 /m²-day. The cumulative duration DO curve for this post-AWT simulation is shown on Figure 3. To simulate the probable impact of urban stormwater treatment after AWT facilities are operating in Springfield, the post-AWT

CSPSS data set was modified to include storage and treatment of urban stormwater. The results of these simulations did not alter the resulting cumulative duration curves enough to justify plotting a line separate from the post-AWT line shown on Figure 3.

MODEL VERIFICATION

In the fall of 1981, additional DO data for the Frazier Bridge calibration point became available for water years 1978, 1979, and 1980. Data for the last 2 years (1979 and 1980) were used to construct an observed post-AWT cumulative duration DO curve. Records for water year 1978 were not used since this was considered a transition year between pre-AWT and post-AWT conditions. These additional data provide a unique opportunity to compare post-AWT conditions predicted by the 1978 CSPSS simulations (Scholl and Wycoff, 1981) to actual post-AWT conditions observed during 1979 and 1980. The observed post-AWT cumulative duration curve is shown on Figure 3 along with the predicted post-AWT curve. This data verifies that the predicted DO curve for post-AWT conditions is reasonably close to the observed DO curve, especially in the range of 0 to 9 mg/l. Statistical characteristics of the post-AWT verification are presented in Table 3.

A probable cause of disagreement between predicted and observed post-AWT cumulative duration curves above 9 mg/l, is the low monthly mean temperatures observed during January and February of 1979 and 1980. For the calibrated CSPSS simulation, a mean monthly temperature of 11.0°C was used for both January and February. Observed monthly mean temperatures for the period 1979-1980 were 4.8 and 6.5°C for January and February, respectively. Thus, the predicted post-AWT cumulative duration curve does not account for the lower temperatures and higher DO concentrations observed during 1979 and 1980.

Comparing the pre- and post-AWT cumulative duration curves on Figure 3 at a DO concentration of 5.0 mg/l indicates that the observed decrease in the frequency of exceedance was 44.5 percent. The decrease predicted by CSPSS was 42 percent. In addition, the area between observed pre- and post-AWT curves indicates that the average increase in DO concentrations at Frazier Bridge was approximately 3.30 mg/l. The average increase predicted by CSPSS was approximately 2.90 mg/l.

Based on this analysis, it appears logical to conclude that urban stormwater was not the cause of low DO and subsequent fishkills on the James River. Rather, it appears that the poor quality secondary effluent of the WWTP was the likely cause of low-DO fishkills.

CONCLUSIONS

1. Continuous rainfall/runoff/receiving water quality simulation such as provided by the CSPSS and other available models can be a valuable tool in AWT planning and can quantify the water quality response of alternative pollution control strategies.
2. Continuous problem-oriented water quality monitoring programs are

extremely valuable aids to the decision-making process and should be encouraged. Such programs can provide a sound basis for the optimum investment of public monies.

ACKNOWLEDGEMENTS

This work was fully funded by the Facility Requirements Division of the EPA as part of the 1982 Needs Survey, Contract No. 68-01-5890. James A. Chamblee was the project officer.

REFERENCES

1. Scholl, J.E., and Wycoff, R.L. 1981. "Continuous DO Simulation at Springfield, Missouri," Journal of the Environmental Engineering Division, ASCE, Vol. 107, No. EE1, Proc. Paper 16021, pp 69-82.
2. Tsivolgou, E.C., and Neal, L.A. 1976. "Tracer Measurement of Reaeration: III. Predicting the Reaeration Capacity of Inland Streams," Journal of the Water Pollution Control Federation, Vol. 48, No. 12, pp 2669-2689.
3. Wycoff, R.L., and Mara, M.J. 1979. "Continuous Stormwater Pollution Simulation System--User's Manual," EPA-430/9-79-004, U.S. Environmental Protection Agency, Washington, D.C.

Table 1
USGS GAUGING STATIONS ON WILSONS CREEK AND JAMES RIVER

<u>Location</u>	<u>Station No.</u>	<u>Period of Record</u>	<u>Drainage Area (mi²)</u>	<u>Type of Data Collected</u>
Wilsons Creek near Springfield, MO	07052100	9-Years (1972-81)	31.4	Flow, continuous DO concentrations, and temperature
Wilsons Creek near Battlefield, MO	07052160	11-Years (1968-70) (1972-81)	55.0	Flow, continuous DO concentrations, and temperature
US James River near Springfield, MO	07050700	26-Years (1955-81)	246.0	Flow only
James River near Nixa, MO	07050750	12-Years (1966-75) (1977-80)	273.0	Daily water temperature only. Discontinued 1980.
James River near Wilsons Creek, MO	07051600	14-Years (1967-81)	329.0 ^a	Monthly water quality only
James River near Boaz, MO	07052250	8-Years (1972-80)	462.0	Flow, continuous DO concentrations, and temperature. Discontinued in 1980.

^aEstimated drainage area from USGS quadrangle map.

Table 2

CALIBRATED JAMES RIVER RECEIVING WATER VARIABLES

<u>Receiving Water Variable</u>	<u>Calibrated Value</u>
Mean annual upstream flow ^a , cfs	325.0
Carbonaceous waste decay rate, K_1 , day ⁻¹ for stormwater and upstream flow	1.00
Carbonaceous waste decay rate, K_1 , day ⁻¹ for WWTP effluent	1.42
Atmospheric reaeration rate, K_2 , day ⁻¹	3.06
Nitrogenous waste decay rate, K_3 , day ⁻¹	0.30
Sediment oxygen demand, $\frac{\text{g oxygen}}{\text{m}^2\text{-day}}$	1.00
Maximum monthly temperature ^b , °C	30.50
Mean upstream BOD ^b , mg/l	1.89
Mean upstream TKN ^b , mg/l	0.34
Mean upstream DO deficit ^b , mg/l	1.34

^aObserved daily flow values for a representative 5-year period were input to CSPSS.

^bMonthly mean values were input to CSPSS.

Table 3

STATISTICAL CHARACTERISTICS OF SIMULATED
PRE-AWT AND POST-AWT CUMULATIVE DO CONCENTRATIONS

<u>Statistical Parameter</u>	<u>Pre-AWT Value</u>	<u>Post-AWT Value</u>
Number of data points	11	12
Average error, % of time equal to or less than indicated DO concentration	2.08	5.17
Relative error, % of time equal to or less than indicated DO concentration	0.03	0.08
Standard error of estimate, % of time equal to or less than indicated DO concentration	4.35	11.76
Coefficient of variation	0.07	0.19
Linear regression intercept, % of time equal to or less than indicated DO concentration	0.27	4.00
Linear regression slope	0.96	0.86
Linear regression correlation coefficient	0.995	0.975

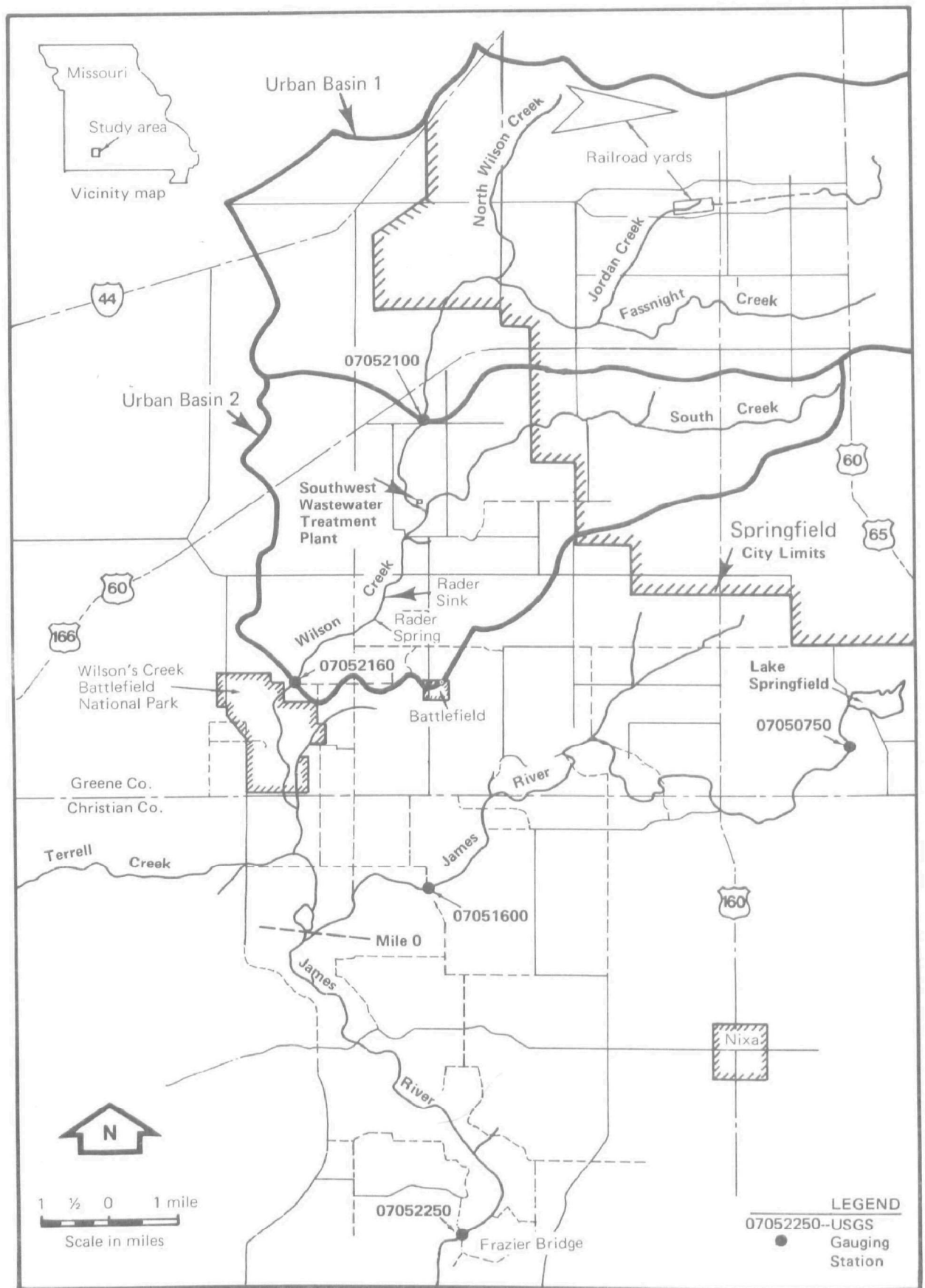


FIGURE 1. Map of Springfield, Missouri, Study Area (1 mile = 1,607 m).

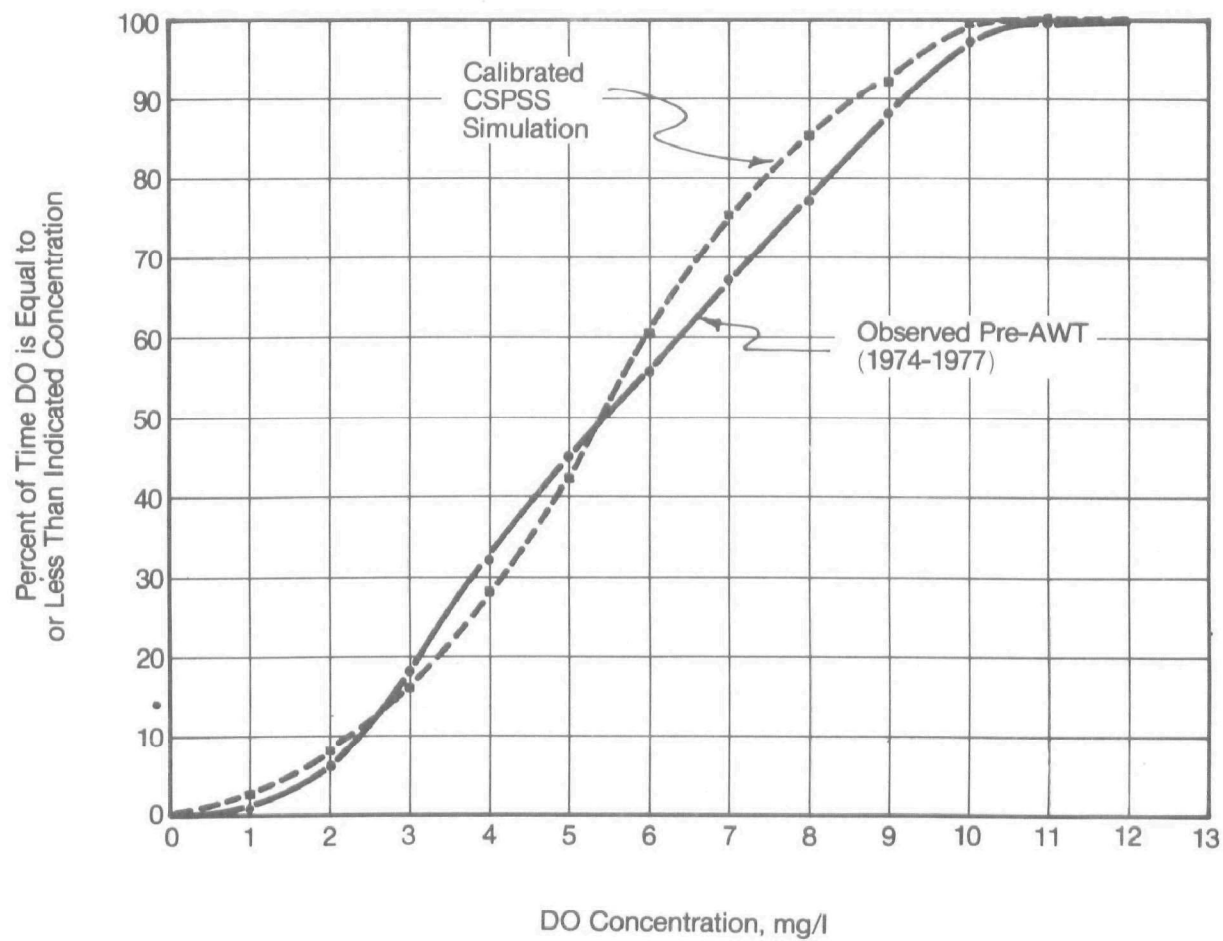


FIGURE 2. Calibration of DO on James River at Frazier Bridge.

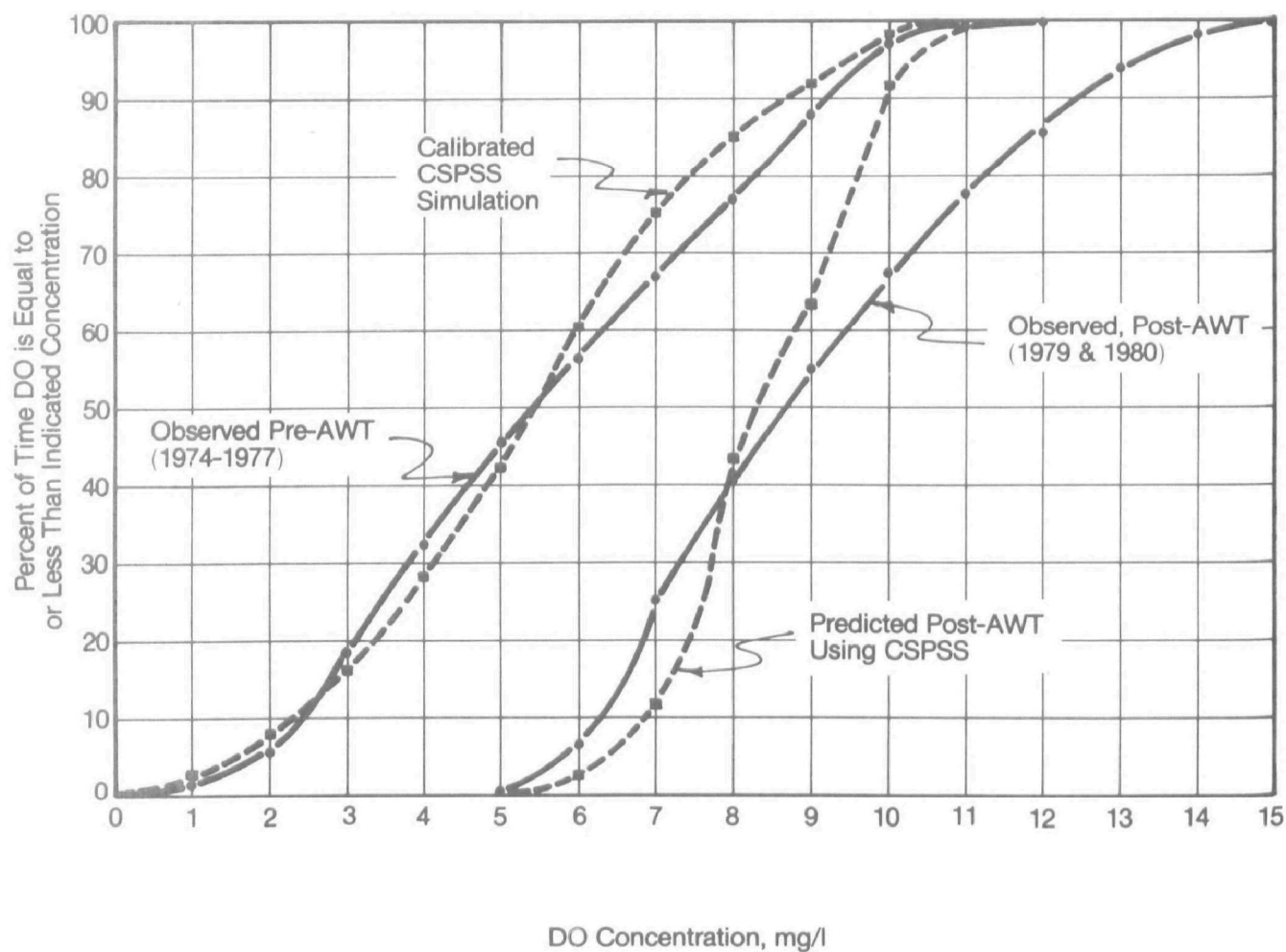


FIGURE 3. Calibration and verification of continuous DO response on the James River near Springfield, Missouri.

The work described in this paper was not funded by the U.S. Environmental Protection Agency. The contents do not necessarily reflect the views of the Agency and no official endorsement should be inferred.

USE OF CONTINUOUS SIMULATION MODEL CALIBRATION
TECHNIQUES TO DEVELOP NONPOINT POLLUTION LOADING FACTORS

By John P. Hartigan¹, Thomas F. Quasebarth²,
and Elizabeth Southerland³

Introduction

This paper describes the derivation of nonpoint pollution loading factors for a River Basin Model (1) of the 64,000 sq mi drainage area of Chesapeake Bay (see Figure 1). The purpose of the River Basin modeling study was to compare the delivery of point source and nonpoint pollution loadings of nitrogen and phosphorus to the Bay's estuarine system and to study locational differences in pollutant contributions. The River Basin Model was also used to evaluate alternate eutrophication management strategies for the Bay's estuarine system.

To develop nonpoint pollution loading factors for rural-agricultural and urban land use categories, a version (2) of USEPA's NPS model (3) was calibrated to several test watersheds characterized by relatively homogeneous hydrologic characteristics and a single land use. A total of 25 test watersheds were monitored from late 1979 through mid-1981 under a \$2.5 million study funded by the EPA Chesapeake Bay Program (4). An earlier twelve-month monitoring study (1976-1977) of 16 urban test watersheds in the Virginia suburbs of Washington, D.C. produced the majority of the urban nonpoint pollution loading data (2). This paper focuses on the development of rural-agricultural loading factors and the verification of 1976-1977 urban loading factors described elsewhere (2) through the calibration of the NPS model to the EPA Chesapeake Bay Program test watersheds. River Basin Model simulations which verified the nonpoint pollution loading factors are also described.

Test Watershed Monitoring Studies

In most cases, the test watershed sites covered only one of the following land use categories: forest; pasture; high tillage cropland; low tillage cropland; and urban residential. Since urban land uses only represent approximately 3% of the Chesapeake Bay drainage area, the test watershed studies focused on rural-agricultural land uses.

As shown in Figure 1, the test watersheds monitored under the EPA Chesapeake Bay Program were located in Coastal Plain and Piedmont river basins in the vicinity of the Bay's estuarine system. A summary of the test watershed monitoring sites is presented below:

¹Director, Engineering-Planning Division, Northern Virginia Planning District Commission (NVPDC), 7630 Little River Turnpike, Annandale, VA 22003

²Environmental Planner-Engineer, NVPDC

³Environmental Engineer, NVPDC

RIVER BASIN	LOCATION	NO. OF SITES	INVESTIGATOR
Occoquan River	Northern Virginia	5	Virginia Polytechnic Institute & State University
Ware River	Southeastern Va.	3	Va. Institute of Marine Science
Pequea Creek	Lancaster, Pa.	3	U.S. Geological Survey
Patuxent River	Maryland	5	State of Maryland
Chester River	Maryland	9	State of Maryland

Each test watershed site was equipped with a flowmeter, automatic sampler, and was served by a continuous recording raingage located within or nearby the site. Either a natural (e.g., ephemeral stream) or artificial (e.g., H-flume, Parshall flume) drainage control was typically used to establish stage-discharge relationships at the outlet of each watershed. The sampling interval was generally automatically initiated by the flowmeter at the start of a runoff event. For studies which relied upon flow-composite sampling methods, the flowmeter activated the sampler at preselected increments of runoff volume. For studies which relied upon



Figure 1. Map of Chesapeake Bay Basin Showing Locations of River Basins with Test Watersheds: Pequea Creek (A), Chester River (B), Patuxent River (C), Occoquan River (D), and Ware River (E)

sequential-discrete sampling methods (i.e., collection of discrete samples at numerous points along the runoff hydrograph), the flowmeter activated the sampler at preselected stage increments. At the larger sites which exhibited dry weather flow, baseflow samples were periodically collected. Runoff and baseflow samples were analyzed for plant nutrients and total suspended solids, with periodic analyses for organics.

At the time the test watershed monitoring studies were designed and implemented, a work program for data management and model calibration had not yet been developed, although a follow-up modeling study was under consideration. The absence of a modeling study work program at the start of the monitoring studies tended to significantly complicate data reduction/management activities during the modeling effort and to reduce the amount of monitoring data that was suitable for model calibration studies. The final section of this paper discusses specific problems and recommendations for coordinating future test watershed monitoring and modeling investigations.

Data Reduction/Management Requirements for Model Calibration

Introduction. The test watershed monitoring investigators reduced the data required to characterize the runoff pollution loadings from each runoff and baseflow sample. Investigators who relied upon flow-composite sampling techniques reported mean flow rate and mean concentration data for the runoff or baseflow sampling interval, while investigators who relied upon sequential-discrete sampling methods reported instantaneous flow rate and instantaneous concentration for each runoff or baseflow sample. All other meteorologic and hydrologic data required for model calibration typically had to be reduced by the modeling investigator.

Meteorologic Data. Since the test watersheds were relatively small, a 15-minute time step was required for the continuous rainfall record to ensure that the rainfall interval was not significantly greater than the watershed's time of concentration. Drum raingage stripcharts used at the Pequea Creek and Ware River basin sites were manually reduced, while other rainfall stripcharts were reduced with a Numonics digitizer equipped with software to create files with the appropriate time-step. Approximately 1.0-1.5 yrs of stripchart record was reduced for the modeling studies. Since the monitoring investigators were only required to report and analyze water quality monitoring data, raingage maintenance appeared to receive the lowest priority of all equipment checks and considerable gaps were found in the onsite records. During periods when the sampling station was shut down due to a breakdown of either the flowmeter or automatic sampler, the raingage was sometimes shut down until water quality sampling was resumed. Since a continuous simulation model requires rainfall records covering the periods between monitored runoff events in order to calculate antecedent soil moisture and sediment accumulations for each monitored storm, missing rainfall records for periods when the onsite raingage was shut down had to be constructed from a nearby raingage. Separate software was developed to create a continuous rainfall file for input to the NPS model.

The other meteorologic input file required for the NPS model calibration study is a time series of daily potential evapotranspiration for the test watershed monitoring period. A continuous potential ET record was developed for each river based upon meteorologic data at the nearest NWS station.

Hydrologic Data. Since it is advisable to use a long-term runoff record to calibrate a continuous simulation model, the reported flow records for runoff events with water quality samples were expanded to include all flow records collected during the monitoring period. Although all monitoring sites were equipped with continuous recording flowmeters, the Pequea Creek test watersheds were the only sites with a complete daily streamflow record. The flow records at some sites were restricted to those runoff events with water quality samples. Stripcharts with additional flow records were reduced with the same digitizer software used to construct rainfall records.

Since the quality control programs of most monitoring investigators concentrated on laboratory analyses, the modeling investigator was required to perform most of the quality assurance checks on the hydrometeorologic datasets. The digitized rainfall and runoff records were integrated for each storm event and rainfall and runoff volumes were compared to identify potential water balance problems due to such factors as backwater, an incorrect stage-discharge relationship or an error in the reported flowmeter setting. Flow stripcharts for monitored storms were also checked for "flat-top" hydrographs which indicated that the maximum stage exceeded the full-scale setting of the flowmeter. In cases of spurious rainfall/runoff ratios or "flat-top" hydrographs, the runoff and water quality data were deleted from the observed dataset for model calibration.

Water Quality Data. Software was developed to calculate total storm loads from datasets with mean or instantaneous flow rates and concentrations for each runoff sample. For test watersheds with flow-composite samples, the product of mean flow rate and mean concentration was multiplied by the storm duration to calculate total load. For test watersheds with sequential discrete samples, the time series of instantaneous loading rates (i.e., product of instantaneous flow rate and concentration) was numerically integrated between the first and last sample time to calculate total loads for each storm. Mean storm concentrations were also calculated for the sequential discrete sampling datasets. Dry weather flow concentration statistics were calculated for test watersheds with significant amounts of baseflow.

Test Watershed Data. Land use and drainage area data was typically based upon maps, drawings, and tables compiled by the monitoring investigator, which were checked through site inspections and with available aerial photographs and topographic maps. At one test watershed where a check of rainfall/runoff ratios revealed a serious water balance problem, the authors performed a plane-table survey which produced a significant increase in the drainage area and more reasonable rainfall/runoff relationships. For urban test watersheds, percent imperviousness was determined by planimetering aerial photographs or site plans.

Soils characteristics for each test watershed were derived from county soil series maps and surveys. The predominant hydrologic soil group was determined and average values of permeability, total water holding capacity, and erodibility were calculated for use in deriving hydrologic and nonpoint pollution model parameters.

Average overland flow slope was typically reported by the monitoring investigator. Reported values were checked with 1:24,000 scale maps of the test watershed and surrounding areas.

For cropland sites, data on monthly vegetative cover and the timing and extent of tillage activities are required to accurately model soil loss. Based upon discussions with local SCS staff and information on the timing and extent of harvest and tillage operations at the test watershed, a time series of monthly ground cover was derived for each cropland site. Since the NPS model does not permit the user to alter ground cover time series from year-to-year, two different input datasets were sometimes required to model cropland watersheds with more than one year of monitoring data due to changes in harvest and or tillage dates from one year to the next. The monthly ground cover time series and tillage parameter values were refined during model calibration to help achieve acceptable agreement between simulated and observed sediment loadings.

Although the monitoring investigators made an effort to select test watersheds which included only one land use, finding an acceptable catchment with a single land use was not always possible. For test watersheds with a mixed land use pattern, aerial photographs of the test watershed were checked to determine the character and extent of any secondary land uses. In cases where nonpoint pollution loading rates from the secondary land use were significantly higher than the loading rates for the primary land use, the complexity of the model calibration study was significantly greater. An example is the forestland test watershed (Site #2) in the Pequea Creek basin which included a high-tillage cropping site (approximately 13% of drainage area) that contributed the majority of the nonpoint pollution loads during major storm events. In such a case, loading factors for the secondary land use had to be set based on model calibration for a similar test watershed prior to model calibration at the mixed land use site. Also, the monitoring dataset had to be screened to identify those storm events (e.g., minor runoff events in the case of Pequea #2) which are least likely to be characterized by major nonpoint pollution loading contributions from the secondary land use.

Description of NPS Model

Introduction. NPS is a continuous simulation model which includes hydrologic and nonpoint pollution loading submodels that are executed sequentially. A flow chart summarizing the processes represented by the model is shown in Figure 2.

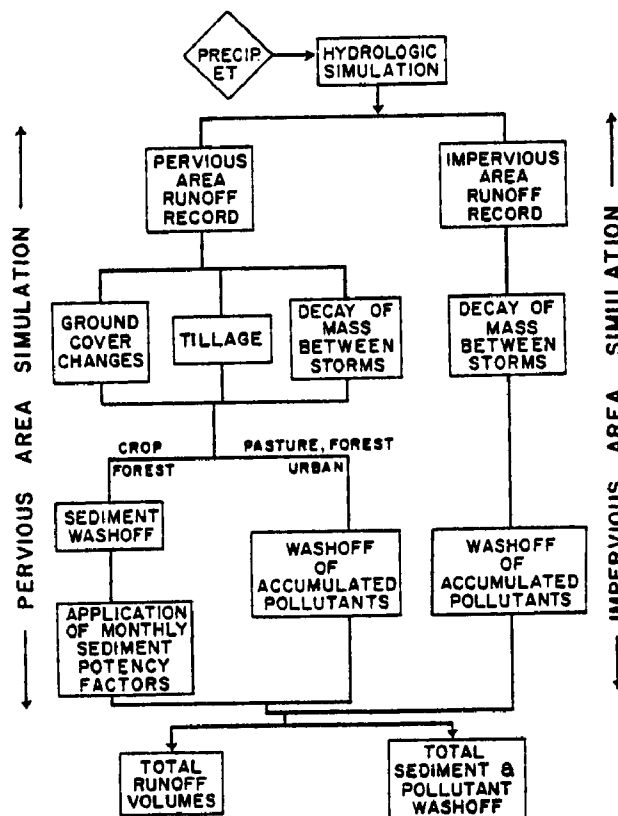


Figure 2. Hydrologic and Nonpoint Pollution Loading Processes Represented by NPS Model

Hydrologic Submodel. Based upon a modified version of the Stanford Watershed Model (5), this submodel is operated with 5-minute, 15-minute, or hourly rainfall records and daily evaporation records. It calculates the amount of rainfall converted to runoff, a continuous record of soil moisture, and subsurface recharge of stream channels. Included among the most sensitive model parameters are the infiltration rate (INFIL), which is based on soils characteristics such as hydrologic soil group and permeability, and the soil moisture storage capacities (LZSN and UZSN) which are based upon the soil's water holding capacity (2,6). A discussion of hydrologic model calibration procedures is presented elsewhere (6). During storm periods, rainfall is distributed among surface runoff and soil moisture storage compartments based upon adjusted infiltration rates and the nominal storage capacities assigned to different sections of the soil profile. Between rainstorms, water storage in soil moisture zones is depleted by mechanisms such as evapotranspiration and subsurface recharge of streams, thereby freeing up soil moisture storage capacity for rainfall inputs from the next storm.

For the model calibration studies of the small test watersheds, channel routing was neglected due to the short times of concentration. Previous model calibration studies for small watersheds are described elsewhere (2).

Nonpoint Pollution Submodel. The nonpoint pollution loading submodel of the modified NPS model (2) operates on rainfall intensity records and on the hydrologic submodel's output of surface runoff and subsurface flow records. Unlike other options available in the HSPF package, such as the ARM model (7), the NPS model treats all constituents conservatively and does not transport pollutants between the idealized soil moisture storage compartments.

For cropland, the model assumes that sediment generation and washoff are the driving forces for loadings of all pollutants. Cropland loadings of sediment, which are calculated from 15-minute rainfall records with a soil loss algorithm related to the Universal Soil Loss Equation, are assigned sediment "potency factors" (i.e., ratio of pollutant mass to sediment mass) to calculate loadings of other pollutants. For urban and pasture land uses, nonpoint pollution washoff algorithms relate the washoff of accumulated pollutant loads to the simulated runoff rate in each time-step. Accumulated pollutant loads at the start of a rainstorm are calculated from the "daily pollutant accumulation rates" (lbs/ac/day) assigned to each land use classification to represent the buildup of pollutants on the land surface and in the atmosphere (i.e., air pollution). For the forestland category, pollutant loading calculations are based upon soil loss/potency factors as well as daily pollutant accumulations, with the former more prominent during periods of low leaf cover and the latter more prominent during periods of high leaf cover.

Given the state-of-the-art of nonpoint pollution loading models, loading factors such as sediment potency factors and daily pollutant accumulation rates are probably best viewed as empirical factors which can provide a reasonable approximation of a land use's nonpoint pollution loading potential, much like the C coefficient in the "rational formula" is viewed as an empirical factor that relates rainfall intensity to peak runoff. The model has the capability to use monthly variations in pollutant loading factors. This feature permits a representation of variations in the pollutant loading potential of cropland areas due to such factors as fertilizer/manure applications, crop harvest, etc. Subsurface flow loadings based upon user-specified concentrations are added to hourly runoff pollution loadings and delivered to the outlet of the test watershed.

Test Watershed Model Calibration

Introduction. Not all of the test watersheds were characterized by sufficient land use homogeneity and hydrometeorologic data to permit NPS model calibration. Sufficient hydrometeorologic and water quality data was available to calibrate the NPS model to 11 of the 12 acceptable sites in the Occoquan River, Ware River, and Pequea Creek basins. A summary of the sites with monitoring records suitable for model calibration is shown in Table 1. Due to the late start of the Maryland test watershed studies, insufficient hydrometeorologic data was available for model calibration of the single land use sites in the Patuxent and Chester basin sites. Therefore, analyses of monitoring data from the Maryland test watersheds were restricted to standard statistical tests. Following model calibration studies of the Virginia and Pennsylvania test watersheds, linear regression analyses of

monitoring datasets were used to relate the calibrated loading factors to the Maryland test watershed data.

Table 1

SUMMARY OF MODELED TEST WATERSHED CHARACTERISTICS AND HYDROLOGY CALIBRATION RESULTS

LAND USE/SITE	AREA (acres)	REGRESSIONS OF SIMULATED AND OBSERVED FLOW VOLUMES					
		MONITORED STORMS			DAILY STREAMFLOWS		
		N	SLOPE	R ²	N	SLOPE	R ²
A. HIGH TILLAGE CROPLAND							
A. PEQUEA #3	115.2	15	0.76	0.88	492 ^a	0.98	0.70
B. WARE #7	16.2	7	0.72	0.99	--	--	--
B. LOW TILLAGE CROPLAND							
A. OCCOQUAN #2	26.6	8	0.98	0.98	--	--	--
B. OCCOQUAN #10	25.8	7	1.03	0.99	--	--	--
C. PASTURE							
A. OCCOQUAN #1	31.3	5	0.81	0.95	--	--	--
B. OCCOQUAN #5	18.8	5	1.07	0.90	--	--	--
D. FOREST							
A. PEQUEA #2	128.0	18	0.69	0.62	222 ^b	0.7	0.79
B. OCCOQUAN #9	75.8	7	1.11	0.95	--	--	--
C. WARE #8	17.4	9	1.15	0.97	--	--	--
E. RESIDENTIAL							
A. PEQUEA #4	147.2	26	0.86	0.98	374 ^c	0.96	0.84
B. WARE #5	6.2	17	0.80	0.92	--	--	--

^aMay 23, 1979 - September 26, 1980

^bMay 23, 1979 - December 31, 1979

^cMay 23, 1979 - May 31, 1980

For most test watersheds, the nonpoint pollution monitoring records were not extensive enough to permit subdividing the dataset into separate calibration periods. Consequently, the entire test watershed monitoring dataset was used for NPS model calibration. The calibrated NPS loading factors were verified through applications to mixed land use river basins in the Chesapeake Bay drainage area. Even in the absence of verification in the Chesapeake Bay river basins, it is felt that the risk of producing biased calibration results from the test watershed modeling studies are significantly reduced by the use of continuous simulation calibration techniques which involve long-term simulations and parameter adjustments that are not keyed to individual storm events.

Hydrology Calibration. Due to the relatively small size of the test watersheds, subsurface flows were often not detectable at the monitoring stations and therefore, baseflow and interflow components of runoff had to be suppressed in hydrologic model calibrations for most sites. Typically, baseflow and interflow were only included in models of forested watersheds where the dry weather flow component represented a significant fraction of monitored flows.

For most test watersheds, hydrologic calibration focused on achieving acceptable agreement between simulated and observed storm volumes. Each test watershed model was iteratively executed with a continuous rainfall record which bracketed the 1-2 year monitoring period, and agreement with monitored flows was checked for each model parameter set. A 3-6 month antecedent rainfall period was used for most test watersheds to minimize the impacts of the assumed soil moisture conditions at the start of the simulation period. Scatterplots and simple linear regressions of simulated and observed runoff volumes were generated for each calibration run to guide parameter adjustments. Sample comparisons of the final simulated and observed runoff volumes for monitored storm events are shown in Figure 3. Based on the goodness-of-fit regression statistics for monitored storms presented in Table 1, it was concluded that acceptable hydrology calibration had been achieved at the 11 test watersheds. For the three Pequea Creek test watersheds, continuous daily flow records were also available for calibration. As shown in Table 1, acceptable regression statistics were achieved for all three Pequea Creek test watersheds. The lower slope term for the forested watershed (Pequea #2) is probably due in large part to the underlying Conestoga Valley limestone formations which appeared to contribute subsurface flows that originated outside the drainage area.

Nonpoint Pollution Loading Calibration. After achieving an acceptable hydrologic calibration, nonpoint pollution loading factors were calibrated for each test watershed by iteratively executing the NPS model with continuous meteorologic records for the entire monitoring period and checking model projections for monitored storms. The calibration of nonpoint pollution loading factors for total P and total N focused on the agreement of simulated loadings with monitored storms which exhibited acceptable hydrologic simulations. Goodness-of-fit evaluations were based upon conventional and nonparametric statistical analyses.

For urban land uses, daily pollutant accumulation rates developed by the earlier study (2) for pervious and impervious fractions were tested with the Chesapeake Bay Program monitoring data. The calibration techniques used to derive separate loading factors for the pervious and impervious fractions are described elsewhere (2). These urban loading factors were held constant in the models for Pequea #4 and Ware #5 to see how well they represented loadings in different regions under different meteorologic conditions. As was the case in the previous urban modeling study, the daily pollutant accumulation rates were held constant from month to month.

For cropland test watersheds, monthly variations in sediment potency factors were required to account for such factors as fertilizer/manure applications and crop harvest, with the higher potencies generally

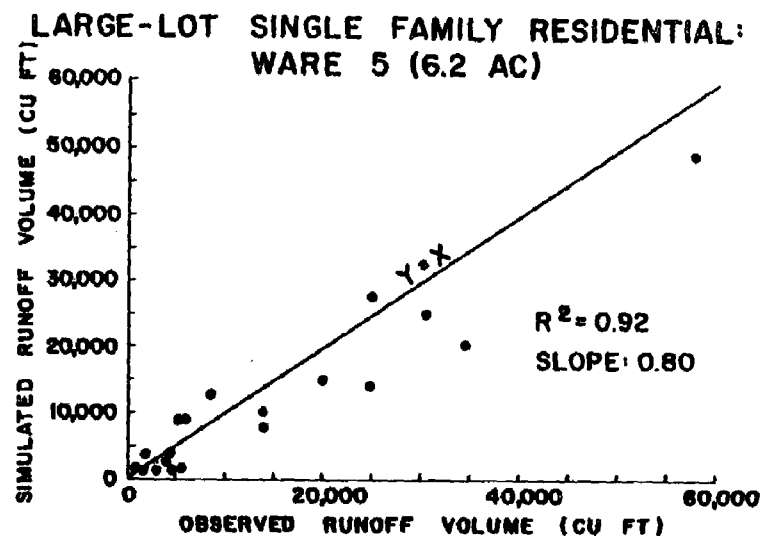
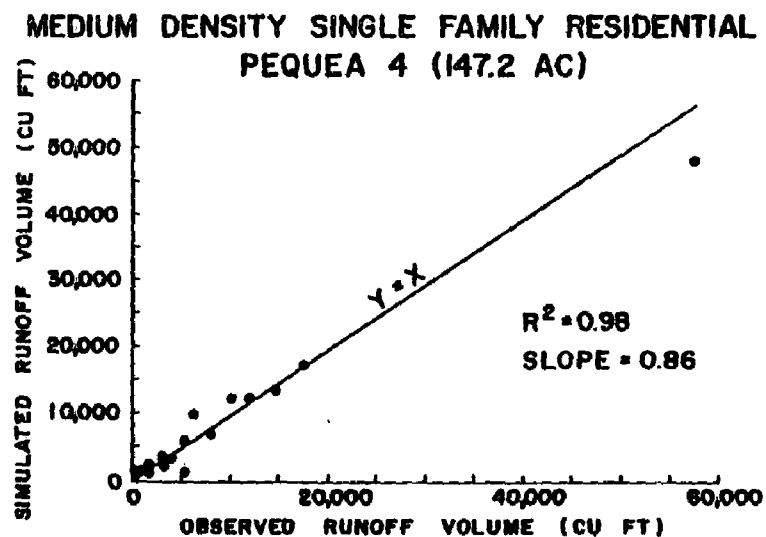
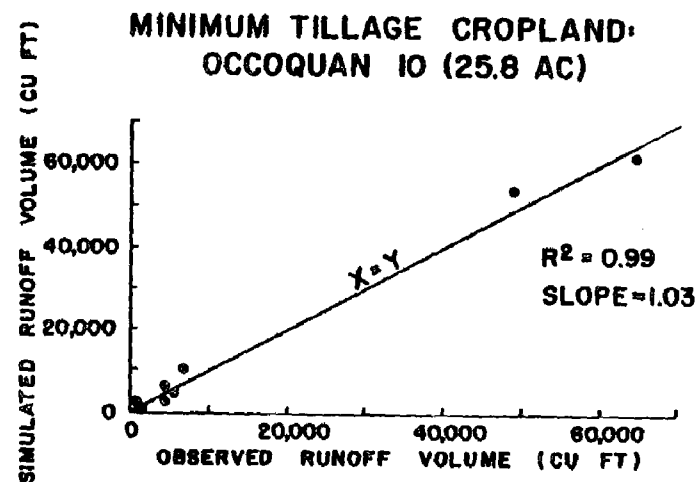
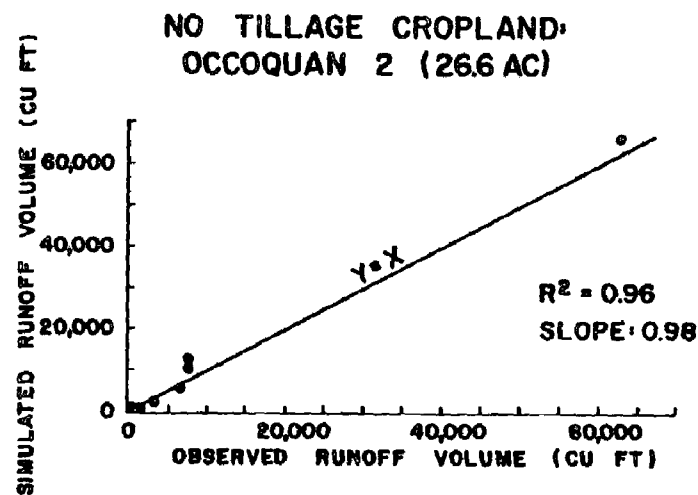


Figure 3. Sample Regressions of Simulated and Observed Runoff Volumes for Monitored Storm Events: Occoquan #2, Occoquan #10, Pequea #4, and Ware #5

associated with the months characterized by highest percentages of vegetative cover and vice versa. The monthly distribution of potency factors is established during model calibration by deriving the upper limit for the summer months of high ground cover and the lower limit for the winter months of low ground cover. For forestland test watersheds, monthly variations in sediment potency factors and daily pollutant accumulation rates were required to account for the variations in ground cover and leaf litter. Table 2 illustrates the relationship between monthly potency factor and monthly ground cover for cropland and forest land uses. For pasture test watersheds, monthly variations in sediment potency factors were generally not required to achieve an acceptable calibration.

The conventional goodness-of-fit evaluations included scatterplots and linear regressions of simulated and observed storm loads and comparisons of simulated and observed volume-weighted mean concentrations for the entire monitoring period. The simulated volume-weighted mean concentration was calculated by summing the loads and runoff volumes for all storm events within the simulation period, including storms which were not covered by the monitoring study. The protocol for NPS loading factor adjustment after each calibration placed greater emphasis on the agreement of volume-weighted mean concentrations, since long-term loading trends were felt to provide the best indication of the need for and direction of further loading factor adjustments. In other words, whenever a parameter adjustment decision involved choosing between improving volume-weighted mean concentration vs. improving the storm load scatterplots and linear regression statistics, the former usually governed.

Comparisons of simulated and observed volume-weighted mean concentrations for the calibrated NPS loading factors are shown in Table 3. As may be seen, the ratios of simulated to observed mean concentrations typically fell within the range 0.75-1.25 which is comparable to the typical errors inherent in hydrometeorologic gaging and laboratory analyses. Thus, Table 3 indicates that the calibrated NPS loading factors provide a good representation of long-term nonpoint pollution loads per unit volume during the monitoring period.

Some of the better scatterplots and regression results for storm loads are shown in Figure 4. As may be seen, agreement between simulated and observed storm loads was quite good for selected sites. However, regression statistics for several other test watersheds were insufficient to demonstrate goodness-of-fit for storm loads. It is felt that much of the difficulty in achieving acceptable regression statistics for storm load comparisons can be attributed to the lower power of conventional normal statistics for evaluations of small sample sizes characterized by skewed (i.e., non-normal) distributions.

To provide a visual check of agreement between simulated and observed frequency distributions, box and whisker plots were developed for the simulated and observed storm load datasets for each test watershed. As illustrated in Figure 5, the box and whisker plot displays the 25th, 50th, and 75th percentile values in the frequency distribution as well as the upper and lower extremes. The departure of the 25th and 75th percentile

Table 2

Nonpoint Pollution Loading Factors Applied to Chesapeake Bay Drainage Area:
Monthly Distributions for Potomac and James River Basins

LAND USE/PARAMETER	JAN	FEB	MAR	APR	MAY	JUN	JUL	AUG	SEP	OCT	NOV	DEC
A. FOREST												
1. GROUND COVER (%)	95%	95%	98%	100%	100%	100%	100%	100%	100%	98%	95%	95%
2. SEDIMENT POTENCY: TOTAL N (%)	1.06	1.06	1.06	1.06	1.06	1.88	1.88	1.88	1.88	1.06	1.06	1.06
3. SEDIMENT POTENCY: TOTAL P (%)	0.15	0.15	0.15	0.15	0.15	0.26	0.26	0.26	0.26	0.15	0.15	0.15
B. HIGH-TILLAGE CROPLAND												
1. GROUND COVER (%)	0.0%	0.0%	0.0%	0.0%	20%	50%	85%	90%	95%	20%	0.0%	0.0
2. SEDIMENT POTENCY: TOTAL N (%)	0.98	0.98	1.22	1.22	1.22	1.22	1.83	1.83	1.83	0.98	0.98	0.98
3. SEDIMENT POTENCY: TOTAL P (%)	0.31	0.31	0.38	0.38	0.38	0.38	0.58	0.58	0.58	0.31	0.31	0.31
C. LOW-TILLAGE CROPLAND												
1. GROUND COVER (%)	40%	60%	75%	85%	92%	99%	99%	99%	99%	70%	30%	40%
2. SEDIMENT POTENCY: TOTAL N (%)	2.06	2.06	2.06	2.52	3.20	3.20	3.43	3.43	3.43	2.06	2.06	2.06
3. SEDIMENT POTENCY: TOTAL P (%)	0.17	0.17	0.17	0.21	0.27	0.27	0.28	0.28	0.28	0.17	0.17	0.17
D. PASTURE												
1. GROUND COVER (%)	100%	100%	100%	100%	100%	100%	100%	100%	100%	100%	100%	100%
2. SEDIMENT POTENCY: TOTAL N (%)	1.52	1.52	1.52	1.52	1.52	1.52	1.52	1.52	1.52	1.52	1.52	1.52
3. SEDIMENT POTENCY: TOTAL P (%)	0.26	0.26	0.26	0.26	0.26	0.26	0.26	0.26	0.26	0.26	0.26	0.26
E. SINGLE FAMILY RESIDENTIAL												
1. GROUND COVER (%)	100%	100%	100%	100%	100%	100%	100%	100%	100%	100%	100%	100%
2. ACCUMULATION RATE: TOTAL N (LBS/AC/DAY)												
a. PERVIOUS FRACTION	0.02	0.02	0.02	0.02	0.02	0.02	0.02	0.02	0.02	0.02	0.02	0.02
b. IMPERVIOUS FRACTION	0.08	0.08	0.08	0.08	0.08	0.08	0.08	0.08	0.08	0.08	0.08	0.08
3. ACCUMULATION RATE: TOTAL P (LBS/AC/DAY)												
a. PERVIOUS FRACTION	0.0035	0.0035	0.0035	0.0035	0.0035	0.0035	0.0035	0.0035	0.0035	0.0035	0.0035	0.0035
b. IMPERVIOUS FRACTION	0.01	0.01	0.01	0.01	0.01	0.01	0.01	0.01	0.01	0.01	0.01	0.01

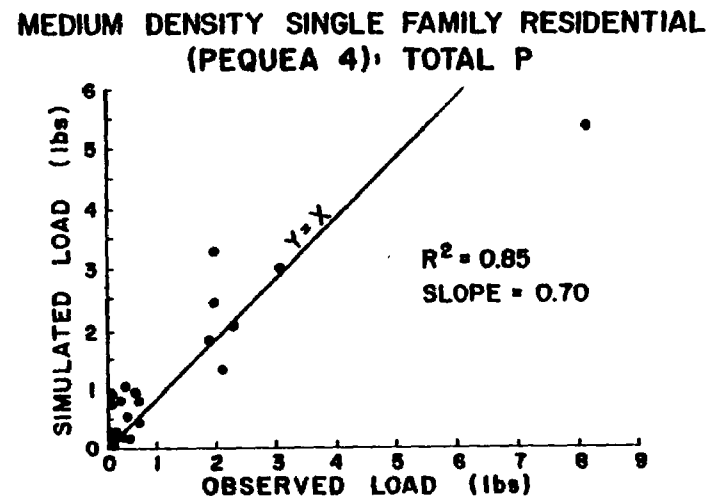
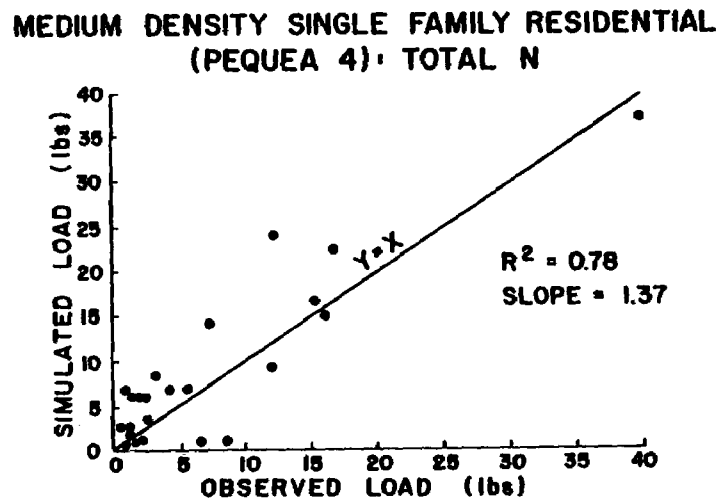
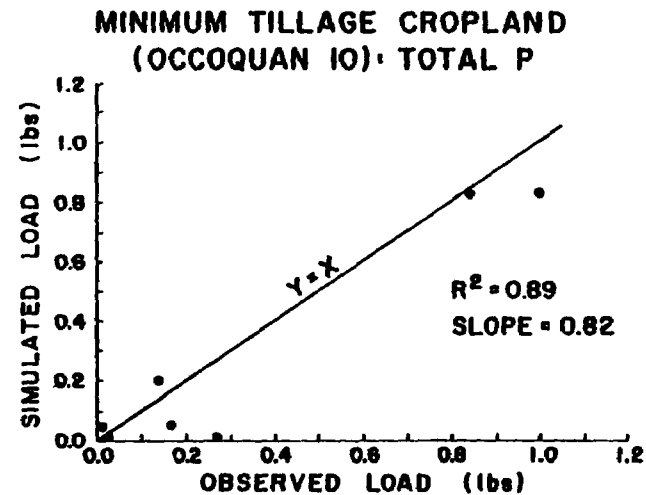
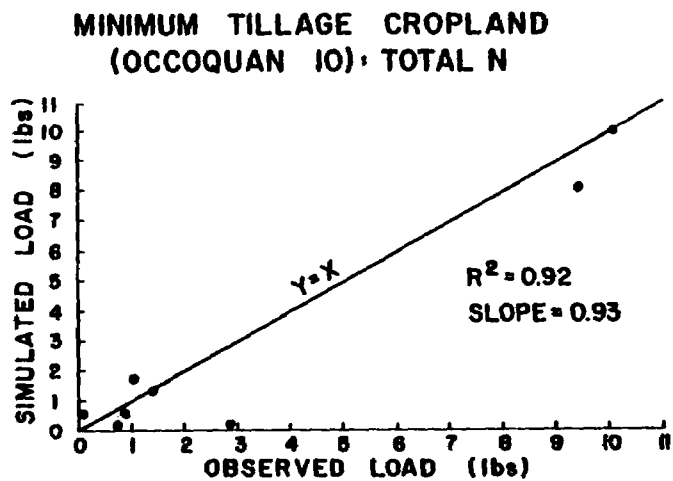


Figure 4. Sample Regressions of Simulated and Observed Loadings for Monitored Storms:
Occoquan #10 and Pequea #4

Table 3

Comparison of Simulated and Observed Volume-Weighted Mean Concentrations

SITE (LAND USE)	OBS. N	SEDIMENT			TOTAL P			TOTAL N		
		SIM. (MG/L)	OBS. (MG/L)	RATIO	SIM. (MG/L)	OBS. (MG/L)	RATIO	SIM. (MG/L)	OBS. (MG/L)	RATIO
PEQUEA 3 (H.T. CROP)	17	783	829	0.94	4.53	4.70	0.96	18.7	19.2	0.98
WARE 7 (H.T. CROP)	10	272	222	1.23	0.70	0.62	1.13	1.6	1.30	1.20
OCC. 2 (L.T. CROP)	16	370	361	1.02	1.96	1.67	1.17	6.8	6.6	1.03
OCC. 10 (L.T. CROP)	13	138	121	1.14	0.47	0.40	1.18	4.6	3.8	1.22
OCC. 9 (FOREST)	15	83	70	1.19	0.13	0.13	1.0	1.1	0.9	1.22
PEQUEA 2 (FOREST)	21	99	169	0.58	0.1	0.13	0.74	3.8	3.6	1.05
WARE 8 (FOREST)	34	64	71	0.90	0.05	0.06	0.83	0.37	0.4	0.93
OCC. 1 (PASTURE)	27	561	670	0.84	0.94	1.12	0.84	5.3	6.2	0.86
OCC. 5 (PASTURE)	11	166	145	1.14	0.43	0.38	1.13	2.5	2.2	1.15
PEQUEA 4 (RESID.)	52	115	194	0.56	0.24	0.30	0.80	1.8	2.4	0.75
WARE 5 (RESID.)	30	50	38	1.32	0.12	0.10	1.23	0.95	0.70	1.36

Table 4

Nonparametric Goodness-of-Fit Statistics for Test Watershed Model
 Calibration: Runoff Volumes (R.O.) and Total Phosphorus (TP),
 Total Nitrogen (TN), and Sediment (SED) Loadings (lbs)

SITE (LAND USE)	RUNOFF INTERVAL (IN.)	SIM. STORMS	OBS. STORMS	TWO-SIDED K-S TEST				WILCOXON RANK SUM TEST			
				LEVEL OF SIGNIFICANCE				LEVEL OF SIGNIFICANCE			
				R.O.	TP	TN	SED	R.O.	TP	TN	SED
PEQUEA 3 (H.T. CROP)	>0.025	28	13	0.20	>0.20*	>0.20*	>0.20*	0.58	0.96	0.65	0.83
WARE 7 (H.T. CROP)	(0.01-0.125 + HURR.)	26	9	0.10	>0.20*	>0.20*	>0.20*	0.17	0.23	0.42	0.84
OCC. 2 (L.T. CROP)	>0.015	29	6	>0.20*	>0.20*	0.10	>0.20*	0.71	0.91	0.20	0.39
OCC. 10 (L.T. CROP)	>0.025	19	8	>0.11*	>0.11*	>0.11*	>0.11*	0.65	0.97	0.94	0.98
OCC. 9 (FOREST)	>0.03	30	9	>0.20*	>0.20*	>0.20*	N/A	0.56	0.45	0.80	N/A
PEQUEA 2 (FOREST)	<0.09	91	16	0.42	0.34	0.26	N/A	0.30	0.61	0.18	N/A
WARE 8 (FOREST)	(0.075-0.9)	20	24	>0.20*	0.10	0.10	N/A	0.86	0.31	0.13	N/A
OCC. 1 (PASTURE)	(0.025-0.5)	15	9	>0.10*	>0.10*	>0.10*	N/A	0.40	0.95	0.81	N/A
OCC. 5 (PASTURE)	>0.01	21	8	>0.20*	>0.20*	0.20	N/A	0.37	0.54	0.25	N/A
PEQUEA 4 (RESID.)	>0.025	86	25	0.94	0.39	0.44	N/A	0.76	0.70	0.48	N/A
WARE 5 (RESID.)	>0.09	43	24	0.58	0.22	0.29	N/A	0.31	0.64	0.34	N/A

*EXCEEDS MAXIMUM PROBABILITY VALUE CURRENTLY REPORTED IN STATISTICAL TABLES FOR SAMPLE SIZES

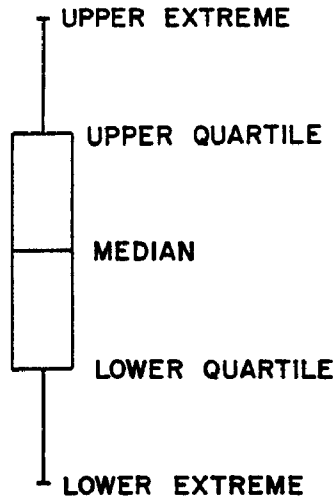


Figure 5. Configuration of a
Box and Whisker Plot

lines from the median line provides an indication of skewness of the distribution. The mean value is sometimes plotted on the box and whisker diagram to highlight departure from the median value and the non-normality of the distribution. Box and whisker plots for the calibrated NPS loading factors are shown in Figures 6, 7, and 8 for cropland, forest/pasture, and urban land uses, respectively. To provide an indication of non-normality, the location of the mean in each plot is indicated by an "o". Since sediment is the driving force for simulated cropland loadings, sediment data is presented for the cropland test watersheds in Figure 6.

As was the case with the simulated volume-weighted mean concentrations reported in Table 3, the simulated box and whisker plots are based on all storms which occurred during the test watershed monitoring period, including those which were not monitored. The inclusion of all storms tended to automatically skew the simulated distribution in the direction of minor storms which typically were not monitored in the field due to the very small runoff volumes. This skewness can be attributed to the fact that whereas the mathematical model will calculate runoff volumes and loads from minor storms, the test watershed monitoring studies relied upon runoff volume thresholds associated with more significant rainfall events. Since similar runoff volume distributions are required to ensure meaningful statistical comparisons of storm loading datasets, minor storms were generally deleted from the simulated dataset prior to the development of the box and whisker plots shown in Figures 6-8. The establishment of the cutoff for minor storms was based upon iterative analyses of box and whisker plots and nonparametric statistics for the simulated and observed runoff volume datasets. The storm runoff volume thresholds which resulted in box and whisker plots and nonparametric statistics that indicated acceptable agreement between the simulated and observed runoff volume distributions and median values are summarized in the "runoff interval" column of Table 4. A check of the total runoff volume and nonpoint pollution load produced by

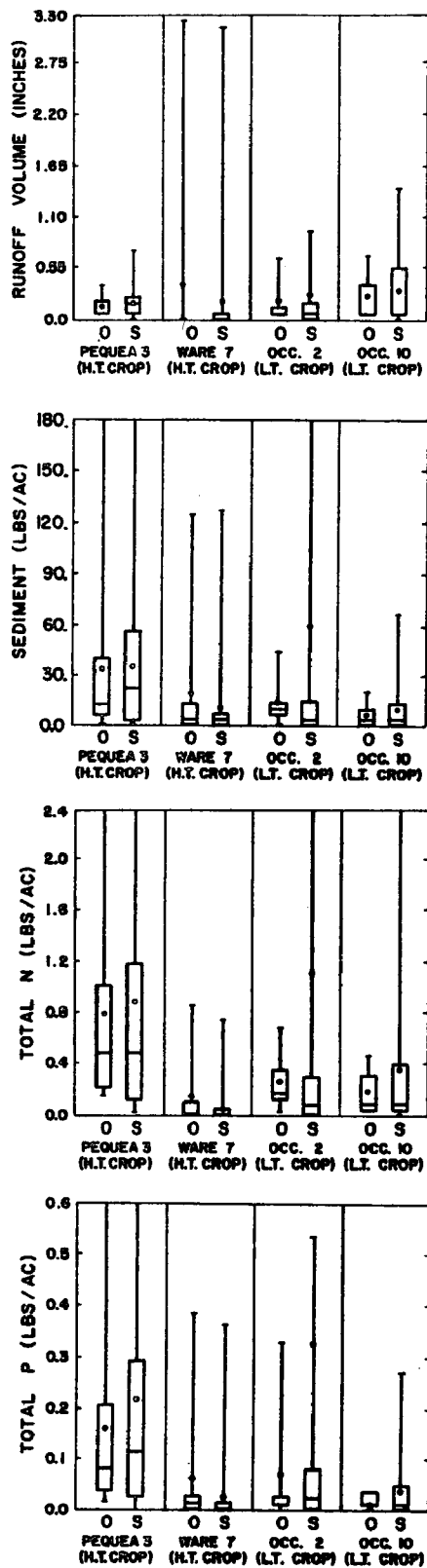


Figure 6. Comparison of Simulated (S) and Observed (O) Box and Whisker Plots for Cropland Watersheds

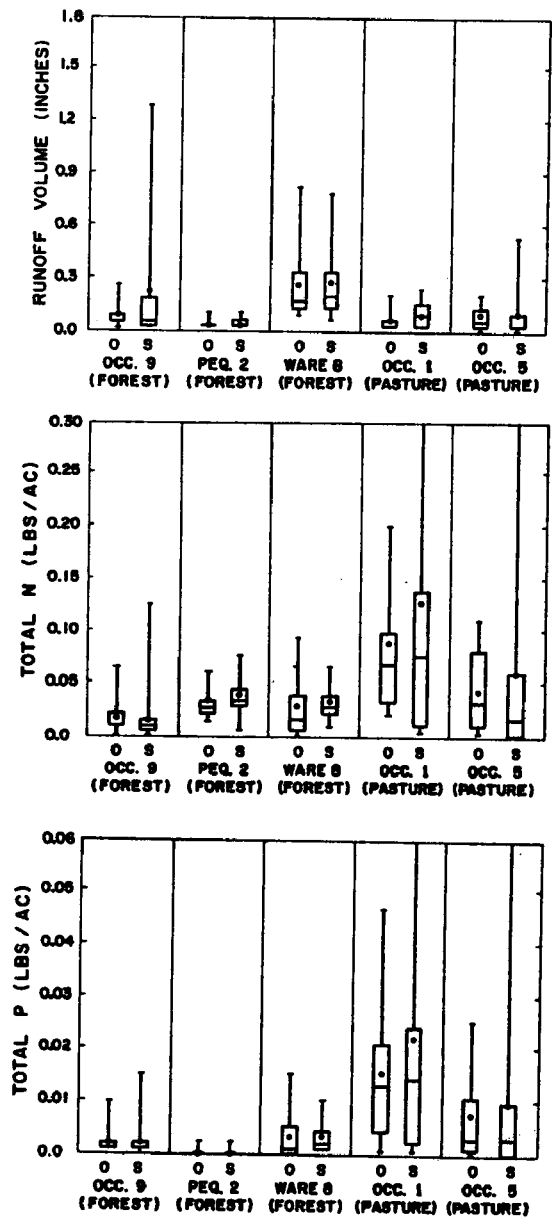


Figure 7. Comparison of Simulated (S) and Observed (O) Box and Whisker Plots for Forest and Pasture Watersheds

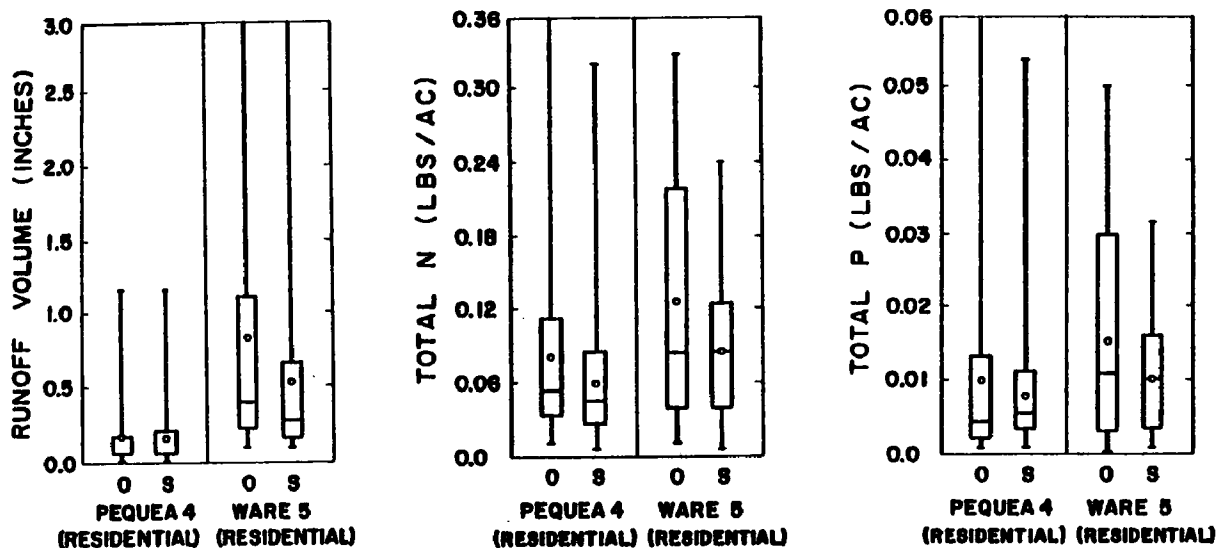


Figure 8. Comparisons of Simulated (S) and Observed (O) Box and Whisker Plots for Single-Family Residential Watersheds

storm events which fall within the specified runoff interval indicates that typically 90% or more of the total volume or load produced during the monitoring period was generated by these storms. This check suggests that the minor storms deleted from the simulated and observed datasets were relatively insignificant in terms of seasonal or annual loads.

The runoff intervals shown in Table 4 were used as the basis for the box and whisker plots of simulated and observed datasets in Figures 6-8. Inspection of these box and whisker plots confirms the highly skewed distributions of the runoff and nonpoint pollution loading datasets. The similarities between the simulated and observed plots, in terms of distribution and median value, also serves as graphical evidence of model goodness-of-fit.

Nonparametric statistical tests (8) were performed for a quantitative assessment of the goodness-of-fit for the datasets plotted in Figures 6-8. Nonparametric statistics assume no shape for the population distribution and therefore are valid for both normal and skewed distributions. Consequently, nonparametric statistical techniques have a much higher power than normal statistical techniques for analyses of datasets, such as the monitored storm load dataset, which are characterized by small sample sizes and skewed distributions. The results of two-sided Kolmogorov-Smirnov (K-S) and Wilcoxon Rank Sum tests are summarized in Table 4. The K-S analysis is a test for any significant deviation of the simulated distribution from the observed distribution. The analysis involves checking the maximum difference between simulated and observed distributions to determine if it exceeds a critical value. Since it is a broad alternative test, the K-S test has lower power for any specific alternative, such as a difference in median values. The Wilcoxon Rank Sum analysis compensates for this deficiency since it is designed to test for differences in median values, under the assumption that the simulated and observed distributions may

differ only with respect to this value. The Wilcoxon Rank Sum test assigns ranks to the combined dataset of simulated and observed values and calculates the sum of the data ranks for each dataset. If the simulated median value differs significantly from the observed median value, the sum of the simulated data ranks will be higher or lower than the sum of the observed data ranks.

Based on a 0.05 probability cutoff for the 95% confidence interval, the level of significance statistics in Table 4 indicate that the simulated runoff volumes and nutrient loads do not vary significantly from those monitored in each test watershed. The high significance levels of the nonparametric tests summarized in Table 4 meet the primary objective of a goodness-of-fit evaluation by indicating a low probability of accepting a false model as true (Type II error).

Determination of Representative NPS Loading Factors. The purpose of the test watershed studies was the development of nonpoint pollution loading factors for application throughout the 64,000 sq mi drainage area of Chesapeake Bay. Of the 11 modeled test watersheds, only the two urban sites relied upon a single set of loading factors for the land use category. Since the urban loading factors developed by a previous study (2) provided a good representation of urban loadings in two different sections of the study area, it was decided that these loading factors would be used for all residential and commercial land uses in the Chesapeake Bay Basin. The transferability of urban nonpoint pollution loading factors is not surprising because impervious cover is such an important contributor to urban nonpoint pollution loadings (2) and an urban land use tends to exhibit similar impervious cover patterns regardless of location.

Differences in calibrated loading factors at the test watersheds in each rural-agricultural land use category can be attributed to variations in management practices and in the significance of sediment loadings. For each land use category, volume-weighted mean concentrations for modeled and unmodeled (i.e., Patuxent and Chester rivers) test watersheds were compared to ascertain long-term loading differences among the testing sites. For the forest land use category, a review of long-term loading statistics for 3 modeled and 3 unmodeled sites indicates that Occoquan #9 is characterized by mean concentrations which are similar to the mean concentrations at most other forest sites. Therefore, the calibrated sediment potency factors and pollutant accumulation rates for Occoquan #9 were selected as the most representative forest loading factors for application throughout the Chesapeake Bay drainage area.

The selection of representative pastureland loading factors was influenced by the limitations of the land use database for the Chesapeake Bay Basin which is based upon interpretations of LANDSAT satellite images from the period 1977-1979. The LANDSAT data interpretations tend to emphasize reasonably well-managed pasture (e.g., Occoquan #5) rather than poorly-managed pastureland (e.g., Occoquan #1) since the latter is difficult to distinguish from low-tillage cropland. Therefore, the calibrated loading factors for Occoquan #5 were felt to be most appropriate for application to the Chesapeake Bay Basin.

For the cropland land use categories, variations in management practices such as manure applications produced different monthly and average annual potency factors for each watershed. Because sediment is modeled as the driving force for nonpoint pollution loadings, comparisons of test watersheds to identify representative loading factors were based upon average annual sediment potency factors. Monitored pollutant loads were regressed with monitored sediment loads for each site, and the slope of the regression line was designated as an average annual sediment potency factor (i.e., pollutant mass/sediment mass) which could be used to compare site loading factors with factors for the high tillage or low tillage cropland datasets. The monitored storm load datasets were then pooled by land use category, and separate pollutant load vs. sediment load regressions were performed for the high-tillage cropland and low-tillage cropland datasets. In this manner, pollutant loading factors for test watersheds which were not suited to model calibration could be compared with factors for modeled watersheds. Likewise, average annual sediment potency factors for calibrated watersheds could be compared with average annual values for the entire high tillage cropland or low tillage cropland datasets. The "land use:site" ratios of the regressed sediment potency factors were multiplied by the calibrated average annual sediment potency factors for Pequea #3 and Occoquan #10 to develop average annual sediment potency factors for high-tillage cropland and low-tillage cropland, respectively. The average annual potency factor was then distributed to monthly values based upon the distributions calibrated for Pequea #3 and Occoquan #10.

The resultant NPS loading factors for rural-agricultural and urban land use categories are summarized in Table 2. Based on test watershed model calibration results, monthly ground cover (COVVEC) for urban and pasture land uses was set at 100% so that pervious area loadings are governed entirely by the calibrated pollutant accumulation rate rather than soil loss. For the other land use categories, ground cover was based upon the calibrated values for the test watershed used to derive the representative loading factors: Occoquan #9 for forestland, Pequea #3 for high-tillage cropland, and Occoquan #10 for low tillage cropland. The forestland and cropland ground cover values shown in Table 2 were used to model the river basins in the southern half of the Chesapeake Bay drainage area (e.g., Potomac and James river basins). For the Susquehanna River Basin, which occupies the northern half of the Bay's drainage area, the ground cover and corresponding sediment potency factors were shifted one month to represent the shorter growing season and earlier crop harvest.

In order to compare annual nonpoint pollution loadings from the various land use categories, the NPS model was set up on a hypothetical single-land use watershed with silt loam soils typical of the Piedmont Province and a 2% overland flow slope. The NPS model was executed with hourly rainfall records from the Virginia suburbs of Washington, D.C. to simulate annual loadings for each land use based upon the NPS loading factors in Table 2 and in Hartigan *et al.* (2). Annual loadings were developed for a year of average wetness (1967) characterized by 40.6 in of rainfall, and a relatively wet year (1975), characterized by 54.1 in of rainfall. The simulated annual unit area loadings of total N and total P are summarized in Table 5. As may be seen, high tillage cropland produces the highest unit

area loads of total N and total P while forestland produces the lowest unit area loads. Also of note are the higher loadings for wet year conditions. For example, Table 5 shows significantly higher cropland loadings for wet year conditions which can be attributed to percentage increases in soil loss that are much greater than runoff increases, while urban land uses exhibit increases proportional to runoff increases.

Verification of Test Watershed Loading Factors

A five-step procedure was followed to scale-up from the test watershed models to the Chesapeake Bay river basin models.

First, the river basin models were subjected to an independent hydrology calibration/verification study which is described elsewhere (6). Calibration/verification gages are shown in Figure 9. Hydrologic parameter sets developed from the test watershed model calibration could not be applied directly to the river basin models because the subsurface flow component was often not detectable at the testing sites. Further, the independent hydrology calibration for the river basin model permits an accurate simulation of overland flow transport to the stream channel system. An accurate representation of overland flow transport eliminates the need for application of a "sediment delivery ratio" to simulated

Table 5

Simulated Annual Surface Washoff of Total N (as N) and Total P (as P)
For Average and Wet Years: Silt Loam Soils Typical of Piedmont Province

LAND USE	TOTAL N LOAD (lbs/acre/yr)		TOTAL P LOAD (lbs/acre/yr)	
	AVG. YR.	WET YR.	AVG. YR.	WET YR.
FOREST	0.6	0.8	0.08	0.12
PASTURE	2.6	3.0	0.45	0.52
SINGLE FAMILY RESIDENTIAL (18% impervious)	6.0	6.8	0.86	0.97
COMMERCIAL (90% impervious)	10.7	12.2	1.29	1.46
LOW TILLAGE CROPLAND	6.3	33.2	0.52	2.74
HIGH TILLAGE CROPLAND	17.9	62.7	5.64	19.82

NOTE: BASED ON RAINFALL RECORDS FOR NORTHERN VIRGINIA GAGES

o AVG. YR. (1967) = 40.6 in.

o WET YR. (1975) = 54.1 in.

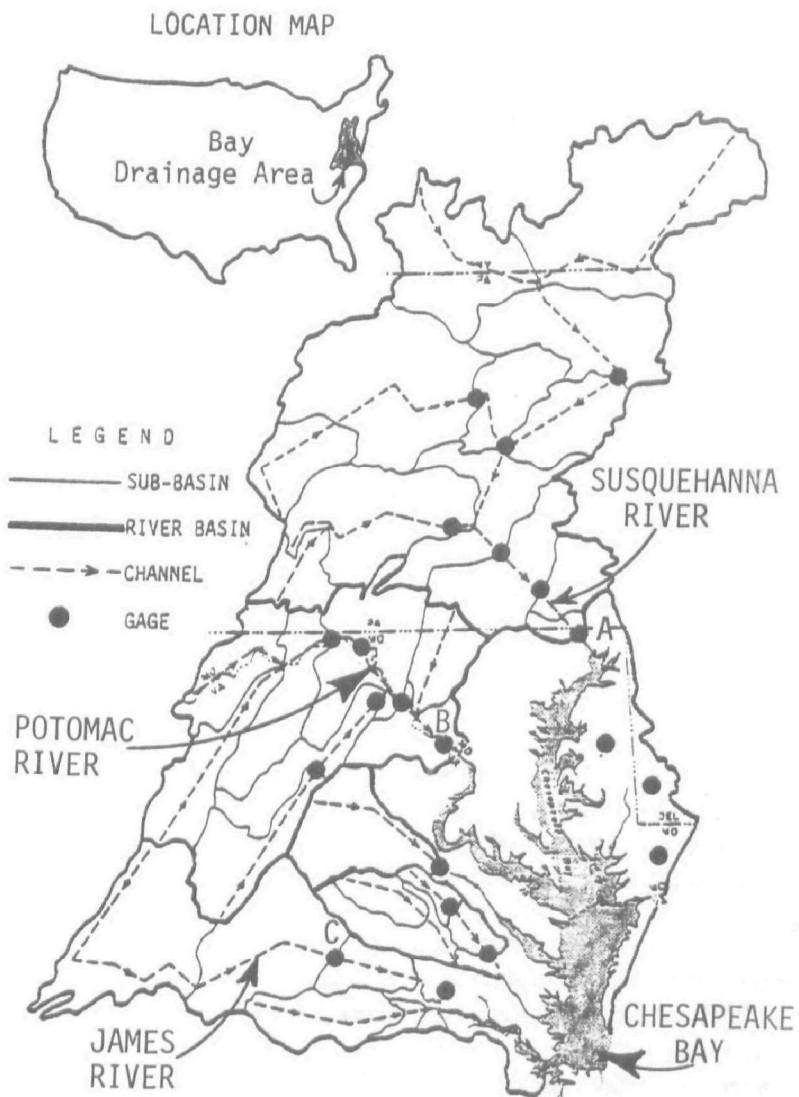


Figure 9. Map of Chesapeake Bay Basin Showing Sub-Basin/Channel Network for Basin Model and Calibration/Verification Gages (Susquehanna River at Conowingo, MD (A), Potomac River near Washington, DC (B), and James River at Cartersville, VA (C))

sediment and sediment-related loads. Based upon test watershed model sensitivity studies, the river basin models relied upon a transport coefficient (KSER) equal to 0.4 which provides a stable representation of runoff transport of detached pollutants.

Second, an erodibility factor (KRER) was assigned to each sub-basin based upon average soils characteristics. Since the NPS loading factors for each land use category are the same in each river basin, the erodibility factor is one of the most important parameters to represent locational differences in cropland nonpoint pollution loadings. For example, high tillage cropland in a sub-basin with highly erodible soils will produce higher NPS loads of total N and total P than the same land use in a sub-basin with less erodible soils, even though the sediment potency factors are the same in both sub-basins.

Third, the NPS loading factors shown in Table 2 were assigned to the land use categories in each sub-basin.

Fourth, a receiving water model with point source discharge files was iteratively executed in a quasi-steady state mode for a typical low flow condition (i.e., 25th percentile flow). Simulated baseflow concentrations were compared to low flow monitoring data to establish an initial estimate of baseflow/interflow concentrations.

Fifth, the sub-basin/receiving water models of each river basin were calibrated for a two-year period (January 1974-December 1975) and verified for a three-year period (January 1976-December 1978). The models were iteratively executed for the two-year calibration period with the NPS loading factors assigned in Step 3 to set instream process parameters and to derive a final set of baseflow/interflow concentrations for each sub-basin. The NPS loading factors were not adjusted during the calibration/verification of the river basin models. Adjustments to instream process parameters and subsurface flow concentrations were based upon comparisons between simulated and observed water quality at two different levels: (1) concentration time series (i.e., typically biweekly observations) for USGS monitoring stations; and (2) nonpoint pollution loading records at USGS fall line stations. A USGS fall line monitoring study (9) from January 1979 through April 1981, which focused on wet-weather loadings at the Susquehanna River, Potomac River, and James River fall lines, produced an acceptable database to verify the NPS loading factors in the river basin models. Since sufficient NWS rainfall records were not available for the 1979-1981 monitoring period, regression equations (9) relating observed daily streamflow and pollutant loads were used to synthesize a daily loading database for the calibration/verification period. The period 1974-1978 was selected for model calibration/verification because land use, wastewater discharges, and flow-duration curves at the three fall line gages were reasonably similar to conditions during the 1979-1981 monitoring study. Comparisons of simulated loadings with flow-loading relationships from the USGS fall line monitoring study were made on a daily, monthly, and annual basis. Daily loading comparisons provided a rigorous test of the nonpoint pollution loading factors derived from the test watershed modeling studies, while the monthly and annual loading comparisons were used to guide

adjustments to receiving water model parameters and baseflow/interflow concentrations. Following calibration, the receiving water model was verified by operating it for the period January 1976-December 1978 with constant instream process parameter sets and baseflow/interflow concentrations. Since nonpoint pollution loading factors were not adjusted during either the calibration or verification model runs, the test watershed model calibration results were actually verified for a 5-yr period. Comparisons of simulated fall line loads and synthesized loading records based on the USGS fall line monitoring study are shown in Figures 10 and 11 for the Susquehanna and Potomac rivers, respectively. The good agreement between simulated and synthesized nutrient loading records at the mouths of the major river basins indicates that the testing site loading factors provide a reasonable representation of loadings from mixed land use river basins.

Recommendations for Future Test Watershed Studies

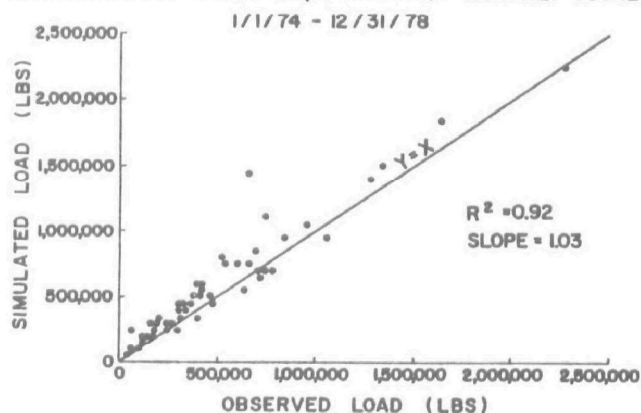
Outlined below are recommendations for improved coordination between the monitoring and modeling efforts to ensure maximum usefulness of the test watershed database. The recommendations address problems with site selection and certain elements in the monitoring work program which were encountered during the modeling study described herein.

Site Selection. One problem which reduced the applications of monitoring data from certain test watersheds was the selection of mixed land use catchments with significantly different loading factors. Secondary land uses which represent a relatively small percentage of the total catchment area can distort monitoring characterizations of the primary land use if runoff concentrations for the secondary land use are significantly higher. While it may not always be possible to identify single land use watersheds for monitoring studies, mixed land use catchments with a secondary land use that is characterized by much higher NPS loading factors than the primary land use should not be designated as test watersheds.

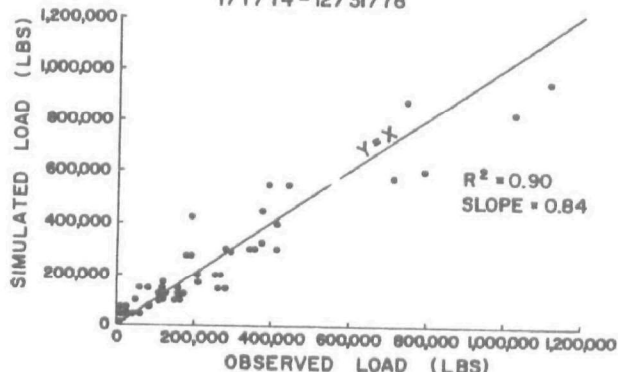
Two of the test watersheds in the Pequea Creek basin were located over limestone formations that affected the quantity and probably the quality of monitored baseflow during dry weather and storm periods. Since the purpose of test watershed monitoring studies is to collect nonpoint pollution loading data that are representative of larger basins, care should be taken during site selection to ensure that underlying geology as well as land use and upper soils characteristics are representative of the river basins in which the data is to be applied.

Monitoring Work Program. As previously indicated, the test watershed monitoring studies were designed and initiated in the absence of a specific watershed modeling work program. The earlier start-up of the monitoring study was intended to ensure sufficient time for modeling studies of the monitoring data. However, if the monitoring and modeling work program had been developed and implemented concurrently, it is likely that: some different site selection decisions would have been made; collection of the continuous rainfall and runoff records required for model calibration would have received a higher priority in order to increase the amount of data

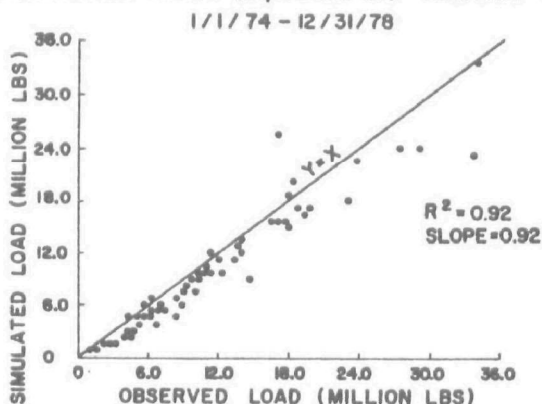
SUSQUEHANNA RIVER (27,100 SQ. MI.): MONTHLY TOTAL P



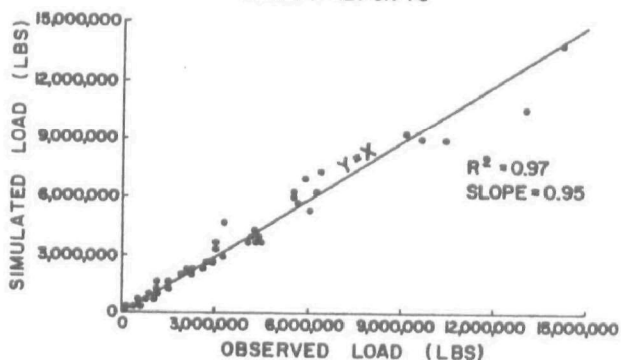
POTOMAC RIVER (11,560 SQ. MI.): MONTHLY TOTAL P



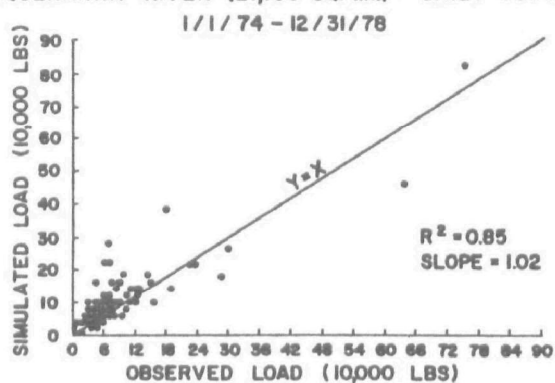
SUSQUEHANNA RIVER (27,100 SQ. MI.): MONTHLY TOTAL N



POTOMAC RIVER (11,560 SQ. MI.): MONTHLY TOTAL N



SUSQUEHANNA RIVER (27,100 SQ. MI.): DAILY TOTAL P



POTOMAC RIVER (11,560 SQ. MI.): DAILY TOTAL P

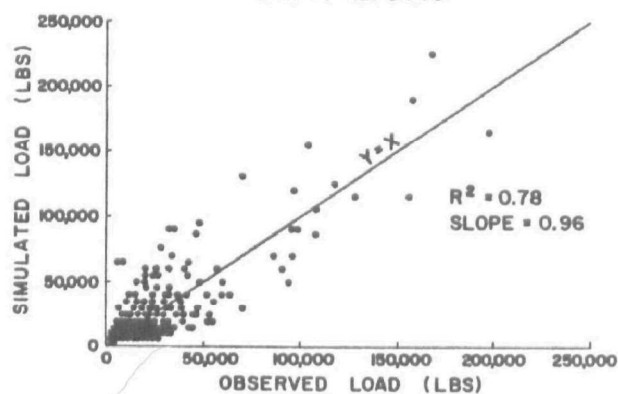


Figure 10. Regression of Simulated and Observed Loadings for the Susquehanna River at Conowingo, MD (Jan. 1, 1974-Dec. 31, 1978): Monthly Total P, Monthly Total N, and Daily Total P

Figure 11. Regressions of Simulated and Observed Loadings for the Potomac River near Washington, D.C. (Jan. 1, 1974-Dec. 31, 1978): Monthly Total P, Monthly Total N and Daily Total P

available for model calibration; data reduction requirements could have been reduced considerably; and the results of model calibration studies would be improved due to the expanded database. After the monitoring studies have started, periodic interactions between the modeling and monitoring investigators can facilitate any mid-course corrections necessary to enhance the applications of the monitoring database. While it is often necessary to initiate test watershed monitoring studies at the earliest possible date to ensure the maximum amount of monitoring data and/or a sufficient amount of time for data analysis, the advantages of better coordination between the monitoring and modeling efforts from start to finish merits consideration.

The majority of the hydrometeorologic data reduction required for model calibration was performed by the modeling investigator. The monitoring investigators were not required to reduce rainfall stripcharts and reductions of flow stripcharts were generally restricted to the storms which produced water quality samples. Consequently, the modeling investigator was required to perform most of the quality assurance checks on hydrometeorologic data for the majority of the test watersheds. These checks included assessments of rainfall-runoff relationships and comparisons of runoff volumes recorded at the test watersheds in each river basin. Due to the later start-up of the modeling study and delayed transmittal of monitoring data to the modeling investigator, initial quality assurance checks on the hydrometeorologic dataset were not completed until most test watershed monitoring studies had ended. As a result, onsite experiments to resolve hydrometeorologic data problems could not be performed, and mid-course corrections involving additional instrumentation, further instrument calibration, or the selection of substitute testing sites could not be considered. Further, an earlier quality assurance effort focusing on model calibration needs probably would have flagged the significant gaps in the hydrometeorologic records required for model calibration in time to produce an expanded database. Therefore, it is recommended that extensive quality assurance checks be performed on the hydrometeorologic data very early in the test watershed monitoring study so that problems and anomalies can be identified in time for mid-course corrections.

For certain test watersheds, relatively long sampling periods (e.g., 24-72 hrs) resulted in the inclusion of excessive baseflow volumes in the flow-composite samples for monitored storm events. As a result, the separation of baseflow volumes and loadings from the reported storm volumes and loadings was very difficult for these test watersheds, and model calibration studies were significantly complicated. To ensure the development of a reliable nonpoint pollution loading dataset by test watershed monitoring studies, it is recommended that the sample collection/retrieval schedule be designed to minimize baseflow contributions during monitored storms.

For test watershed monitoring studies in four of the five river basins, separate raingage and flowmeter recorders were used for the majority of the monitoring period. The use of separate recorders generally resulted in unsynchronized rainfall and flow records due to inevitable differences in chart speeds. Consequently, one of the more time-consuming data reduction tasks involved scanning the individual stripcharts to match rainfall and

flow records for monitored storms. The use of a dual-pen recorder for the raingage and the flowmeter would not only reduce data reduction requirements for continuous simulation studies but would also facilitate the quality assurance checks of hydrometeorologic data recommended above.

Acknowledgements

The work described herein was funded through a Cooperative Agreement (No. CR807816-01) with the U.S. Environmental Protection Agency's Chesapeake Bay Program. James T. Smullen was the EPA Project Officer.

Several NVPDC engineer interns assisted with this project. Susan M. Lees participated in the hydrologic and nonpoint pollution model calibration tasks. Mark D. Taylor participated in the hydrologic model calibration tasks. Cynthia D. Burch coordinated the reduction of the majority of the hydrometeorologic data and participated in hydrologic model calibration tasks. Mary Jo Rimkus participated in data reduction and hydrologic model calibration tasks.

References

1. Southerland, E., et al., "A Modeling Study of Nonpoint Pollution Loadings and Transport in the Chesapeake Bay Basin," Proceedings of Thirteenth Annual Pittsburgh Conference on Modeling and Simulation, School of Engineering, Univ. of Pittsburgh, Pittsburgh, PA, 1982.
2. Hartigan J.P., et al., "Calibration of Urban Nonpoint Pollution Loading Models," Proceedings of ASCE Hydraulics Division Specialty Conference on Verification of Mathematical and Physical Models in Hydraulic Engineering, ASCE, New York, NY, August 1978, pp. 363-372.
3. Donigian, A.S. and Crawford, N.H., "Modeling Nonpoint Pollution from the Land Surface," EPA-600/3-76-083, U.S. Environmental Protection Agency, Environmental Research Laboratory, Athens, GA, July 1976.
4. USEPA Chesapeake Bay Program, "Monitoring Studies of Nonpoint Pollution in Chesapeake Bay Test Watersheds: Final Completion Report," U.S. Environmental Protection Agency, Annapolis, MD. (In Press).
5. Crawford, N.H and Linsley, R.K., "Digital Simulation in Hydrology: Stanford Watershed Model IV," Dept. of Civil Engineering Technical Report 39, Stanford University, Stanford, CA, 1966.
6. Cavacas, A., et al., "Hydrologic Modeling for Studies of Pollutant Loadings and Transport in Large River Basins," Proceedings of Stormwater and Water Quality Model Users Group Meeting: March 25-26, 1982, U.S. Environmental Protection Agency, Environmental Research Laboratory, Athens, GA, 1982.
7. Donigian, A.S. and Davis, H.H., "User's Manual for Agricultural Runoff Management (ARM) Model," EPA-600/3-78-080, U.S. Environmental Protection Agency, Environmental Research Laboratory, Athens, GA, August 1978.

8. Hollander, M. and Wolfe, D.A., Nonparametric Statistical Methods, John Wiley and Sons, New York, NY, 1973.
9. U.S. Geological Survey, "Water Quality of the Three Major Tributaries to the Chesapeake Bay, January 1979-April 1981: Estimated Loads and Examinations of Selected Water Quality Constituents," prepared for USEPA Chesapeake Bay Program, November 1981.

The work described in this paper was not funded by the U.S. Environmental Protection Agency. The contents do not necessarily reflect the views of the Agency and no official endorsement should be inferred.

HYDROMETEOROLOGICAL DATA AQUISITION: INNOVATIVE,
HIGH-RESOLUTION PROGRAMMABLE INSTRUMENTATION FOR
STORMWATER MANAGEMENT

BY

William James, Hector Haro, Mark A. Robinson,

Dale Henry and Reuven Kitai

Civil Engineering Department and

Electrical and Computer Engineering Department,

McMaster University, Hamilton, Ontario, Canada L8S 4B8

ABSTRACT

The paper describes difficulties with existing instrumentation, a new raingauge for sensing rainfall intensity at a high time resolution, and associated new instrumentation. The data logger incorporates an audio cassette unit for data retrieval and a single chip microcomputer programmed to record appropriate time series data in compact form. The data on the retrieved cassettes is input and stored on removable hard-disc packs via a PDP 1123 microcomputer through a specially devised decoder, also incorporating a single chip microcomputer. Special interactive FORTRAN applications software on the 1123 processes the time series data files and plots hyetographs on a desk-top plotter. Sample input/output is provided. The entire system is designed to be inexpensive, using cheap, mass-produced components. The system is being extended to monitor water depth (discharges), temperature, conductivity and pH. The system is designed for use in real-time control.

INTRODUCTION

Our hydrometeorological field program started in the summer of 1980. The data abstracted from these two field years enable calibration of stormwater management models for the city of Hamilton. These models are used in turn to determine average daily, monthly and annual amounts of stormwater runoff and pollutant loadings entering Coote's paradise and Hamilton Harbour, the receiving waters (Robinson and James, 1982). The pollutants investigated include:

- Suspended Solids
- BOD5
- Nitrogen
- Phosphate
- Coliforms

The models are also being used to investigate a wide range of design alternatives and strategies for minimising pollutant overflows due to stormwater from the city of Hamilton (or for example Kibler and Aron, 1980).

In the field program, rainfall intensity, stormwater quantity and quality samples are collected from various field stations located throughout the Hamilton-Wentworth region. Figure 1 presents an overview of the data acquisition network, based on conventional instrumentation.

CONVENTIONAL FIELD INSTRUMENTS

For the benefit of readers not familiar with field work, the purpose here is to review the general difficulties associated with



Figure 1 Hydrometeorological Monitoring Network
for the City of Hamilton

conventional instruments, and to elaborate on the new microcomputer-based instruments.

For a general review of the subject, see Alleg (1977). Readers familiar with conventional instruments should skip this part of the paper.

TIPPING BUCKET RAINGAUGES

Three types of tipping bucket raingauge (TBRG) were used in our field work. The Atmospheric Environment Service (AES) provides a standard TBRG which is used throughout Canada. It consists of a 10 inch (25.4 cm) diameter brass funnel, an AES standard bridge and bucket assembly and a heavy gauge brass and steel casing. Not all AES TBRGs are calibrated to 0.2 mm per tip (0.00787 in. per tip). Older Imperial gauges can be readily converted to metric standards by recalibrating them using a Calibration Checking Device and a No. 2 nozzle and rainfall simulator (Environment Canada, 1980).

Two other TBRGs were also used, manufactured in the United States by the Belfort Instrument Company and Weathertronics Incorporated. Both of these instruments were similar to the AES raingauge, except the bridge and bucket assembly incorporates the use of a mercury switch instead of a magnetic microswitch.

WATER LEVELS

Our pneumatic level sensors used air or nitrogen bubbles flowing at a constant rate through a tube, to exit at an appropriate location (e.g. weir). The components of a pneumatic level sensor site are a weir, an air supply and tube, a bubble gauge, a recorder, a power supply and

rating curves. Steven's float recorders, also used in our field work, are simple and easy to use if properly installed and maintained. The necessary components of this instrument are a stilling well, a recorder in a waterproof recorder housing, a weir in a stable channel and a rating curve. The recorder is powered by a clock which is driven by a weight. The water level is sensed by a float inside the stilling well.

MAINTENANCE OF CONVENTIONAL INSTRUMENTS

With experience it was found advisable to carry out maintenance twice a week. The following point by point maintenance schedule for the pneumatic level sensors is presented to illustrate the effort involved:

1. Rewind spring operated clock to ensure accurate paper transport.
2. Check air or nitrogen pressure. If pressure is below 500 psi, install a new gas cylinder.
3. Check bubbling rate to ensure that the apparatus is still operating. One bubble emitted every 2 or 3 seconds is adequate.
4. Check battery to ensure adequate power supply.
5. On a monthly basis clean the upstream side of the weir to ensure that the water level is unaffected by sedimentation.

Maintenance of chart recorders was as follows:

1. Indicate timing marks to ensure accurate timing.
2. Top off ink well and inspect ink nib.
3. Check chart paper to ensure sufficient quantity is available (new rolls last two weeks).
4. Check battery to ensure an ample power source for the pen.

However, conventional spring-driven instruments failed to operate for short periods at random intervals. The most common mechanical failures experienced in our field work were:

1. Recorder ink running out before the next maintenance check. This failure was caused by the lack of ink in the ink well, air bubbles in the ink well (i.e. pen not primed) or pen releasing ink too rapidly.
2. Recorder ink smearing causing distortions.
3. Chart paper ripping and/or jamming.

4. Electric failures (i.e. 110V and/or battery).
5. Erratic bubbler rate.
6. Bubble tube blocked.
7. Float sticking to side of stilling well.

DATA ABSTRACTION FOR CONVENTIONAL EQUIPMENT

The strip charts from the various rain recorders were removed after each storm event. Timing marks were noted and timing errors manually corrected. One minute rainfall intensities were calculated using tipping capacities of 0.254 mm/tip or 0.200 mm/tip. A typical chart strip recording and hyetographs is shown in Figure 2. The hyetographs were plotted on a plotter using the software described below. It is clear from the above descriptions that conventional instruments require continuous maintenance and manual data massaging.

MICROCOMPUTER-BASED DATA ACQUISITION SYSTEM

Modern microcomputers, on the other hand, provide an excellent tool for stormwater management (James and Robinson, 1980).

A microcomputer is a digital integrated circuit (or group of integrated circuits) containing all the functions required in a digital processing system. A typical digital microcomputer consists of: central processor unit (CPU), program memory, data memory and input/output ports (I/O).

The program memory serves as a place to store instructions, the coded pieces of information that direct the activities of the CPU. In data memory the information processed by the CPU is stored. The input ports are used by the CPU to receive information from an external device

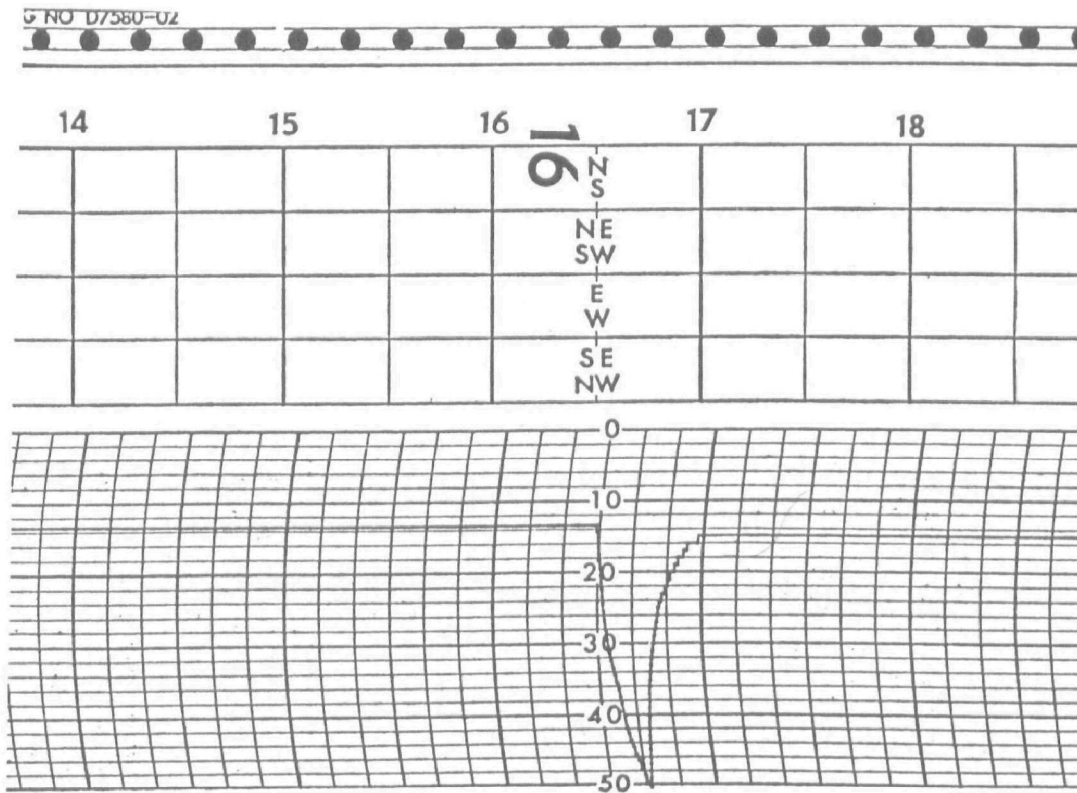
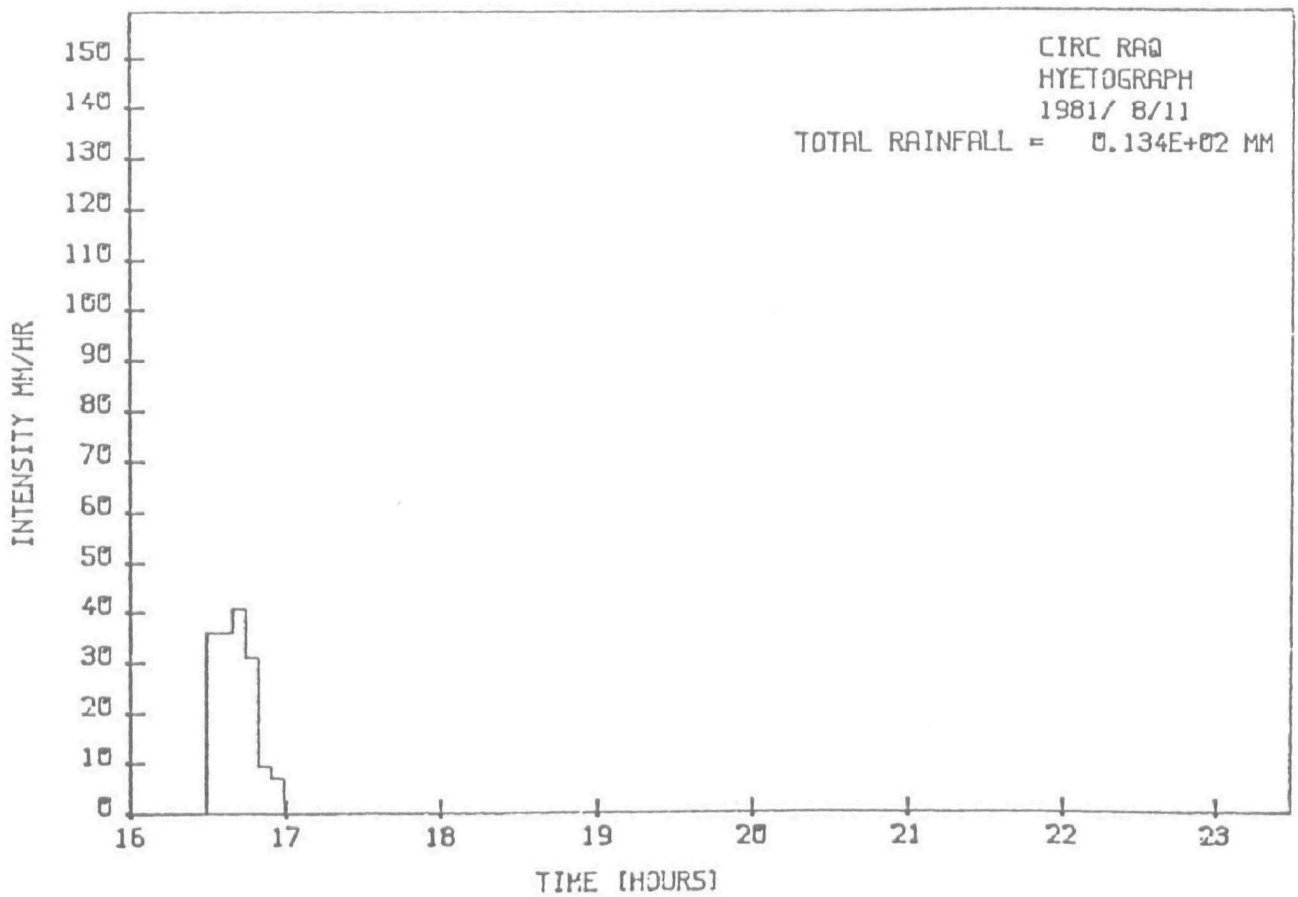


Figure 2 Strip Charts for the Rustrak and 30 Day Recorders

such as: memory, paper tape reader, floppy disk, etc. at high rates of speed and in large volumes. A computer also requires one or more output ports that permit the CPU to communicate the results of its processing to the outside world. The CPU controls the functions performed by all the other components. The CPU must be able to fetch instructions from memory, decode their contents, and execute them and output the results. It must also be able to reference memory and I/O ports in the execution of an instruction. Figure 3 presents a simplified overview of the components in a microcomputer.

A microcomputer can receive digital information from rain gauges or streamflow sensors and process the information into a useful format, store this data on cassette tape and transmit the data to other remote devices such as a central site computer.

A microcomputer-based system is more reliable, efficient and accurate and also less expensive than a conventional data acquisition system. Manual data manipulation is not necessary. Processed data is stored permanently at each transducer on cassette tape recorders, and at the central site where the processed data is dumped by the central mini-computer onto magnetic tape. The processed data can be accessed by an operator at the console for any desired time period. The processing and transmitting procedures are so quick that real time control is readily adaptable to this type of data acquisition system. At present all programming in our existing raingauge microcomputers takes up only 370 milliseconds of the 60 second cycle time.

Mechanical failures are very unlikely. There are no moving parts such as gears and switches to wear out and replace. Power input to the system is minimal and a small power pack could supply the unit for a

long period. Timing errors are eliminated since the internal timing mechanism is extremely accurate. Synchronization of the entire data acquisition network is easily obtained within an estimated acceptable tolerable error of thirty seconds for the drainage control system.

Electronic devices require little maintenance. Remote devices can be monitored by the operator at the central receiving site, thereby reducing the number of field inspection trips. Faulty microcomputers are easily replaced.

NEW MICROPROCESSOR-BASED RAINGAUGE

Conventional TBRGs and recorders are large, cumbersome and expensive to purchase and maintain. Recorder parts and data recording papers are expensive. We have accordingly attempted to produce a lower cost, higher precision, reliable and automatic system for rainfall data measurement, logging and presentation.

As shown in Figure 4, our raingauge consists basically of three major components:

- (A) The rain sensor collects precipitation and converts it into water drops of almost constant size to be counted by the data logger.
- (B) The data logger senses the drops and counts them for a programmable time interval. The logger processes the time series and stores it on standard audio cassette magnetic tape.
- (C) The cassettes are removed, transported to our computational laboratory, and read and interpreted by a decoder. The decoder communicates the rainfall time series data to a PDP 1123 computer, operating in a multi-user environment.

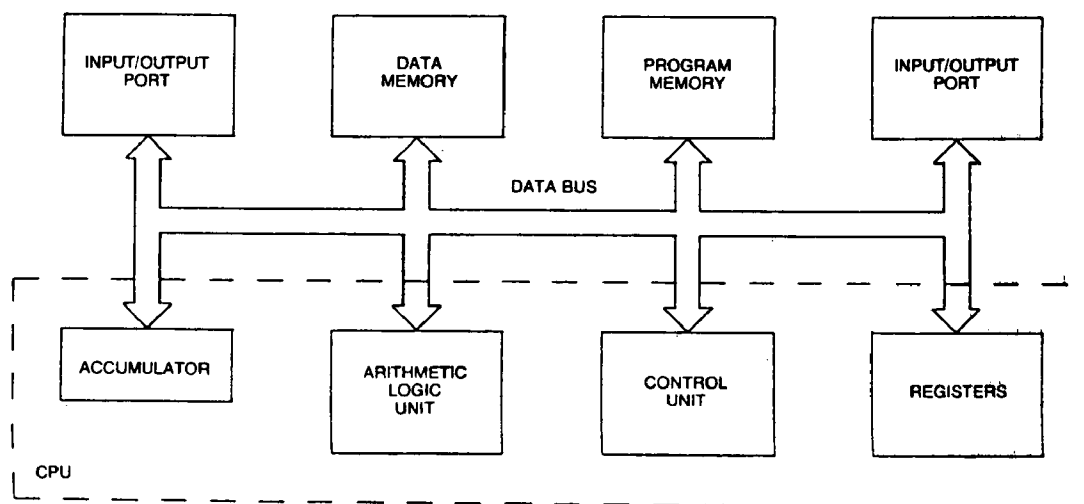


FIGURE 3

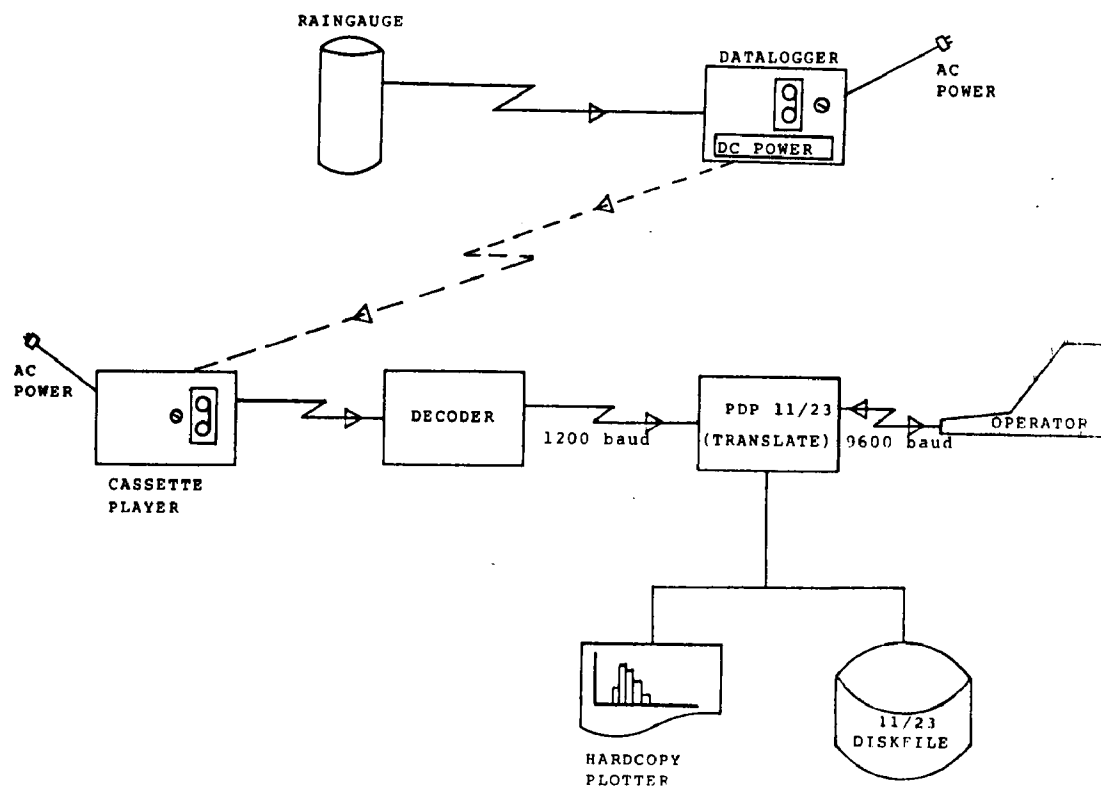


FIGURE 4

The microprocessor raingauge stations were not completed until late 1981. Therefore no complete storm event data were collected using these instruments in 1981. Rigorous testing is now being completed at the Canada Centre for Inland Waters (CCIW) in Burlington to ensure that the microprocessor raingauge is functioning as expected. Ten gauges are now being used in the field (1982) in Hamilton, and other are to be used elsewhere (Ottawa, North West Territories, Precipitation sampling sites in Ontario).

The raingauge is contained in two cylinders, numbers (1) and (2) in Figure 5. Cylinder (1) contains the sensor while cylinder (2) is used as the base. Both cylinders are easily assembled and the screws (3) are used to clamp them together.

Inside cylinder (1) there is a plastic funnel (4) whose function is to collect the rain. The rubber stopper (5) is pierced by a capillary glass tube (6). The lower part of the funnel (7) supports the sensor (8) which consists of two electrically conducting points.

The sensor is connected electrically to the connector (10) mounted inside cylinder (1) and its sensor system may be separated mechanically as well as electrically from cylinder (2).

At the top of the funnel inside the cylinder, there is a removable coarse mesh (9) whose function is to trap leaves, etc. Under this mesh at the point where the funnel shape changes, there is another dome-shaped fine mesh (11) to prevent dust entering the glass tube.

The plastic surrounding (12) the top of cylinder (1) provides a good aerodynamic shape, to reduce air turbulence above the gauge.

A clamp (13) secures the cable (14) to cylinder (2). Cable (14) feeds the sensor to the electronic system.

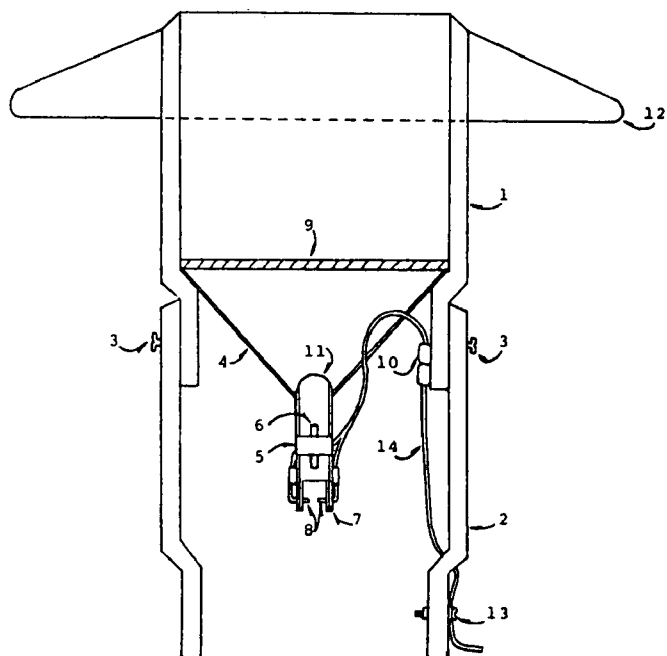


FIGURE 5

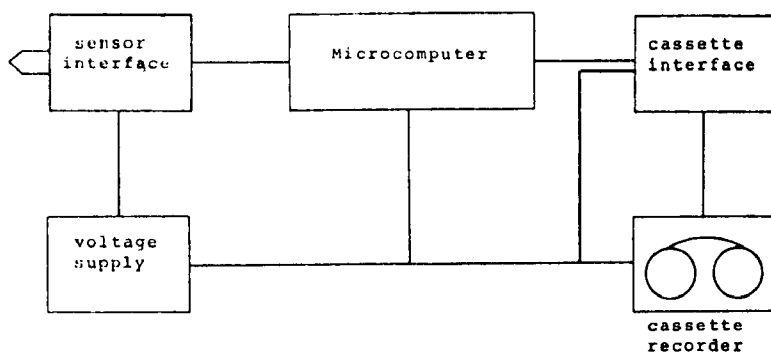


FIGURE 6

The electronic system consists of five parts as shown in Figure 6.

The sensor interface senses the drops and converts them into electrical pulses for the microcomputer. The microcomputer counts these pulses and stores the count in memory for a time interval which is predetermined when the microcomputer is programmed. At the end of this time interval, the microcomputer turns on the cassette recorder through the cassette interface and records the acquired information together with the time the data was acquired.

A single chip microcomputer is used for temporary storage as well as data processing.

The cassette interface controls the recorder power supply as well as the signals to be recorded. The recorder is a mass-produced product that has been modified slightly. Frequency shift keying is used because of the limited frequency response of the recorder.

Power is normally provided by A.C. mains supply. A rechargeable battery backup provides continuity of supply in the event of main supply failure.

The novel aspects of this device are as follows:

1. The raingauge is constructed from low-cost mass-produced plastic components that are manufactured for other primary purposes.
2. A microcomputer in conjunction with peripheral electronic devices is used to detect and count drops, together with precision time measurement.
3. Digital rainfall rate and time are stored on audio magnetic tapes.

Limitations of the apparatus are as follows:

For very high intensity rainfall, the flow changes from drops to a continuous jet. The tests show that continuous jet flow commences only above 25 millimeters of rain per minute, which is a very rare event.

The two meshes have to be wetted before the water can pass through the funnel. Also, as the diameter of the glass tube is small to form the drops, some water necessarily collects above the tube before surface tension is overcome and drops pass the detectors.

The total initial water required to "wet" the funnel, from the dry state, is of the order of 0.03 mm. of rain, roughly 15% of that required to tip a standard tipping bucket type rain gauge. This is considered negligible in most measurements.

Technical details for the raingauge are listed in Table 1 and for the data logger in Table 2.

TABLE 1: RAINGAUGE DETAILS

Collecting surface	8 107 mm. ²
Drop size	31 mm. ³
	3.81E-3 mm. of rain
Drop size variation (max.)	± 2.17 mm. ³
Maximum capacity	18.6 cm. ³ /min.
	137 mm/hr of rain
Water retention from dry state	350 mm. ³
Size: Height	235 mm.
Width	235 mm.

TABLE 2: DATA LOGGER DETAILS

Microcomputer	Intel 8748
Storage media:	
Magnetic cassette tape	Audio
Modulation	Frequency shift keying
Carriers	1.8 and 2.7 Khz.
Baud rate	300 bps.
Format	50 bytes/block
	11 bits/byte
Data block	10 bytes of synchronism
	20 bytes of data
	20 bytes of timing
Error relation	Less than 1 error in 10^6
Recorder capacity	7 days of continuous rain
	5 years of no rain
Operating temperature	+10°C to +50°C.
Power requirements	115 V.a.c.
Steady state	75 ma. @ 5 V.d.c.
peak (at last 4 sec. each 20 mins.)	225 ma. @ 5 V.d.c.
Battery back-up	17 hrs. 6 C size batteries
	(Self Charging)

TABLE 3

```

system number 10010010050010080010110010160010210010270010310010360010380010420
01046001056001064001090001094001138001175001178001181001183001185001187001188001
18900119100119200119400119500119700119900120200120700121100121300121500121800122
00012270012330012400000990011250011580012340012400000720011050011320011410012400
00072001220001240000052001085001103001114001137001159001184001220001240000036001

```

```

STORM EVENT  START  MARCH,16,1982  12:02
              FINISH  MARCH,17,1982  10:00

```

APPLICATIONS SOFTWARE FOR DATA PRESENTATION

A sample of the data stored on the data logger is presented in Table 3. In order to present this information in a form readily comprehended by hydrologists/engineers and also in a format for input to SWMM, a considerable amount of program development was necessary.

The TRANSLATE and INTERPRETATION procedures developed for the PDP1123 were written in a transportable subset of FORTRAN. The overall flowcharts for the programs are presented in Figures 7-9 inclusive.

These programs interpret the information stored on the data logger and prepare the plotting files for a Houston Instruments Plotter (Gausch and Lomb, 1981). A typical hyetograph was presented in Figure 3.

FUTURE DEVELOPMENTS

REAL-TIME MICROCOMPUTER-BASED CONTROL SYSTEM

Using our existing calibrated continuous SWMM model of the drainage network, simpler relations for the prediction of real time stormwater flow (or water level) have been developed (Robinson and James, 1982). Statistical analyses of the input and output from our calibrated model, including multiple regressions, serial cross-correlations and auto-lag correlations, provide reliable local prediction equations. It is our intention to use these equations in existing field microcomputers on a continuous basis.

The entire real time microcomputer control system envisaged would include the following items (Figure 10):

FLOWCHART - GENERAL TRANSLATE PROCEDURE

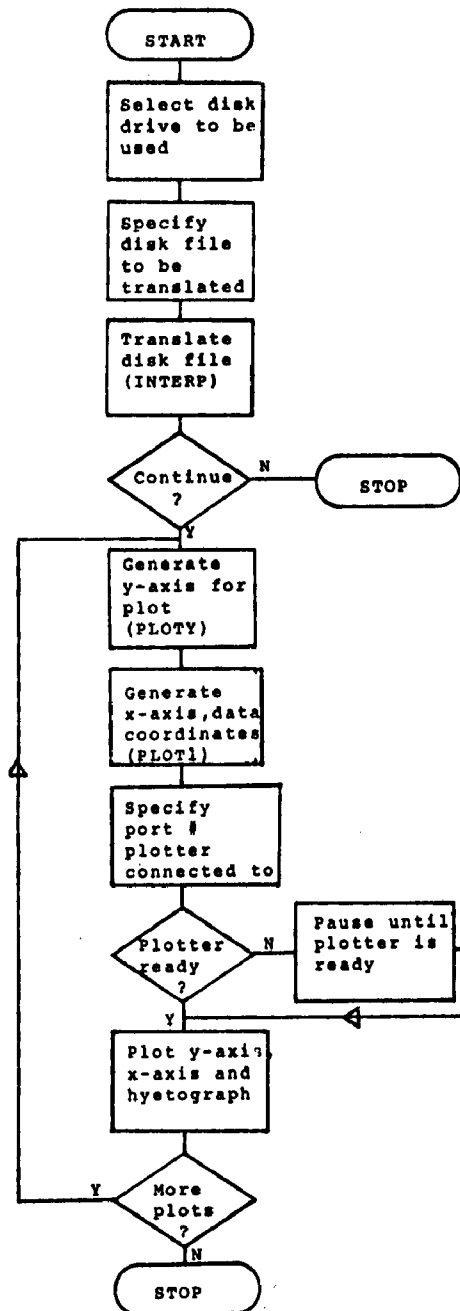


FIGURE 7

FLOWCHART - PROGRAM INTERP

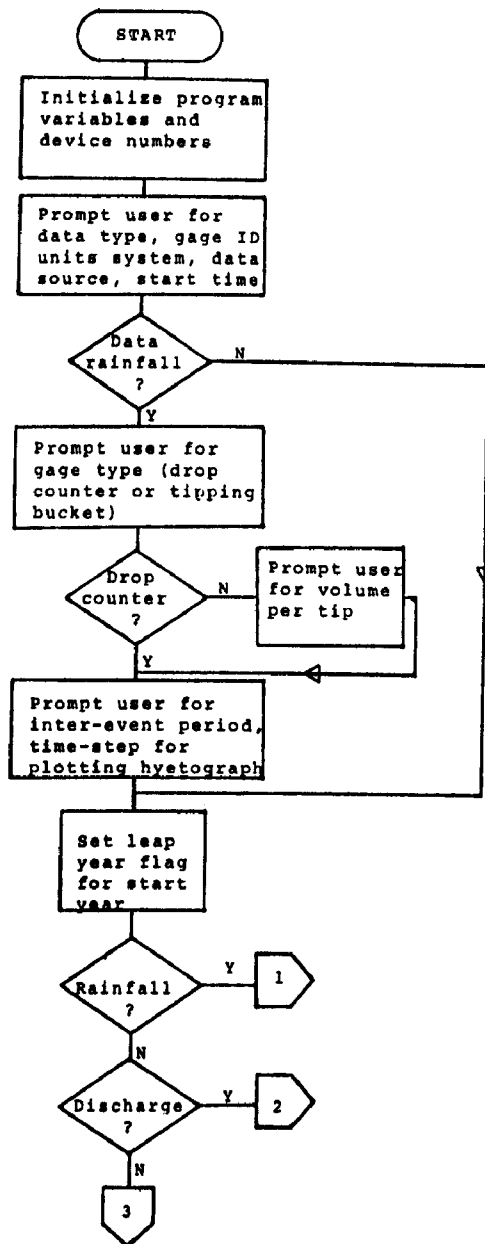


FIGURE 8

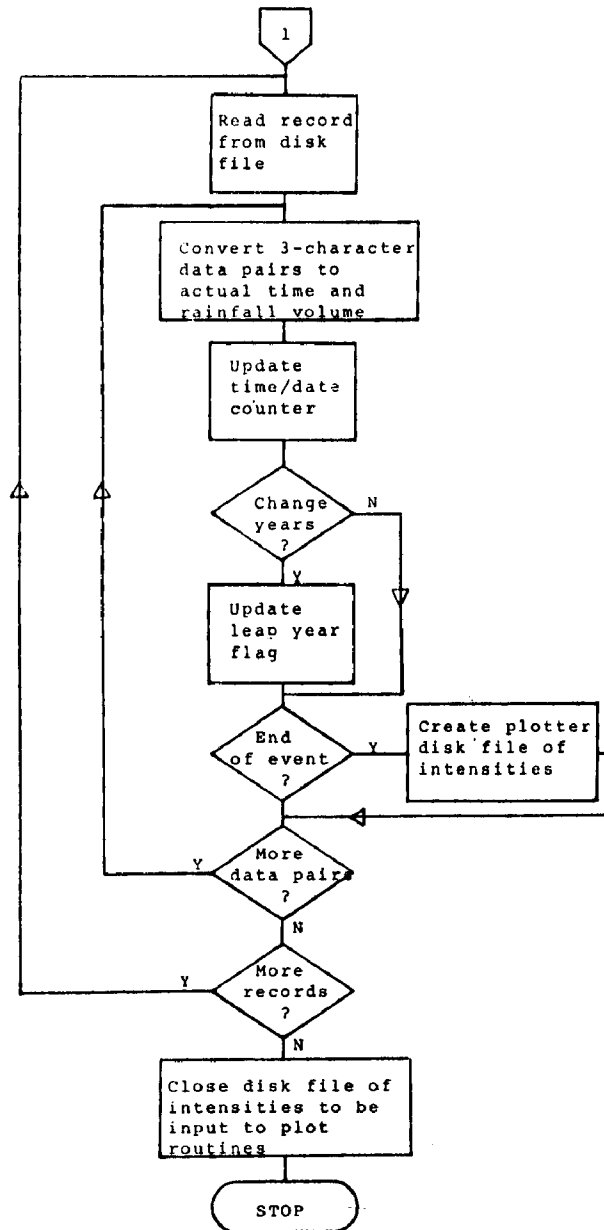


FIGURE 9

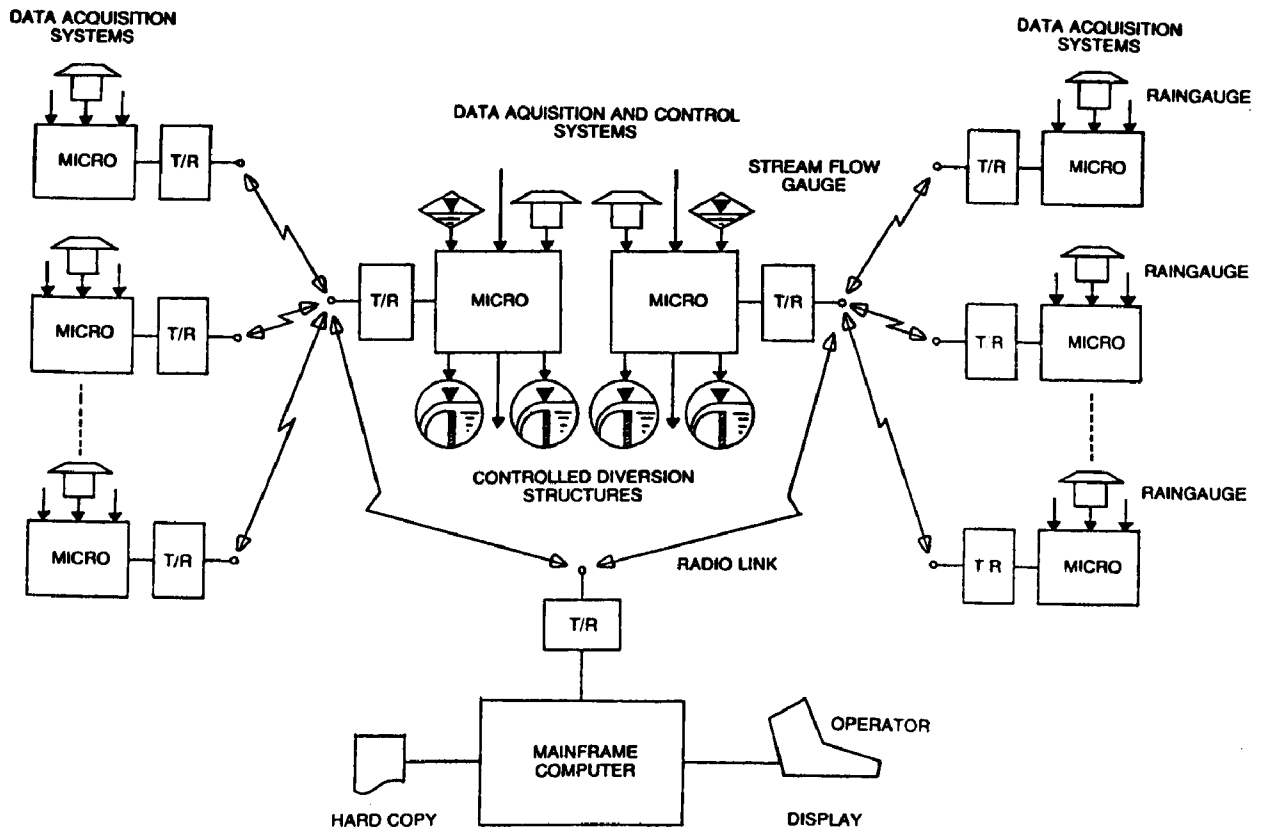


FIGURE 10: Proposed Real Time Control System

1. remote monitoring and telemetering stations each with microcomputer and cassette recorders,
2. communication network (radio or existing leased telephone lines),
3. microcomputer controlled diversion structures (initially only one is suggested),
4. central minicomputer with display, operator control console and magnetic tape archive. Our existing PDP 1123 would be a suitable machine for this.

Following the approach used elsewhere (EPA, 1980; McPherson and Ammon, 1980), the microcomputer system will be programmed for the following operational strategies:

1. Only these structures diverting combined sewage from catchments lying in the storm track will be activated (Schtifter, 1981).
2. As much of the first flush as possible will be transported to the sewage treatment plant (STP).
3. Discharges from the "dirtiest" catchment areas will have the highest priority for transport to the STP.
4. The diversion gates close in a preset order; the least polluted first, and to the sensitive outfall areas (if any) last.
5. When in-line storage to the STP becomes available, gates open in the order of the more polluted runoff first, based on instantaneous indicators.
6. Maximum inflow to the sanitary interceptor is increased to a carefully computed increased proportion of dry weather flow, eg. 4 times DWF. Manual override for all structures is provided.

Advantages of the proposed system are briefly listed below:

1. Inadvertent discharges to the natural receiving waters due to erroneous storm forecasts are reduced.
2. Stormwater is selectively discharged so that the "dirtiest" flow is directed to the sewage treatment plant first.
3. Stormwater is anticipated so that maximum storage can be reserved for highly polluted flows.
4. The central control site has an improved capability to divert some or all of the stormwater from the drainage network. At the present time this is not possible. The central site will know the likely pollutional loadings from the contributing areas, from the results of our current modelling studies.
5. The improved system control could reduce the possibility of basement flooding, through better monitoring and control.
6. Blockages of overflow structures are hard to detect at the present time. The proposed system is able to detect them almost as soon as they occur.
7. A good stormwater data base is archived for future studies.

8. The microcomputer-based control system can be easily expanded. For example, extra storage facilities can be added to the drainage network using better estimates of cost-effectiveness from the simulation programs.
9. Structural changes in the drainage system occur frequently; re-evaluation of the prediction equations can easily be incorporated in the microcomputers.
10. The storage available in most existing drainage networks is minimal. The total amount of available storage in Hamilton, converted to depth of water over the Central Business District (CBD) amounts to only 1.2 mm. or about 4 mm. of rain on all directly connected impervious areas of the CBD. Additional storage would provide further control but would of course be expensive. Additional storage can easily be incorporated in the system programs.
11. The present continuous SWMM model for downtown industrial land uses in the CBD has not yet been expressly calibrated for either discrete or continuous storm events. New automatic sampling equipment will facilitate calibration in the near future. New calibration parameters can easily be incorporated into the microprocessors.

ACKNOWLEDGEMENTS

The Computational Hydraulics Group at McMaster University, is a small organization dedicated to researching and developing innovative solutions for urban drainage and their environmental problems. The group comprises nine members: W. James, Director, two full-time research engineers (Mark Robinson and Dale Henry), one research assistant (Carol Brown), a full-time text processor (Brenda Bon) and five full-time graduate students (Hector Haro, Ron Scheckenberger, B. Shivalingaiah, Alaa ElZawahary and Ali Unal). Two part-time undergraduate members are Mark Stirrup and Peter Nimmrichter. Four summer students and a visiting professor from Sweden usually join the group each year.

The Ministry of the Environment and the Hamilton-Wentworth Regional Engineering Department jointly provided funds for investigations on the urban drainage system in the city of Hamilton. Other studies have been funded by the Natural Science and Engineering Research Council, and Environment Canada, to develop computer software for stormwater management, including pollutants washed off street surfaces.

The group possesses a Burroughs B1985 computer, with magnetic tape and disc drives, line printer and six terminals, made available by Burroughs Inc. The group also has a PDP 1123 with hard disc drives, plotter, line printer, word processor and six terminals, obtained through an NSERC grant.

REFERENCES

- Environmental Protection Agency, "Urban Stormwater Management Technology: Case Histories", August, 1980, Report No. EPA-600/8-80-035, 329 pp.
- Kibler, D.F. and Aron, G., "Urban Runoff Management Strategies", Journal of the Technical Councils, ASCE, Vol. 106, No. TC1, August 1980, pp. 1-12.
- Schtifter, Z., "A Kinematic Storm Model for an Urban Drainage Study", M.Eng. Thesis, McMaster University, Hamilton, 1981, 152 pp.
- James, W., and Robinson, M., "Potential Coordinated Multiprocessing System for Field Data Acquisition and Real Time Control of Urban Drainage in Hamilton", McMaster University, Hamilton, Ontario, 1980, 20 pp.
- McPherson, M.B. and Ammon, D.C., "Integrated Control of Combined Sewer Regulations Using Weather Radar", Municipal Environmental Research Laboratory, Office of Research and Development, USA, EPA, R806702, 1980, 87 pp.
- Alley, W.H., "Guide for Collection, Analysis and Use of Urban Stormwater Data", ASCE New York, 1977, 115 pp.

Environment Canada, "Field Test of Accuracy for Bridge and Bucket Assemblies (Tipping Bucket Raingauge)", Atmospheric Environment Services, Willowdale, Toronto, October, 1980, 10 pp.

Gausch and Lomb, "Houston Instrument, Hi-Plot, Operator's Instructions", Gausch and Lomb, One Houston Square, Austin, Texas, 1981, 35 pp.

Robinson, M. and James, W., "Continuous SWMM Modelling of Hamilton Summer Stormwater Including Certain Quality Indicators - Preliminary Output Time Series Using Discrete-event Calibration for Non-industrial Areas", published by CHI Publications (about 200 pages), March 1982.

The work described in this paper was not funded by the U.S. Environmental Protection Agency. The contents do not necessarily reflect the views of the Agency and no official endorsement should be inferred.

The Separation of Boundary Layer And Flow Turbulence Of Center-Feed Circular Sedimentation Basins

by

Tieh-lin Yin, M. ASCE
Project Manager/Engineer
Maryland-National Capital Park and Planning Commission
Upper Marlboro, Maryland

(I) Introduction

Sedimentation has been one of major treatments for purification of waste and wastewater for many years. Settling tanks are efficient in removal of suspended solids at relatively less cost. It is believed that they will continue to be one of the primary unit operations in wastewater treatment process.

The efficiency of most wastewater treatment processes are largely a function of hydraulic efficiencies of operations; and the sedimentation is especially of the case. Several researchers have investigated the methods of determination of the hydraulic efficiencies of sedimentation basins.

Basically the hydraulic efficiency of sedimentation basins are evaluated through the analysis of the types of flow. The types of flow may be considered plug flow and complete mixing flow, the former being the ideal settling flow and never existing and the latter having the assumption that any content, such as suspended solids or a dye, will immediately and completely disperse throughout the volume of the whole tank at the beginning of the influent. Both are extreme cases and the real basin falls in between.

By plan view, sedimentation basins are generally either rectangular or circular. The circular basins are further classified as center-feed and peripheral-feed depending on the location of inlet. Generally accepted through previous studies is that the hydraulic performance of rectangular settling tanks are better than that of circular tanks, and the peripheral-feed circular settling tanks have better hydraulic efficiency than center-feed circular settling tanks.

In previous research little emphasis has been focused on the explanation into insight of the above fundamental phenomenon in sedimentation basins. In this report it is intended to analyze the boundary layer flow separation in center-feed circular basins, which is believed to be the major reason for the difference of hydraulic efficiency between rectangular and circular settling basins.

Primarily, this paper presents the analysis in an analytical approach adopting some classical treatments of the problem, to prove the occurrence of boundary layer flow separation in center-feed circular settling basins.

(II) Fundamentals of Boundary Layer Flow Separation

There are certain phenomena in fluid flows, which cannot be dealt solely by the frictionless flow theory. One example is that a submarine with constant cruising speed under water experiences drag force due to viscous friction of the water. Another example is the experimental fact that the relative velocity between solid surface and the flowing fluid is zero. Actually there is a thin layer immediately adjacent to solid surface called boundary layer where frictionless flow theory ceases to be completely valid.

Boundary Layer Approximations

It is a basic assumption that in the study of boundary layer, for flows with large Reynolds numbers the boundary layers are thin compared with the characteristic dimensions of the problem. Based on this assumption we can have the following simplifying approximations.

- (1) Within the boundary layer the pressure is approximately constant in the direction normal to the surface, and can be calculated from frictionless flow theory.
- (2) The flow within the boundary layer is basically parallel and the shearing stress on a fluid element can be approximated by $\tau = \mu \left(\frac{\partial u}{\partial y} \right)$, where μ is dynamic viscosity of the fluid, u is the tangential component of the fluid velocity and y is the distance normal from the body surface.
- (3) The thickness of boundary layer is thin compared with the body and with radius of curvature of the body surface.

The following boundary layer equations are based on these assumptions.

Boundary Layer Equations

The following two equations are called Prandtl's boundary layer equations, the derivation of which are primarily due to L. Prandtl.

$$\frac{\partial u}{\partial x} + \frac{\partial v}{\partial y} = 0 \quad (1)$$

$$\frac{\partial u}{\partial t} + u \frac{\partial u}{\partial x} + v \frac{\partial u}{\partial y} = -\frac{1}{\rho} \frac{dP}{dx} + \nu \frac{\partial^2 u}{\partial y^2} \quad (2)$$

For the case of steady flow, Prandtl's boundary layer equations are simplified to:

$$u \frac{\partial u}{\partial x} + v \frac{\partial u}{\partial y} = -\frac{1}{\rho} \frac{dP}{dx} + \nu \frac{\partial^2 u}{\partial y^2} \quad (3)$$

$$u \frac{\partial u}{\partial x} + v \frac{\partial u}{\partial y} = -\frac{1}{\rho} \frac{dP}{dx} + \nu \frac{\partial^2 u}{\partial y^2} \quad (4)$$

The derivation of Prandtl's boundary layer equations will not be discussed here. In above equations, v is velocity component along y ; P is pressure; ν is kinematic viscosity, and ρ is fluid density.

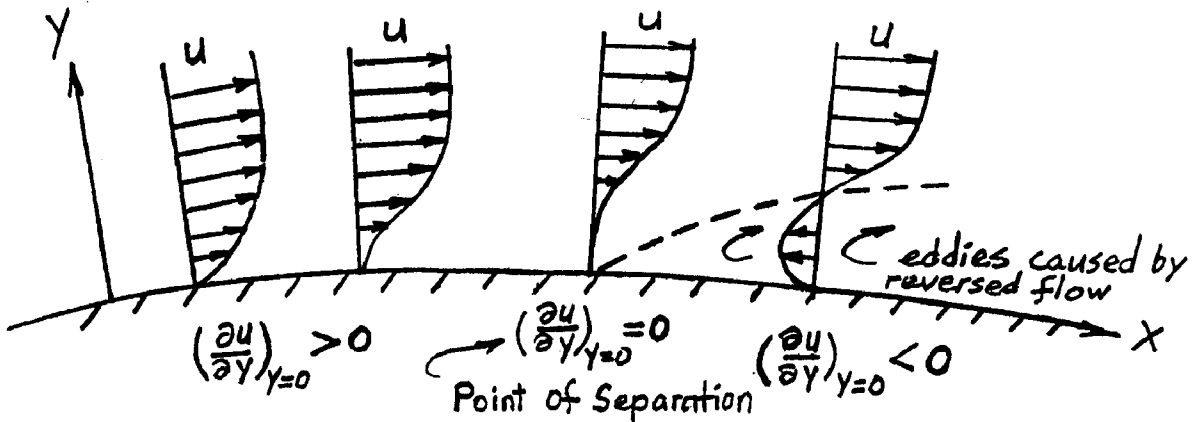
Solution of Prandtl's Boundary Layer Equations

A number of solutions of boundary layer equations has been developed in past years. Because of their mathematical complication some approximate solutions have also been developed, a famous one of which was attributed to Karman and Pohlhausen. Basically this technique is used to prove the occurrence of boundary layer separation in center-feed circular sedimentation basins, as will be discussed later.

The problem of boundary layer is to find the solutions $u(x,y)$ and $v(x,y)$ for equations (3), (4) for a given solid body in a flow with large Reynolds number. The solutions must satisfy the following conditions:

- (1) On the body surface $y=0$, $u=v=0$
- (2) At the outer edge of boundary layer $u=U(x)$, the velocity calculated from frictionless flow theory. $P(x)$ and $U(x)$ are related by Bernoulli's equations $P + \frac{1}{2} \rho U^2 = \text{constant}$.
- (3) At some upstream points in the boundary layer, the velocity profile must satisfy some initial conditions, such as $X=0$, $U=0$ at stagnation point.

Boundary Layer Separation:



Along the streamwise direction, the pressure can either increase or decrease depending on physical conditions, which will make different consequences on the development of boundary layers. If the pressure decreases it is called favorable; if the pressure increases, it will be called unfavorable. As the fluid element within boundary layer experiences retarding viscous stress, the favorable pressure gradient tends to accelerate the fluid element in the boundary layer, thus helping it to overcome the viscosity. In the case of unfavorable pressure, the increasing pressure will add some retarding force to the fluid element in the boundary layer. Near the bottom, the fluid elements have to overcome not only the increasing pressure but also the wall shear stress which is extremely large here compared with that in outer edge. Therefore it may be a point downstream where the flow begins to be forced in reverse direction near the bottom. This point is called separation point.

In mathematical expressions, the above argument can be as follows: since the velocity profile is reversed at bottom part and at the point of separation where the tangent is zero, there must be a point of inflexion in the profile. In other words, the separation can only occur when the flow is retarded.

Mathematically,

$$\mu \left(\frac{\partial^2 u}{\partial y^2} \right)_{y=0} = \frac{dP}{dX} > 0 \quad (5)$$

$$\text{or, } \left(\frac{\partial^2 u}{\partial y^2} \right)_{y=0} > 0 \quad (6)$$

is a necessary condition for the separation.

$$\text{Only } \left(\frac{\partial u}{\partial y} \right)_{y=0} = 0 \quad (7)$$

is the definition of and sufficient condition for the boundary layer separation.

After the point of separation, the flow is reversed in direction near the bottom and becomes highly turbulent due to possible vertical eddies, involving energy dissipation and making the suspended solids difficult to settle. As to how to quantify the turbulence and its effect on the sedimentation of suspended solids, additional study involving experiments is needed.

(III) Boundary Layer Separation and Flow Turbulence

In this section it is intended to show that in center-feed circular sedimentation tanks boundary layer separation occurs and it makes the flow highly turbulent in the bottom area of the tank. We try to obtain the conclusion through analytical approach based on some mathematical developments about the boundary layer problem.

This effort of trying to investigate insights of the efficiency of circular sedimentation tanks has reached an explanation agreeable with previous experimental results concerning hydraulic or sedimentation efficiency of different kinds of settling basins.

Based on Van Kaman-Pohlhausen:

It is defined that

$$Z = \frac{\delta_z^2}{\nu} \quad (8)$$

$$K = Z \frac{dU}{dx} \quad (9)$$

where, δ_z = memetum thickness of bounday layer; and ν = kinematic viscosity.

At separation the velocity profile shape factor $\Lambda = -12$ or -10 . Λ is defined as

$$\Lambda = \frac{\delta^2}{\nu} \frac{dU}{dx}, \quad \delta = \text{boundary layer thickness} \quad (10)$$

If $\Lambda = -10$ is chosen, the corresponding value of K is -0.1369 as derived by Holstein and Bohlen.

Therefore,

$$Z = K / \frac{dU}{dx} = -0.1369 (U')^{-1}$$

$$\text{Or, } \frac{dZ}{dx} = 0.1369 \frac{U''}{(U')^2} \quad (11)$$

$$\text{Let } \sigma = \frac{U U''}{(U')^2} \quad (12)$$

$$\text{Then equations (11) become } U \frac{dZ}{dx} = 0.1369 \sigma \quad (13)$$

From mementum equation

$$U \frac{dZ}{dx} = F(K) = 1.523 \text{ for } \Lambda = -10 \text{ also by Holstein and Bohlen.}$$

$$\text{Therefore, } \sigma = \frac{U U''}{(U')^2} = 11.13 \approx 11 \quad (14)$$

$$\text{If } \sigma > 11 \quad \text{no separation} \quad (15)$$

$$\sigma < 11 \quad \text{separation}$$

For the center-feed circular settling tank, the following relationships hold as derived by Chiu assuming point source of influent.

$$U = \frac{m}{X} \quad (16)$$

$$\frac{dU}{dX} = -\frac{m}{X^2} \quad (17)$$

$$\frac{d^2U}{dX^2} = \frac{2m}{X^3} \quad (18)$$

where m is a constant.

Substitute equations (16) (17) (18) into equation (14)

$$\sigma = \frac{UU''}{(U')^2} = \frac{\frac{m}{X} \cdot \frac{2m}{X^3}}{\left(-\frac{m}{X^2}\right)^2} = 2 < 11$$

This result leads to conclude that the pressure increase rate in center-feed circular settling tanks is so large that separation is far from being able to be avoided.

In real circular settling tanks, no point source of influent exists. X should begin at X_0 instead of zero. Therefore,

$$U(x) = U_0 \frac{X_0}{X} \quad (19)$$

$$U'(x) = -U_0 \frac{X_0}{X^2} \quad (20)$$

$$U''(x) = 2 U_0 \frac{X_0}{X^3} \quad (21)$$

Substituting equations (19) (20) (21) into equation (14) also gives $\sigma = 2 < 11$ as explained before.

Based on Curle and Skan's solution of Boundary layer equation,

$$x^2 C_p \left(\frac{dC_p}{dx} \right)^2 = 1.04 \times 10^{-2} = K \quad (22)$$

Where:

x = position of separation

$$C_p = (P - P_0) / \left(\frac{1}{2} \rho U_m^2 \right) = 1 - \frac{U^2}{U_m^2} \quad (23)$$

U_m = max. main stream velocity.

K = Function of pressure distribution

For the circular tank, substitute equations (19) (20) (21) into equation (22) and get the following:

$$x^2 \left(1 - \frac{U^2}{U_m^2} \right) \left[\frac{d}{dx} \left(1 - \frac{U^2}{U_m^2} \right) \right]^2 = 1.04 \times 10^{-2} \quad (24)$$

Equation (24) becomes:

$$X^6 - 384.4154 X_0^4 X^2 + 384.4154 X_0^6 = 0 \quad (25)$$

As the solution of the equation (25), X has two values. One is $X = 1.002 X_0$ and another one is $X = 4.369 X_0$. The first value implies the physical meaning that the flow separation occurs almost immediately after the influent point. The physical meaning of the second value $X = 4.369 X_0$ is perhaps more significant. It contains the possibility that the boundary layer would go further turbulent at around $X = 4.369 X_0$ due to continuous pressure increases after the flow separation occurs at $X = 1.002 X_0$. Alternatively, but consistently with the foregoing interpretation, the physical meaning can be conceived as follows: Since the flow faces a continuous pressure increase along the outwardly radial direction, the boundary layer is unstable almost at the beginning of the influent, and the separation occurs at approximately $X = 4.369 X_0$. After this point, the boundary layer becomes turbulent due to the flow separation and subsequent reversed flow and vertical eddies.

In other words, it can be concluded as follows: The center-feed circular settling tank has such a large unfavorable pressure gradient that the laminar boundary layer almost cannot exist and the bottom flow is turbulent, especially after the flow separation at $X = 4.369 X_0$, all the way to the point of outlet. This conclusion is parallel to the previous result that $\zeta = 2 \ll 11$, which indicates that the pressure increase makes the bottom flow much more turbulent than mere occurrence of boundary layer separation. Obviously, experimental observation is needed to quantify the turbulence under this condition.

Another approach can also lead to the similar result.

Also based on Kaman-Pohlhausen solution of boundary layer equations, the velocity profile parameter $\Lambda = \frac{\delta^2}{\nu} \frac{dU}{dx}$ determines the shape of velocity profile and occurrence of flow separation.

For the center-feed circular tank the boundary layer thickness at x is:

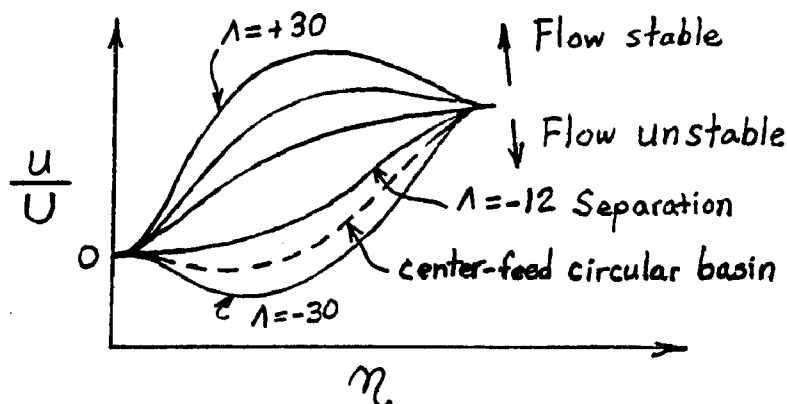
$$\delta_x = 5 \sqrt{\frac{\nu x}{U_x}} \quad (26)$$

Substituting $U_x = U_0 \frac{X_0}{X}$, $\frac{dU_x}{dX} = -U_0 \frac{X_0}{X^2}$ and equation

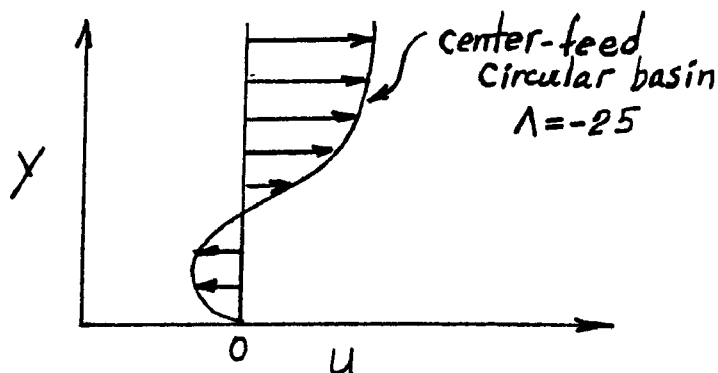
(26) into definition equation of Λ gives

$$\begin{aligned} \Lambda &= \frac{\delta^2}{\nu} \frac{dU_x}{dX} \\ &= -25 \ll -12 \end{aligned}$$

$\Lambda = -12$ is the value meaning occurrence of boundary layer separation. This, also agreeable with the previous result, may be interpreted as bottom flow being almost turbulent everywhere in center-feed circular tanks. This can be further shown in a family of curves derived by Kamen & Pohlhausen, involving $\eta = y/\delta$.



The above picture can be technically converted into the following one with the conversion factor omitted.



This converted y-u figure indicates that the boundary layer of center-feed circular settling basins, with shape factor $\Lambda = -25$, has the phenomenon of reversed flow. The reversed flow at the bottom of the basin would cause vertical eddies and, therefore, turbulence of the flow. This turbulence would make it relatively difficult for suspended particles to settle.

All the analytical results discussed in this paper support the argument that center-feed circular settling basins have less efficiency than rectangular basins, with the occurrence of boundary layer flow separation and its subsequent reversed flow and eddies believed as the main cause of the difference in the settling efficiency.

(IV). Conclusion

- (1) In center-feed circular settling basins, the boundary layer flow separation does occur and also the subsequent reverse flow and vertical eddies at bottom of the settling basins, due to the continuous increase of pressure. Location of flow separation is analytically obtained.
- (2) The flow separation, reversed flow and eddies which cause turbulence of flow at basin bottom are believed to be the fundamental reason for less settling efficiency of center-feed settling basins compared with rectangular ones.
- (3) For practical purposes, it needs further study to quantify the impact of boundary layer flow separation on the turbulence of bottom flow and on the settling efficiency.
- (4) The reduction of settling efficiency due to boundary layer flow separation in center-feed circular basins may be considered not as important as some other factors in practical wastewater treatment operations and design. However, the analysis of the insight of the phenomenon and the location of the separation point of bottom flow might lead to improvement of design in circular settling basins or other related hydraulic structures.

References:

1. Chiu, Y., "Boundary Layer Separation Concept", ASCE, Journal of the Environmental Eng. Division, Dec., 1974.
2. Schlichting, H., "Boundary Layer Theory", 1968.
3. Karman, Von; Millikan, C.B., "On the Theory of Laminary Boundary Layers Involving Separation", 1934, NACA Report.
4. Camp, T.R., "Sedimentation on the Design of Settling Tanks" Transaction, ASCE Vol. III Paper No. 2285, 1946.
5. Goda, T., "A Study on the Mechanism of Transportation of Suspended Sediment and Its Application to Increasing the Efficiency of Sedimentation Basin", Kyoto University, Kyoto, Japan, Vol. 15, No. 4, 1953.
6. Dague, R.R., "Hydraulics of Circular Settling Tanks by Model - Prototype Comparison "M.S. Thesis, Iowa State University, 1960.
7. Tekippe, R. J. and Cleasby, J. L., "Model Studies of a Peripheral-Feed settling Tank", ASCE, Journal of Sanitary Eng. Division, Feb., 1968.
8. Prandtl, L., "The Essentials of Fluid Dynamics" Hafner Publishing Co., 1952.

The work described in this paper was not funded by the U.S. Environmental Protection Agency. The contents do not necessarily reflect the views of the Agency and no official endorsement should be inferred.

DYNAMIC MODEL ADJUSTMENT

by

Dong Hoang
City of Portland, Oregon

MODEL DEVELOPMENT CONCEPT :

Generally all storm sewer computer models are composed of two parts : the runoff and the transport.

The first part is designed to compute flows versus time generated by rainfall over watersheds which connect to the minor sewer system. The flow time curves are called hydrographs.

The watersheds and the minor sewer system are represented by a series of numerical values which represent the area of the watershed, the coefficients of the Horton equation for infiltration, the slope, the diameter, the shape, the length, the flow resistance of the pipe...

The hydrographs are then used as input flows to the major sewer system. The hydrographs are input at points called inlets which are the connections between minor and major sewer system.

The difference between the runoff and the transport models (or blocks) is in the degree of sophistication between the two models.

The transport model uses the dynamic and continuity equations for gradually varied unsteady flow to represent the behavior of the flow in time and space. Besides, with the idea of computing, for each time step, and for each node of the sewer system, a surface area which is the sum of individual water surface areas in each half length pipe connecting to the node, the transport model allows the effect of back water to be considered. With those sophistications, the flows are more realistically represented in the major sewer system.

Before simulating the flow with the transport model, it is necessary to make sure that the runoff is properly simulated. This process is called model calibration. The model calibration is a series of computer simulation runs which attempt to match the simulated with the measured hydrograph. The discrepancies between the simulated and the measured hydrographs are believed, for simplicity, to be influenced only by the percentage of imperviousness. After a number of tries, each with a different percentage of imperviousness, the adequacy of the calibration is judged by visual comparison of the simulated and the measured hydrographs in terms of total volume of runoff and the shape of the hydrograph.

This commonly used procedure of model calibration is empirical and subjective; and due to the oversimplification of the process, flow distortions are always apparent. Besides, it doesn't provide any quantifiable measure which allows the computation of the model accuracy which is an impartial criterion to judge the reliability of the simulation.

As we all know, the calibration is a much more complexed process, involving a multitude of factors to be jointly considered, than the commonly used one.

In fact the calibration can never be correctly realized if attempts are made to adjust each influencing variables individually.

Theorically, a mathematical calibration model should take into account all the influencing factors of all types which can be classified into two categories. One is of statistical nature, the other regarding quantities which can be expressed by mathematical formulas.

To build a calibration model, in which all types of variables are involved regardless of their nature, requires effort and resource which are economically disproportionate to the field measurement accuracies. Not to mention the difficulty of handling it.

Logically, the calibration process aims at adjusting the a-pri-ori simulation in which all the variables of statistical nature have been taking care of by a careful model set-up which tries to properly and realistically distribute the water over the subcatchments, the minor and major sewer system. See appendices.

The calibration model is then reduced to the one of reasonable size with manageable number of variables to be handled.

MATHEMATICAL MODEL :

In general, no matter how careful the model is set-up, the flows simulated never match the flows measured at the corresponding monitoring station. The errors are caused by choosing wrong coefficients of pipeflow-resistance, wrong coefficients of discharge of the diversion-devices, wrong constants of Horton's equation for infiltration.

If Q_S is the simulated flows and Q_M is the measured flows of the corresponding pipe, then :

$$Q_M = Q_S + (q_I + q_{f1} + q_{f2} + \dots + q_{D1} + q_{D2} + \dots + q_E) \quad (2-1)$$

Where :

q_I : correction due to infiltration,

q_{f1} : correction due to choosing wrong pipe-flow-resistance

q_{f2} : coefficients of the major sewer system used in the

q_{fN} : transport block,

q_{D1} : correction due to choosing

- q_{D2} wrong discharge coefficients
 q_{DN} of the diversion-devices (if any),
 q_E : extraneous water which is not formulated in the model.

Using the dynamic and continuity equations for gradually varied unsteady flow, the rate of change of flows over time " r " can be established in the following manner :

With reference to Fig-1 and by the energy principle the general dynamic equation for gradually varied unsteady flow can be expressed in the following form :

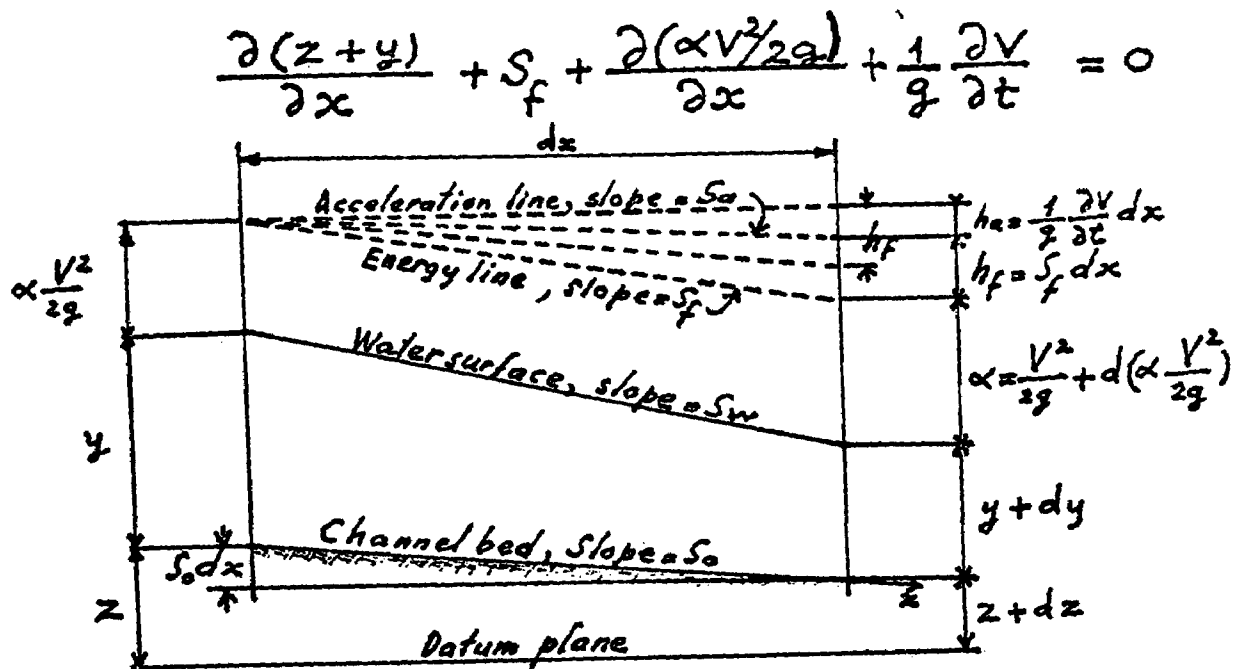


Fig-1

Now let $z+y=H$; $\alpha=1$; $Q=AV$. And let use the continuity equation for unsteady flow in open channels :

$$\frac{\partial Q}{\partial x} + \frac{\partial A}{\partial t} = 0$$

Then we have :

$$\frac{\partial Q}{\partial t} = 2V \frac{\partial A}{\partial t} + V^2 \frac{\partial A}{\partial x} - gA \frac{\partial H}{\partial x} - gAS_f \quad (2-2)$$

From Manning's Equation :

$$S_f = \frac{f}{gA} \cdot \frac{Q|V|}{R^{4/3}}$$

Where

$$f = \left(\frac{n}{1.49} \right)^2 g \quad (2-3)$$

$$Q^2 = QVA$$

Substitute the value of S_f derived from Manning's equation into equation (2-2) and let $\Delta x = L$ equation (2-2^f) becomes :

$$Q_{t+\Delta t} - Q_t = \frac{fVQ_{t+\Delta t}}{R^{4/3}} \Delta t + 2V \frac{\Delta A}{\Delta t} \Delta t + V^2 \frac{A_2 - A_1}{L} \Delta t - gA \frac{H_2 - H_1}{L} \Delta t$$

Solving for $Q_{t+\Delta t}$ gives :

$$Q_{t+\Delta t} = \left[\frac{1}{1 + f\Delta t|V|/R^{4/3}} \right] \left[Q_t + 2\bar{V}\Delta A + V^2 \frac{A_2 - A_1}{L} \Delta t - gA \frac{H_2 - H_1}{L} \Delta t \right]$$

From the above equation, the following dynamic equation, in finite form, used to route the flows through the conduit system of the transport block is derived

$$r = \frac{\partial Q}{\partial t} = \frac{Q_{t+\Delta t} - Q_t}{\Delta t}$$

$$r = \left[\frac{1}{1 + f\Delta t|\bar{V}_t|/\bar{R}^{4/3}} \right] \left[-\frac{f|\bar{V}_t|Q_t}{\bar{R}^{4/3}} + 2\bar{V}_t \frac{\bar{A}_t - \bar{A}_{t-\Delta t}}{\Delta t} + \bar{V}_t^2 \frac{A_j - A_i}{L} - g\bar{A}_t \frac{(H_j - C_1 u_j^2/2g) - (H_i - C_2 u_i^2/2g)}{L} \right] \quad (2-4)$$

Where :

Q : discharge,

V : velocity,
 A : cross-sectional area of the flow,
 H : hydrolic head,
 S_f : friction slope,
 x : distance along conduit,
 t : time
 n : Manning's roughness coefficient,
 R : hydrolic radius,

C_1, C_2 : coefficients of entrance and exit losses in the conduit.
 The subscript i, j refer to upstream and downstream nodes respectively; m refers to midpoint of the conduit. The barred symbol for R , V and A represent a weighted average along the conduit, eg.

$$\bar{R}_t = 1/4 (R_i + 2R_m + R_j)_t$$

The error dr due to errors committed by f and Q is :

$$dr = \frac{\partial r}{\partial f} df + \frac{\partial r}{\partial Q} dQ + \dots \quad (2-5)$$

$$dr = -df \left[\frac{|\bar{V}_t| \Delta t / \bar{R}^{4/3}}{1 + f |\bar{V}_t| \Delta t / \bar{R}^{4/3}} r \right] - df \left[\frac{|\bar{V}_t| / \bar{R}^{4/3}}{1 + f |\bar{V}_t| \Delta t / \bar{R}^{4/3}} Q_t \right] - dQ_t \left[\frac{f |\bar{V}_t| / \bar{R}^{4/3}}{1 + f |\bar{V}_t| \Delta t / \bar{R}^{4/3}} \right] \quad (2-6)$$

$$\text{If} \quad -f |\bar{V}_t| \Delta t / \bar{R}^{4/3} = T \quad (2-6b)$$

$$\text{then} \quad |\bar{V}_t| / \bar{R}^{4/3} = -T / f \Delta t$$

Equation (2-6) becomes :

$$dr = -df \left[\frac{-T}{f(1-T)} r \right] - df \left[\frac{-T}{f \Delta t (1-T)} Q \right] - dQ \left[\frac{-T}{\Delta t (1-T)} \right] \quad (2-7)$$

For the time interval Δt , an error in the rate " r " induces an error in ΔQ . In other words, during Δt , an error $d(\Delta Q)$ is committed in the conduit.

$$d(\Delta Q) = dr \Delta t$$

$$\begin{aligned} d(\Delta Q) &= \left[\frac{\tau}{1-\tau} \right] \left[\frac{df}{f} (r \Delta t + Q) + dQ \right] \\ d(\Delta Q) &= \left[\frac{\tau}{1-\tau} \right] \left[\frac{Q_{t+\Delta t}}{f} df + dQ \right] \end{aligned} \quad (2-8)$$

From equation (2-3)

$$f = n^2 \frac{g}{(1.49)^2}$$

we have

$$\frac{df}{f} = 2 \frac{dn}{n} \quad (2-9)$$

Substitute the value of df/f defined by (2-9) into equation (2-8) gives :

$$d(\Delta Q) = \left[\frac{\tau}{1-\tau} \right] \left[\frac{2 Q_{t+\Delta t}}{n} dn + dQ \right] \quad (2-10)$$

dQ of equation (2-10) is composed of $q_I, q_{D1}, q_{D2} \dots q_E$ defined in (2-1). It's now to express various q in function of the appropriate independent variables. The infiltration equation is expressed in the following form (Horton-Equation)

$$I = k_1 + (k_2 - k_1) e^{-k_3 t}$$

Error d_I is induced due to errors committed in choosing wrong values k_1, k_2, k_3 .

$$\begin{aligned} dI &= \frac{\partial I}{\partial k_1} dk_1 + \frac{\partial I}{\partial k_2} dk_2 + \frac{\partial I}{\partial k_3} dk_3 \\ dI &= (1 - e^{-k_3 t}) dk_1 + e^{-k_3 t} dk_2 - t e^{-k_3 t} (k_2 - k_1) dk_3 \end{aligned}$$

For a point in time t , over a pervious area A , an error q_I is committed :

$$q_I = (1 - e^{-k_3 t}) A d k_1 + e^{-k_3 t} A d k_2 - t e^{-k_3 t} (k_2 - k_1) A d k_3$$

$$\text{If } (1 - e^{-k_3 t}) A = AA \quad (2-11)$$

$$e^{-k_3 t} A = BB \quad (2-12)$$

$$- t e^{-k_3 t} (k_2 - k_1) A = CC \quad (2-13)$$

then

$$q_I = AA d k_1 + BB d k_2 + CC d k_3 \quad (2-14)$$

The diverted flow over the diversion device Q_D is in error by a quantity q_D . This error is induced by choosing a wrong discharge coefficient C . Using the weir formula, q_D can be evaluated :

$$\begin{aligned} Q_D &= C L \left[\left(h + \frac{V^2}{2g} \right)^a - \left(\frac{V^2}{2g} \right)^a \right] \\ dQ_D &= \frac{\partial Q}{\partial C} dC \\ dQ_D &= L \left[\left(h + \frac{V^2}{2g} \right)^a - \left(\frac{V^2}{2g} \right)^a \right] dC \\ dQ_D &= \frac{Q_D}{C} dC \end{aligned} \quad (2-15)$$

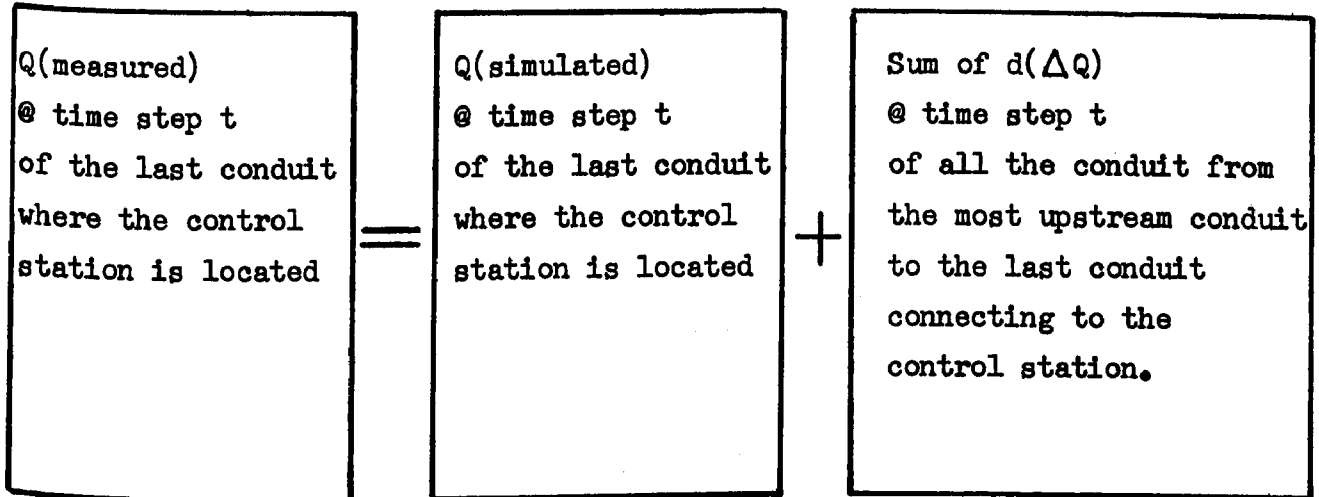
Substituting various values of q_I, q_D from equations (2-11), (2-12), (2-13), (2-15) respectively in equation (2-10) we have :

$$\begin{aligned} d(\Delta Q) &= \left[\frac{T}{1-T} \right] \left[\frac{2Q_{t+\Delta t}}{n} dn + AA d k_1 + BB d k_2 \right. \\ &\quad \left. CC d k_3 + Q_D \frac{dC}{C} + q_E \right] \end{aligned} \quad (2-16)$$

The factor $(T/1-T)$ which is a function of the flow resistance coefficient, the velocity, the hydraulic radius and the time interval is called dynamic coefficient. For each time step, each conduit has different value of dynamic coefficient. Equation (2-16) is the error committed in each conduit during the flow routing with the transport block.

MODEL ADJUSTMENT BASED ON FLOW :

The basic formula used to form the observation equation is :



In each tributary area, controlled by a control station the following independent variables are to be determined :

1. d_{n1} : correction to pipe-flow-resistance of the major sewer system,
2. d_{k1} : correction to Horton's equation constant k_1 ,
3. d_{k2} : correction to Horton's equation constant k_2 ,
4. d_{k3} : correction to Horton's equation constant k_3 ,
5. d_{C1} : correction to diversion-device discharge coefficient,
6. EQ : under a rainfall, EQ is a constant flow in cfs. For each conduit and for each time step t , q_E is determined as follows :

$$q_E = EQ \cdot \frac{A_{IMP}}{\sum A_{IMP}} \cdot \frac{QM - QS}{QM}$$

A_{IMP} : impervious area contributing to an inlet node,

$\sum A_{IMP}$: total impervious area of the tributary area,

QM : flow measured at time step t of the last conduit connecting

to the control station,

QS : flow simulated at time step t of the last conduit connecting to the control station.

In total, if x is the number of pipe-flow-resistance coefficients of the major sewer system, and y is the number of diversion-devices-discharge coefficients, the number of independent variables are : (4 + x + y).

At each time step, the general form of $\sum d(\Delta Q)$ is :

$$\begin{aligned} \sum_1^m d(\Delta Q) &= dn_1 \sum_1^{m1} \left[\left(\frac{T}{1-T} \right) \frac{2Q_{t+\Delta t}}{n_1} \right] + dn_2 \sum_1^{m2} \left[\left(\frac{T}{1-T} \right) \frac{2Q_{t+\Delta t}}{n_2} \right] \\ &+ dk_1 \sum_1^m \left[\left(\frac{T}{1-T} \right) AA \right] + dk_2 \sum_1^m \left[\left(\frac{T}{1-T} \right) BB \right] \\ &+ dk_3 \sum_1^m \left[\left(\frac{T}{1-T} \right) CC \right] + dc_1 \left(\frac{T}{1-T} \right) \frac{QD_1}{C_1} + dc_2 \left(\frac{T}{1-T} \right) \frac{QD_2}{C_2} \\ &+ EQ \sum_1^m \left[\left(\frac{AIMP}{\sum AIMP} \right) \frac{QM - QS}{QM} \right] \left[\frac{T}{1-T} \right] \end{aligned} \quad (2-17)$$

Equation (2-17) is called observation equation for time step t.

m : total number of conduits,

m1, m2 : number of conduits having flow-resistances n1 , n2 respectively.

In general, if "v" is the residual flow, the following system of equation is called system of observation equations ;

$$\left. \begin{aligned} Q_M @ t_1 &= Q_S @ t_1 + \sum_1^m d(\Delta Q) @ t_1 + v_1 \\ Q_M @ t_2 &= Q_S @ t_2 + \sum_1^m d(\Delta Q) @ t_2 + v_2 \\ \dots\dots\dots \\ Q_M @ t_N &= Q_S @ t_N + \sum_1^m d(\Delta Q) @ t_N + v_N \end{aligned} \right\} \quad (2-18)$$

AA, BB, CC are computed from (2-11), (2-12), (2-13) for each time step over all the subcatchments contributing to each inlet-node.

MODEL ADJUSTMENT BASED ON DEPTH :

The sum of error in Q committed by different lines at time step t :

$\sum d(\Delta Q)$ will cause an error in cross-sectional area of the control conduit which is expressed as follows :

$$\frac{\sum d(\Delta Q)_t}{V_t} = dA_t \quad (2-19)$$

V_t is the velocity of the control conduit at time step t and dA_t is the error of the cross-sectional area of the control conduit.

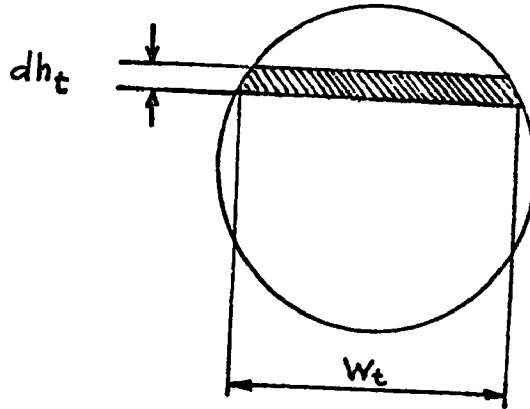


Fig-2

dA_t is also determined by :

$$dA_t = dh_t \times w_t \quad (2-20)$$

dh_t , w_t are respectively the error of the flow depth and the width of the control conduit at time step t . From equation (2-20) :

$$dh = dA_t / w_t \quad (2-21)$$

Substituting value of dA_t given by equation (2-19) into equation (2-21) giving:

$$dh_t = \frac{\sum d(\Delta Q)_t}{V_t \cdot W_t} \quad (2-22)$$

Divide equation (2-17) by $V_t \cdot W_t$ one obtains :

$$\begin{aligned} H_{M@t} = & H_{S@t} + dn_1 \frac{1}{V_t \cdot W_t} \sum_1^{m_1} \left[\left(\frac{T}{1-T} \right) \left(\frac{2Q_t + \Delta t}{n_1} \right) \right] \\ & + dn_2 \frac{1}{V_t \cdot W_t} \sum_1^{m_2} \left[\left(\frac{T}{1-T} \right) \left(\frac{2Q_t + \Delta t}{n_2} \right) \right] + \dots \\ & + dk_1 \frac{1}{V_t \cdot W_t} \sum_1^m \left[\left(\frac{T}{1-T} \right) (AA) \right] + dk_2 \frac{1}{V_t \cdot W_t} \sum_1^m \left[\left(\frac{T}{1-T} \right) (BB) \right] \\ & + dk_3 \frac{1}{V_t \cdot W_t} \sum_1^m \left[\left(\frac{T}{1-T} \right) (CC) \right] + dc_1 \frac{1}{V_t \cdot W_t} \left[\left(\frac{T}{1-T} \right) \left(\frac{QD_1}{C_1} \right) \right] \\ & + dc_2 \frac{1}{V_t \cdot W_t} \left[\left(\frac{T}{1-T} \right) \left(\frac{QD_2}{C_2} \right) \right] + \dots \\ & + EQ \frac{1}{V_t \cdot W_t} \sum_1^m \left[\left(\frac{T}{1-T} \right) \left(\frac{AIMP}{\sum AIMP} \right) \left(\frac{QM - QS}{QM} \right) \right] * \end{aligned} \quad (2-23)$$

Equation (2-23) is called observation equation for time step t .

$H_{M@t}$: Flow-depth measured @ time step t @ the control conduit,

$H_{S@t}$: Flow-depth simulated @ time step t @ the control conduit.

As for the case of flow adjustment a system of observation equations can be derived

$$\left. \begin{aligned} H_{M@t_1} &= H_{S@t_1} + \frac{\sum_1^m d(\Delta Q)_{t_1}}{V_{t_1} \cdot W_{t_1}} + v_1 \\ H_{M@t_2} &= H_{S@t_2} + \frac{\sum_1^m d(\Delta Q)_{t_2}}{V_{t_2} \cdot W_{t_2}} + v_2 \\ &\dots \dots \dots \\ H_{M@t_N} &= H_{S@t_N} + \frac{\sum_1^m d(\Delta Q)_{t_N}}{V_{t_N} \cdot W_{t_N}} + v_N \end{aligned} \right\} \quad (2-24)$$

The rest of the notations are explained in the previous section.

* See page 23 (INHY.FOR Program).

THE LEAST - SQUARES TECHNIQUE :

System (2-18) is now presented in detail (similar presentation for system 2-24) :

$$QM_1 - QS = a_{11}dn_1 + a_{21}dn_2 + \dots + a_{31}dk_1 + a_{41}dk_2 + a_{51}dk_3 +$$

$$a_{61}dC_1 + \dots + a_{71}EQ + v_1 = b_1$$

----- (2-25)

$$QM_N - QS_N = a_{1N}dn_1 + a_{2N}dn_2 + \dots + a_{3N}dk_1 + a_{4N}dk_2 + a_{5N}dk_3 +$$

$$a_{6N}dC_1 + \dots + a_{7N}EQ + v_N = b_N$$

Since the observation are not perfect, we must find the most probable system of values which, by the principle of least-squares, makes the sum of the square of the residuals $[v^2]$ minimum.

$$SSE = \sum_{i=1}^N (v^2)$$

$$SSE = \sum_{i=1}^N (b_i - a_{1i}dn_1 - a_{2i}dn_2 - a_{3i}dk_1 - a_{4i}dk_2 - a_{5i}dk_3 - a_{6i}dC_1 - a_{7i}EQ)^2$$

Since the variables are independent, the condition that SSE is a minimum is that the partial differentials of function SSE with respect to each independent variable must be zero. Realizing that condition, we generate the following set of normal equations :

$$dn_1 \sum_1^N a_{1i}^2 + dn_2 \sum_1^N a_{1i}a_{2i} + dk_1 \sum_1^N a_{1i}a_{3i} + dk_2 \sum_1^N a_{1i}a_{4i} + dk_3 \sum_1^N a_{1i}a_{5i} +$$

$$dC_1 \sum_1^N a_{1i}a_{6i} + EQ \sum_1^N a_{1i}a_{7i} = \sum_1^N a_{1i}b_i$$

$$dn_1 \sum_1^N a_{2i}a_{1i} + dn_2 \sum_1^N a_{2i}^2 + dk_1 \sum_1^N a_{2i}a_{3i} + dk_2 \sum_1^N a_{2i}a_{4i} + dk_3 \sum_1^N a_{2i}a_{5i} +$$

$$dC_1 \sum_{i=1}^N a_{2i} a_{6i} + EQ \sum_{i=1}^N a_{2i} a_{7i} = \sum_{i=1}^N a_{2i} b_i$$

$$dn_1 \sum_{i=1}^N a_{7i} a_{1i} + dn_2 \sum_{i=1}^N a_{7i} a_{2i} + dk_1 \sum_{i=1}^N a_{7i} a_{3i} + dk_2 \sum_{i=1}^N a_{7i} a_{4i} + dk_3 \sum_{i=1}^N a_{7i} a_{5i} +$$

$$dC_1 \sum_{i=1}^N a_{7i} a_{6i} + EQ \sum_{i=1}^N a_{7i}^2 = \sum_{i=1}^N a_{7i} b_i$$

N : Number of observation equations. For simplicity purpose, we assume that there are only 2 " dn " & 1 " dC " in the system above. Therefore the normal equations are composed of 7 unknowns and 7 equations.

In terms of matrix, the normal equations can be written :

$$A X = G$$

where :

$$X = \begin{bmatrix} dn_1 \\ dn_2 \\ dk_1 \\ dk_2 \\ dk_3 \\ dC_1 \\ EQ \end{bmatrix}$$

$$G = \begin{bmatrix} \sum_{i=1}^N a_{1i} b_i \\ \sum_{i=1}^N a_{2i} b_i \\ \text{---} \\ \sum_{i=1}^N a_{7i} b_i \end{bmatrix}$$

and

$$A = a'a$$

where a' is the transpose of matrix a regarding the system of observation equations (2-25).

If matrix A is nonsingular, we can write the solution for the normal equations as :

$$X = A^{-1}G$$

STANDARD ERROR :

Standard error of a single observation is computed by the following :

$$\sigma = \sqrt{\frac{[v^2]}{N-1}}$$

Standard error of the mean value can be computed by one of the following :

$$\sigma_o = \sqrt{\frac{[v^2]}{N(N-1)}}$$

$$\sigma_o = \sigma / \sqrt{N}$$

N : Number of observation equations,

v : Difference between corrected values and measured values.

VANCOUVER DRAINAGE BASIN :

The data blocks of this drainage basin are called DVANR.DAT for run-off and DVANT.DAT for transport.

The model is simulated with an integration time of 30 seconds.

It is adjusted based on flow monitored by HYDRA STATION-18 of February 9, 1979 (Hydrologic Data Retrieval & Alarm System) Flows are recorded in cubic feet per second and inches for every 5 seconds for flows and depth respectively.

The calibration for this model is based on flow.

In the simulation, base-flows are input into nodes as net constant-flows (QINST variable of the SWMM model).

The number of independent variables to be solved for this model is 6 including 2 Manning's n ; 3 Horton's equation coefficients K ; and One extraneous water EQ. See Table-1.

ADJUSTED VARIABLES

VARIABLE	ESTMATED VALUE	CORRECTION	CORRECTED VALUE
n1	0.015	+0.00033	0.01533
n2	0.013	-0.00131	0.01169
k1	0.400	-0.00595	0.39405
k2	0.800	-0.00360	0.79640
k3	0.00115	-0.00005	0.00110
EQ		+5.13746	5.13746

TABLE-1

TIME	FLOW MEASURED QM	FLOW SIMULATED QS*	QM - QS	FLOW ADJUSTED QA**	QM - QA
6h30	1.30	1.18	+0.12	2.25	-0.95
7.00	1.30	1.50	-0.20	1.31	-0.01
7.30	2.80	1.67	+1.13	2.37	+0.43
8.00	3.80	1.82	+1.98	3.73	+0.07
8.30	3.50	1.97	+1.53	3.83	-0.33
9.00	3.80	2.10	+1.70	3.86	-0.06
9.30	5.50	2.96	+2.54	4.86	+0.64
10.00	5.50	4.33	+1.17	5.38	+0.12
10.30	5.50	7.76	-2.26	6.90	-1.40
11.00	7.90	8.68	-0.78	8.09	-0.19
11.30	12.60	14.34	-1.74	13.93	-1.33
12.00	11.50	15.05	-3.55	14.18	-2.68
12.30	10.50	10.48	+0.02	10.26	+0.24
13.00	7.40	9.84	-2.44	9.00	-1.60
13.30	5.50	5.05	+0.45	4.96	+0.54
14.00	3.80	3.64	+0.16	3.78	+0.02
14.30	3.80	5.70	-1.90	4.39	-0.59
15.00	7.40	6.56	+0.84	6.39	+1.01
15.30	5.30	5.83	-0.33	5.80	-0.30
16.00	5.50	5.59	-0.09	5.54	-0.04
16.30	6.50	5.57	+0.93	5.95	+0.55

* See pages 92-94

** See pages 89-91

TIME	FLOW MEASURED QM	FLOW SIMULATED QS	QM - QS	FLOW ADJUSTED QA	QM - QA
17.00	4.20	5.57	-1.37	4.85	-0.65
17.30	3.80	3.58	+0.22	3.38	+0.42
18.00	2.40	2.60	-0.20	2.46	-0.06
18.30	2.40	2.44	-0.04	2.31	+0.09
19.00	1.90	2.41	-0.51	1.79	+0.11

$$\sigma_{\text{A-pri-ori}} = \sqrt{\frac{53.3558}{26}} = 1.43251$$

$$\sigma_{\text{Adjusted}} = \sqrt{\frac{17.8709}{26}} = 0.82906$$

The work described in this paper was not funded by the U.S. Environmental Protection Agency. The contents do not necessarily reflect the views of the Agency and no official endorsement should be inferred.

AN IMPROVED SURCHARGE COMPUTATION IN EXTRAN

by John A. Aldrich and Larry A. Roesner
Camp Dresser & McKee
Annandale, Virginia

What is EXTRAN?

EXTRAN is the Extended Transport Block of the Stormwater Management Model. It is one of a select few models able to dynamically route gradually varied flow through urban drainage systems and, in certain cases, natural streams. This is accomplished by explicitly solving the full Navier-Stokes equation for a wide variety of hydraulic conditions, including free surface flow, pressure flow or surcharge, tidal and non-tidal backwater, and flow reversals. EXTRAN represents a drainage system as a series of links (pipes and channels) and nodes (pipe junctions and flow diversion devices). The "link-node" concept permits the user to model a wide range of system configurations, including parallel pipes, branched and looped systems, and flow diversion devices (orifices, weirs, and pumps).

EXTRAN was developed as the Transport Block of the San Francisco Stormwater Model (1,2) by Water Resources Engineers (now part of Camp Dresser & McKee, Inc). It was first included in EPA's SWMM package in 1974, providing detailed analysis of complex system configurations and special hydraulic conditions which existing, simpler models in the SWMM package were unable to simulate. At this time the model was renamed Extended Transport to differentiate it from the University of Florida's Transport Block. Since then, EXTRAN has been expanded and refined to more fully meet the needs of SWMM users. Version III of SWMM, which has just been released, contains the latest set of revisions to EXTRAN. The most important of these is a modification to the surcharge computation routine.

Shortcomings of Previous EXTRAN Surge Computations

The original WRE Transport Model treated a system surcharge as if the excess water rose into a surge chamber located at the junction node. In many hydraulic situations, however, this resulted in minor, and in a few cases, major misrepresentations of the system flows. To remedy this, a new approach was taken in more recent versions of the model. This approach is based on the fact that the continuity equation for a surcharged node j at time t is:

$$\sum Q_j(t) = 0 \quad (1)$$

If $\partial Q / \partial H_j$ is computed for each link connected to node j , the continuity equation can be rewritten as

$$\sum (Q(t) + \frac{\partial Q(t)}{\partial H_j} \Delta H_j(t)) = 0 \quad (2)$$

and solved for a head correction,

$$\Delta H_j(t) = - \sum Q(t) / \sum \frac{\partial Q(t)}{\partial H_j} \quad (3)$$

in the half and full time steps. It has been found, however, that the solution is more stable when only half of the head correction is applied in the half time step. Also, only 0.3 and 0.6 of the correction are applied in the half and full steps, respectively, at upstream terminal nodes to prevent oscillations in head at these points.

Surcharges computed in the above manner were found to give accurate results under most surcharge conditions. When several consecutive nodes are in surcharge simultaneously, though, predicted heads and flows can be significantly underestimated, especially when no lateral inflows exist.

The University of Ottawa has been studying this problem (3). They tested a system consisting of a long series of pipes with a restricted outfall. Figure 1 shows a comparison of the surcharge heads obtained from EXTRAN and a similar model, the HVM Dorsch model. The Dorsch model is

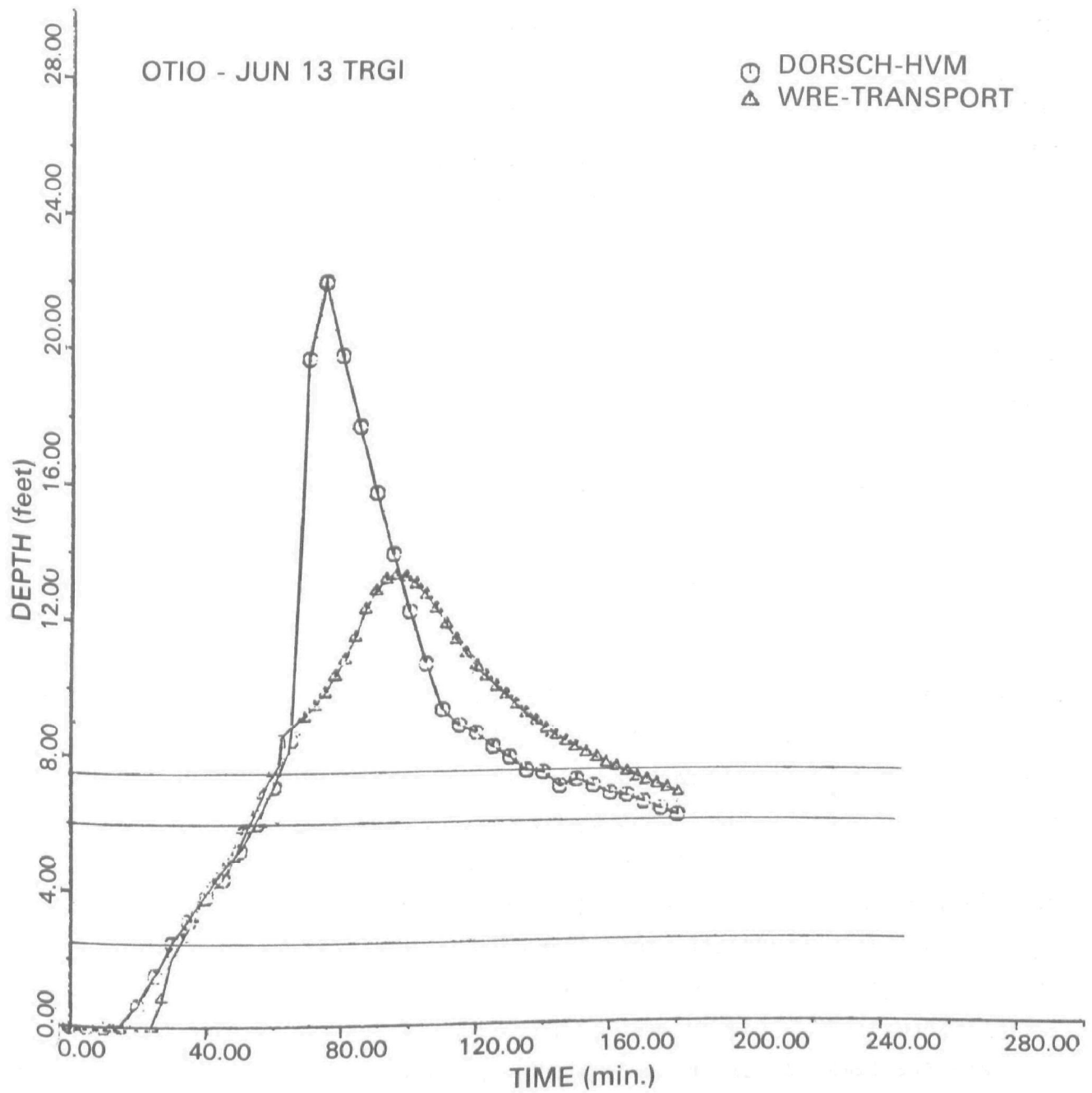


Figure 1 - Comparison of HVM Dorsch Model and
EXTRAN Without Surge Iterations

designed to handle the same hydraulic conditions as EXTRAN, but by using an implicit solution technique rather than EXTRAN's explicit solution. The implicit character of the Dorsch model makes it a reliably accurate prediction tool, therefore its results are considered a good basis of comparison. This accuracy is gained, however, through a much larger expenditure of computer time than is required by EXTRAN.

The findings of the University of Ottawa indicated that the flexibility and, consequently, the ultimate usefulness of EXTRAN was limited, even though only the most severe surcharge conditions cause errors of this magnitude. It thus was important to understand where the physical realities of surcharged flow, represented mathematically by equations 1-3, and the model differed.

Analysis of The Explicit Surcharge Solution Technique

The most basic difference between a physical situation and a model of this situation is, of course, the mathematical approximations required to solve the fundamental flow equations, and it was here that the deficiency of the surcharge calculation was found. The explicit solution technique used by EXTRAN is advantageous for computational efficiency because the unknowns in the present time step are computed solely from previous values in time of that quantity. Storage requirements are thus kept small and complicated arithmetic such as matrix inversion is unnecessary. Unfortunately, the simplification and efficiency acquired from an explicit solution does not permit any spacial interrelationships, thus the computation of the head correction, ΔH_j , is independent of other head corrections for adjacent nodes.

Another cause of error in computing surcharge heads rests in the fact that computed values are approximations. Therefore, the continuity equation at a surcharged node is approximated as:

$$\sum Q_j(t) = \epsilon_j \quad (4)$$

where ϵ_j = small nodal flow differential. At each surcharged node, this computational error is an insignificant fraction of the flow passing through the junction. Thus if only a few isolated nodes surcharge, the net flow pattern in the system will not be drastically affected and EXTRAN's results will be reliable.

When several adjacent nodes surcharge, there is net flow within the entire surcharge area, i.e.

$$\sum Q_{\text{entire surcharge section}}(t) = 0 \quad (5)$$

Computationally, however, a small flow error exists at each surcharged node. Since an explicit solution technique is used, no relationship exists between these nodes and individual nodal errors accumulate, giving:

$$\sum Q_{\text{entire surcharge section}}(t) = \sum \epsilon_j \quad (6)$$

This cumulative error can be a large fraction of the flow in the surcharge section under certain conditions and can significantly alter the net flow pattern, even though total system continuity is preserved. The problem is especially apparent for a long line (many links) where there is little or no lateral inflow. Therefore a refinement to the explicit solution technique is needed to compute surcharge heads and flows.

Semi-Implicit Surcharge Iteration Loop

In modifying the surcharge routine, a balance was sought in which the area in surcharge could be considered as an entity while the explicit character of the general solution technique would be retained. To do this, the full-step computations for heads and flows in areas undergoing surcharge were placed in an iteration loop. The iterations continue until the sum of inflows to and outflows from all surcharged nodes in equation 6 is sufficiently small, i.e.

$$\sum \epsilon_j \approx 0$$

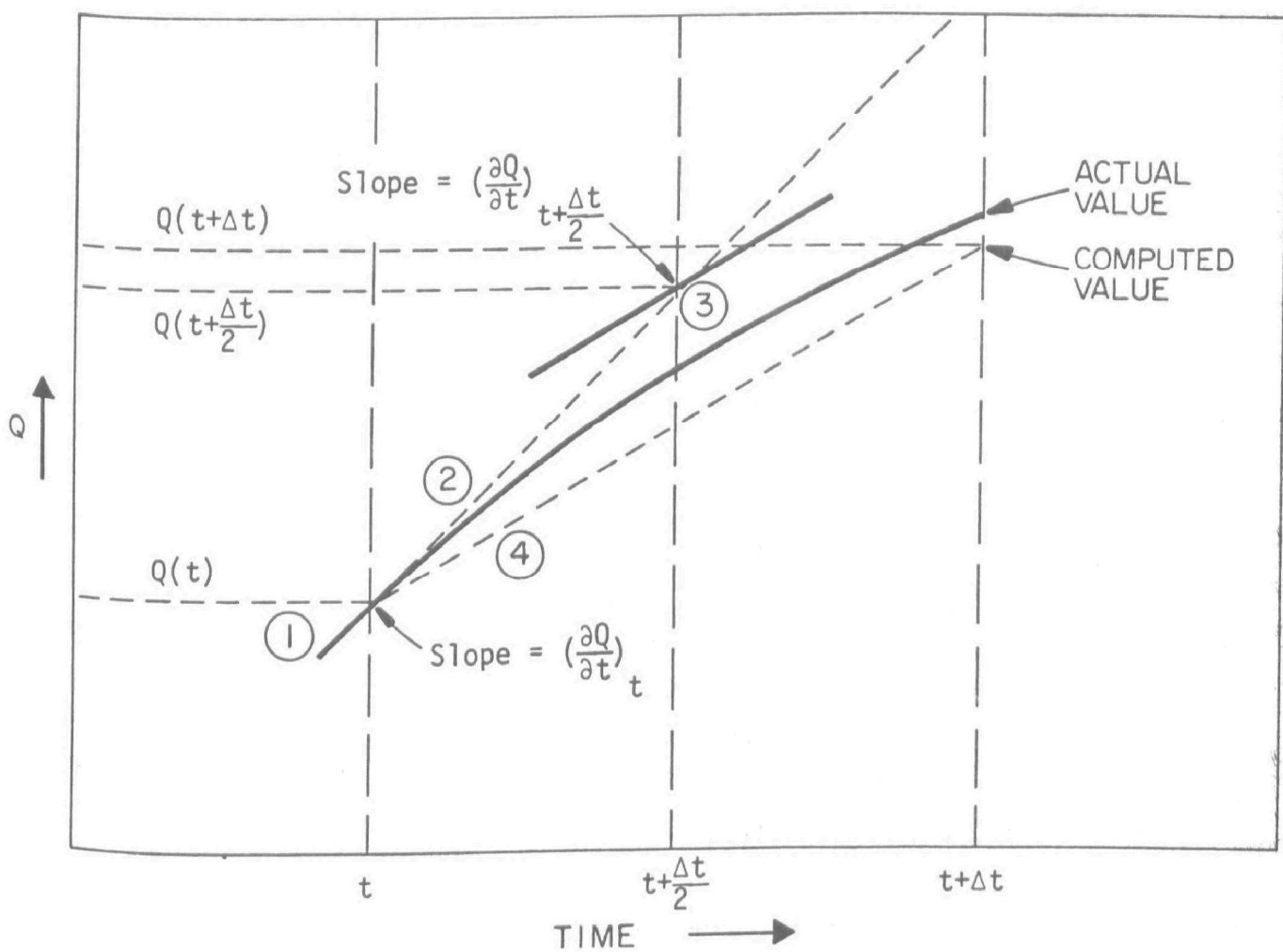
(7)

This technique achieves a relationship between the surcharged nodes, giving the surcharge computation a semi-implicit character.

To demonstrate the effectiveness of the semi-implicit iteration loop, a closer look at the computation method employed in EXTRAN is required. Figure 2 shows how this technique, the Modified Euler method, is used to compute discharge. Steps 1 and 2 show that the half step flow and, consequently, head are based solely on system properties at time t which are assumed to be true. Since values at time t cannot be altered, an iteration of the half-step computation would be useless. Therefore, the iteration is restricted to the full-step computations, steps 3 and 4.

Once an estimate of the flow is made in the half-step, $Q(t + \Delta t/2)$, the average of the flows in all links connected to surcharged nodes is computed. A fraction of this average flow, input by the user as SURTOL, is then used as a check on the convergence of the iteration. This test, in essence, simply checks the validity of equation 7 above. Once an initial estimate of full step flows and heads is made, the sum of the flow differentials at nodes under surcharge is compared with the test differential computed above. If the computed flow differential is greater than the test value, the full step computations are repeated for surcharged nodes and their connecting links. This continues until either the computed flow differentials are sufficiently small or, to prevent a possible infinite loop, until a user-input maximum number of iterations is exceeded.

The surcharge iteration loop was found to dramatically improve the accuracy of EXTRAN under severe surcharge conditions. Figure 3 demonstrates this improvement by superimposing the results from the surcharge iteration loop version of EXTRAN onto Figure 1. EXTRAN is now found to closely



- ①. Compute $(\frac{\partial Q}{\partial t})_t$ from properties of system at time t
- ②. Project $Q(t + \frac{\Delta t}{2})$ as $Q(t + \frac{\Delta t}{2}) = Q(t) + (\frac{\partial Q}{\partial t})_t \frac{\Delta t}{2}$
- ③. a. Compute system properties at $t + \frac{\Delta t}{2}$
 b. Form $(\frac{\partial Q}{\partial t})_{t + \frac{\Delta t}{2}}$ from properties of system at time $t + \frac{\Delta t}{2}$
- ④. Project $Q(t + \Delta t)$ as $Q(t + \Delta t) = Q(t) + (\frac{\partial Q}{\partial t})_{t + \frac{\Delta t}{2}} \Delta t$

Figure 2 - Modified Euler Solution Method For Discharge Based on Half-Step, Full-Step Projection

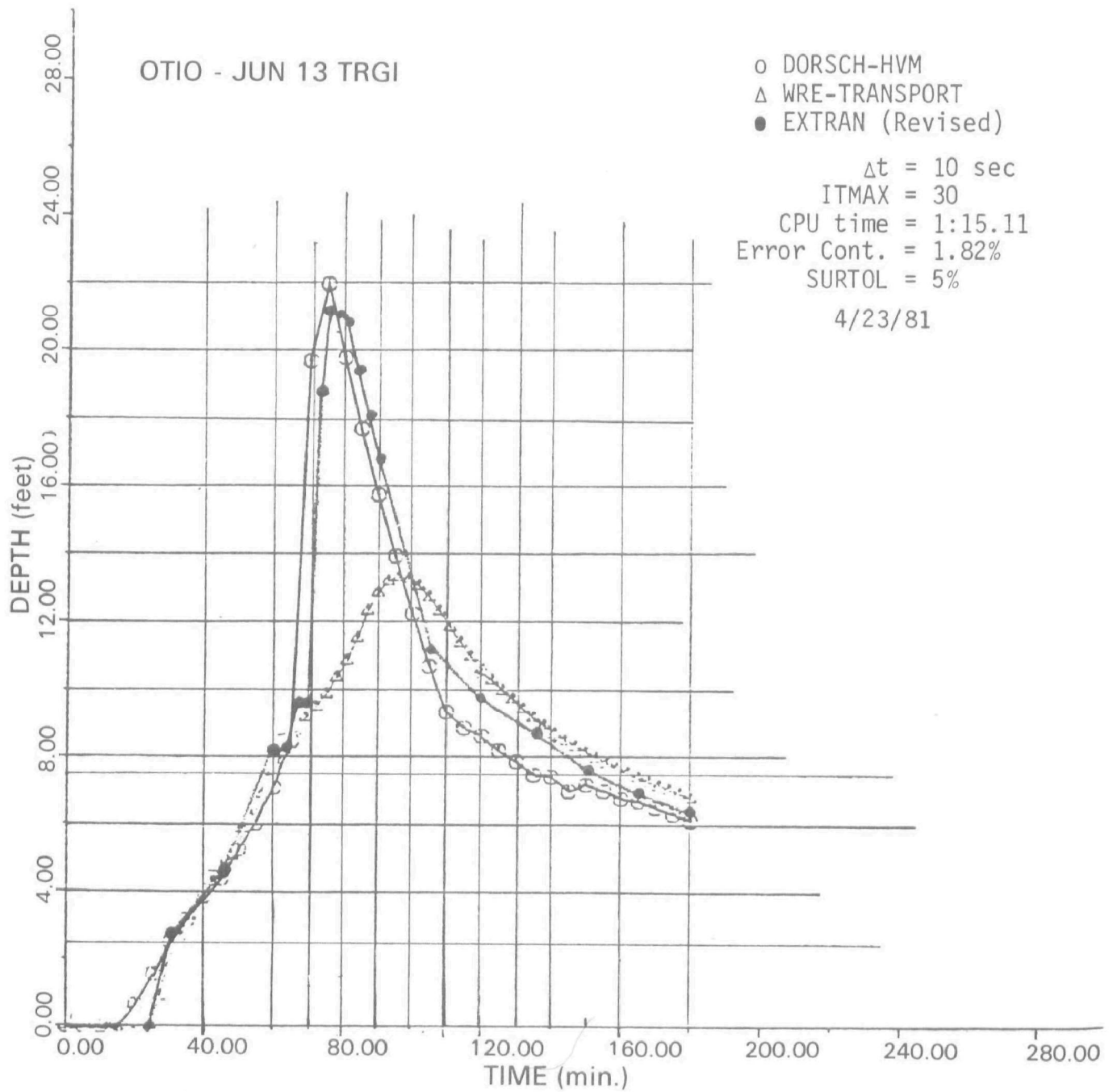


Figure 3 - Comparison of HVM Dorsch Model and EXTRAN With and Without Surcharge Iterations.

approximate the Dorsch results while using less computer time. In addition, the use of smaller values of SURTOL further increased the accuracy of EXTRAN, but also increased the computation time required.

User Control of the Iteration Loop

There is, of course, a certain amount of experience required to efficiently and accurately utilize the iteration loop. The two variables which control the loop, the fraction SURTOL of the average surcharge flow and the maximum number of iterations ITMAX, act both individually and jointly. It is clear that a small SURTOL along with a large ITMAX will yield the highest degree of accuracy. This is gained, however, at the expense of computer time. The user, therefore, has a tradeoff between accuracy and efficiency.

To assist in the optimization of SURTOL and ITMAX, EXTRAN's intermediate printout shows the sum of the surcharge flow differentials and the iterations required in each print cycle where iterations occur. It may be advisable, then, to design a small, short problem similar to a portion of a system prone to surcharge in order to adjust these two variables. It is also advisable in any case to initially set SURTOL = 0.05 and ITMAX = 30, values which have been shown to give good results.

Another troublesome situation which is likely to arise in large complex systems concerns the case where two or more separate areas of the system are in surcharge at the same time. In this situation, the net flow in each surcharge area could easily differ by a significant amount. EXTRAN, however, computes the cutoff for the surcharge iteration as a fraction of the average flow through all surcharged sections. This means that equation 7 may be satisfied in one surcharged section but not in another if the flows are relatively different in each section.

Several ways exist to compensate for this problem. The sum flow differential, $\sum \epsilon_j$, may remain relatively large only in surcharge areas with flow substantially less than the gross average surcharge flow. Therefore, errors in these sections may not impact the flows in the system as a whole simply by the fact that these flows are small. If, on the other hand, reliable values of flow are desired in these sections of the system, the value chosen for SURTOL can be reduced to lower the cutoff value for the iteration. This would give more accurate results overall, but at a cost of computer time. Finally, EXTRAN could be revised to check the conveyance of each surcharge area individually. It was determined, though, that the effort involved and loss of computational efficiency rendered by these changes would hardly be warranted by greater automation of the surcharge computation. In addition, the authors believe that the user should always check the intermediate printout to determine the accuracy of the surcharge procedure rather than blindly accept EXTRAN's solution of complex flow patterns.

Interpretation of the intermediate results for partially surcharged systems is straightforward. As noted above, the actual sum flow differential and number of iterations required is printed at each print cycle where iterations occur. Also, nodes in surcharge are designated with an asterisk. If nodes in unconnected areas are found in surcharge at the same time, a quick calculation can determine the sum flow differential in each section in the same way that EXTRAN computes it for all surcharged nodes. Figure 4 demonstrates how this is done for one large area in surcharge. First, the links connecting to each surcharged node need to be found in the internal connectivity summary within the input data echo. The flow differential at each node, ϵ_j , is simply

$$\epsilon_j = \sum Q_j \quad (8)$$

where inflows to the node are positive and outflows are negative. These flows are shown in the intermediate printout using the sign convention established by the user. Once the differentials are found, they can be summed over each area in surcharge and compared with the average flow in this

CYCLE 426 TIME 1 HRS - 21.00 MIN FLOW DIFFERENTIAL IN SURCHARGED AREA= -4.21CFS ITERATIONS REQUIRED= 8

JUNCTIONS / DEPTHS

106/ 16.35*	1/ 16.71*	2/ 17.05*	3/ 17.40*	4/ 17.74*	5/ 18.08*	6/ 18.42*	7/ 18.76*
8/ 19.09*	9/ 19.43*	10/ 19.76*	11/ 20.10*	12/ 20.43*	13/ 20.77*	14/ 2.50	

CONDUITS / FLOWS

100/ 82.24	101/ 82.59	102/ 82.93	103/ 83.27	104/ 83.61	105/ 83.94	106/ 84.26	107/ 84.56
108/ 84.89	109/ 85.19	110/ 85.48	111/ 85.77	112/ 86.02	113/ 86.16	90015/ 86.16	

Surcharged Junction Number	Upstream		Downstream		ϵ_j
	Conduit	Flow	Conduit	Flow	
100	Lateral in flow	81.94	100	82.24	-0.30
1	100	82.24	101	82.59	-0.35
2	101	82.59	102	82.93	-0.34
3	102	82.93	103	83.27	-0.34
4	103	83.27	104	83.61	-0.34
5	104	83.61	105	83.94	-0.33
6	105	83.94	106	84.26	-0.32
7	106	84.26	107	84.58	-0.32
8	107	84.58	108	84.89	-0.31
9	108	84.89	109	85.19	-0.30
10	109	85.19	110	85.48	-0.29
11	110	85.48	111	85.77	-0.29
12	111	85.77	112	86.02	-0.25
13	112	85.02	113	86.16	-0.14
14	113	86.16	90015	86.16	0.0

$$\sum \epsilon_j = -4.21$$

Figure 4 - Example Computation of the Sum Flow Differential Within a Surcharged Area

section. If the user finds this value to be too large, say greater than 5 or 10 percent of the average flow, he can reduce SURTOL and re-run EXTRAN. In this way, an acceptable degree of accuracy can be gained. It is clear, however, that this determination should be made if possible before a major run of EXTRAN is attempted to avoid unnecessary computer expense.

Future Research

EXTRAN has been in use for several years and in most cases has been found to give reliable results. It has also been continually revised, both by the authors and by the many users of the model. Most verification of the model's accuracy, however, has been done by comparing the results with similar models, as was done against the HVM Dorsch model by the University of Ottawa, or by running simple cases which can be checked with hand calculations.

Camp Dresser and McKee, Inc. is presently preparing to further verify EXTRAN using a large data base collected on a major metropolitan sewer system. The author's believe that this data is diverse enough to fully utilize all features of EXTRAN and demonstrate its accuracy as well as point out any remaining shortcomings and sources of error. The results of this study, which should be of interest to all EXTRAN users, will be reported at a future date.

References

1. Shubinski, R. P., and L. A. Roesner. Linked Process Routing Models, paper presented at the Symposium on Models for Urban Hydrology, American Geophysical Union Meeting, Washington, D.C., 1973.
2. Kibler, D. F., J. R. Mouser, and L. A. Roesner. San Francisco Stormwater Model, User's Manual and Program Documentation, prepared for the Division of Sanitary Engineering, City and County of San Francisco, Water Resources Engineers, Walnut Creek, California, 1975.
3. Personal Communication with Atef M. Kassem, Research Associate, University of Ottawa, Ottawa, Ontario, Canada, November 27, 1980.

The work described in this paper was not funded by the U.S. Environmental Protection Agency. The contents do not necessarily reflect the views of the Agency and no official endorsement should be inferred.

PREPARING A DESIGN STORM

By

Stephen A. McKelvie, P. Eng.

Project Manager

Gore & Storrie Limited

Toronto, Ontario.

Introduction

The application of all individual event oriented models analyzing an urban drainage problem requires that the user establish various characteristics to accurately describe both the rainfall and the watershed. The decisions regarding the rainfall used are generally the most important as this input has the greatest effect on the runoff from the watershed under consideration. Thus it is important that the user of SWMM or any of the other hydrologic models fully understand the basis for the rainfall selected and entered into the model. It is hoped that the comments presented herein will aid SWMM users in understanding the rainfall input of the watershed model.

Use of Design Storms

The concept of a design storm dates back to the development of the Rational Method. The design storm has maintained its popularity until relatively recent times when the widespread use of computer models have made the use of continuous modelling or historical storms a real possibility and in many cases desirable.

In spite of this, in most practical applications in Ontario design storms have continued to be used. This is largely due to the encouragement of provincial and municipal governments who in many cases specify the rainfall to be used in urban drainage analyses. At the SWMM Users Group Meeting (1) held in Montreal in 1979 it was concluded by those present that, while the use of "synthetic" design storms presents many advantages, their selection is an important part of the modelling process and should be analyzed on a case-by-case basis.

In Ontario the most commonly used synthetic design storms are the "Chicago" design storms, the SCS Type II distribution and the direct use of Intensity-Duration-Frequency (I.D.F.) curve. Some authorities specifically provide the design storms, others suggest various design storms based on the particular analysis.

In order to understand the "synthetic" design storm, one must understand how it is generated.

Construction of the Synthetic Design Storm

Construction is an appropriate word to use in conjunction with synthetic design storms as it is often built by using various blocks of actual storms. The origins of most synthetic design storms or in the case of the Rational Method, the design storm is the Intensity-Duration-Frequency (I.D.F.) curve.

The I.D.F. curves are based on statistical relationships of the return period of the average intensity of rainfall for a specific duration. For example, the highest annual rainfalls in a 10-minute period for the length of available records would be statistically analyzed with the result being the 1/2 year design average intensity, the 1/5 year design average intensity and so on. This procedure is repeated for various durations and the results are plotted in a manner shown on Figure 1, (2). As can be envisioned from this procedure, one design rainfall event is built of blocks of rainfall from several actual rainfall events, not from one rainfall.

Thus, the design storm is a storm that never really occurred. This fact is not always recognized, but is important to understand.

The decision to use a design storm, continuous rainfall or historical rains will have to be considered carefully by those involved in the analysis. A detailed discussion of the merits of the various type of rainfalls that could be used is beyond the scope of this presentation.

Some of the perceived benefits of design storms are as follows:

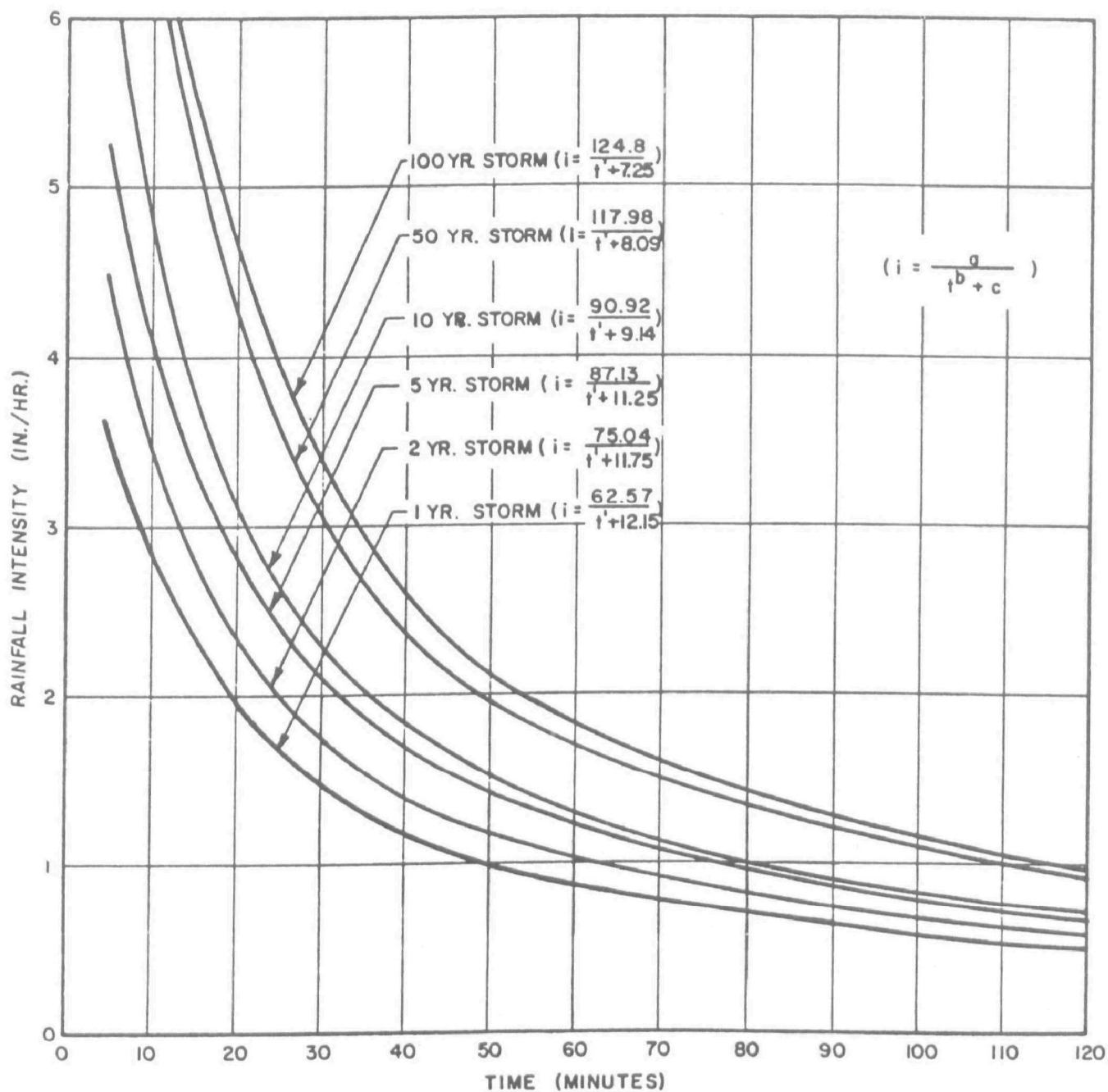


FIGURE 1 - RAINFALL INTENSITY-DURATION-FREQUENCY CURVES

- a jurisdiction may want to use a design storm to maintain a consistency of design standards.
- in most cases, use of a design storm yields conservative results (i.e. high peak discharge rates and volumes) when compared to actual storms.
- the use of design storms is relatively inexpensive and not very time consuming.

On the other hand, there are a number of concerns that must be realized when a modeller and other people involved with stormwater runoff use design storms.

- a basic misinterpretation is often made that the flows generated from various design storms of a given frequency have the same probability of occurring as the design rainfall itself. One must realize that there are many other factors that influence stormwater runoff.
- methods to construct a design storm may be misinterpreted
- design storms usually do not cover all the possibilities (i.e. early peak rainfall, late peak rainfall, snowmelt combined with rainfall etc.)
- usually design storms do not generate the levels of runoff (i.e. long duration, relatively high flows) that can cause problems in detention/retention facilities.

All of these concerns must be realized before one proceeds with the use of a design storm.

Preparing Intensity-Duration-Frequency Curves

In Canada, the Atmospheric Environmental Service of the Department of the Environment operates the weather stations from coast to coast. These weather stations can provide the necessary information to formulate Intensity-Duration-Frequency curves. In most urban areas of Canada a copy of the continuous strip chart of the rain gauge record is available from the Atmospheric Environment Service. This will provide sufficient detail of historical rainfall events for further processing. By referring to annual summaries, one can quickly "zero-in" on the significant rainfall events of that year and thus, an entire year of continuous strip chart records will not have to be analyzed.

In many urban areas there are several weather stations that may be used as the data base for the design storms. The three most important factors in the comparison of several stations are:

- (1) length of period of record
- (2) distance from the study area
- (3) climatic similarity to the study area

The influence of these factors must be carefully considered when reviewing the records at several stations close to the study area.

For the statistical analysis of the rainfall data up to a return period of 10 years a partial duration series is usually used. In a partial duration series the extreme values are analyzed without regard for the year of occurrence. Thus, for example, if one was analyzing the maximum rainfall during 30 minutes for a period of 12 years, one would select the 12 largest 30 minute rainfall events for analysis rather than the largest 30 minute rainfall for each of the 12 years.

The partial duration series can be converted to an annual series by the empirical factors (4) shown in Table 1 as follows;

TABLE 1
FACTORS TO CONVERT PARTIAL-DURATION
SERIES TO ANNUAL DURATION SERIES

<u>Return Period</u> <u>(years)</u>	<u>Conversion</u> <u>Factor</u>
2	0.88
5	0.96
10	0.99
>10	1.00

In deriving intensity-duration-frequency relationships, rainfall intensity values for each selected duration are considered independently from other durations. The initial step being a separate ranking of rainfall intensities for each selected duration in descending order of size. A mathematical fit is made to the array of intensities for each selected duration using the Gumbel analysis or the Log-Pearson Type III analysis. The Gumbel Method is generally accepted for extreme value analysis of rainfall events and is used by the Atmospheric Environment Service in Canada.

The Gumbel Extreme Value Type I Distribution is as follows (6);

$$p = 1 - e^{-e^{-y}} \quad - (1)$$

where p = probability of being equaled or exceeded

e = base of napierian logarithms

y = reduced variate (function of probability)

This distribution may be written as

$$X = \bar{X} + K (S) \quad - (2)$$

where \bar{X} = mean value of annual maxima

S = standard deviation of annual maxima

K = frequency factor

X = rainfall value

TABLE 2
VALUES OF K FOR EXTREME-VALUE (TYPE-I) DISTRIBUTION

RETURN PERIOD YEARS	PROBABILITY	RECORD LENGTH, YEARS											
		15	20	25	30	40	50	60	70	75	100	200	∞
1.58	0.63		-0.492		-0.482	-0.476	-0.473				-0.464	-0.459	-0.450
2.00	0.50		-0.147		-0.152	-0.155	-0.156				-0.160	-0.162	-0.164
2.33	0.43		0.052		0.038	0.031	-0.026				0.016	0.010	0.001
5	0.20		0.919		0.866	0.838	0.820				0.779	0.755	0.719
10	0.10	1.703	1.625	1.575	1.541	1.495	1.466	1.446	1.430	1.423	1.401	1.36	1.30
20	0.05	2.410	2.302	2.235	2.188	2.196	2.086	2.059	2.038	2.079	1.998	1.94	1.87
25	0.04	2.632	2.517	2.444	2.393	2.326	2.283	2.253	2.230	2.220	2.187		
50	0.02	3.321	3.179	3.088	3.026	2.943	2.889	2.852	2.824	2.812	2.770	2.70	2.59
75	0.013	3.721	3.563	3.463	3.393	3.301	3.241	3.200	3.169	3.155	3.109		
100	0.01	4.005	3.836	3.729	3.653	3.554	3.491	3.446	3.413	3.400	3.349	3.27	3.14
200	0.005		4.49		4.28	4.16	4.08					3.83	3.68
400	0.0025		5.15		4.91	4.78	4.56					4.40	4.23
1000	0.001	6.265	6.006	5.847	5.727	5.476	5.478		5.359		5.261		

The frequency factor, K , varies with the return period and record length. The values of K , for the extreme value Type I distribution are given on Table 2, (5, 6).

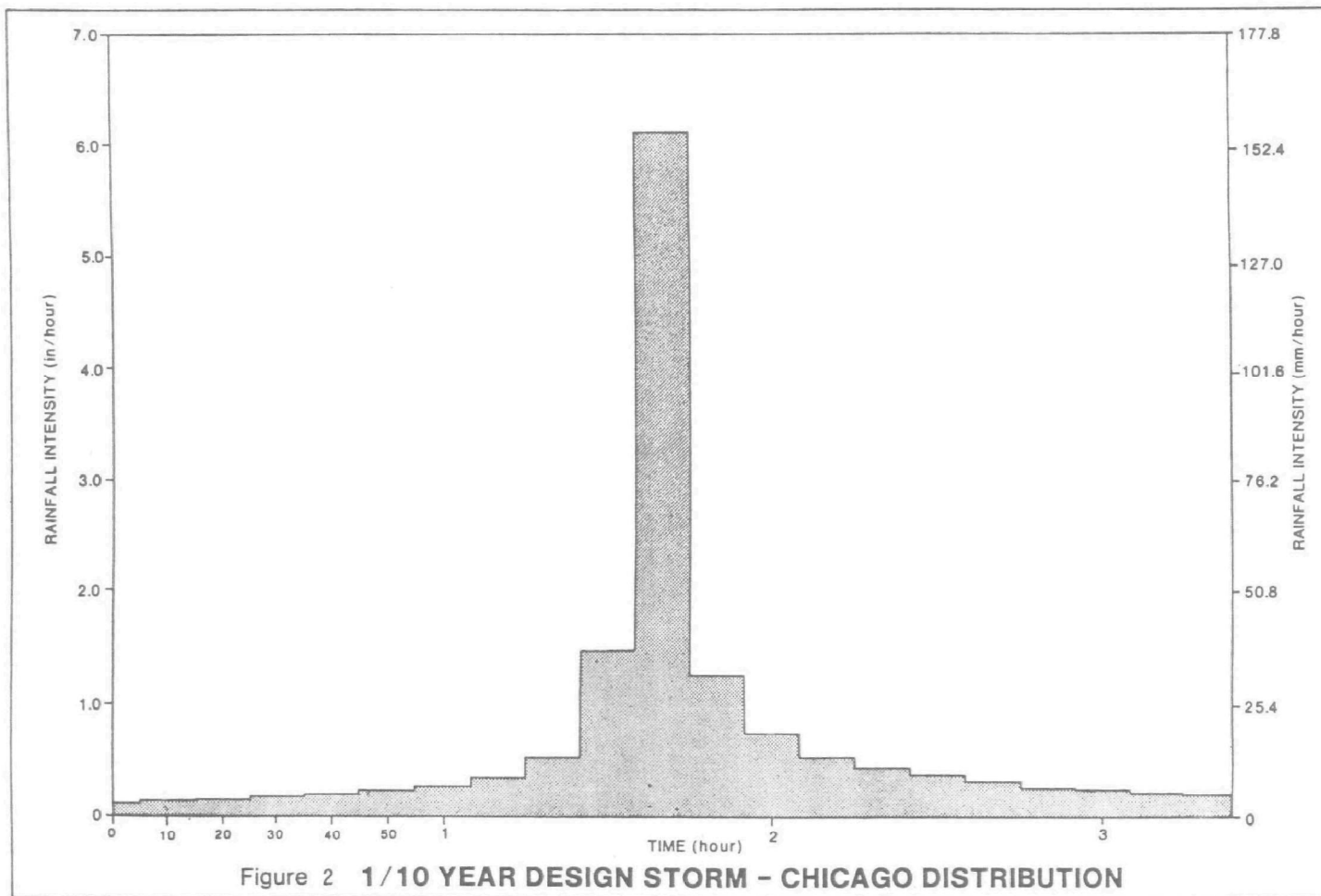
The foregoing analysis is usually used to determine the extreme values of rainfall for the rainfall events with a return frequency of 2, 5, 10, 25 and 100 years, although one or two other storms may be required. For erosion control projects the return period of concern may be the 2 month rainfall event.

The rainfall durations that are usually computed are 5, 10, 15, 20, 30, 60, 120, 180, 360, 720 and 1440 minutes. This provides sufficient data to use the Rational Method, the SCS procedures or the many rainfall-runoff models in use.

The information resulting from this analysis is commonly displayed in the form of the Intensity-Duration-Frequency Curves as shown on Figure 1. The information in this form is suitable for use in the Rational Formula which is still frequently used in small watersheds. It is important to realize that the frequency curves link occurrences that are not necessarily from the same storm. They do not represent a sequence of intensities during a single storm, but only the average intensity of rainfall expected for the specified duration.

Due to the effect of the length of rainfall records it is important that the intensity-duration-frequency data and consequently all other data derived from it, be reviewed and revised if necessary, at periodic intervals of about five years. Of course this depends upon the length of rainfall records used initially.

In order to use the information provided in the Intensity-Duration-Frequency curves in computer aided calculations it is usually necessary to determine the equation of the rainfall curves. The most common forms of the equations used to describe these curves are as follows:



$$i = \frac{a}{t^b + c} \quad - (3)$$

$$i = \frac{a}{(t + c)^b} \quad - (4)$$

where i = average intensity
 t = duration of rainfall
 a, b, c = constants

The suitability of these equations will depend upon the shape of the Intensity-Duration-Frequency curves.

The constants in these equations are obtained for each return period by fitting the Gumbel intensity-duration data to the general form of Equations 3 and 4 and using regression equations of the following forms;

For Equation 3;

$$\text{Log } i = \text{Log } a - \text{Log } (t^b + c) \quad - (5)$$

For Equation 4;

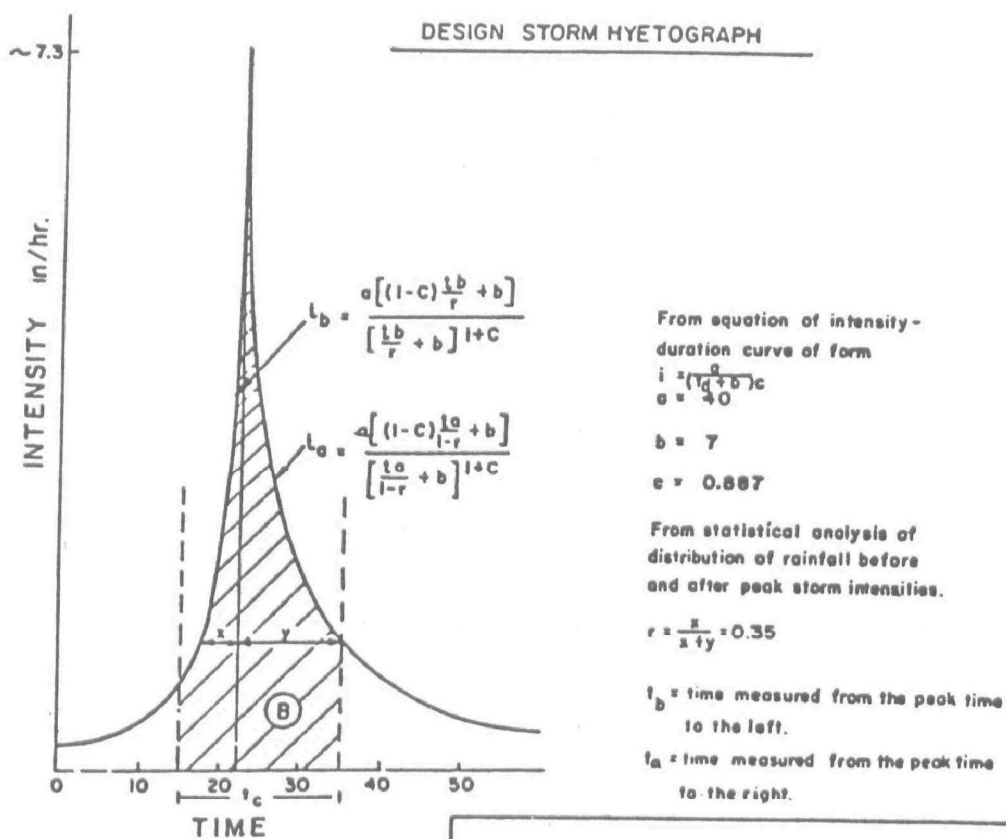
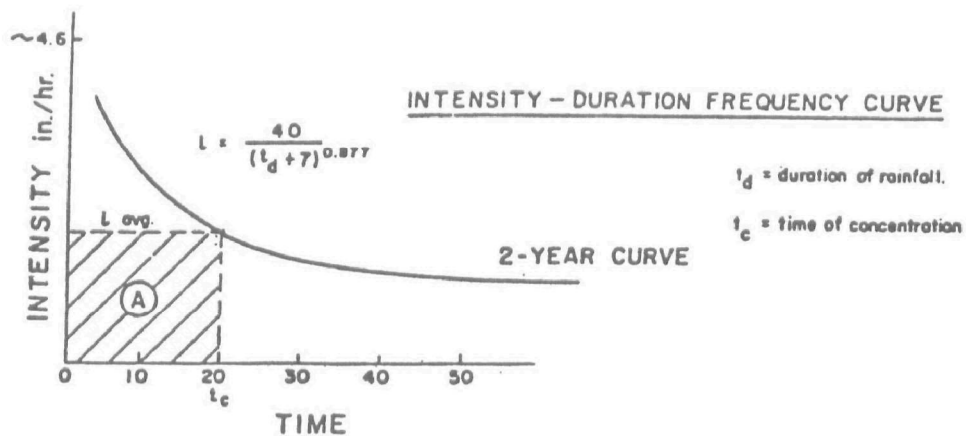
$$\text{Log } i = \text{Log } a - b \text{ Log } (t + c) \quad - (6)$$

For most design storms in Ontario, Equation 4 provides the best fit.

One of the most frequently used types of rainfall distribution used for SWMM analysis in Ontario is the "Chicago type" hyetograph. A typical hyetograph is shown on Figure 2, (3).

For Intensity-Duration-Frequency curves similar to Equation 3 the following distribution is used, (7);

$$i = a \frac{\left[(1 - b) \left(\frac{t_b}{r} \right)^b + c \right]}{\left[\left(\frac{t_b}{r} \right)^b + c \right]^2} \quad - (7)$$



VOLUME (A) = VOLUME (B)

DERIVATION OF 2 YEAR
DESIGN STORM FROM
INTENSITY-DURATION
FREQUENCY CURVE

FIGURE 3

After the Peak

$$i = a \frac{\left[(1 - b) \left(\frac{t_a}{1-r} \right)^b + c \right]}{\left[\left(\frac{t_a}{1-r} \right)^b + c \right]^2} \quad - (8)$$

where t_b = time before peak

t_a = time after peak

r = advancement of storm pattern

The measurement of the storm advancement, r , is the elapsed time from the beginning of the design storm to its peak, divided by the total duration of the design storm.

For Intensity-Duration-Frequency curves similar to Equation 4 the following distribution is used, (8);

Before the peak

$$i = a \frac{\left[(1 - b) \left(\frac{t_b}{r} \right) + c \right]}{\left[\left(\frac{t_b}{r} \right) + c \right]^{1+b}} \quad - (9)$$

After the Peak

$$i = a \frac{\left[(1 - b) \left(\frac{t}{1-r} \right) + c \right]}{\left[\left(\frac{t_a}{1-r} \right) + c \right]^{1+b}} \quad - (10)$$

where t_b = time before peak

t_a = time after peak

r = advancement of storm pattern

These "Chicago-type" storms attempt to distribute rain such that for any time interval the average intensity is equal to that of the intensity-duration-frequency curves. This is shown on Figure 3, (11).

The location of the peak rainfall intensity rates, r , for the design storm is based on observed storm characteristics. Table 3 presents values of r used in various cities in Canada.

TABLE 3

<u>City</u>	<u>Country</u>	<u>r</u>
Kitchener	Canada	0.40
Burlington	Canada	0.46
Oakville	Canada	1/2-0.345, 1/5-0.366, 1/10-0.488
Richmond Hill	Canada	0.35
Winnipeg	Canada	0.31
East York	Canada	0.35
Nepean	Canada	0.41
Mississauga	Canada	0.30
SCS Type II	U.S.A.	0.50

It is not possible to draw any significant conclusions from this comparison other than the typical range of the storm advancement, r , is from 0.30 to 0.50. The storm advancement should be investigated with respect to local experience.

The selected duration of the design storm should be based on the size of the watershed and more specifically on the watershed response. The duration of the design storm should be longer than the time of travel from headwater to outlet of the largest watershed. In most urban municipalities, the duration is 3 - 4 hours is sufficient. In the analysis of pre-development or rural conditions, the duration may have to be significantly longer.

In many design storms based on the Chicago type design storm the peak rainfall intensity is significantly greater than in the I.D.F. curve on which it is based. This may be one of the causes of the reputation that the Chicago type storms are "peaky". In some cases the volume of rainfall during the duration of the storm may be different than that obtained by using the intensity-duration-frequency curve.

When the design storm hyetograph is prepared it should be compared to the I-D-F curve on which it was based. The differences, if any, should be identified and understood by all parties. This becomes important when comparing flows estimated by the direct use of the I.D.F. curves with those estimated by use of the hyetograph. The most important considerations when comparing the I.D.F. curves with the hyetograph is the peak rainfall intensity and the average rainfall intensity and hence the rainfall volume.

As mentioned previously, in Ontario the Intensity-Duration-Frequency curves are most often of the general form described by Equation 4. Thus, Equations 9 and 10 are used to describe the hyetograph. However, for modelling purposes, the hyetograph curve will usually have to be discretized.

In urban areas hyetographs are usually discretized into time steps of 5 - 15 minutes. The size of the time step has a significant effect on the peak rainfall intensity. This will affect the generated peak flows in highly impervious areas. The selected time step for the discretized hyetograph should not be less than 5 minutes in most cases as the intensity-duration-frequency curves which are the basis for the hyetograph usually do not provide rainfall intensity data for duration less than 5 minutes.

The method recommended by the Ontario Ministry of the Environment to discretize the hyetograph curves (9) as identified by Equations 9 and 10 is as follows;

1. Select the time step, Δt
2. Compute the peak rainfall intensity using the following equation

$$i_p = \frac{a}{(\Delta t + c)^b} \quad - (11)$$

3. Distribute the time interval selected (Δt) around the peak as $r \Delta t$ before the peak and $(1 - r) \Delta t$ after the peak.
4. Compute additional points before and after the peak by integrating the design curve and calculating the intensity value by equating the volumes for each time increment of Δt .

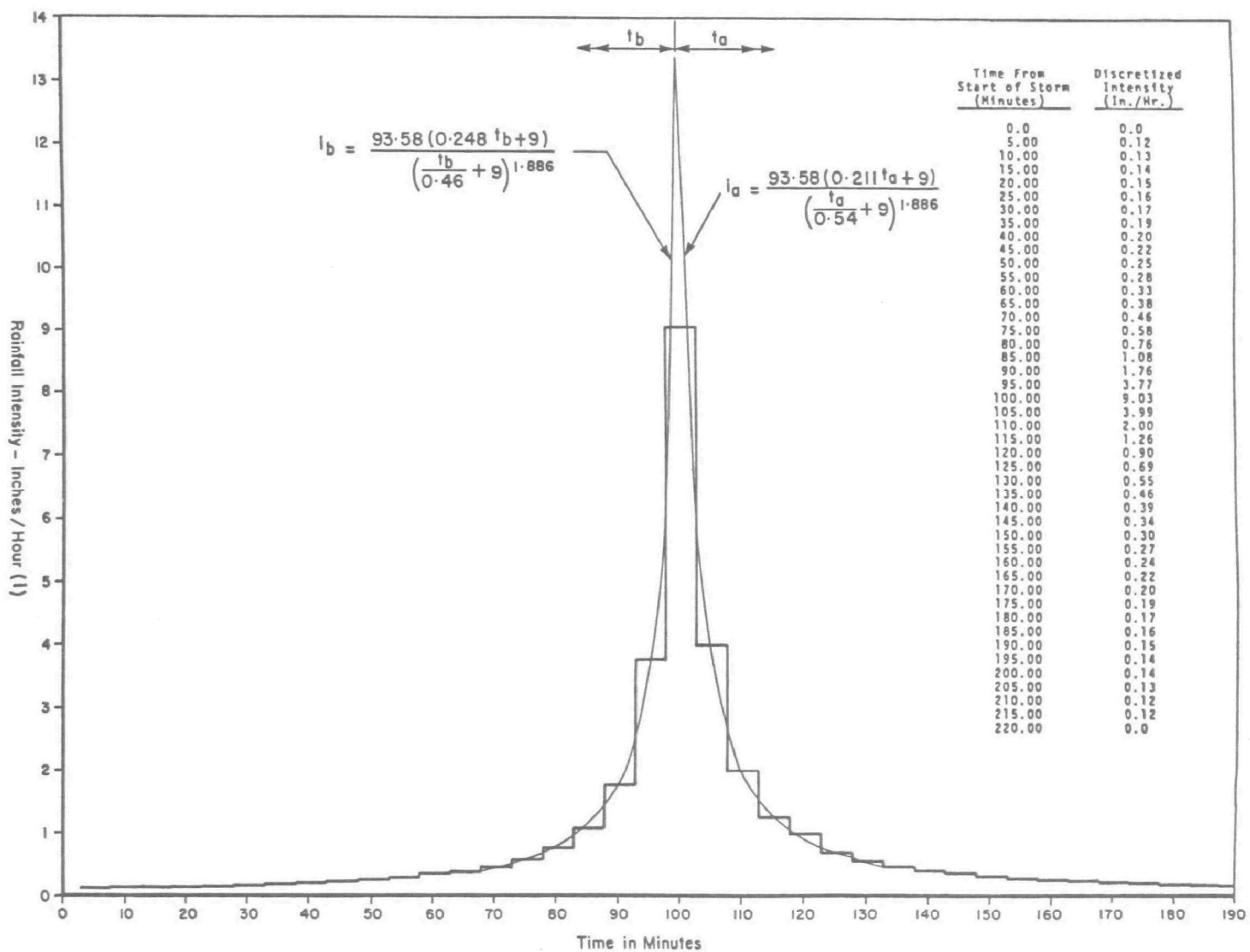


FIGURE 4 - DISCRETIZED DESIGN STORM HYETOGRAPH

The general integral form of the hyetograph curve before the peak is given by Equation 12, (9).

$$\int_{t_{b1}}^{t_{b2}} i_b dt_b = \left[\frac{at_b}{\left(c + \frac{t_b}{r}\right)^b} \right]_{t_{b1}}^{t_{b2}} \quad - (12)$$

The general integral form of the hyetograph curve after the peak is given by Equation 13, (9).

$$\int_{t_{a1}}^{t_{a2}} i_a dt_a = \left[\frac{at_a}{\left(c + \frac{t_a}{1-r}\right)^b} \right]_{t_{a1}}^{t_{a2}} \quad - (13)$$

If this procedure is used similarity between the intensity-duration-frequency curve and the design storm hyetograph is maintained. This is important as the intensity-duration-frequency curve is based on recorded rainfall information. An example of this is shown as Figure 4, (10).

Design storm hyetographs can easily be converted into mass rainfall curves that are required for some hydrologic models such as HYMO.

As mentioned previously the SCS Type II distribution is used frequently in Ontario. The SCS Type II distribution takes the total rainfall over a given period of time, usually 6, 12 or 24 hours and distributes the rainfall throughout that period by a mass curve shown on Figure 5, (12). Used in this manner, the distribution of rainfall intensity within the duration of the rainstorm is not related to historical data at a particular location.

The SCS Type II distribution is usually expressed in hourly and half-hourly intervals and is most applicable in this form to larger rural

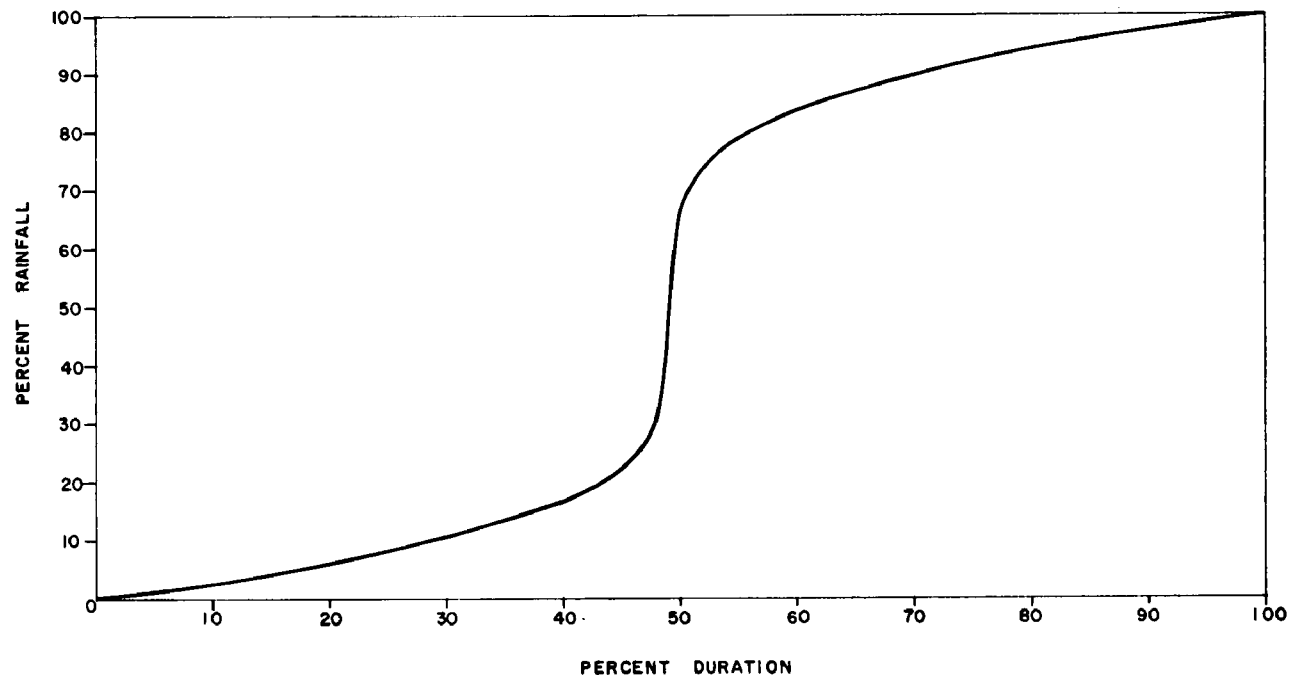


FIGURE 5 – NORMALIZED SCS TYPE II RAINFALL DISTRIBUTION

watersheds. This distribution can be used in pipe system analysis if the time interval is smaller. In the analysis of urban drainage systems, the rainfall period is usually not required to be longer than 12 hours. Long duration storms may be of interest to test the performances of detention/retention facilities.

For the 1/10 year SCS Type II distribution of the rainfall at the Toronto Bloor Street Station the observations shown on Table 4 are interesting. As can be seen in Table 4 the 12 hour storm duration is the best fit to the I.D.F. curve with respect to peak and average rainfall intensities in this case. This may vary for other locations.

TABLE 4
Comparison of I.D.F. Curves/SCS Type II Rainfall Distribution
Toronto Bloor Street Station 1/10 Year Rainfall

<u>Storm Duration</u>	<u>Ave. Intensity mm/hr.</u>	<u>Total Rainfall mm</u>	<u>Peak SCS 12 min. mm/hr.</u>	<u>Peak I.D.F. 12 min. mm/hr.</u>	<u>SCS Peak/Ave.</u>	<u>I.D.F. Peak/Ave.</u>
24 hour	3.10	74.4	83.7	113.7	27.0	36.7
12 hour	5.68	68.2	114.2	113.7	20.1	20.0
6 hour	10.30	61.8	119.9	113.7	11.6	11.0
3 hour	17.30	51.9	127.9	113.7	7.4	6.6

$$\text{Intensity} = \frac{875}{(t + 3)^{0.75}} \text{ mm/hr.}$$

When using design storms, the modeller and others involved in stormwater management should fully understand the procedures used to develop the design storm and the limitations inherent of the design storm concept. It is hoped that this commentary will aid in this matter.

REFERENCES

1. Summary - Seminar on the Design Storm Concept - "Proceedings Stormwater Management Model (SWMM) Users Group Meeting - May 24 - 25, 1979" U.S. Environmental Protection Agency - EPA 600/9-79-026.
2. Gore & Storrie Limited - "Storm Water Management for Nepean, Merivale Area" Research Report No. 89, Canada-Ontario Agreement on Great Lakes Water Quality.
3. Andrew Brodie Associates Inc. "Town of Oakville Storm Drainage Policies and Criteria" 1979.
4. V.T.Chow "Handbook of Applied Hydrology" McGraw Hill Book Company.
5. Viessman, Knapp, Lewis, & Harbaugh - "Introduction to Hydrology" Second Edition Harper & Row Publishers Inc.
6. Linsley, Kohler, & Paulhus - "Hydrology for Engineers" Second Edition, McGraw Hill Inc.
7. C.J. Keifer & H.H. Chu - "Synthetic Storm Pattern for Drainage Design" Proceedings ASCE, August 1957.
8. M. Bandyopadhyay - "Synthetic Storm Pattern and Run-off for Gauhati, India" Journal of the Hydraulics Division, ASCE HY5, May 1972.
9. Ontario Ministry of the Environment and Municipal Engineer's Association - "Training Manual - Sewer and Watermain Design Course" September 1981.
10. M.M. Dillion Limited - "City of Burlington Storm Drainage Manual" 1977.
11. "Second Canadian Stormwater Management Model Workshop" October 19 - 21, 1976.
12. K.R. Cooley - "Erosivity Values for Individual Design Storms" Journal of the Irrigation and Drainage Division, ASCE, IR2 June, 1980.

The work described in this paper was not funded by the U.S. Environmental Protection Agency. The contents do not necessarily reflect the views of the Agency and no official endorsement should be inferred.

A PREDICTIVE MODEL FOR HIGHWAY RUNOFF POLLUTANT CONCENTRATIONS AND LOADINGS

by

Brian W. Mar, Richard R. Horner (1)

Introduction

Highway runoff is not recognized in most literature as a separate constituent in nonpoint source pollution (Browne and Grizzard, 1979; Browne, 1981). Its threat to water resources has traditionally been aggregated with general urban runoff and characterized by mass/unit area/unit time loadings, as well as concentrations. Another approach has been to hypothesize a pollutant deposition model for the periods preceding storms and a washoff model for contaminant removal in runoff from individual storms (Sartor and Boyd, 1972; Sylvester and DeWalle, 1972; Meinholz et al., 1978; Kobriger et al., 1981). There was reason to believe that these approaches do not adequately represent the important operative factors in determining the character of highway runoff for impact assessment in the climatic conditions prevalent in the Pacific Northwest. Accordingly, the Washington State Department of Transportation funded a five-year research effort to improve the understanding of these factors and model highway runoff pollutant loadings for use in impact analysis.

One of the first issues faced in the research program was whether to base monitoring on discrete samples collected throughout storms or composites representing entire storms. A system was developed to economically collect composite samples from a storm, and it was decided to sacrifice the better characterization of the pollutographs of a relatively few storms through discrete samples for storm composite data for many events. We have used the system to sample approximately 500 storms at nine locations in Washington State.

Experimental Design

Figure 1 illustrates the composite sampling system schematically. Its major elements are a calibrated flow splitter and composite sample collector. Flow splitters were sized to capture a set proportion of the design storm for each site, typically about 1 - 2 percent.

The data collected at each site included continuous, automatic traffic counts and, for each storm, precipitation and runoff volumes. Samples were analyzed for total suspended solids (TSS), three metals (lead, zinc, copper), nutrients (total phosphorus, total Kjeldahl nitrogen, nitrate-plus-nitrite-nitrogen), and general measures of organic constituents (chemical oxygen demand, total organic carbon). Measured concentrations and flow volumes were used to estimate pollutant loadings. Tests demonstrated that comparable

(1) Environmental Engineering and Science Program; Department of Civil Engineering, University of Washington, Seattle, Washington 98195.

Approximate Scale 1" = 2.5'

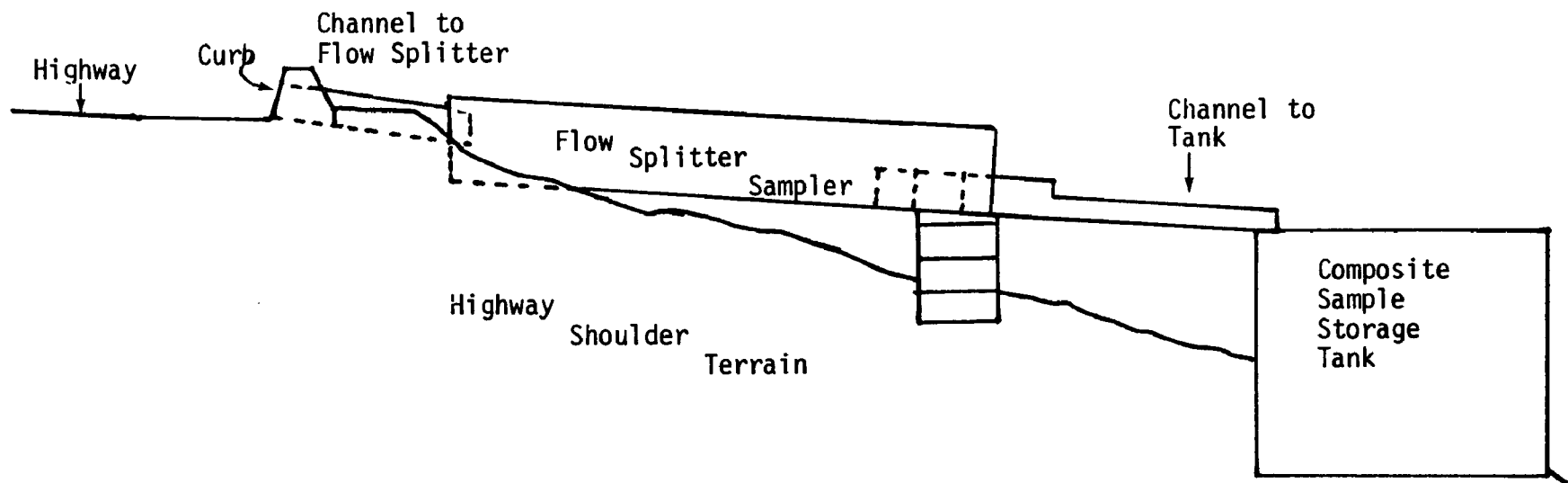


Figure 1: Layout of the Composite Sampling System on a Curbed Highway

loading estimates resulted from using samples from the composite tank and composites made from discrete samples collected simultaneously by an automatic sampler (Clark et al., 1981).

Pollutant Transport Mechanisms

Figure 2 illustrates the pollutant deposition mechanisms considered to be operating, including contributions from the surroundings, traffic deposition, pavement wear, maintenance operations, and spills. Data collected suggested that vehicles traveling during storms were a very important source of pollutants in the extended wet periods of Western Washington. Vehicles apparently pick up and retain contaminants, which are then spray-washed from their undercarriages while driving on wet roads.

Mechanisms tending to remove pollutants from highways, diagramed in Figure 3, include hydrologic and vehicular scrubbing, maintenance, and natural and traffic-generated winds. The eruption of Mt. St. Helens midway in the project provided an opportunity to directly observe the latter mechanism, and we consider it to be of major importance in pollutant removal. In the Pacific Northwest transport of highway pollutants appears to be more a function of kinetic energy provided by moving vehicles than by the low-intensity rainfall.

Pollutant Loading Model

As the data base developed, we investigated the associations among pollutant loadings and a number of site and storm characteristics, including volume, duration, and intensity of precipitation, antecedent dry period, total traffic, and vehicles traveling during storm periods. The analysis exhibiting the most consistent pattern for the various sampling sites and contaminants monitored was cumulative pollutant mass per unit highway length versus cumulative vehicles during storms (VDS), pictured in Figure 4 for TSS at one station. The relationship assumed a "stair-step" form, the steps being associated with the occurrences of winter sanding or, on a few occasions, volcanic eruptions. The fall and spring periods were characterized by linear relationships. Viewed for all sites (Figure 5), the slopes of the lines differed among sites and between winter and other seasons at each site.

Observing these differences, it was natural to hypothesize that site runoff coefficients (RC) should have a major influence on the cumulative pollutant mass loading entering the runoff. When this variable was introduced, TSS runoff rates at the various stations grouped as shown in Figure 6. The elevated rates at arid Eastern Washington locations result from deposition of the loose soils on roadways by relatively high and continuous winds. The relationships illustrated can be expressed by a model in which TSS loading is proportional to the product of VDS and runoff coefficient:

$$\text{TSS Loading} = (K) (\text{VDS}) (\text{RC})$$

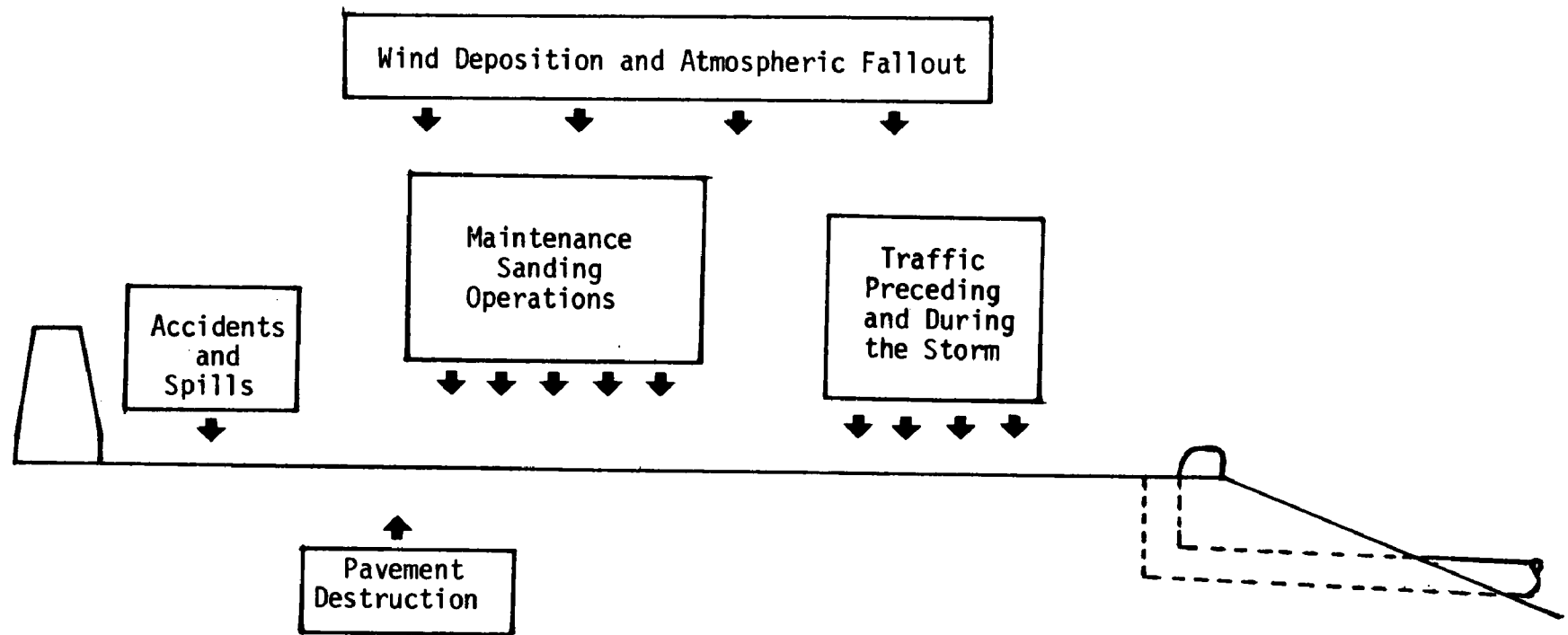


Figure 2: Total Suspended Solids and Pollutant Deposition Mechanisms

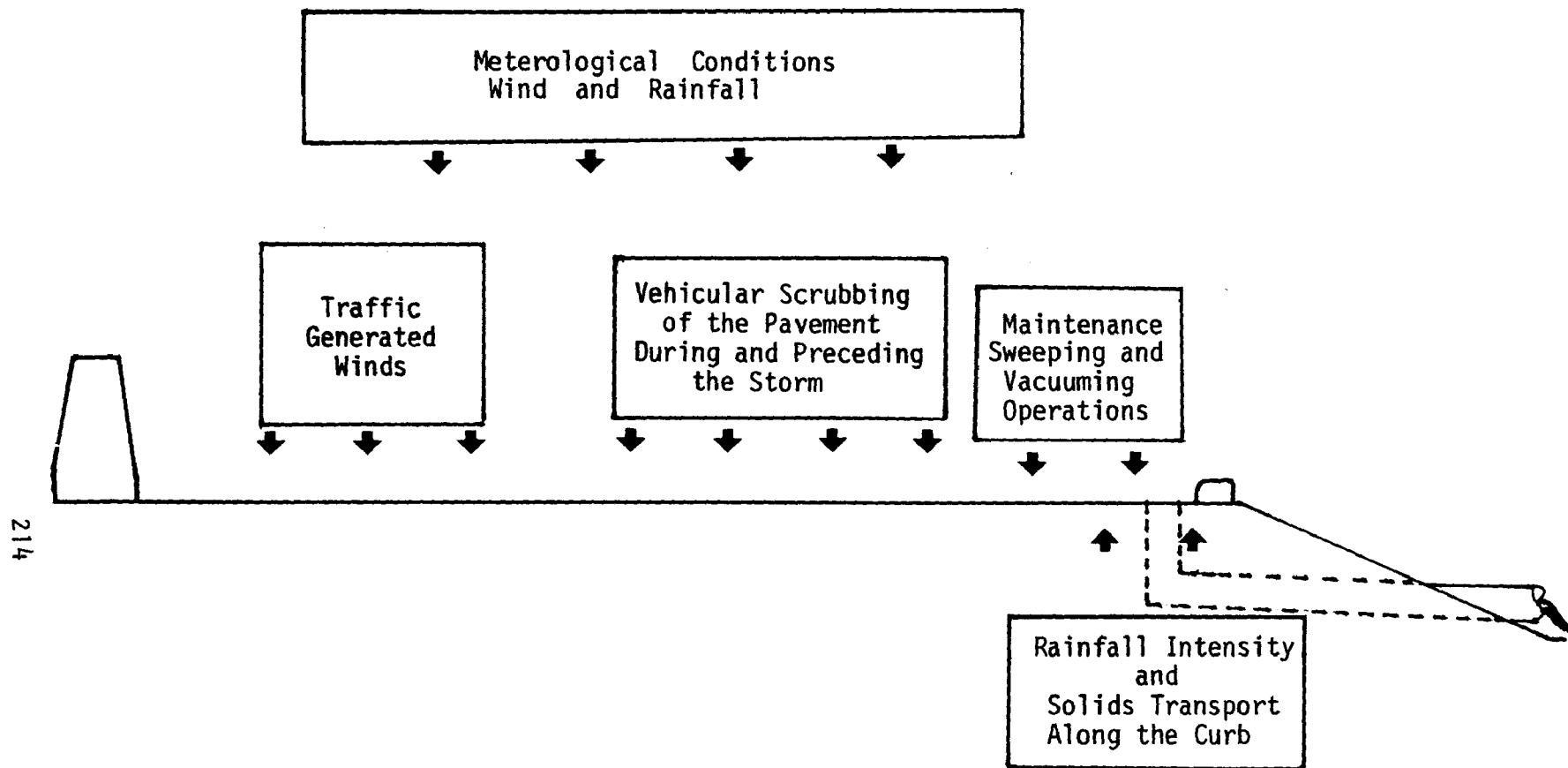


Figure 3: Total Suspended Solids and Pollutant Removal Mechanisms

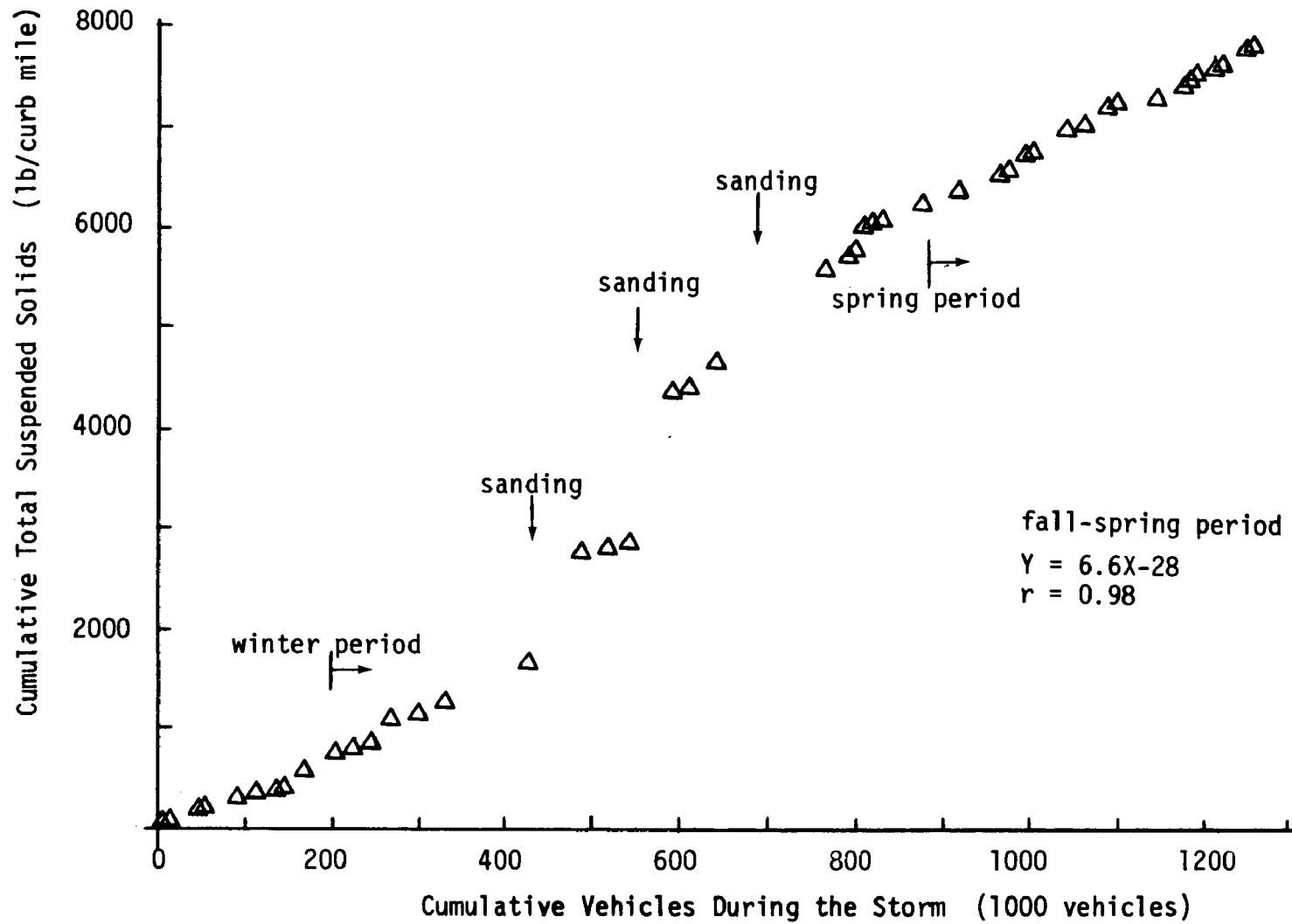


Figure 4: Cumulative Total Suspended Solids Versus Cumulative Traffic Volumes During the Storm for the SR-520 Site

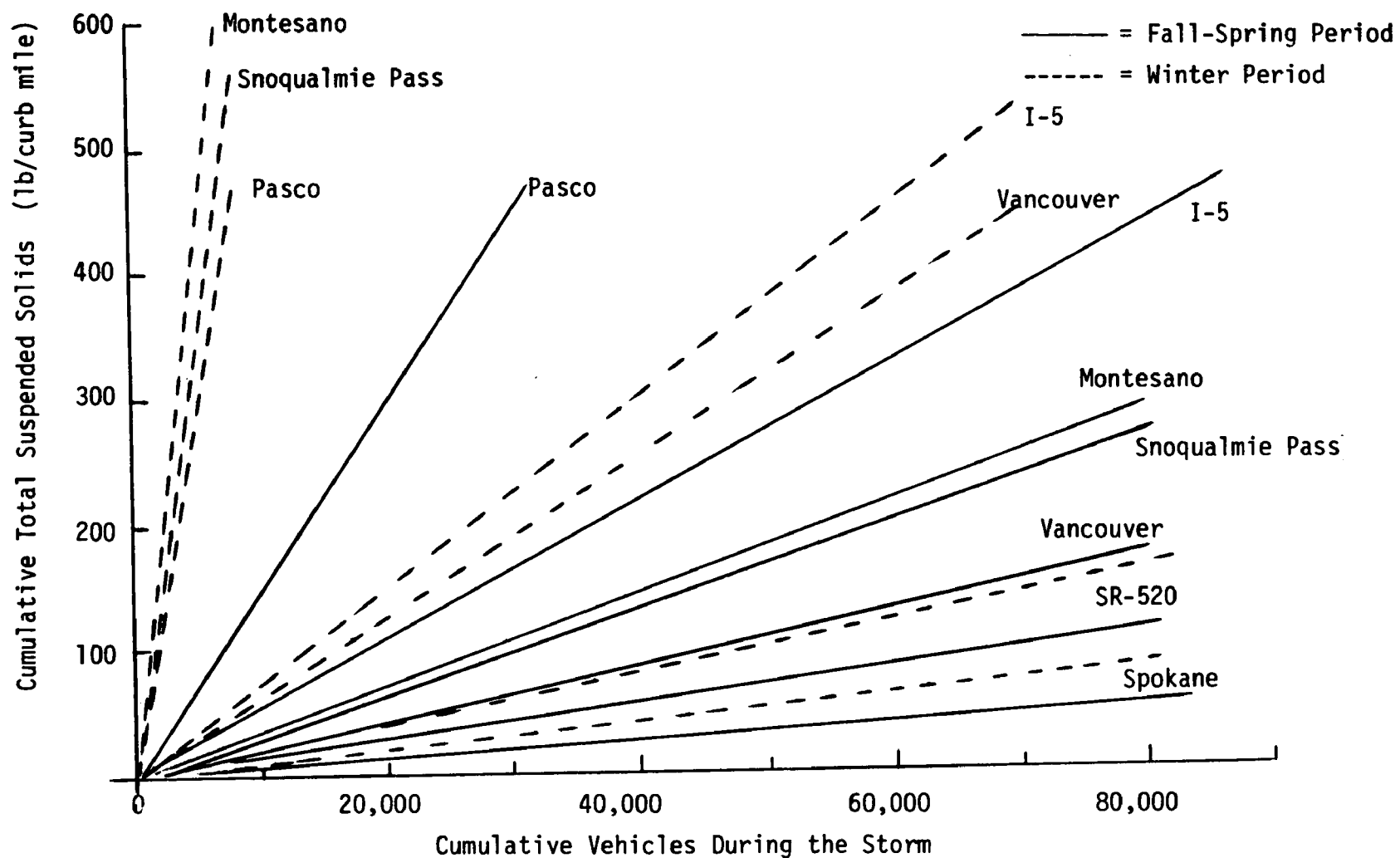


Figure 5: Estimated Seasonal TSS Runoff Rates for the Various Runoff Sites*

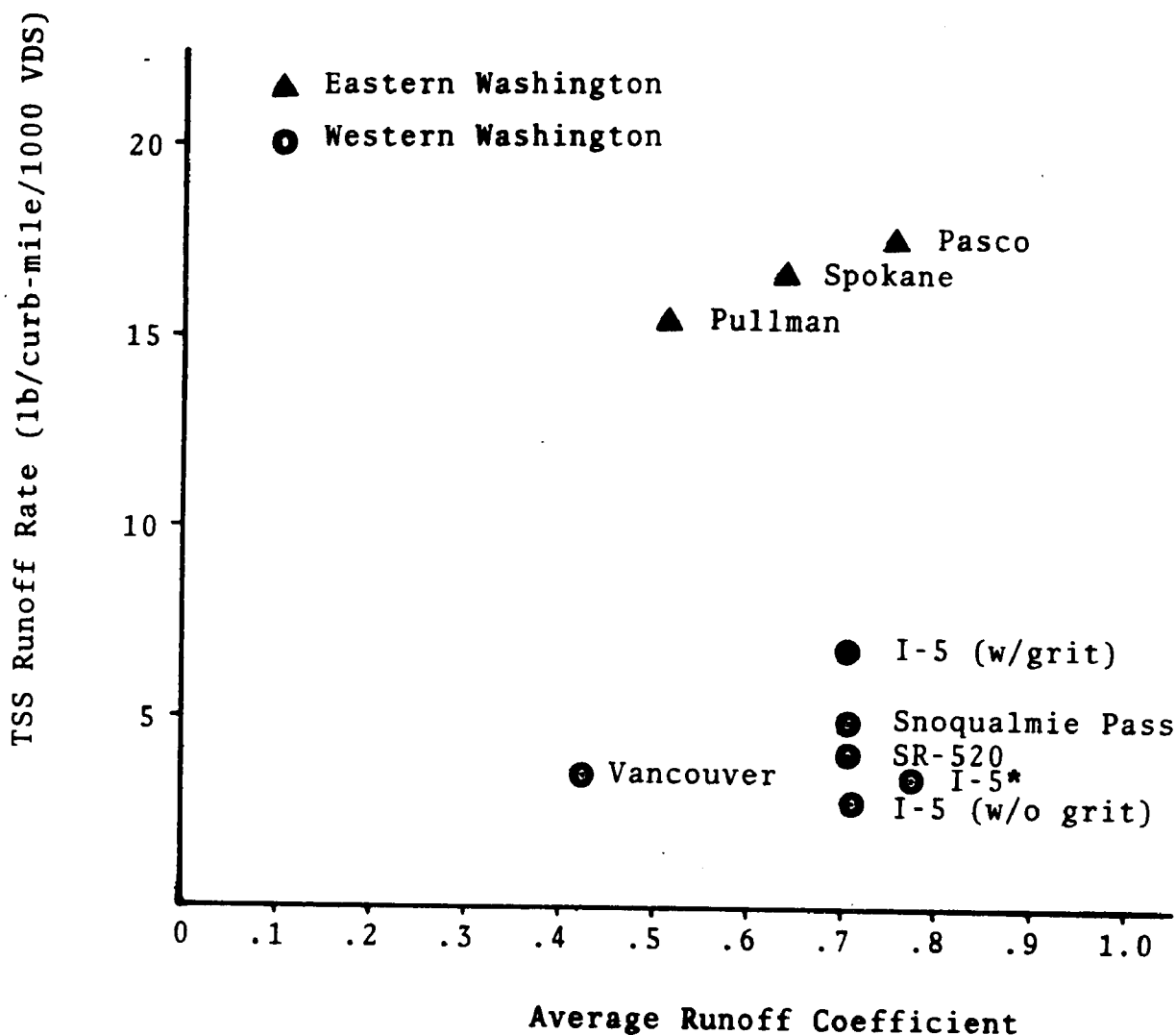


Figure 6: TSS Runoff Rate versus Average Runoff Coefficient for All Sites.

The constant of proportionality (K), which is the TSS runoff rate at a runoff coefficient of 1, may be established as follows, since TSS loading is directly proportional to runoff flow rate:

$$K_{(RC=1)} = \frac{K_{(RC=n)}}{n}$$

The mean constant (+ one standard error) for Western Washington locations is 6.4 ± 0.8 lb/curb-mi/1000 VDS. It was found by observing runoff following large, intense storms which thoroughly cleaned highway surfaces that the constant fell to approximately 3 lb/curb-mi/1000 VDS under those conditions, representing the direct contribution of vehicles alone and excluding import from adjacent land uses. The reduction in the loading factor is short-lived, and one or more dry days restores enough solids to return it to approximately the mean value. K for Eastern Washington locations was estimated on the basis

of considerably less data than available for Western Washington to be 26 lb/curb-mi/1000 VDS.

Other pollutants generally observed a relationship to cumulative VDS similar to that of TSS. Illustrated as an example (Figure 7) is the chemical oxygen demand plot for one sampling site. Again, a linear relationship during the spring and fall was evident, broken by steps coincident with sanding. The similarities of form among the plots suggested that loadings of the various contaminants could be estimated as proportions of TSS loadings:

$$\text{Specific Pollutant Loading} = (P)(\text{TSS Loading})$$

The coefficients of proportionality (P) are analogous to potency factors employed in SWMM, STORM and other models. The coefficients derived from the data (Table 1) may be taken as constants at any Washington State location for some pollutants or as linear functions of traffic for other contaminants. We are continuing to refine this aspect of the model, with a particular interest in expressing loadings of the soluble, more biologically available forms of the metals.

The model was developed on the basis of cumulative measures and thus is applicable to assessing total loadings over a time span encompassing a number of storms (monthly or annually). We have also adopted an approach to characterizing individual storm loadings, as discussed below.

Table 1: Expressions of Specific Pollutant Ratios Recommended for Use with Washington State Highway Runoff Model.

Pollutant	Expression	R ²	Specifications
VSS	$P_{VSS} = .2$	--	For all sites
COD	$P_{COD} = .4$	--	For all sites
TOC	$P_{TOC} = .8$	--	For all sites
Pb	$P_{Pb} = 2 \times 10^{-5} + (8.55 \times 10^{-8}) * (ADT)$.987	For all sites except Pasco
Zn	$P_{Zn} = 4.48 \times 10^{-4} + (2.37 \times 10^{-8}) * (ADT)$.820	For all sites except Spokane
Cu	$P_{Cu} = 7.05 \times 10^{-5} + (2.89 \times 10^{-9}) * (ADT)$.888	For all sites
TKN	$P_{TKN} = 2 \times 10^{-3}$	--	For Western Washington sites
	$P_{TKN} = 5.36 \times 10^{-3} + (3.06 \times 10^{-9}) * (ADT)$.995	For Eastern Washington sites
NO ₃ + NO ₂ - N	$P_{NO_3 + NO_2 - N} = 2 \times 10^{-3}$	--	For all sites
TP	$P_{TP} = 2 \times 10^{-3}$	--	For all sites

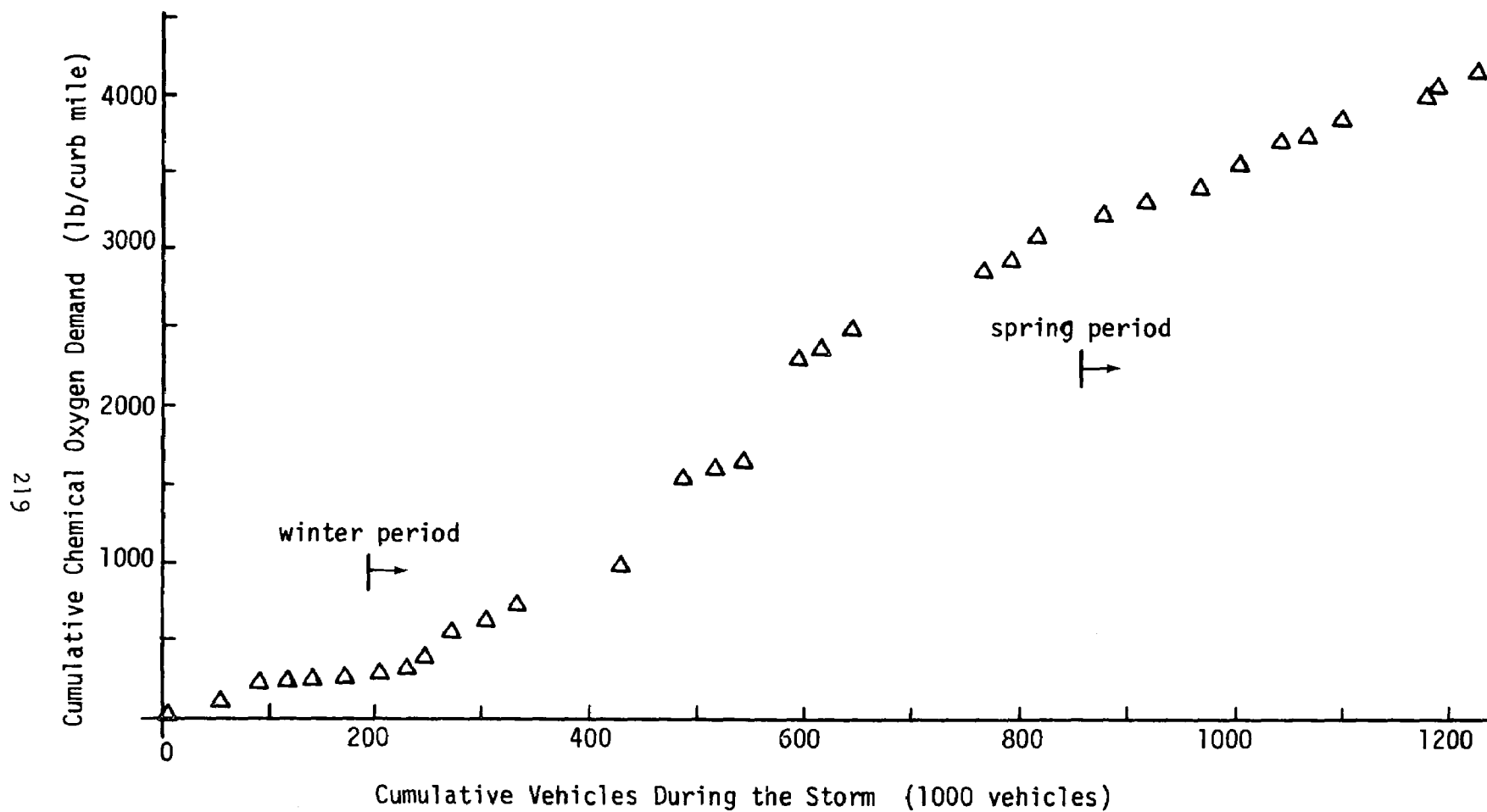


Figure 7: Cumulative Chemical Oxygen Demand Versus Cumulative Traffic Volumes During the Storm for the SR-520 Site

Analysis of Individual Event Runoff Concentrations and Loadings

To this point this paper has dwelled on pollutant loadings and said nothing about concentrations, which generally are of more direct biological significance. Loadings are primarily useful to evaluate the relative stresses on aquatic biota in two given situations and to assess the accumulation of contaminants in sinks such as sediments and standing bodies of water of long residence times. Toxic responses in dynamic systems are more a function of concentrations, however. The plot in Figure 8, often termed a pollutograph, illustrates a typical storm runoff concentration pattern with time, with greatly elevated concentrations in the first fraction of an hour declining rapidly to fairly stable, low levels. Of course, this pattern is not always observed; sometimes intense bursts of precipitation midway in a storm result in concentrations far higher than the "first-flush".

Considering this variability in discrete sample concentrations and the lack of knowledge to assess the consequences of brief, high level exposures, we decided to base our analysis on the concentrations in composite samples, which are the event mean values. This approach admittedly neglects the maximums; nevertheless, it should represent the approximate conditions affecting receiving water biota for all but very short periods. We reinforced this procedure with bioassays enabling direct observation of impacts (although presentation of the results of these experiments is beyond the scope of this paper).

The composite samples from our various monitoring stations exhibited wide concentration ranges. It appeared that many variables would greatly complicate any deterministic or stochastic attempt to express concentrations in terms of those variables. Inspired by the technique being applied to the Nationwide Urban Runoff Program data (U.S. Environmental Protection Agency, 1981), our solution to the problem of expressing individual storm loadings and concentrations was to analyze cumulative distributions to determine the probability of exceeding specific values with given storm and site conditions.

After we plotted the individual site distributions, it became clear that aggregation of the data into Eastern and Western Washington groupings would again be warranted. As shown in Figure 9 for TSS concentrations, plotting the aggregated cumulative distributions on logarithmic axes against concentrations (or loadings) produced straight lines useful in plotting probability distributions. Using TSS concentration in Western Washington highway runoff as an example (Figure 10), these distributions demonstrate that the data are essentially log-normal. In addition to showing the probability of surpassing any given concentration in any storm in untreated runoff, the graphs include lines representing various levels of pollutant reduction through treatment, dilution by receiving waters, or a combination of the two. Where available, criteria were shown to provide a basis for judgment.

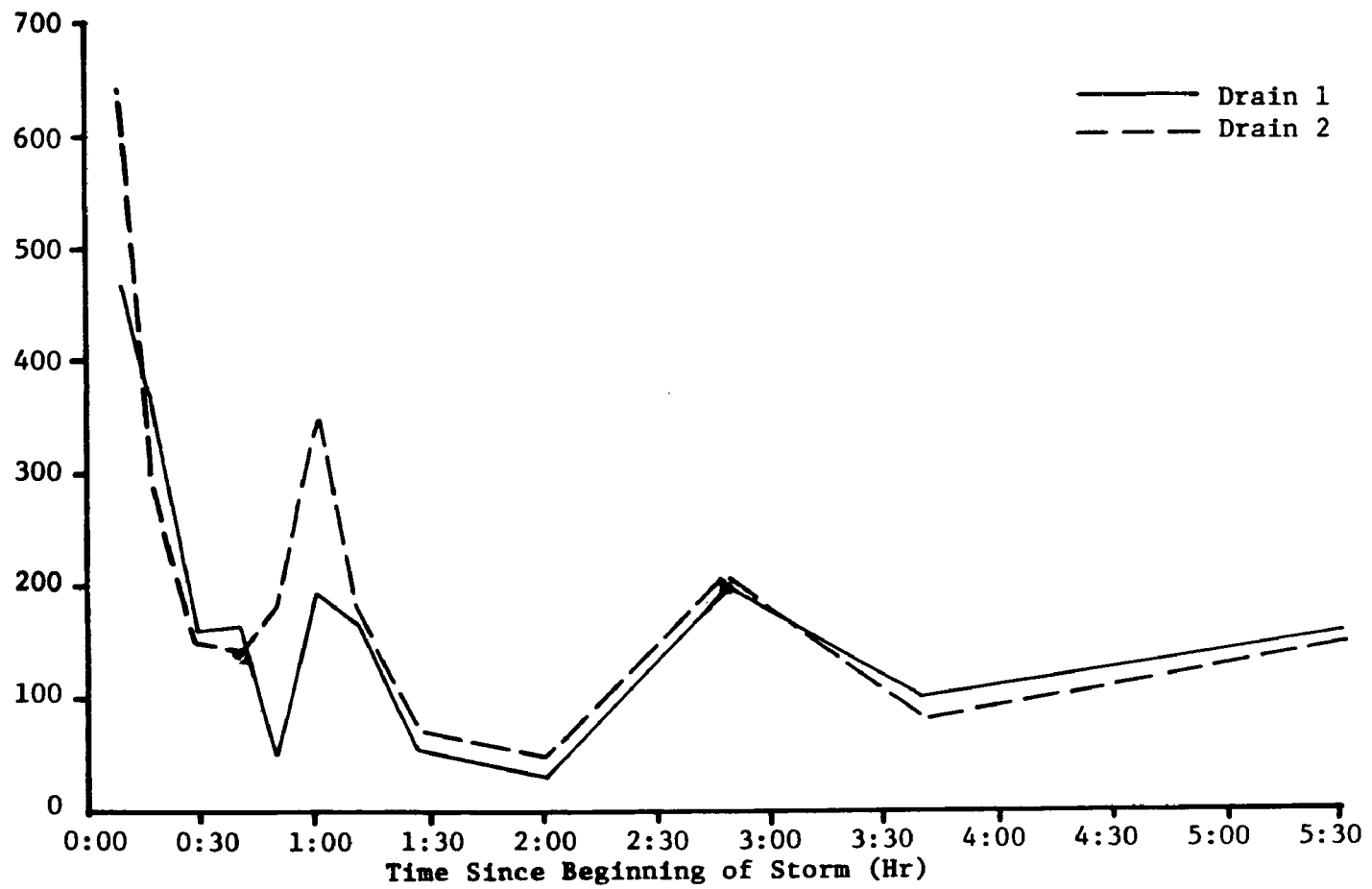


Figure 8: Total Suspended Solids Concentration versus Time, SR-520, 2/25/78.

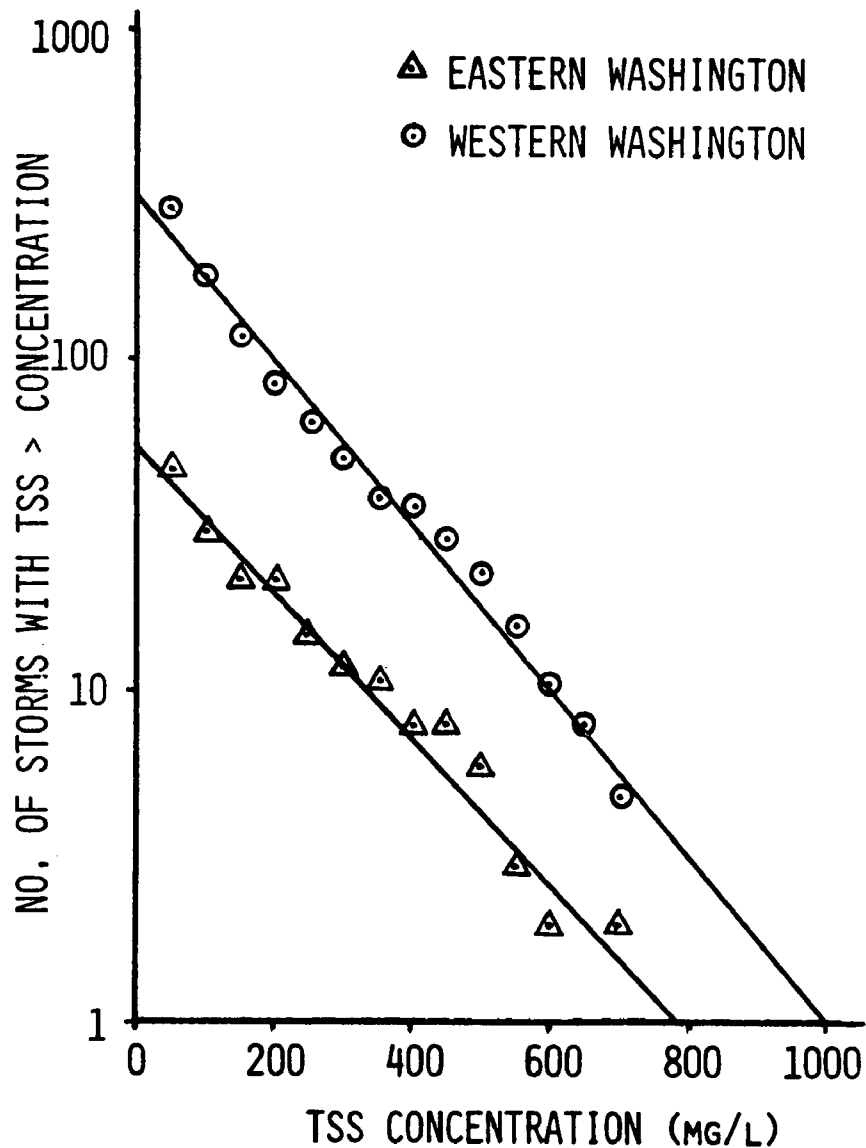


Figure 9: Cumulative Distributions of TSS Concentrations.

Conclusions

Our model thus consists of a component for predicting total pollutant loadings over an extended time period, plus a series of charts with which individual event impacts may be assessed probabilistically. These elements have been assembled in a guidebook for evaluating aquatic impacts due to highway operations and maintenance. We believe that the specific research findings and the proposed impact assessment procedures apply throughout the Pacific Northwest and that the techniques used to monitor storms and analyze the data are more generally applicable.

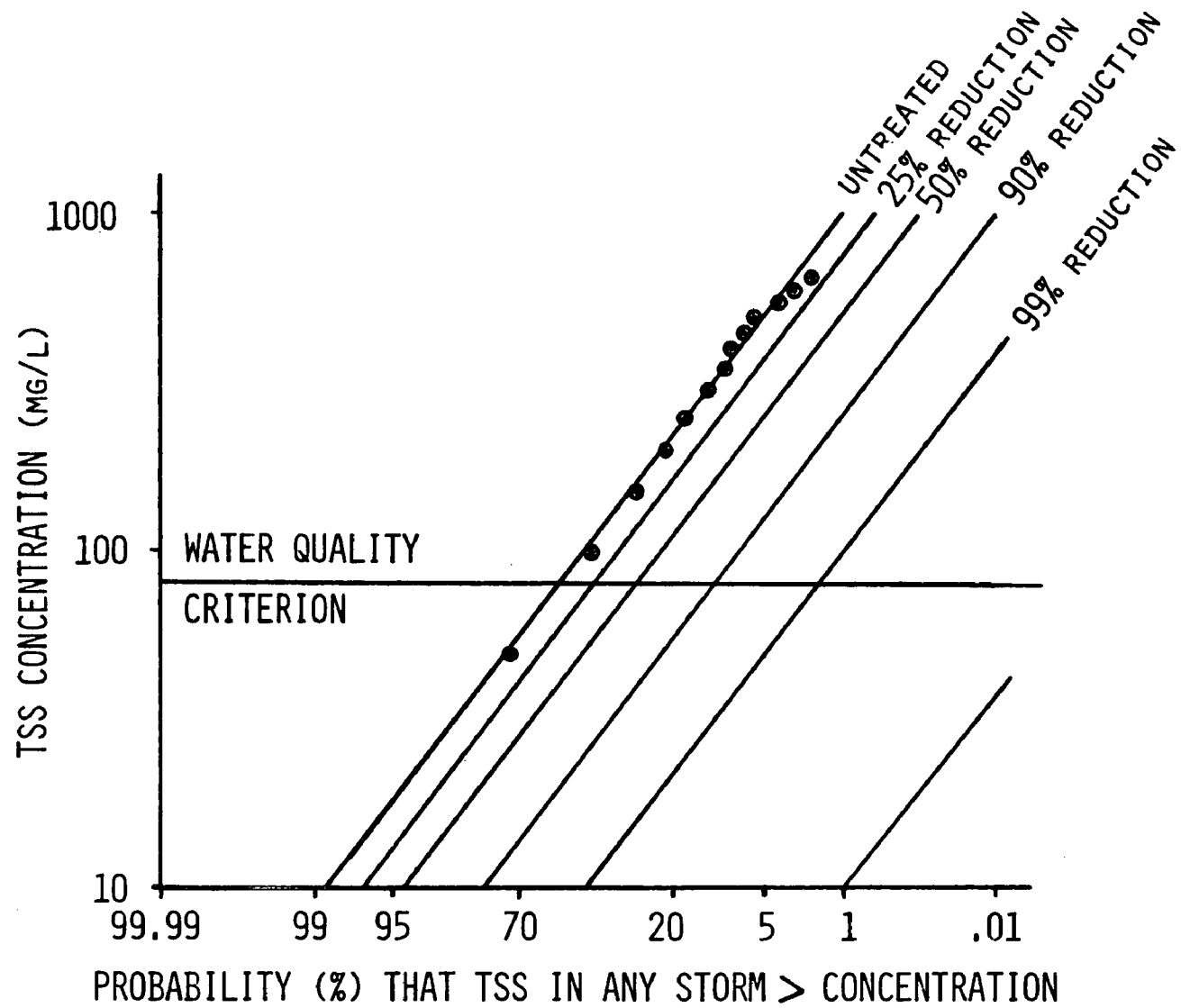


Figure 10: TSS Concentration-Probability Distributions for Western Washington Storms.

REFERENCES

- Browne, F.X. and T.J. Grizzard, "Non-point Sources", J. Water Poll. Control Fed., 51, No. 6, June 1979, pp. 1428 - 1444.
- Browne, F.X., "Non-point Sources", J. Water Poll. Control Fed., 53, No. 6, June 1981, pp. 901 - 908.
- Clark, D.L., R. Asplund, J. Ferguson, and B.W. Mar, "Composite Sampling of Highway Runoff", J. Environ. Eng. Div. ASCE, 107, No. EE5, October 1981, pp. 1067 - 1081.
- Kobriger, N.P., T.L. Meinholz, M.K. Gupta, and R.W. Agnew, "Constituents of Highway Runoff, Vol. III: Predictive Procedure for Determining Pollutant Characteristics in Highway Runoff", FHWA/RD-81/044, Envirex, Inc., Milwaukee, WA, 1981.
- Meinholz, T.L., N.P. Kobriger, M.K. Gupta, and R.W. Agnew, "Predictive Procedure for Determining Pollutant Characteristics in Highway Runoff, Vol. III, Final Report", Report to U.S. Department of Transportation, Federal Highway Administration by Envirex, Inc., Milwaukee, WI, 1978.
- Sartor, J.D. and G.B. Boyd, "Water Pollution Aspects of Street Surface Contaminants", EPA-R2-72-081. U.S. Environmental Protection Agency, Washington, D.C., 1972.
- Sylvester, R.O. and F.B. DeWalle, "Character and Significance of Highway Runoff Waters: A Preliminary Appraisal", Report to Washington State Highway Commission by Department of Civil Engineering, University of Washington, Seattle, WA, 1972.
- U.S. Environmental Protection Agency, "Preliminary Results of the Nationwide Urban Runoff Program", Vol. I (Draft), USEPA Water Planning Division, Washington, D.C., 1981.

Highway Runoff Water Quality Reports

Report No. 1. Horner, R.R. and E.B. Welch, "Effects of Velocity and Nutrient Alterations on Stream Primary Producers and Associated Organisms," November 1978.

Velocity and nutrient studies at 12 sites in Western Washington streams indicated that 50 cm/sec is the critical average current velocity where the productive base of the food web is impacted. Swiftly flowing streams rich in nutrients should not be slowed to this value, and slowly flowing streams should not be altered to have velocities greater than this value.

Report No. 2. Horner, R.R., S.J. Burges, J.F. Ferguson, B.W. Mar, and E.B. Welch, "Highway Runoff Monitoring: The Initial Year," January 1979.

This report covers the initial 15 months of effort to review the literature, select a prototype site, compare the performance of several automatic sampling devices, and install a prototype sampling site on I-5 north of Seattle.

Report No. 3. Clark, D.L. and B.W. Mar, "Composite Sampling of Highway Runoff: Year 2," January 1980.

A composite sampling device was developed that can be installed at less than ten percent of the cost of automatic sampling systems currently used in Federal highway runoff studies. This device was operated for one year, along-side an automatic sampler at the I-5 site, to demonstrate that the two systems provide statistically identical storm composites.

Report No. 4. Vause, K.H., J.F. Ferguson, and B.W. Mar, "Water Quality Impacts Associated with Leachates from Highway Woodwaste Embankments," September 1980.

Laboratory and field studies of a woodchip fill on SR-302 demonstrated that the ultimate amounts of COD, TOC and BOD per ton of woodchips can be defined and that this material is leached exponentially by water. After a year the majority of the pollutant has been removed, suggesting that pre-treating of the woodchips prior to use in the fill can reduce the pollutant release from a fill. Thus, chips should be protected from rainfall and groundwater intrusion to avoid the release of leachate. Release of leachate onto tidal lands can cause beach discoloration, and an underground deep outfall may be required.

Report No. 5. Aye, R.C., "Criteria and Requirements for Statewide Highway Runoff Monitoring Sites," July 1979.

Criteria for selecting statewide monitoring sites for highway runoff were established to provide representative combinations of climate, traffic, highway, land use, geographic and topographic characteristics. Using these criteria, a minimum of six sites were recommended for use in this research.

Report No. 6. Asplund, R., J.F. Ferguson, and B.W. Mar, "Characterization of Highway Runoff in Washington State," December 1980.

A total of 241 storm events were sampled at ten sites during the first full year of statewide monitoring of highway runoff. Analyses of these data indicate that more than half of the observed solids in this runoff is traced to sanding operations. The total solids loading at each site was correlated with traffic during the storm. The ratio of other pollutants to solids was linear when there was sufficient traffic-generated pollutants to saturate the available solids.

Report No. 7. Mar, B.W., J.F. Ferguson, and E.B. Welch, "Year 3 - Runoff Water Quality, August 1979 - August 1980," January 1981.

This report summarizes findings detailed in Report Nos. 4 and 6 plus the work of Zawlocki on trace organics in highway runoff. Several hundred compounds tentatively identified by GC-MS were grouped into nine categories, which were not mutually exclusive. Major components of these categories were petroleum products used by vehicles and incompletely combusted hydrocarbons. The concentrations of these trace organics groups were low compared to criteria proposed for protection of aquatic life.

Report No. 8. Eagen, P.D., "Views of Risk and Highway Transportation of Hazardous Materials - A Case Study in Gasoline," November 1981.

While gasoline represents one-third of all hazardous materials transported in the country by trucks, the risk associated with gas transportation, as viewed by the private sector, is small. Public perceptions of risk are much greater due to lack of knowledge on probabilities and consequences of spills. Methods to improve knowledge available to the public on gasoline spills and methods to improve estimates of environmental damages from gasoline spills is presented. Generalization of methodologies to hazardous materials in general are discussed.

Report No. 9. Zawlocki, K.R., J.F. Ferguson, and B.W. Mar, "A Survey of Trace Organics in Highway Runoff in Seattle, Washington," November 1981.

Trace organics were surveyed using gas chromatography coupled to mass spectrometry for highway runoff samples from two Seattle sites. The characterization of the organics exhibited concentrations of aliphatic, aromatic and complex oxygenated compounds. Vehicles, including exhaust emissions, were concluded to be the source of many of the organics.

Report No. 10. Wang, T.S., D.E. Spyridakis, R.R. Horner, and B.W. Mar, "Transport, Deposition and Control of Heavy Metals in Highway Runoff," January 1982.

Mass balances conducted on soils adjacent to highways indicated low mobility of metals deposited on well-vegetated surfaces. Grass drainage channels were shown to effectively capture and retain metals (e.g. a 60 m channel removed 80 percent of the original Pb concentration). Mud or paved channels, however, demonstrated little or no ability to remove metals from runoff. Metal release studies suggested that acid precipitation could release metals bound in the soil, especially where low buffering capacity exists.

Report No. 11. Portele, G.J., B.W. Mar, R.R. Horner, and E.B. Welch, "Effects of Seattle Area Highway Stormwater Runoff On Aquatic Biota," January 1982.

The impacts of stormwater runoff from Washington State freeways on aquatic ecosystems were investigated through a series of bioassays utilizing algae, zooplankton and fish. Algae and zooplankton were adversely affected by the soluble fraction of the runoff, while suspended solids caused high mortalities of rainbow trout fry. In addition, BOD₅ values similar to those reported in the stormwater literature were measured; however, there were indications that results were influenced by toxicity to microbial populations.

Report No. 12. Chui, T.W., B.W. Mar, and R.R. Horner, "Highway Runoff in Washington State: Model Validation and Statistical Analysis," November 1981.

Results of the second year of full-time operation of nine monitoring sites in the State of Washington produced 260 observations of highway storm runoff. A predictive model was developed based on the data from two years of observation for total suspended solid loads. A high correlation was demonstrated between total suspended solids and COD, metals and nutrients. The major factor controlling pollution loads from highways in Washington State is the number of vehicles passing during each storm, not those preceding storms.

Report No. 13. Mar, B.W., J.F. Ferguson, D.E. Spyridakis, E.B. Welch, and R.R. Horner, "Year 4 - Runoff Water Quality, August 1980 - August 1981."

This report summarizes findings presented in Report Nos. 10 - 12. Included are the results of studies aimed at improving and extending Asplund's solids loading model, increasing data on the ratios of various pollutants to TSS in the runoff, investigating the fate of heavy metals in drainage systems, and conducting bioassays on sensitive organisms exposed to highway runoff.

Report No. 14. Horner, R.R. and B.W. Mar, "Guide for Water Quality Impact Assessment of Highway Operations and Maintenance." (Draft issued Fall, 1981).

Procedures particularly applicable to Washington State have been developed to assist the highway designer in evaluating and minimizing the impacts of highway runoff on receiving waters. The guide provides computation procedures to estimate pollutant concentrations and annual loadings for three levels of analysis which depend on the watershed, the discharge system and traffic. It further provides means to judge the potential impacts of the runoff on receiving waters.

Report No. 15. Horner, R.R. and E.B. Welch, "Impacts of Channel Reconstruction in the Pilchuck River." (To be issued Winter, 1982.)

Report No. 16. Report on dissertation project during Year 5. (To be issued Summer, 1982.)

Report No. 17. Final report. (To be issued Summer, 1982.)

Please send me copies of Report No. 1, 2, 3, 4, 5, 6, 7, 8, 9, 10, 11, 12,
13, 14

Name _____

Address _____

Phone () _____

Return to: B.W. Mar
 Department of Civil Engineering
 University of Washington
 307 More Hall, FX-10
 Seattle, WA 98195

There is a charge of \$2.00 per report to cover copying and postage. Please enclose a check to the University of Washington.

The work described in this paper was not funded by the U.S. Environmental Protection Agency. The contents do not necessarily reflect the views of the Agency and no official endorsement should be inferred.

CHIMNEY HILL OFF-SITE DRAINAGE STUDY
Jerome M. Normann, P.E.¹ and
Edward R. Estes III, EIT²
March 26, 1982

Introduction

The City of Virginia Beach, Virginia, is one of the most rapidly developing cities in the United States. It is located on the Atlantic Coast in the Tidewater area of Virginia (Figure 1). The topography of the Tidewater area is very flat and lowlying, with a high groundwater level.

The shoreline areas of Virginia Beach and the Chesapeake Bay, are already extensively developed, and residential growth is now occurring in the large interior land areas of the city. These inland areas are drained by a system of long drainage canals with large cross sections, which discharge into tidal estuaries. Systems of feeder canals, in turn, drain the subdivisions and convey the water to the main drainage canals.

Many of these feeder canals are very wide, retain water continuously, and have aesthetic appeal as well as serving a storm drainage function.

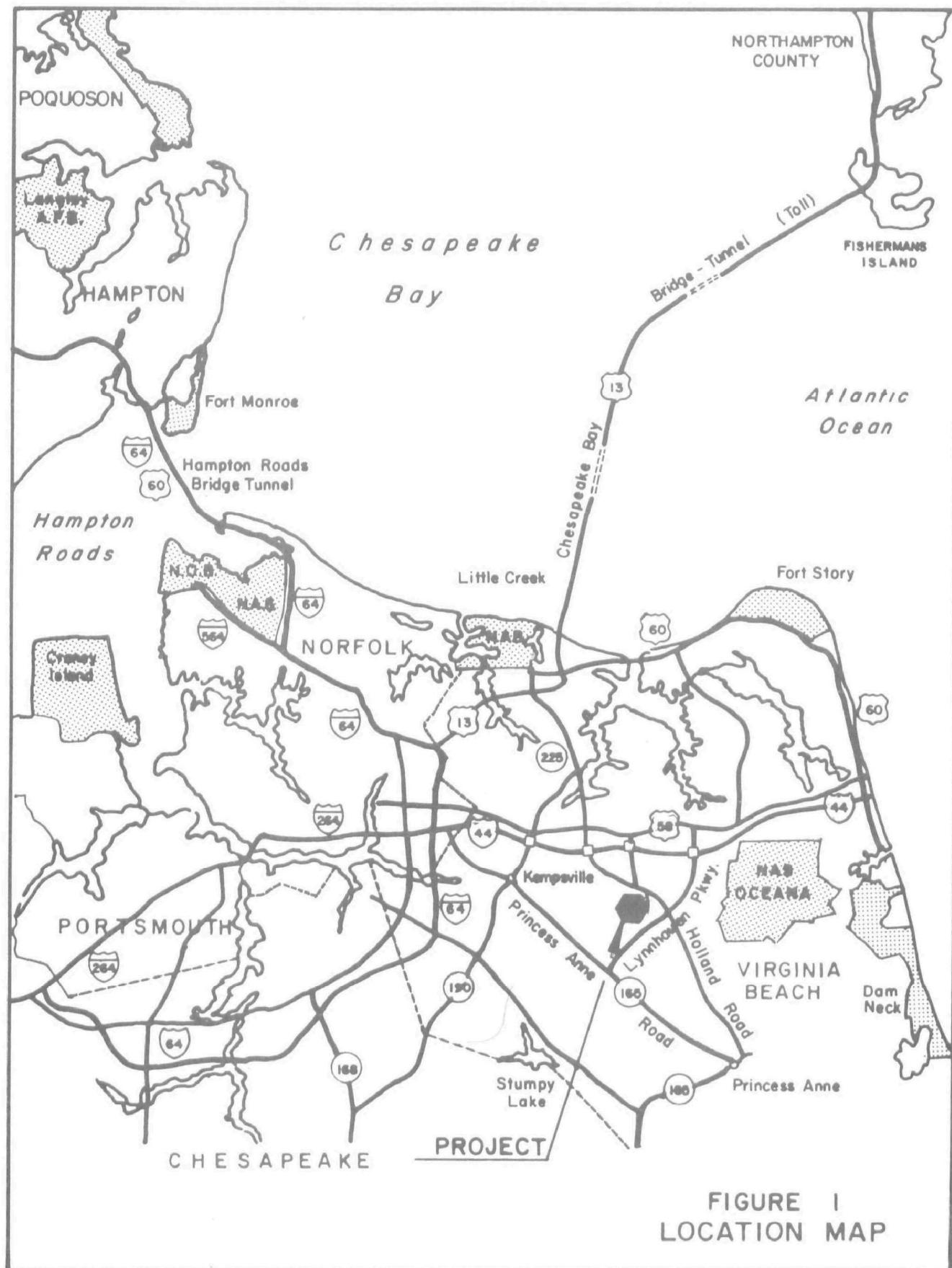
Chimney Hill is one of the city's many subdivisions. Chimney Hill and the adjacent developments comprise about 800 acres, which are drained by seven feeder canals in series, with a total length of about 13,000 feet, interconnected by culverts under roadways and draining into Canal No. 2, one of the city's main drainage canals (Figure 2).

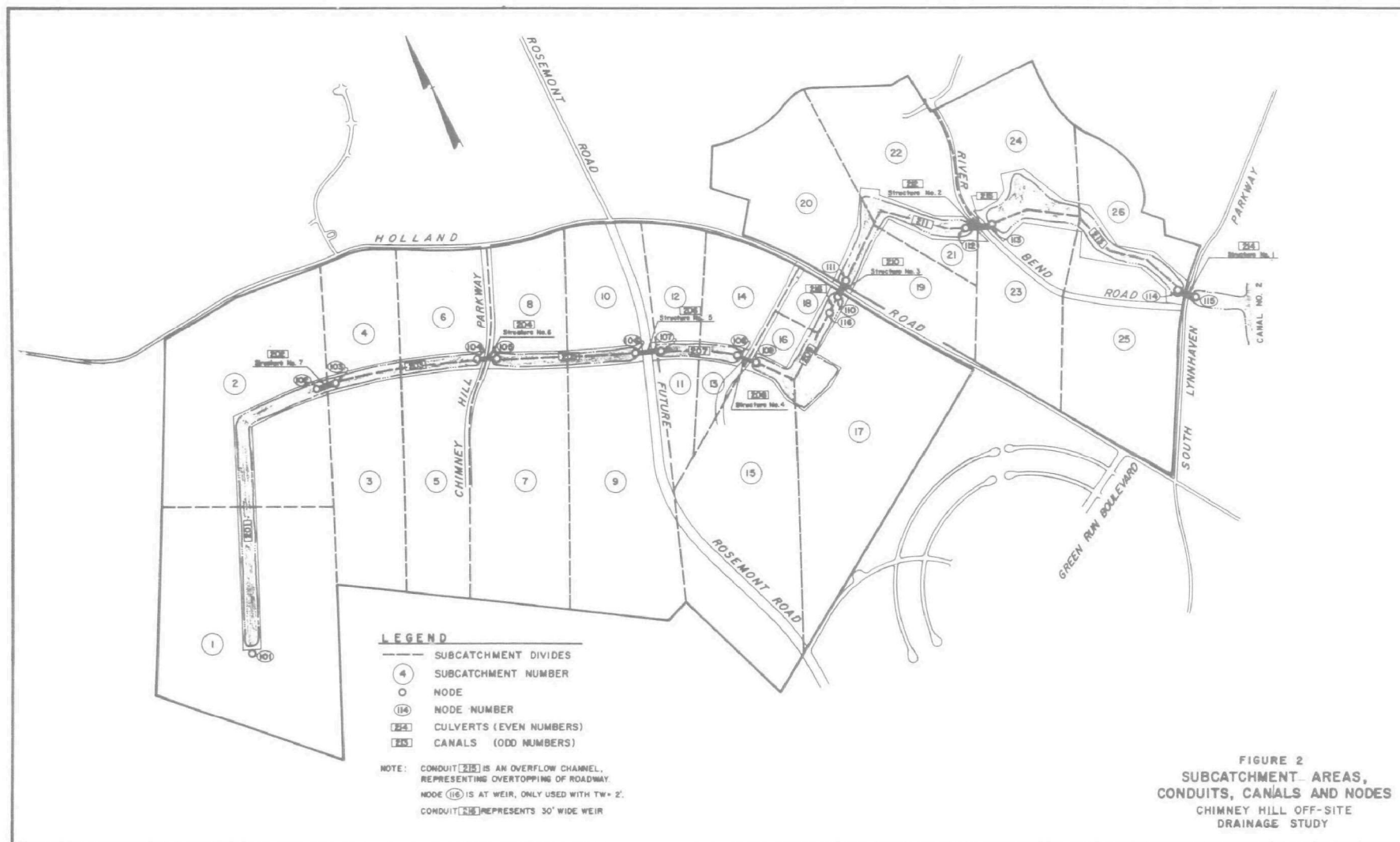
Several routing calculations were performed previously by hand to determine flow conditions in the feeder canals during the design storm. However, due to the flat longitudinal slopes of the canals, it was suspected that flow might move upstream in some canals during the early part of the runoff event, invalidating the results of the simple routing calculations which proceeded from the upstream to the downstream end of the canal system.

In order to evaluate flow conditions in the system of large feeder canals, it was decided to attempt to apply the SWMM Version II model to the problem on an experimental basis. The Extended Transport module of the program was

1/.Director of Water Resources, MMM Design Group, Norfolk, Virginia

2/.Civil Hydraulic Engineer, MMM Design Group, Norfolk, Virginia.





selected due to the flat slopes and high tidal tailwater conditions in the canals.

This paper describes the application of the SWMM model to the rather complex drainage system, and the results of that study.

The Watershed

The watershed drained by the system of canals is shown in Figure 2. The development consists of commercial areas, multi-family housing, and single-family housing. Since the purpose of the study was to test the capabilities of the EXTRAN module of the SWMM model, no attempt was made to perform a detailed analysis of the watershed runoff.

The 800 acre drainage basin was subdivided into 26 subcatchment areas as shown in Figure 2. Subcatchment areas and the composition of the development in each subcatchment area are shown in Table 1.

TABLE 1

Subcatchment Areas and Types of Development

Sub-catchment Nos.	Total Area, Acres	Canal Acres	Commercial Acres	Multi Family Acres	Single Family Acres
1,2	149.0	13.9	21.0	108.6	5.5
3,4,5,6	125.1	6.3	9.6	41.2	92.9
7,8,9,10	129.1	5.6	30.6	0.0	68.0
11,12,13,14	67.1	4.4	42.7	0.0	20.0
15,16,17,18	116.9	7.4	0.0	20.2	89.3
19,20,21,22	72.6	7.0	15.6	0.0	50.0
23,24,25,26	133.9	9.0	42.2	15.7	67.0

The following parameters were chosen for the subcatchment areas .

Percent Imperviousness: A weighted percentage of imperviousness was calculated for each subcatchment based on the percentages of subcatchment area associated with each type of development. The following values were assumed;

based on observed development characteristics in the subcatchments:

<u>Type of Development</u>	<u>Percent Impervious</u>
Single-Family	50
Multi-Family	70
Commercial	85
Water Surfaces	100

Slope: A generalized slope of 0.003 ft./ft. was used for all subcatchments. These values could be adjusted based on more detailed topographic information.

Resistance Factors: A Manning n value of 0.013 was selected for impervious areas, and a value of 0.100 was chosen for grassy, pervious areas.

Surface Storage: The SWMM program default values, 0.062 inch of storage for impervious areas and 0.184 inch of storage for pervious areas, were used.

Infiltration Rates: Based on soil conditions in Virginia Beach (6) and discussions with the local office of the Soil Conservation Services (5) the following infiltration rates were assumed for the Horton Equation used by the SWMM model:

Maximum infiltration rate : 2.0 in/hr.
Minimum infiltration rate : 0.4 in/hr.
Decay rate (default value): 0.00115 1/sec.

Rainfall

The synthetic rainfall hyetograph was developed based on the 50 year recurrence interval rainfall values given in Technical Paper No 40 (1). While more up-to-date rainfall information is available from the National Weather Service (2) and state sources, it was decided to use the values from Technical Paper No. 40 to provide for comparisons with the previous runoff studies which had also utilized that publication.

A small computer program entitled "Rain", obtained from the U S Army Corps of Engineers, was used to derive the synthetic rainfall hyetograph, which is tabulated in Table 2 and shown in Figure 3. The resultant hyetograph is somewhat conservative, because it is synthesized to contain all storms shorter than 24 hours in duration with a 50 year recurrence interval. For example, the peak 30 minute period

has a total rainfall of 2.89 inches or an average intensity of 5.78 inches per hour over the 30 minute period. Given total rainfall in inches for various durations, the "Rain" program develops a 24 hour rainfall distribution for the requested time increment. The peak rainfall intensity is located at the center of the hyetograph, and decreasing intensities alternate to either side of the peak.

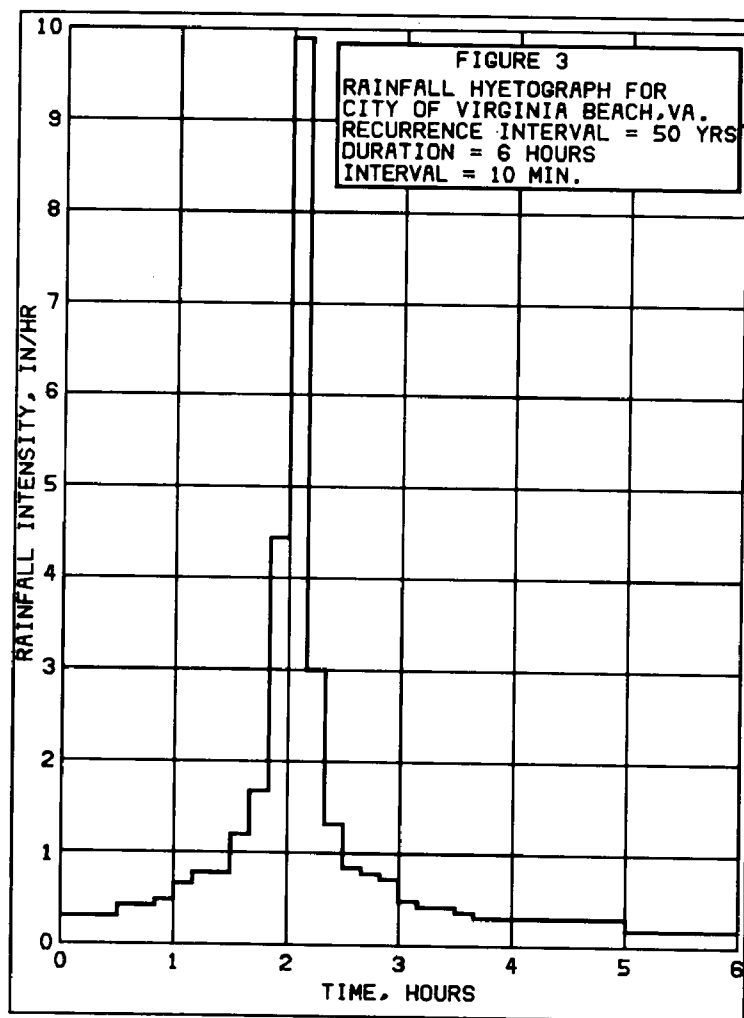


Table 2
Rainfall Distribution for Virginia Beach, Virginia
based on Technical paper 40 (1)

Time		Rainfall	
Hour	Minute	Inches	Inches/Hour
0	10	0.05	0.30
	20	.05	0.30
	30	.05	0.30
	40	.07	0.42
	50	.07	0.42
1	00	0.08	0.48
	10	.11	0.66
	20	.13	0.78
	30	.13	0.78
	40	.20	1.20
	50	.28	1.68
2	00	0.74	4.44
	10	1.65	9.90
	20	.50	3.00
	30	.22	1.32
	40	.14	.84
	50	.13	.78
3	00	.12	0.72
	10	.08	.48
	20	.07	.42
	30	.07	.42
	40	.06	.36
	50	.05	.30
4	00	0.05	0.30
	10	.05	.30
	20	.05	.30
	30	.05	.30
	40	.05	.30
	50	.05	.30
5	00	0.05	0.30
	10	.03	.18
	20	.03	.18
	30	.03	.18
	40	.03	.18
	50	.03	.18
	60	.03	.18

A six hour segment was selected from the 24 hour hyetograph for this simulation, with about two hours of antecedent precipitation prior to the peak rainfall. A ten minute time increment was used since the response time for the watershed was estimated to be much longer than ten minutes; on the order of one to two hours.

Any other recurrence interval rainfall, such as the 100 year rainfall, could easily be inserted in the model and the resultant runoff calculated.

Evaporation Rate

Due to the short time duration of 6 hours used in the program run, losses due to evaporation are negligible in the analysis. The program default value of 0.1 inch/day was used.

Tidal Conditions

Canal Number 2, into which the canal system under consideration discharges, has complex tidal characteristics. The canal connects to two separate tidal estuaries; Lynnhaven Inlet on the north and West Neck Creek, leading to Currituck Sound, on the south. The canal has been studied extensively by the Corps of Engineers for the Canal No. 2 Project, and it would be possible to define a tidal cycle at the exit of the Chimney Hill Canal system. This may be done in future studies; however, for this preliminary analysis, two constant tailwater elevations were chosen. One elevation, +2.0 ft. MSL, represents the mean spring high tide. The other elevation, +4.75 ft. MSL, represents a tide about halfway between mean high tide and the 100 year tide (+7.8 ft. MSL). (7)

The EXTRAN tidal tailwater elevation option in Version II of the SWMM model did not operate properly due to a coding error. It is hoped that this option in Version III will operate properly, and that this program capability can be used in future simulations.

Selection of Simulation Model

The SWMM model with the Extended Transport module was chosen for evaluation because of its capability to analyze both surcharged flow conditions and tailwater effects. Most other stormwater routing programs, such as the Corps of Engineers HEC-1 program, begin at the most upstream channel or pipe and progress downstream, neglecting back pressure effects due to tailwater.

These programs are inadequate in lowlying tidal areas where backflow can occur and there are nearly always tail-water effects present.

While the SWMM model is normally applied to prismatic drainage conduits rather than to the irregular canals involved in this study, it was decided to attempt to utilize the model because of its potential benefits in improved analysis of the complex hydraulics involved.

Application of the SWMM Model

In this rather unusual application of the SWMM Version II model, several different approaches were formulated and attempted.

One of the first approaches considered involved the representation of the system as a series of very large storage nodes (the canals) linked by conduits (the culverts). This concept was quickly abandoned because adequate representations of the geometry of the canals (storage versus volume relationships) were not possible using vertical walled nodes. Problems with system connections were also encountered in attempting to apply the storage nodes in the above manner.

A more conventional approach was then attempted, representing the canal system as a series of links and nodes, with hypothetical nodes at either end of each canal and culvert. The volumes of the nodes were negligible when compared with the large volumes of the canals in this system.

Both canals and culverts were represented as links in the computer model. Multiple barrels and non-circular culverts were represented as equivalent rectangular conduits on the basis of cross sectional areas and roughness, maintaining the actual heights of the structures due to flow depth considerations. The dimensions of the culverts are given in Table 3.

Canals were first represented as trapezoidal channels with 2 (horizontal) to 1 (vertical) side slopes, based on the original canal designs. This was later found to be in error, and the bottom widths and side slopes were adjusted to match surveyed stage versus volume information as closely as possible. The canal lengths used were actual centerline lengths. By dividing the canal volume by the canal length, cross sectional areas were determined at two water depths of interest. Then, simultaneous equations were formulated and solved for the base width and side slopes as follows:

$$A = Bd + Zd^2$$

Where A is the cross sectional area of the flow prism
d is the corresponding depth of flow
B is the computed bottom width
and Z is the cotangent of the side slope.

Table 3
Descriptions of Culverts

Structure No.	Link No.	No. Barrels & Shape	Material	Size B D	Length	Elev. Inlet Invert	Elev. Outlet Invert	Slope
1	214	3-Rect	Conc	9'x4'	100'	1.30'	1.10'	0.0020
2	212	4-Circ	Conc	6'	132'	-3.50'	-3.50'	0.0000
3 *	210	2-Rect	Conc	9'x6'	116'	-0.92'	-1.10'	0.0016
4	208	3-Circ	Conc	6'	120'	-0.79'	-0.79'	0.0000
	206	3-Circ	Conc	6'	194'	-0.79'	-0.79'	0.0000
6	204	2-Pipe Arch	Corr Metal	10'-1" x7'-1"	110'	-0.79'	-0.79'	0.0000
7	202	3-Circ	Conc	6'	120'	-0.79'	-0.79'	0.0000

* Structure No. 3 has a 30 ft. wide rectangular weir upstream of the structure with a crest elevation of 4.21 feet MSL.. This weir maintains canal levels upstream of Structure No. 3.

Therefore, the canals are represented in the model as prismatic, trapezoidal channels which produce the proper stage versus volume relationships, but which may not physically resemble the actual canals. Table 4 shows the dimensions of the hypothetical canals used in this model.

Table 4
Descriptions of Canals used in Model

Link No.	Length, ft.	Bottom Width, ft.*	Side Slopes
201	3130	91.0	5.0 :1
203	1460	123.0	7.2 :1
205	1400	110.0	8.4 :1
207	800	166.0	9.4 :1
209	1350	200.0	10.5 :1
211	1630	202.0	12.6 :1
213	2170	250.0	3.5 :1

* At a bed elevation of +4.75 ft MSL, (the upper tailwater elevation).

The subcatchments, shown in Figure 2, were divided so that for each canal, one half of its contributing drainage area is directed at each end on the canal. This approximates the true flow condition which is a combination of

of spatially varied flow and point discharges into the canals. No attempt was made to model the details of the drainage subsystems (pipes, small channels, gutters, etc.) in each subcatchment area.

As was expected, no particular problems were encountered in utilizing the runoff module to simulate the surface runoff from the drainage subcatchments, although some fine tuning was performed. Use of the EXTRAN module to model the flows in the canals and culverts was much more difficult. To avoid instability in the relatively short culverts, 10 second time steps were selected for use in the EXTRAN model.

Since the slopes of the canals and culverts were very flat in some reaches, small incremental "Z" values were input; ie., node bottom elevations were staggered slightly to avoid longitudinal conduit slopes of zero.

One of the first major problems encountered was that the Version II EXTRAN module had no method of establishing starting water surface elevations in the canals. Thus, starting with actual invert elevations (Table 3) adjusted to avoid zero slopes, most of the runoff was expended in filling the canals to their proper starting water surface elevations.

This problem led to several attempts at solutions, using trial and error procedures.

First, it was attempted to input a high initial rainfall in the Runoff module to fill the canals and thus reach a stable starting condition prior to inputting the design storm. This ploy worked partially, but the watersheds became so saturated that very low losses occurred when the design hyetograph was finally applied. Thus, almost all of the rainfall ran off of the subcatchments, and very high peak runoff rates were observed.

Then, it was attempted to compensate by raising the invert elevations of the conduits (links), while leaving the nodal inverts at their actual levels. This did not satisfy the initial storage in the canals, and the rainfall was still expended in filling the canals.

It was noticed that the program apparently regards the nodal invert elevations as the starting water surface elevations.

Therefore, on the next trial, it was decided to raise the nodal invert elevations to the desired starting water surface elevations, and to use zero Z values. This seemed to

controlled by a weir where two different starting water surface elevations were necessary. Note that there is a weir upstream of node 110 which maintains water surface elevations at +4.21 upstream, while downstream levels could be at a lower level, such as +2.0 ft. MSL. If the upstream and downstream nodes, with large differences in invert elevations, were connected by a steeply sloping conduit, huge flow rates through the steep conduits would occur early in the run, even before actual runoff had started.

However, for the higher starting tailwater elevations, when the weir at node 110 was submerged, the ploy of raising nodal invert elevations seemed to work quite well. It was necessary to adjust the canal cross sections so as to neglect the portions of the cross sections submerged at the beginning of the run, but this was of little consequence since friction losses in the large canal sections were almost negligible in either case.

Culvert friction losses were also minor in most cases, at least at low flows. Thus, raising culvert inverts tended to increase friction losses slightly, but not to a degree which was of significance. Also, at the peak of the runoff event, water levels are such that the culverts are submerged in either their true physical profile or with their inverts artificially raised to control starting water surface elevations.

In these early successful program runs, reverse or upstream flow was indeed observed in some of the canals. The negative flows appeared to be true flows and not merely products of instability in the model.

However, at this point in the study, it was discovered that our initial canal geometry which had assumed 2 H to 1 V side slopes was incorrect, and the canal geometry was adjusted to match the measured stage versus volume characteristics. This correction in geometry eliminated negative flows of consequence, somewhat to our disappointment.

The model run with a +4.75 ft. MSL starting water surface was performing very well by this time; canal sections had been corrected, and stage and flow output seemed correct. Hand calculations were performed to spot check culvert and canal flow results, which seemed correct. Some flooding of Riverbend Road at conduit 212 was observed, so it was attempted to insert wide weirs at nodes 112 and 114 to simulate flooding across Riverbend Road and, just in case, across Lynnhaven Parkway. It was attempted to simulate the roadways using in-line broad crested weirs. This had been successfully accomplished in an earlier study (3), but, in that case, the flow was discharged from the system

and the weirs were only used as devices to track the total overflow. In this study, it was attempted to reinsert the overflow from node 112 at node 113 downstream, and this did not work, probably due to incorrect connectivity in the model. Therefore, a 275 ft. wide, low rectangular conduit with inverts matching the road elevations was inserted between nodes 112 and 113 to simulate flow across Riverbend Road. The broad crested weir was left at node 114, since the flow leaves the system at that location in any case. As it turned out, there was no flooding at node 114 for the 50 year design discharge.

For the lower system tailwater (El. +2.0 MSL), high flows occurred between nodes 110 (invert elevations 4.21) and node 111 (invert elevation 2.0) at the beginning of the run. In order to preserve the characteristics of culvert 210 under Holland Road, an additional node (No 116) was added upstream of node 110, and a conduit with the same width as the weir (30 ft.) was added to simulate the upstream operation. (A weir at conduit 110 had been tried previously, but had been unsuccessful. Apparently, in-line weirs are not acceptable in the EXTRAN module. This information would be helpful if presented in the User's manual for the program.)

The 30 ft. wide rectangular conduit was set at a rather flat slope (.003 ft. per ft.) by raising the downstream end in node 110 in order to prevent high initial flows. However, the conduit first chosen was only 70 feet long, and use of this hydraulically short pipe resulted in extreme flow instability downstream of culvert 208. Therefore, the 30 ft. wide conduit was lengthened to 150 ft. and the slope was flattened to 0.001 ft. per ft., which eliminated a great deal of the model instability and provided good estimates of flow and water surface elevations in the system. A shorter time increment may be necessary to completely eliminate instability for low tailwater runs.

Results of the Model Applications.

Some representative calculations have been chosen to illustrate the results of the model runs. Figure 4 depicts a typical runoff hydrograph from the subcatchments into Canal No. 201, the most upstream canal in the system. This hydrograph was developed by summing the inflow hydrographs from nodes 101 and 102. The outflow hydrograph through culvert 202 is also shown in Figure 4, illustrating the routing effect of the wide, long canals. Note that the peak flow reduction is due to live storage above elevation +4.75 ft. MSL only.

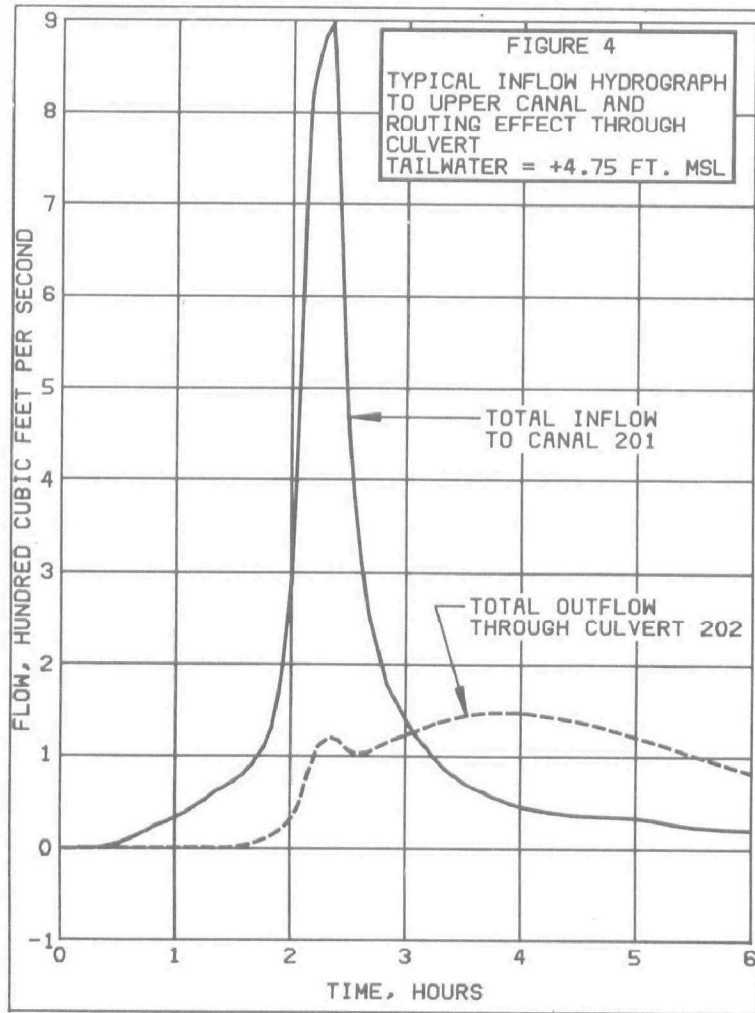


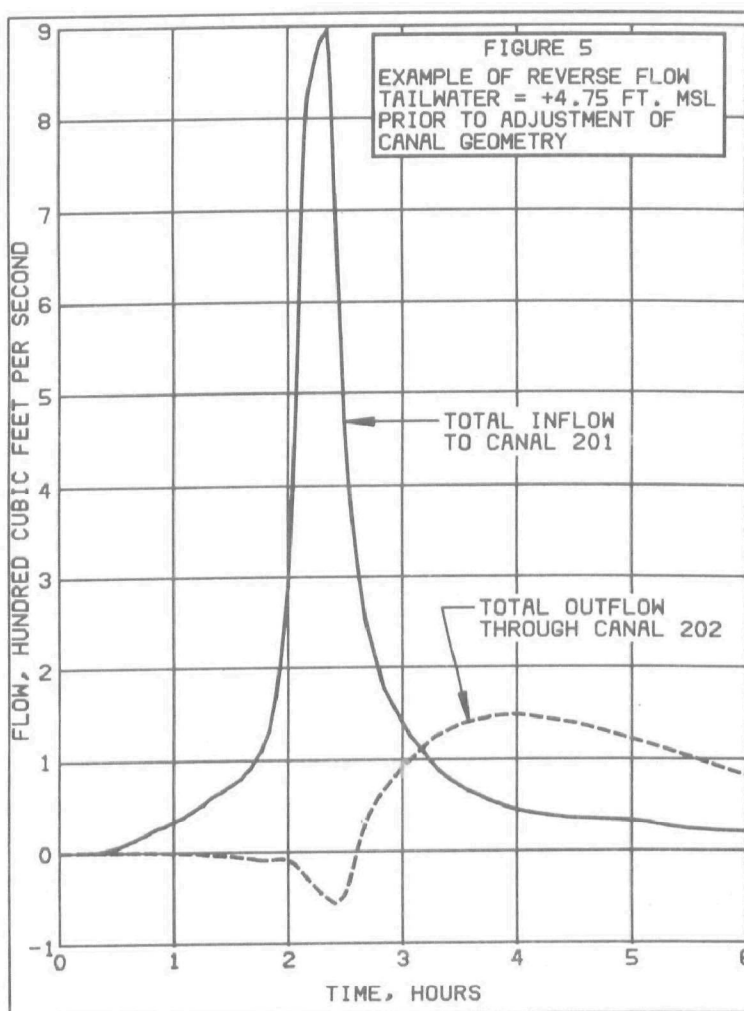
Table 5 shows the peak inflow rates into each canal, also derived by adding the inflows at each end of the canals.

Table 5 Peak Inflows to Canals

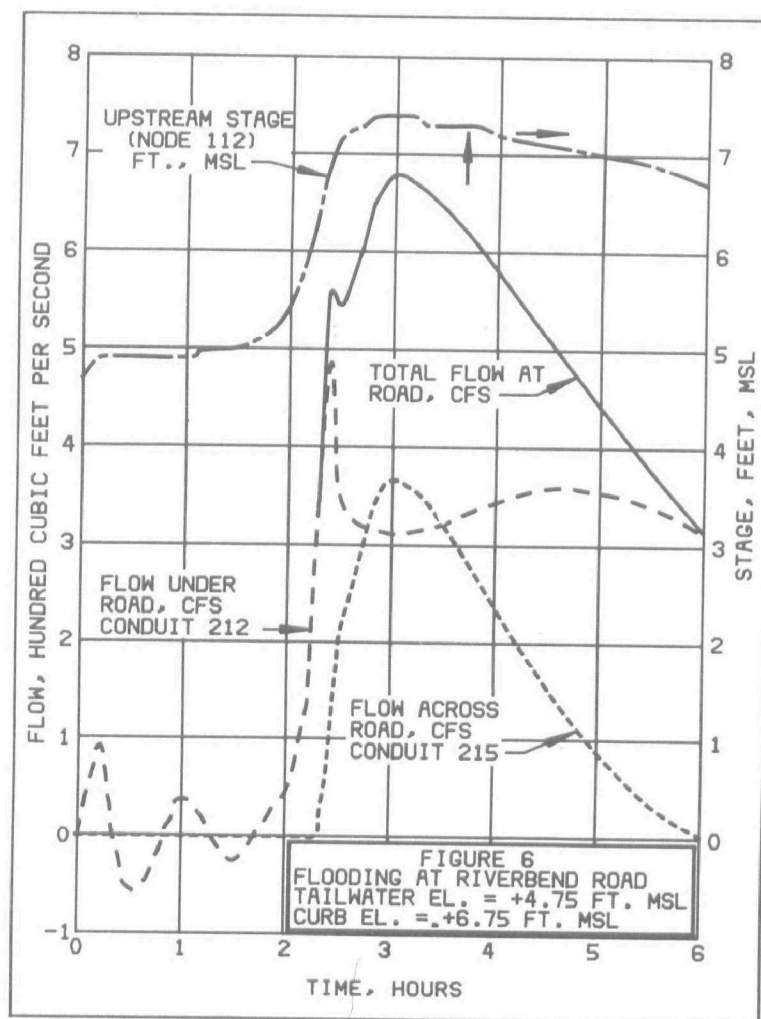
Canal No.	Downstream Structure	Upstream Node	Downstream Node	Peak Inflow, cfs
201	202	101	102	897.
203	204	103	104	624.
205	206	105	106	600.
207	208	107	108	278.
209	210	109	110	578.
211	212	111	112	398.
213	214	113	114	738.

These peak inflow rates were similar to, but higher than the inflow rates derived by using the methods of SCS TR-55 (4) which were utilized in the previous hand calculations.

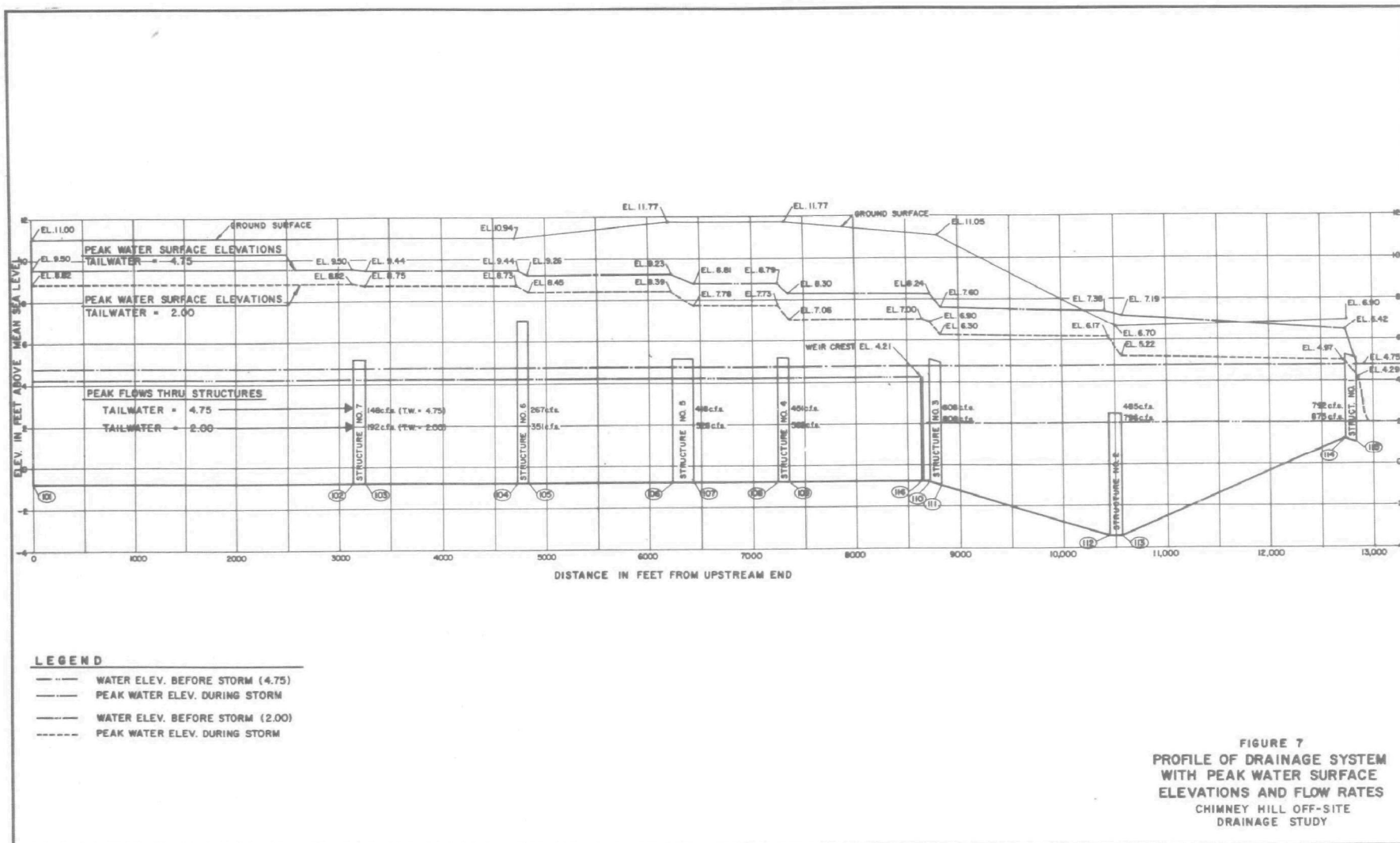
Figure 5 is presented to illustrate the negative flows obtained in early runs of the model prior to correction of the canal geometry. The inflow hydrograph and location are the same as in Figure 4; however, note that at about hour 2.4, a negative flow of about -60 cubic feet per second occurred, even though the inflow hydrograph was rising rapidly. This was a function of canal storage in the upstream and downstream canals, resulting in differential water surface elevations producing upstream flow.



Use of the wide rectangular conduit between nodes 112 and 113 to simulate flow across Riverbend Road is illustrated in Figure 6. Flow under the road is depicted by flow in conduit 212, flow over the road is carried by conduit 215 which is the rectangular conduit 275 feet wide and 1 foot high, and the total flow is represented by the solid curve. The water surface stage upstream of the road is also shown at the top of the figure.



Results of the study are summarized in Figure 7, which shows profiles of peak water surface elevations in all of the canals, as well as peak flow rates, for the two tailwater elevations of interest. Note the friction losses in the culverts, and the fact that water surface profiles in the canals are nearly horizontal, indicating very low friction losses.



For the lower tailwater elevations (+2.0 ft. MSL), supercritical flow exists in conduit 214, indicating that the culvert is in so-called "inlet control." This accounts for the steep water surface profile at that location.

Conclusions

The SWMM Version II model with EXTRAN option has been successfully applied to the simulation of a series of large storage canals, linked by culverts, and discharging into a tidal estuary.

The results from the SWMM Version II model seem reasonable; however, due to shortcomings in the model, it would be beneficial to apply the Version III model to the data. For example, the tidal tailwater option in Version II EXTRAN did not operate properly, and it was not possible to input starting water surface elevations.

A capability which would be very useful in the EXTRAN model would be the ability to simulate in-line weirs, as well as diversion weirs. In this study, weirs were simulated using short conduits, but instability in the model was a problem.

Overall, SWMM Version II worked quite well in simulating the canal system, and the results confirmed the results of the hand calculations performed earlier.

Acknowledgements

The authors wish to express their thanks to the City of Virginia Beach Department of Public Works especially to Mr. Donald R. Trueblood, P.E., City Engineer, and Mr. Keith Slicer, P.E., for their assistance and support during this study.

Appendix References

1. "Rainfall Frequency Atlas of the United States," Technical Paper No. 40, U. S. Department of Commerce, Weather Bureau, Washington D.C., May 1961.
2. "Five-to 60-Minute Precipitation Frequency for the Eastern and Central United States," NOAA Technical Memorandum NWS HYDRO-35, National Oceanic and Atmospheric Administration, Silver Spring, Maryland, June 1977.
3. "Modeling of Storm Drainage in a Coastal City," Normann, Jerome M., Proceeding of the National Symposium on Urban Stormwater Management in Coastal Areas, Hydraulics Division, ASCE, Blacksburg, Virginia, June 20, 1980.

4."Urban Hydrology for Small Watersheds," Technical Release No. 55, Engineering division, Soil Conservation Service, U.S. Dept of Agriculture, Washington, D. C., January 1975.

5. Personal communications with Louis Cullipher, District Conservationist, U. S. Department of Agriculture, Soil Conservation Service, Virginia Beach, Virginia, May 1980.

6."Soil Survey, Norfolk County Virginia," Series 1953, No. 5, U. S. Department of Agriculture, Soil Conservation Service, May 1959.

7. Tidal studies conducted by Norfolk District, Corps of Engineers, in June 1969, file H-31-10-47, and May 1974, Files H-31-10-80(8), J-31-10-80(9), Referenced in Storm Drainage Seminar presented at Old Dominion University, Norfolk, Virginia, October 8, 1975.

The work described in this paper was not funded by the U.S. Environmental Protection Agency. The contents do not necessarily reflect the views of the Agency and no official endorsement should be inferred.

DESK TOP METHODOLOGY FOR
NONPOINT SOURCE LOAD EVALUATION

by

Arun K. Deb, Ph.D., P.E.
Project Director
Environmental Systems Department
Roy F. Weston, Inc.

INTRODUCTION

Nonpoint source pollutants are materials which degrade surface water and groundwater quality and which originate in a diffuse manner from the land surface. Much attention has been given by water quality managers and planners to the problems associated with this form of pollutant loading. Impacts of nonpoint source loading on surface water quality have been studied for limited large urban areas under Section 208 of Public Law 92-500. In such areas, nonpoint pollutant load controls have been analyzed by computer models in developing most cost-effective areawide water quality management. With the completion of a fairly large number of 208 studies, a large amount of nonpoint source data have been developed in characterizing pollutant development in various land use areas. Importance of evaluation of nonpoint source loading from urban and agricultural areas other than 208 study areas and its impact in water quality has been recognized.

The use of computerized calibrated models in nonpoint source loading analysis is expensive and may not be cost-effective in many small water quality management studies. An alternative to computerized approaches for the analysis of the nonpoint pollutant loadings is desktop analysis techniques. A desktop model for nonpoint source pollution assessment is any hand-calculation technique or procedure that can be used to determine the stormwater runoff pollutant loading from a study area. This type of approach involves an estimation of pollution loadings sufficiently comprehensive to provide an environmentally and economically satisfactory basis for realistic decisions concerning nonpoint source pollution impacts.

OBJECTIVES

This paper outlines a simplistic methodology for nonpoint source loading evaluation for areas where rate coefficients and loadings can be estimated. The methodology has limited application and can be used for:

- o First level of analysis;
- o Areas with similar characteristics where rate coefficients and loadings have been developed;
- o Determining the need for a detailed computer modeling.

METHODOLOGY

The methodology used in this paper was developed for island wide urban nonpoint source pollution analysis for Puerto Rico. A detailed calibrated computer modeling method was used to develop nonpoint source loadings for five typical urban areas of Puerto Rico. Using the rate coefficients and pollutant loading rates for various land use groups obtained by field sampling and computer modeling, a desktop methodology was developed for the evaluation of urban nonpoint source loadings for other similar cities on the island.

The simplified methodology developed in this paper contains the following basic elements:

1. Rainfall data analysis and development of a design storm event.
2. Characterization of the drainage basin.
3. Run-off quality and flow characterization.

Essentially, the methodology relates phenomena in the drainage area to their associated effect on stormwater loads. The rate coefficients which depend on the cause and effect relationships of storm events and land use characteristics are determined previously for a similar urban area.

The step-by-step methodology developed in this paper for evaluation of nonpoint source loads incorporates the following steps:

1. Historical rainfall data analysis and selection of a design storm.
2. Determination of the land use pattern of the study area.

3. Determination of the percent of imperviousness of the various land use types.
4. Estimation of the composite run-off coefficient for the study area.
5. Estimation of the stormwater run-off rates.
6. Calculation of pollutant accumulation on each land use at the start of the storm.
7. Estimation of the stormwater run-off loads.

Step 1: Selection of a Design Storm Event

The important parameters for design storm characterization are the duration of a storm event, the dry period between storm events, the maximum hourly intensity, and the total rainfall. The maximum hourly rainfall and the total rainfall parameters are defined by statistical recurrence intervals.

Historical rainfall data can be used to develop design storms for each urban study area. These storms can then be used for the development of nonpoint source pollution loads. The specific technique used consists of the following steps:

- o Select the maximum hourly intensity for the desired design storm in a particular urban study area.
- o Select the average duration for design storms in the urban study area.
- o If the average duration is three or four hours, assume that the maximum hourly intensity occurs during the second hour. If the average duration is two hours, assume that the maximum hourly intensity occurs during the second hour.
- o Select the total design storm volume for the particular design storm in the urban study area.
- o For an urban area, where storms have an average duration of three or four hours, determine the difference between the total rainfall for the design storm and the maximum hourly rainfall, and divide this difference equally between the remaining hours of the design storm. For an urban area where storms have an average duration of two hours, determine the difference between the total rainfall for the design storm and the

maximum hourly rainfall, and assume that this difference occurs during the first hour of the storm.

The rainfall amounts for the different hours of the design storm, along with the dry period before the storm would occur, defines the design storm event. The design storm used in illustrating the methodology is given in Table 1.

TABLE 1

Sample Study Area - Design Storm Characteristics

Total Rainfall	- 0.9 inches
Storm Duration	- 3 hours
Antecedent Dry Period	- 10 days
Rainfall by Hour	
o First	- 0.25 Inch
o Second	- 0.40 Inch
o Third	- 0.25 Inch

Step 2: Estimation of the Land Use Pattern of the Study Area

The key element in making reliable storm load estimates with the desktop methodology is the determination of study area characteristics which are used in relationships that define pollutant concentrations for particular amounts of rainfall which will leave the area as runoff.

Initially, the overall study area, i.e., that area for which nonpoint source loadings are desired, must be defined. The urban study area will typically be defined on the basis of political boundaries. However, in order to evaluate all factors that affect nonpoint source runoff and resulting water quality impacts, it may be necessary to look beyond the political boundaries of the study area.

The type and quantity of nonpoint source loads depend on land use. In order to estimate these loads, it is first necessary to determine the distribution of the land use types in the urban study area, and the areal extent of each land use type. The procedure to use in determining the areal extent of land use types is one of obtaining, from the best possible source, up-to-date land use maps. If no maps are found to be available,

site investigations should be used to define the general land use characteristics of the study area.

The sample study area for this example is assumed to have the land use characteristics listed in Table 2.

TABLE 2

Sample Study Area - Land Use Characteristics

<u>Land Use Type</u>	<u>Area In Acres</u>	<u>Percent of Total Area (LUP)</u>
Single Family Residential	150	7
Multiple Family Residential	1000	50
Commercial	100	5
Industrial	50	3
Open and Park	700	35
	<hr/>	<hr/>
TOTAL	2000	100

Step 3: Estimation of the Percent Imperviousness of the Various Land Use Types

Imperviousness portions of the urban land use type contributes maximum to the nonpoint source pollution loads. Therefore, it is essential that the percent of impervious cover for each land use type should be estimated for the study area. Table 3 lists average percent imperviousness values used for the example.

TABLE 3

Sample Study Area - Percent of Imperviousness
Values for Particular Land Use Types

<u>Land Use Type</u>	<u>Percent of Imperviousness Cover (PIC)</u>
Single Family Residential	52
Multiple Family Residential	63
Commercial	70
Industrial	90
Open or Park	15

Step 4: Determination of the Composite Runoff Coefficient for the Study Area

The volumetric runoff coefficient measures the fraction of the storm volume that reaches the receiving water body as runoff. It is assumed that the average runoff coefficient for impervious sections of an urban drainage area is 0.92, and the value for pervious sections is 0.18. The major portion of urban nonpoint source runoff which impacts a receiving water body originates from the impervious sections of the drainage basin. This is due to the fact that runoff from pervious sections of a predominantly urban drainage basin is attenuated, and possibly even permanently lost to infiltration.

The composite Runoff Coefficient (CRC) for the entire urban study is determined by the following relationship:

$$\text{CRC} = [(\text{IRC} \times \text{PIC}/100) + (1 - \text{PIC}/100) \text{ PRC}] \text{ LUP}$$

where:

CRC = Composite runoff coefficient for impervious areas in each land use type.

LUP = The percentage of the total drainage area in each land use.

IRC = Impervious runoff coefficient.

PRC = Pervious runoff coefficient.

Table 4 illustrates the calculations for determining the CRC for the sample study area.

Step 5: Determination of the Stormwater Runoff Rate

The rate at which rainfall is assumed to run off the drainage basin is defined by the amount of rainfall for the storm event, its intensity, and the Composite Runoff Coefficient (CRC). An additional factor that must be considered when analyzing urban nonpoint source runoff is depression storage. This parameter defines the volume of water that is retained on the surface in small depressions and does not become surface runoff. The value of depression storage that was used in the sample area was 0.02 inches.

TABLE 4

Sample Study Area - Composite Runoff Coefficient
(CRC) Calculations

Land Use CRC Calculation

Land Use Type	Percent of Area	Percent Imperviousness	Pervious Area	Impervious Area	Total
Single Family Residential	7	52	0.18 X 0.48 = 0.08	0.92 X 0.52 = 0.48	0.56
Multiple Family Residential	50	63	0.18 X 0.37 = 0.07	0.92 X 0.63 = 0.58	0.65
Commercial	5	70	0.18 X 0.10 = 0.05	0.02 X 0.70 = 0.64	0.69
Industrial	3	90	0.18 X 0.10 = 0.02	0.92 X 0.90 = 0.83	0.85
Open or Park	35	15	0.18 X 0.85 = 0.15	0.92 X 0.15 = 0.14	0.29

$$\begin{aligned}
 \text{CRC for imperviousness area} &= (0.48 \times 0.07) + (0.58 \times 0.50) + (0.64 \times 0.05) \\
 &\quad + (0.83 \times 0.03) + (0.14 \times 0.35) \\
 &= 0.43
 \end{aligned}$$

$$\begin{aligned}
 \text{CRC for the total area} &= (0.56 \times 0.07) + (0.65 \times 0.50) + (0.69 \times 0.05) \\
 &\quad + (0.85 \times 0.03) + (0.29 \times 0.35) \\
 &= 0.53
 \end{aligned}$$

The relationship for determining total stormwater runoff volume for a study area is:

$$\text{Total Stormwater Runoff} = (\text{Total Rainfall} - \text{Depression Storage}) \times (\text{Composite Runoff Coefficient})$$

For this example, the values in this relationship are:

$$\text{Total Stormwater Runoff} = (0.9 \text{ inches} - 0.02 \text{ inches}) \times 0.53$$

$$\text{Total Stormwater Runoff} = 0.46 \text{ inches}$$

This same runoff relationship can be used to determine the volume of stormwater runoff on an hourly basis. Where hourly Total Stormwater Runoff is desired, hourly Total Rainfall must be provided.

For the design storm being used in this example, Table 1 lists the total rainfall for each hour of the event. The total runoff for each hour is given in Table 5.

TABLE 5

Hourly Runoff

	Rainfall Inches	Runoff	
		Impervious Inches	Total Inches
Hour 1	0.25	0.25 X 0.43 = 0.11	(0.25-0.02) X 0.53 = 0.12
Hour 2	0.40	0.40 X 0.43 = 0.16	0.40 X 0.53 = 0.21
Hour 3	0.25	0.25 X 0.43 = 0.11	0.25 X 0.53 = 0.13

Step 6: Calculation of Pollutant Accumulation on Each Land Use at the Start of the Storm

The washoff of pollutants from an urban drainage area depends on the amount of pollutants that are built up on the area at the start of the storm event. Table 6 lists the specific pollutant accumulation values (in terms of pounds per acre per day) as obtained from detailed studies of similar areas for the land use types used in this example. The pollutant accumulation given in Table 6 can be used to determine the weighted average Pollutant Accumulation Rate (PAR) for the sample study area. The relationship used to determine the weighted average PAR (in pounds/acre/day) is:

$$\text{Weighted Average PAR} = \sum (\text{PAR} \times \text{LUP})$$

where:

PAR = The pollutant accumulation rate, in pounds/acre/day, for each land use (from Table 6)

LUP = The percent of the total drainage area for each land use.

Table 6 also illustrates the calculations required to determine the Weighted Average PAR. The example is presented for biochemical oxygen demand (BOD).

TABLE 6

Sample Study Area - Weighted Average PAR Calculations

<u>Land Use Type</u>	<u>Percent of Total Area</u>	<u>BOD Pollutant Accumulation Rate (pounds/acre/day)</u>
Single Family Residential	7	0.22
Multiple Family Residential	50	0.40
Commercial	5	0.48
Industrial	3	0.50
Open or Park	35	0.20
Weighted Average PAR = (0.22 X 0.07) + (0.40 X 0.50) + (0.48 X 0.05) + (0.50 X 0.03) + (0.20 X 0.35)		
Weighted Average PAR = 0.32 pounds/acre/day		

Step 7: Determination of Stormwater Runoff Loads

Stormwater runoff pollutant loads are a function of the mass of pollutants on an acre, the runoff intensity, and an exponential washoff coefficient. The relationship which incorporates these factors in order to determine pollutant loads is an empirical one based on studies of surface buildup and washoff of pollutants, and is expressed as:¹

$$M_p = P_p (1 - e^{-KR_I})$$

where:

M_p = the mass of a pollutant that is washed from a surface during a given (hourly) time period.

P_p = Accumulated pollutant remaining on the surface at the beginning of the time step.

K = Washoff decay coefficient, assumed to be equal to 2.0 for Puerto Rico urban areas.

R_I = Stormwater runoff rate in inches per hour from the impervious section of the surface

The value for P_p at the beginning of the rainfall event depends on the Weighted Average Pollutant Accumulation Rate, Table 6, the Antecedent Dry Period (Table 6), and the total acreage of the study area. For this example, the total pollutant on the surface at the start of the rainfall event is:

$$P_p = (\text{Weighted Average PAR}) \times (\text{Antecedent Dry Period}) \\ \times \text{Acres in Study Area}$$

$$P_p = 0.32 \text{ pounds/acre/day} \times 10 \text{ days} \times 2000 \text{ acres}$$

$$P_p = 6400 \text{ pounds}$$

Using the empirical pollutant washoff relationship, the total amount of pollutants washed off the total study area during each hour of the design storm is:

Hour 1

$$P_p = 6400 \text{ pounds}$$

$$R_I = 0.11 \text{ inches/hour}$$

$$K = 2.0$$

$$M_p = 6400 (1 - e^{-2.0 \times 0.11})$$

$$M_p = 1264 \text{ pounds}$$

Hour 2 The Pp value at the start of hour 2 is equal to the Pp value at the start of the storm minus the Mp value for the first hour, and so on throughout the storm event.

$$P_p = 6400 \text{ pounds} - 1264 \text{ pounds} = 5136 \text{ pounds}$$

$$R_I = 0.16 \text{ inches/hour}$$

$$K = 2.0$$

$$M_p = 5136 (1 - e^{-2.0 \times 0.16})$$

$$M_p = 1406 \text{ pounds}$$

Hour 3

$$P_p = 5136 \text{ pounds} - 1406 \text{ pounds} = 3730 \text{ pounds}$$

$$R_I = 0.11 \text{ inches/hour}$$

$$K = 2.0$$

$$M_p = 3730 (1 - e^{-2.0 \times 0.11})$$

$$M_p = 737 \text{ pounds}$$

The total pollutant load for this design storm event is therefore the sum of the hourly pollutant loads, or 3407 pounds.

Pollutant Concentration

$$\begin{aligned} \text{Hour 1 Pollutant Concentration} &= \frac{\text{Load}}{\text{Runoff Volume}} \\ &= \frac{1264}{0.12 \times 2000 \times 0.0272 \times 8.33} \\ &= 23.2 \text{ mg/L} \end{aligned}$$

$$\begin{aligned} \text{Hour 2 Pollutant Concentration} &= \frac{1406}{0.21 \times 2000 \times 0.0272 \times 8.33} \\ &= 14.8 \text{ mg/L} \end{aligned}$$

$$\begin{aligned} \text{Hour 3 Pollutant Concentration} &= \frac{737}{0.13 \times 2000 \times 0.027 \times 8.33} \\ &= 12.5 \text{ mg/L} \end{aligned}$$

Average Concentration of Nonpoint Source Pollutant during the storm event =

$$\begin{aligned} \frac{\text{Total Load}}{\text{Total Runoff}} &= \frac{1264 + 1406 + 737}{0.46 \times 2000 \times 0.0272 \times 8.33} = 16.3 \text{ mg/L} \end{aligned}$$

CONCLUSIONS

The desktop methodology discussed in this paper is simple and can be used with minimum available information. However, limitations for using this methodology should be observed and can only be used as first level analysis and extrapolation of analysis to areas where good values of nonpoint source loading rates and rate coefficients are established.

REFERENCE

1. "Storage, Treatment, Overflow, Runoff Model - STORM, User's Manual", The Hydrologic Engineering Center, The Army Corps of Engineers, July 1976.

The work described in this paper was not funded by the U.S. Environmental Protection Agency. The contents do not necessarily reflect the views of the Agency and no official endorsement should be inferred.

CONTINUOUS SIMULATION OF INSTREAM FECAL COLIFORM BACTERIA

A.C.Rowney (1) L.A.Roesner (2)

ABSTRACT

The simulation of fecal coliform bacteria in an urban stream is discussed in light of a recent study of the Rideau River at Ottawa, Canada. As part of this study, it became necessary to verify the use of a one-dimensional advection/dispersion river model incorporating first order decay in the simulation of fecal coliform bacteria. An extensive time-series data base was gathered for calibration and verification of the model QUAL-II. This data base was supplemented with runoff data simulated using STORM. It was found that the selected models provided a good representation of major processes in the test reach selected, certainly adequate for planning purposes. Some preliminary statistics representing the goodness of fit of simulated to observed instream concentrations are presented. In addition, modifications made to QUAL-II to permit simulation of time series input conditions are briefly discussed.

INTRODUCTION

The Rideau River at Ottawa has been the subject of an on-going investigation designed to protect and enhance water quality for several years. This investigation is motivated by a number of general concerns, one of which is that the bathing beaches located on the river and within the city of Ottawa have been closed by the medical officer due to unacceptable indicator bacteria levels.

A major component of the investigations has therefore been to isolate sources of bacterial contamination so that proper management techniques to reduce bacterial levels to acceptable limits may be undertaken. Past studies, discussed during the 1981 SWMM users group meeting in Niagara Falls, have shown that a major contribution to dry-weather sources is likely to be carryover of elevated instream concentrations from one storm event to the next. It is evident, however, that significant non-point sources of dry weather bacterial pollution also exist. Prior to any

- (1) Proctor and Redfern Ltd
- (2) Camp Dresser and McKee Inc.

attempt to institute controls on storm-water related pollution, it is necessary to investigate the likely magnitude of these dry weather sources.

A careful examination of all likely sources of fecal coliform contamination is therefore required, so that the nature and likely relative importance of sources may be estimated. A part of that investigation involves modelling the instream transport of bacteria concentrations, and it is the calibration and verification of the QUAL-II model in this context which is discussed in this paper.

The work discussed herein was carried out by a joint venture between Proctor and Redfern Ltd and Gore and Storrie Ltd in association with Camp Dresser and McKee Inc. on behalf of the Rideau River Stormwater Management Study.

2.0 SELECTION OF TEST REACH

The selected test reach for calibration and verification is depicted in Figure 1. As shown, the test reach is a fairly straight section of river, bounded at the top and bottom by bridges. The section was selected for several reasons. It is known to have a fairly regular cross-section throughout its length, which facilitates simulation of hydraulics. In addition, the area directly tributary to this reach is minimal, which reduces the size of un-monitored stormwater sources and consequently simplifies simulation. The bridges above and below the test reach provided convenient markers for locating monitoring stations, and facilities for 24-hour monitoring and sample storage could be located nearby conveniently.

Unfortunately, the site had some drawbacks, chief of which was its length, some 1.6 km. This short distance means that during high flow periods, changes in bacteria concentration due to die-off are small, and therefore are difficult to assess. However, increasing the length of the test reach would increase the number and size of non-quantified sources, so a balance had to be struck. The test reach shown was the result.

3.0 AVAILABLE DATA BASE

3.1 Hydraulic Data

The Rideau River at Ottawa is characterised by a series of deep and shallow sections. As part of a navigational waterway, the river is highly regulated, and flows within the study section are controlled by backwater effects from the locks and dams at the outlet. For this reason, the option for calculation of hydraulics

using the normal depth trapezoid contained by QUAL-II was abandoned in favour of inputs derived using the backwater HEC-2 model. HEC-2 was set up and run for a range of flows which encompassed the range measured during collection of the bacteria data in the test reach. Examination of the flow and elevation data simulated and observed in the test reach showed that changes in velocity in this section can be well represented by a linear function, and that depths are relatively constant over the range of flows which is of interest. Therefore, QUAL-II was coded to use a constant depth and linear velocity-flow relation.

River flow data during the period of monitoring was taken from a Water Survey of Canada gauge located about 5 km. upstream of the test reach. A separate gauge was established at the outlet of the Sawmill Cr., since flows from this tributary can govern flows in the test reach during storm events. Lateral inflows not accounted for by the two gauges were estimated using runoff volumes calculated by a calibrated STORM model.

3.2 Fecal Coliform Bacteria

Bacteria concentration data were gathered at four instream points and on one tributary. The chosen sites, depicted in Figure 1, are located evenly down the length of the test reach, and on the Sawmill Cr.

Samples were taken hourly on a 24-hour basis for a period of just over one month, beginning on the sixth of July, 1981. Samples were taken at the mid-stream point at a depth of one meter, and were stored in cooler chests in ice for a maximum of six hours prior to shipping to the laboratory for analysis. A membrane filter technique was used in estimating fecal coliform concentrations in the samples so collected.

The measured sources therefore accounted for all runoff related bacteria except for a small local tributary area. This area was simulated using the STORM model, and results were input to QUAL-II along with the measured values.

Bacteria die-off rate parameters were taken from findings of a study of the University of Ottawa, which measured bacteria die-off in plastic bags suspended in the river from floats. An average measured T90 of 43 hours was calculated in these experiments, and a range of 24-48 hours was tested in this study.

4.0 MODIFICATIONS TO QUAL-II

QUAL-II is currently available in a version which only accepts inputs of steady state or initial condition data. Applied in the steady state mode, it is useful for evaluation of continuous discharges during periods of known constant river flow, or for similar applications. The model can be extended to dynamic uses

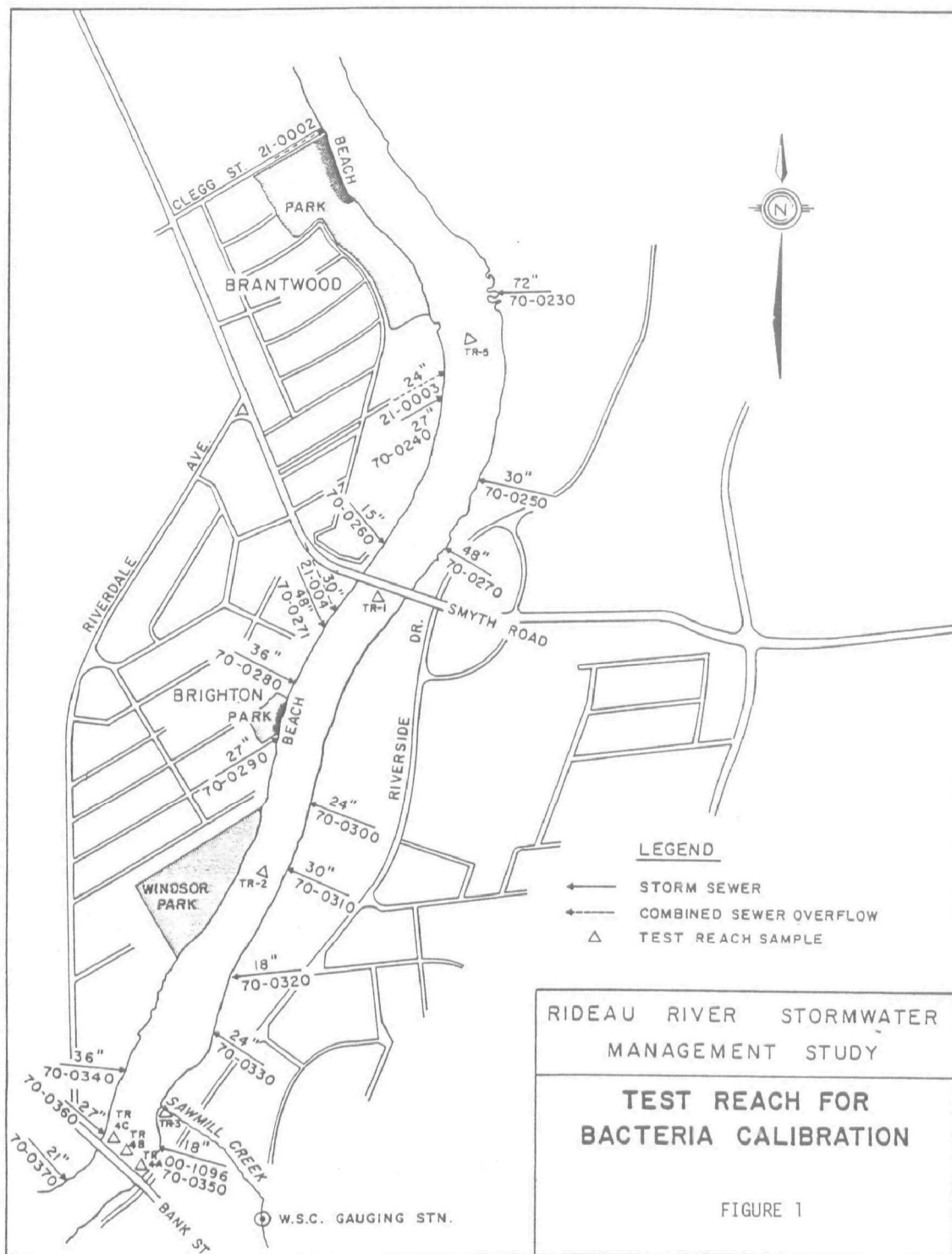


FIGURE 1

if initial conditions resulting from an event are known, since these initial conditions can be specified in the model, and the subsequent recovery of the river can be 'viewed'.

However, it is not possible to simulate time varying inputs of concentration or flow with the standard version of the model. While this was not deemed a necessary condition for completion of modeling in the overall study, this capability was required for calibration to time series data during this specific part of the study. Rather than employ a model already using dynamic inputs, it was decided for reasons of consistency and economy to modify QUAL-II to accept this type of data.

In practice, these changes proved to be quite simple to implement. A number of possible modifications were tested, and a final version of QUAL which allows dynamic input of concentration and flow data at headwater, point source, and uniform lateral load points was devised. The modified MAIN flowchart for QUAL-II is shown in Figure 2.

The new version of QUAL is designed to read data at arbitrary time intervals from disc files, and will accept point source, headwater, and distributed loads that vary independently. Outputs from the model are printed to disc or hard copy devices at user defined time increments in a format which facilitates subsequent computer plotting. In addition, the time series outputs have been made slightly less unwieldy by allowing the user to specify any number of individual elements for display.

To allow a rapid and economical sorting of data by users, a LINK program was also created. This program is a simple utility routine which reads data from coded field observations and interpolates flow and concentration data at any specified time increment and in any combination desired by the user. The primary benefit to this approach is that it allows the user to rapidly evaluate the significance of various combinations of individual sources, and in addition makes it possible to smooth data somewhat by averaging several observations into one value representative of each time increment.

It is interesting to note that the modified QUAL-II reflected hydraulic conditions just as well when headwater flows were held fixed as when they were allowed to vary as observed. This implies that an average flow, velocity, and depth adequately represent hydraulic conditions in this system, which is consistent with observations made in prior studies. However, it was found that the resulting simulation did not accurately represent in-stream concentrations. The model would conserve mass, but without the proper input volumes to calculate dilutions, concentration simulation was not possible. The dynamic hydraulic inputs used in this calibration were therefore provided

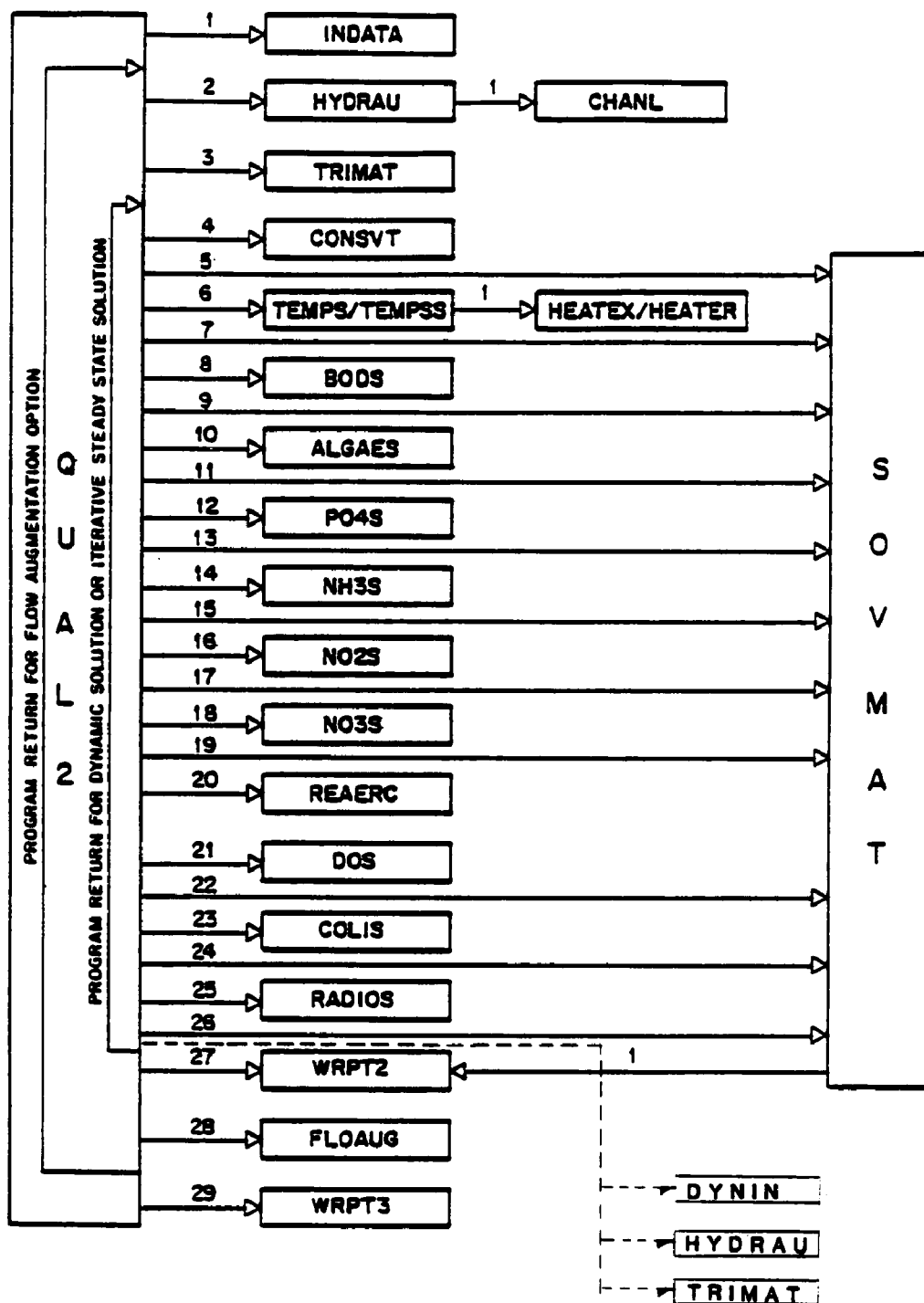


FIGURE 2. MODIFIED QUAL-II STRUCTURE

to allow proper computation of diluted concentrations, rather than for the impact they make on advection parameters.

5.0 MODEL APPLICATION

5.1 Calibration

A calibration period consisting of the last 200 hours of observations was selected for calibration. This period includes about one quarter of the available time series observations, and covered periods representative of both dry and storm flow conditions.

Calibration was a fairly simple process, since flows input to the model were fixed. Parameters available for calibration were therefore advection, dispersion, and die-off.

It was observed that the advection of pollutants, as measured by timing of peak events moving through the system, was fairly well represented as input, and this factor was not altered. The initial flow/velocity relation calculated by HEC-2 was maintained throughout the calibration/verification series.

Dispersion in the model as applied in this study was limited to the numerical dispersion induced by the particular element size and time step incorporated in the model. An associated study showed the impact of dispersion on the model results is not significant, and this factor was not altered during calibration.

Thus, the major parameter left for calibration was the bacteria die-off rate. Since previous die-off studies by the University of Ottawa had quantified this value, the range of die-off rates tested was known. In this case, T90 times averaged 43 hours with a range of approximately 20 to 60 hours.

There was, however, one condition not accounted for in the above set of input and rate parameters, and that is the rate of input of continuous sources of bacterial pollution. These sources which included the combined effect of such things as illegal connections, animal populations, and other diffuse sources, were not quantifiable and therefore had to be input to the model by inference. The model was adjusted so that events causing peaks of concentration (i.e. storms) were well represented, and then the rate of constant distributed side loads was adjusted to increase dry weather levels to observed values.

This proved to be an effective and rapid means of obtaining a good calibration to observed conditions, although as noted below the size of the implied constant source is a direct function of the assumed rate and form of bacterial decay.

5.2 Verification

Once the calibration was completed, the model was verified by completing a run over the entire 800 hour data set with all calibration parameters held constant.

6.0 DISCUSSION OF RESULTS

In general, the model was found to reproduce observations remarkably well, considering the highly variable nature of fecal coliform bacteria. Figure 3 shows part of the calibration data set. It is evident that major peaks are reproduced quite closely, and that base levels do range about the simulated values. Figure 4, representing part of the verification period, presents a similar picture, although somewhat more scattered. Subjectively, one may observe what appears to be a diurnal variation of observed concentration about the simulated level during some dry periods, but the mechanism for this effect is not known for certain.

Comparisons were made of observed and simulated conditions in several ways, as discussed below:

Mean errors were calculated to provide some indication of how well simulations were centered within the range of observed bacterial concentrations.

TABLE 1. MEAN DIFFERENCES BETWEEN SIMULATED AND OBSERVED F.C. CONCENTRATIONS

location	#points	mean error (no/dl)	mean log error log(no/dl)
TR-2	760	-8.9	-0.0646
TR-1	778	15.6	-0.0112
TR-5	353	-52.6	-0.0627

Average concentrations observed were about 300 no/dl at all three stations. Although the plotted curve does not duplicate the observed values exactly, it is (on average) well centered in the range of observed values.

RMS errors were calculated to provide an index of spread about the simulated values.

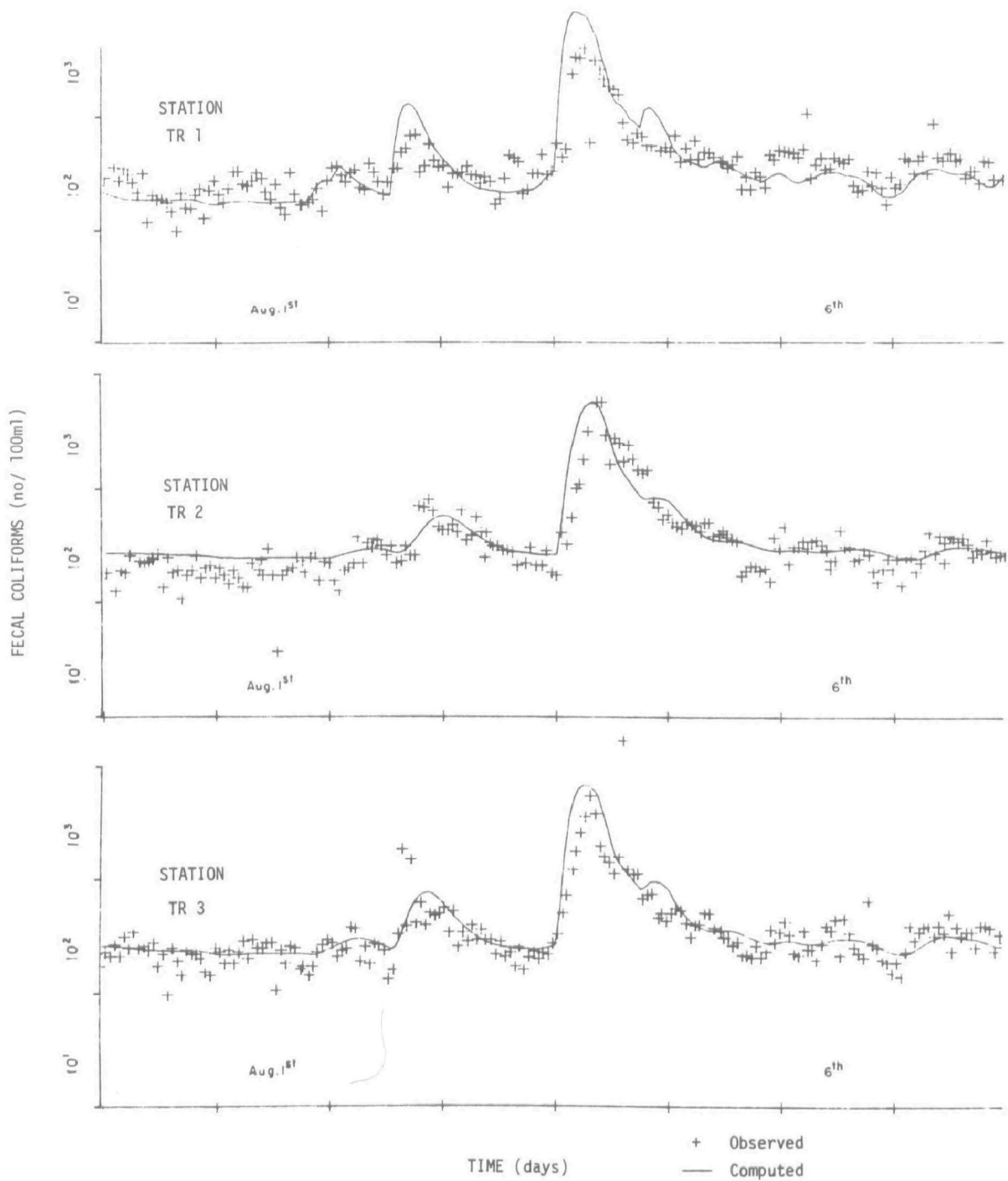


FIGURE 3. CALIBRATION PERIOD

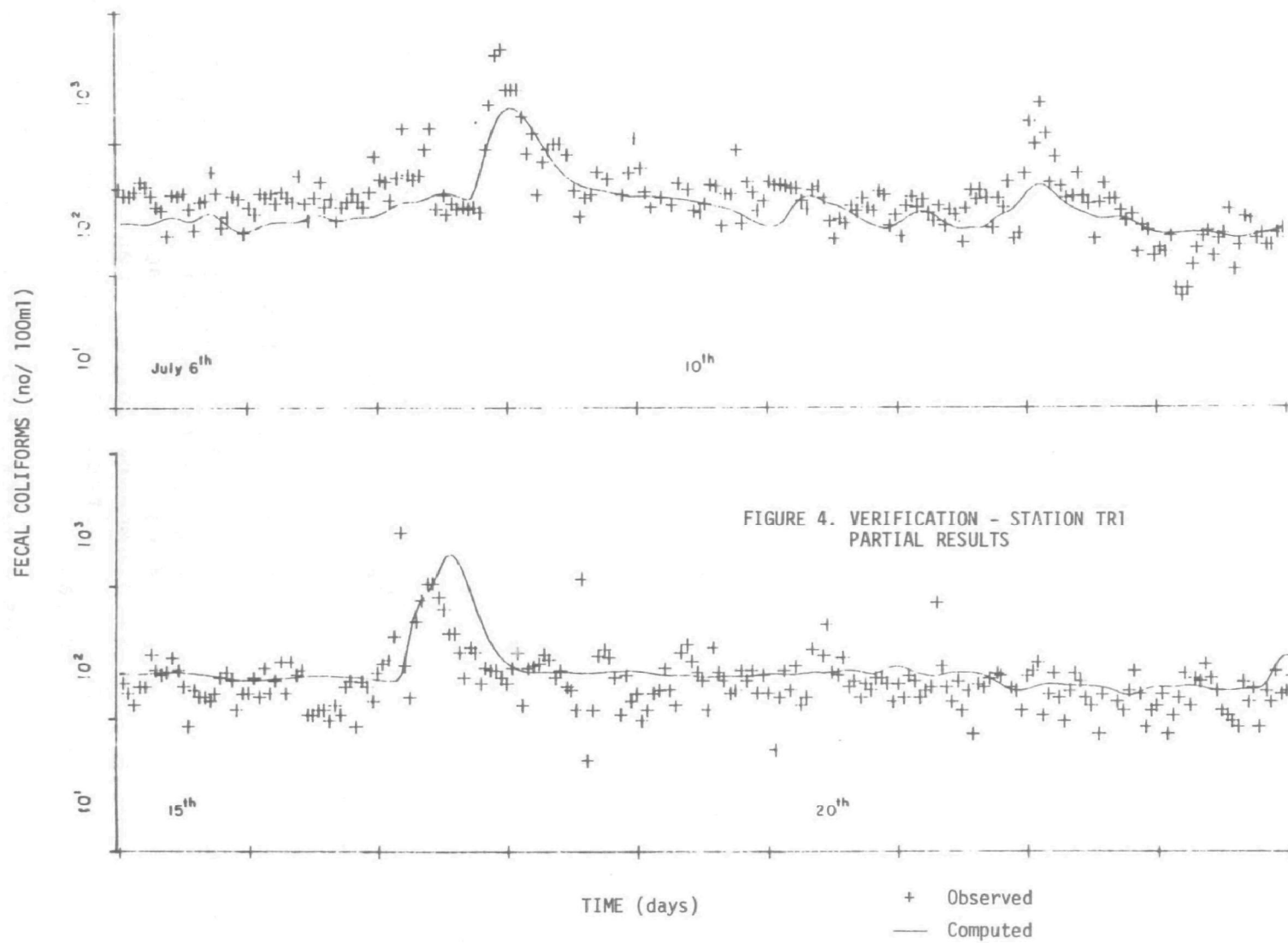


TABLE 2. RMS DIFFERENCES BETWEEN SIMULATED AND
OBSERVED F.C. CONCENTRATIONS

location	#points	RMS error log(no/dl)
TR-2	760	0.2342
TR-1	778	0.1962
TR-5	353	0.1687

The average concentration observed during the above simulation period was about $2.5 \log(\text{no/dl})$.

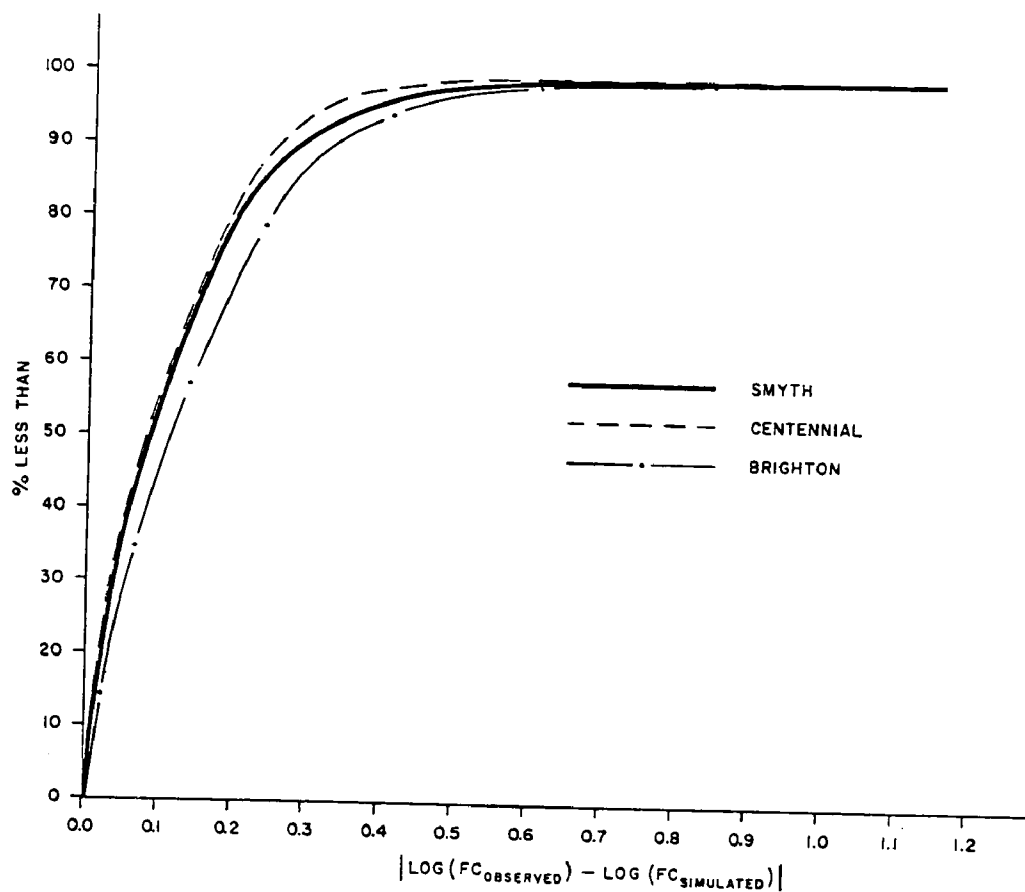
Frequency of departures was calculated. While the RMS shown above is a common measure of fit, it does not provide much information about the likelihood of any given error unless the distribution relating simulations and observations is known. To provide a measure of this factor, the absolute differences between $\log(\text{observed})$ and $\log(\text{simulated})$ results were collected and grouped in classes of width .02. From this data, % less than curves were determined as shown in Figure 5. It is evident from these curves that the three stations are represented approximately equally well, and that for practical purposes all observations may be considered to be within .2 to .3 logs of the simulation. Again, for the variability of the phenomenon, this is quite a good approximation.

Changes in concentration during peak periods were estimated. This was by necessity a subjective assessment, but gives some feel for the 'goodness' of peak event representation. As shown in Table 3, observed changes are on average 6% higher than simulated.

Absolute peaks were compared, again subjectively, to provide some indication of how well peak concentrations are predicted, as shown in Table 4.

In summary, several points are clear from the above results.

- o While the natural variability of fecal coliform bacteria in the environment makes it impossible to exactly duplicate observed values, simple model techniques are capable of providing a reasonable representation of the instream processes affecting the persistence of fecal coliform bacteria.
- o QUAL-II provides a quick, economical, and effective model for use in this type of analysis.



TEST REACH ANALYSIS
DEPARTURE OF OBSERVATIONS FROM
SIMULATED RESULTS

FIGURE 5.

TABLE 3 COMPARISON OF SIMULATED AND OBSERVED CHANGES FROM BASE LEVEL FECAL COLIFORM CONCENTRATIONS

LOCATION	E VENT	CHANGE OBSERVED	(log(no/dl)) SIMULATED	RATIO (O/S)
TR-1	1	1.05	.66	1.59
	2	.75	.33	2.27
	3	.89	.95	.94
	4	.50	.42	1.19
	5	1.45	1.40	1.04
TR-2	1	.70	1.02	.69
	2	.55	.50	1.10
	3	.75	1.25	.60
	4	.35	.78	.45
	5	1.15	1.61	.71
TR-5	4	.40	.35	1.14
	5	1.30	1.38	.94

Average= 1.06

TABLE 4 COMPARISON OF SIMULATED AND OBSERVED FECAL COLIFORM PEAK CONCENTRAIONS

LOCATION	E VENT	PEAK (log(no/dl)) OBSERVED	SIMULATED	DIFFERENCE (O-S)
TR-1	1	3.55	3.22	.33
	2	3.20	2.66	.54
	3	3.00	3.21	-.21
	4	2.72	2.88	-.16
	5	3.70	3.84	-.14
TR-2	1	3.25	3.54	-.29
	2	3.15	2.80	.35
	3	3.00	3.42	-.42
	4	2.80	3.12	-.32
	5	3.65	3.98	-.33
TR-5	4	2.75	2.8	-.05
	5	3.65	3.8	-.15

Average= -.07
Average as %= 17% high

- o In the Rideau river, a significant continuous source of fecal coliform bacteria contamination exists.
- o Quantification of such a continuous source is not in this case possible by direct measurement. It is, however, possible to estimate the size of the source by inference from modelling results. Care must be taken in such a calculation since the estimated rate of bacteria die-off has a great impact on the implied load, and the mechanism of instream die-off is only approximated by a simple first order decay assumption.

Currently, work is underway to resolve some of these uncertainties. For example, improved information on bacterial die-off is being generated from larger scale and longer duration measurements. Subsequent stages of analysis will use the models developed in this study to provide information on bacteria sources sufficient to permit planning of measures to protect the river from further degradation, and if possible to improve the current situation.

The work described in this paper was not funded by the U.S. Environmental Protection Agency. The contents do not necessarily reflect the views of the Agency and no official endorsement should be inferred.

ATMOSPHERIC POLLUTION IN RELATION TO STORM WATER
QUALITY MODELLING; LITERATURE REVIEW FOR AN
INDUSTRIAL CITY

by

Shivalingaiah, B.

and

William James

Civil Engineering Department
McMaster University
Hamilton, Ontario, Canada

ABSTRACT

The atmosphere is one of the largest sources of pollutants in surface runoff in an industrial city. The location of the major industrial areas, wind direction and velocity and source concentrations are important parameters in the prediction of the atmospheric fallout component of surface loadings. Isopleths of atmospheric fallout are correlated with these parameters and superimposed on the discretized catchment. The total accumulated dry weather loading is input to the water quality sections of SWMM-RUNOFF. The water quality algorithms in SWMM III are reviewed and improvements suggested, eg. inclusion of atmospheric fallout and scavenging, street sweeping time series data, separation of pollutant source areas, variable time step hydrology and moving storm analysis.

INTRODUCTION

Atmospheric pollutants are washed out by precipitation or fallout as sediments, or are deposited by chemical processes. The atmosphere is one of the identified sources of nutrients and solids to runoff. The interrelation between atmospheric pollution, rain and storm water contamination has not been fully established. An attempt is made in this paper to review the literature for an industrial city, Hamilton, on atmospheric pollution in relation to storm water quality modelling. A discussion of the SWMM III runoff water quality algorithms and possible areas for improvement concludes the paper.

GEOGRAPHICAL FEATURES OF HAMILTON

Hamilton is highly industrialized and is located on the south western shore of Lake Ontario. The iron and steel industry is the major activity in the city of 306,640 (1980) occupying most of the southern shore of Hamilton Harbour. The downtown area lies to the southwest. The Niagara Escarpment almost surrounds Hamilton and the southern arm divides the city into upper and lower sectors having an average height difference of 325 feet (figure 1). The escarpment is cut by a number of deep valleys, the most important of which is the southwest-northeast aligned Dundas Valley.

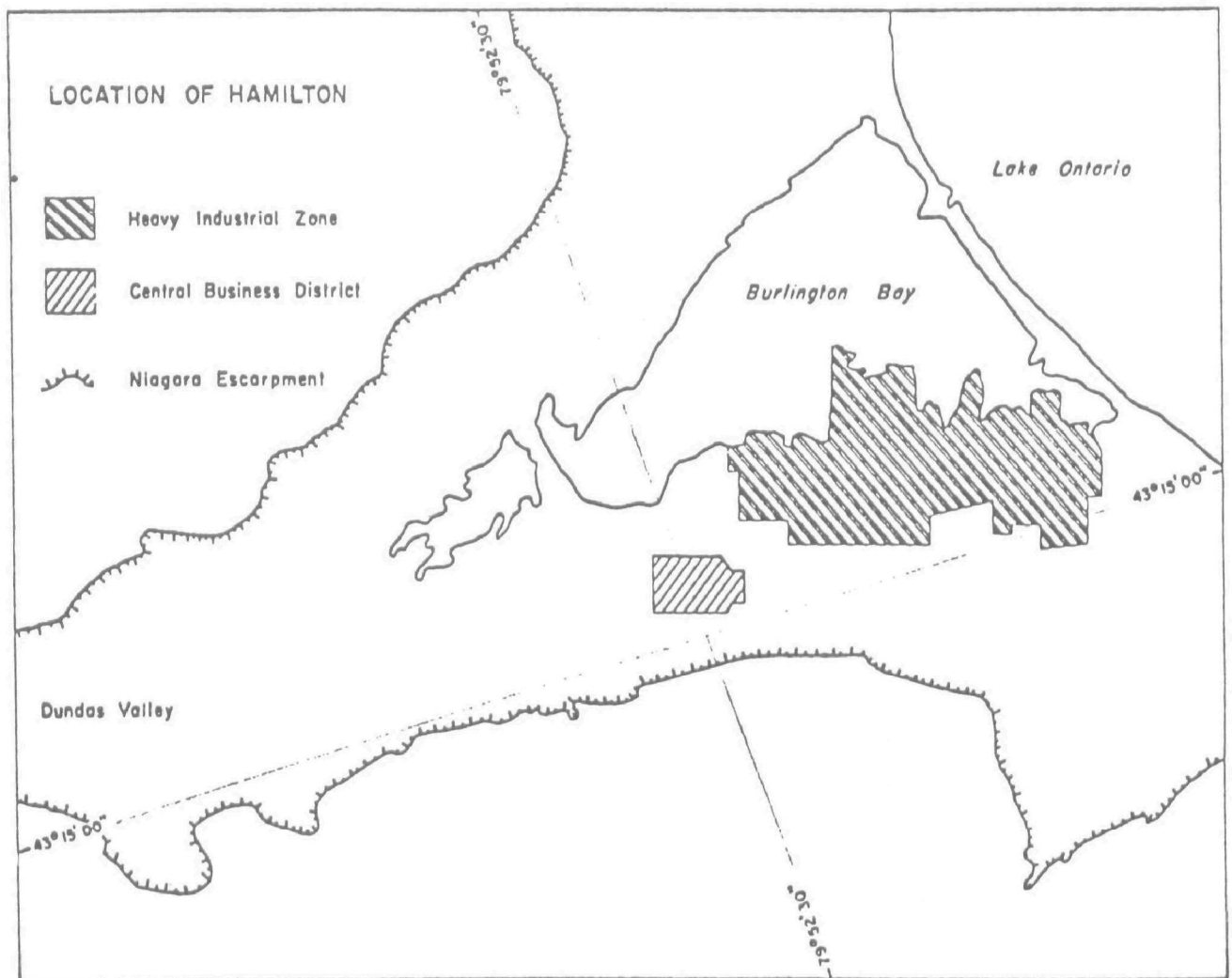


Figure 1: Geographical features of Hamilton

The major steel plants are located in the northeast of Hamilton, with associated industries including machinery, electrical and chemical manufacturing. The business district is made up of a core of multi-storey commercial buildings of limited areal extent surrounded by a lower level of mixed commercial and residential properties. The prevailing wind is dominantly west and southwest. Though the frequency of easterly wind (30-40 percent) is less than westerly wind, easterly wind transports industrial pollutants west across the city. It is especially unpleasant when occasional anti-cyclonic conditions result in light easterly winds which have been cooled over the cold lake surface. Then, very stable lower air layers are created due to the temperature inversion which locks polluted air over most of the lower city.

SOURCES OF ATMOSPHERIC POLLUTANTS

In an urban situation industries, automobiles, house heating and resuspension of solids due to wind and vehicle movements contribute significant quantities of pollutants to the atmosphere. Winds on unpaved areas and unprotected industrial waste products also adds to the problem. The average values of pollutants produced due to combustion are given in Table 1 (Joe O. Ledbetter, 1972).

TABLE 1

COMBUSTION	POLLUTANTS				
	Particu- lates	Oxides of Nitrogen	Organic Hydrocarbons	Aldehydes	
Natural Gas lb/million cu.ft. of gas	15	390	3	-	1.0
Fuel oil lbs/1000 gal of oil	8	140	-	3.2	0.6
Coal lb/million BTU	5	1.9	-	0.4	0.0013
Autos lb/ 1000 gal/fuel	12	113	-	200	4
Diesel lb/ 1000 gal/ fuel	110	222	-	136	10

REMOVAL PROCESSES

Pollutants are removed from the atmosphere by dry and wet processes. In the case of dry process (absence of rain) particles greater than 20 um. size settle under gravitational force and particles less than 20 um. size are transported close to the surface by means of turbulence. Wet processes refer to removal of pollutants by precipitation. This is further divided into washout and rainout processes. Precipitation particles collecting dry particles by inertial collection or, in the case of smaller aerosol particles, by

diffusion and phoretic forces, is known as washout (scavenging). Rainout refers to particles which are nucleated for water condensation and thereby grow into cloud drops and in turn grew into precipitation particles.

Scavenging of gases by water drops due to molecular diffusion occurs in accordance with the vapour pressure and solubility of the free and collected gases (Junge, 1963; Chamberlain, 1960; and Griffiths, 1963). The maximum washout possible at a particular distance, assuming the rain starts as soon as the release of pollutants, is related to source strength, washout coefficient and average wind velocity (Culkowski, 1963; Guthrie and Nichols, 1964).

Among the above processes, wet processes contribute relatively more pollutants to runoff water. During dry days, dust accumulates (dry process) on the surface and washes off during precipitation. Wet processes scavenge pollutants during rain. It is evidently essential to account for both dry and wet processes in modelling surface water quality.

CONTRIBUTION OF ATMOSPHERIC POLLUTANTS TO PRECIPITATION

Increased urbanization and industrialization augments pollutants in rain water. Suspended solids, BOD, COD, TOC, nitrate and phosphates are often commonly measured in rain

and runoff water. The average values of COD and TOC in rain water are 20.7-322 mg/lit and 2.8-18 mg/lit respectively (C.W. Randall et al 1978; Per-Arne Malmquist 1978). Nitrate and phosphate in rain water has been found to exceed the level recommended for controlling eutrophication (Vladimir Novotny 1981, Randall et al, 1978, Rutherford 1967, John A. Frizzola, 1975; Albert Goettle, 1978; Dean Stuart, 1975, Chan and Kantz 1981). The concentration of pollutants in the atmosphere and in rain water may be site specific in an highly industrialized city. Maximum levels of pollutants have been observed to occur during the early stages of rain, similar to the first flush effect observed in runoff water (Randall et al, 1978). The ground surface acts as a net pollutant sink rather than a source of water pollution (Randall 1981). Exceptions to this condition are tilled land and highly impervious business areas.

AIR POLLUTION AND RAINWATER STUDIES IN THE CITY OF HAMILTON

The first report of an air pollution survey was published in December 1956 (Ontario Research Foundation, 1956). Since then a number of studies have been conducted on different aspects such as atmospheric fallout, total suspended solids, soil index, sulphur dioxide, oxides of nitrogen (Stewart, 1968; Mathehson, 1969; Rouse et al, 1970; Heidron, 1978; MOE reports 1977-80; Barton, 1981). The

dust concentration has been increasing even though a decreasing tendency has been observed for other pollutants since 1970. Effective controls for point source emissions have been enforced since 1970 (MOE 1980 Hamilton air quality report). This shows that other pollution sources (industrial and non-industrial) such as blowoff from unpaved areas, excavation, construction, demolition, road traffic (Syd Barton 1981), uncontrolled stockpiles and other non stack industrial emissions are adding to the problem. Yearly average dustfall observations showed that a portion (15 sq. km.) of the lower city and the beach strip near the industrial area was encompassed by the 9.0 gram/sq.m - 30 days isopleth. This is twice the Ontario Ministry of the Environment objective. Another 57 sq. km. was encompassed by 4.5 gram/sq.m.-30 days contour. Remaining areas of the city receive less than 4.5 gram/sq.m.-30 days.

An average concentration of 3.5 ug/cu.m. of nitrate and 3-24 ug/cu.m of organic carbon (5-14% of TSP) (Barton 1981) was observed in suspended particulates over Hamilton. Maximum atmospheric pollution index incidents (32 to 50 level) were observed during a lake breeze regime with moderately consistent winds from the east-northeast at speeds less than 6 miles/hr (Heidorn, 1978).

Not many studies appear to have been conducted on rain

water quality over Hamilton, except for the work of Dean Stuart (1975). Relative to surface waters, precipitation is normally low in conductivity and pH, with elevated heavy metals (10-1000 ug/lit) and nutrients (50-100 mg/litP; 400-2000 mg/litN) concentration. The above mentioned results are mean values obtained at a single station. Samples collected at a number of stations give a better understanding of wet process contributions.

FACTORS AFFECTING SPATIAL DISTRIBUTION OF POLLUTANTS

The dispersion of pollutants in the atmosphere is the result of three dominant mechanisms: (a) the general mean air motion that transports the pollutants downwind, (b) the turbulent velocity fluctuations that disperse the pollutants in all directions and (c) mass diffusion due to concentration gradients. In addition, the general aerodynamic characteristics such as size, shape and weight, affect the rate at which the nongaseous pollutant particles settle to the ground or are buoyed upwards.

The wind patterns near the shore of lakes, oceans, and bays are complicated because of differences in the rate of warming between the land and water. The expansion of the rising warmer air over the land causes a general air movement horizontally from the water to the land (sea or lake

breeze). At night the land surface cools at a faster rate by radiation than does the water. The air over the land gradually becomes cooler and more dense than the air over the water. Hence, a general local horizontal air movement occurs from the land to the water (land breeze). Most large industrial cities in Canada are located near large bodies of water and hence wind patterns over cities are complex. In addition to this, the presence of escarpments, mountains, large hills or prominent drainage valleys near the city further complicates the wind pattern.

Atmosphere stability is related to pollutant dispersal. Under stable conditions, pollutants do not exhibit much vertical mixing or motion. This is of importance in estimating the quantity of air pollutants at a given location.

SWMM III RUNOFF QUALITY ALGORITHMS

Pollutants are assumed to build up on an impervious area during the dry days preceding a storm and then washoff into the drains during a storm. Land use types for pollutant build up rate are the same as those in SWMM II but many more relations (power, linear, exponential or Michaelis-Menton) are included in SWMM III for dust and dirt accumulation. A maximum limit for accumulation of dust and dirt and for specific pollutants is also included in

SWMM III (1982).

Rain causes washoff of dust and dirt from impervious areas for each time step, (POFF), proportional to runoff rate to a power, (WASHPO).

$$- \text{POFF}(t) = d/dt (\text{PSHED}) = -\text{RCOEFX} * (\text{R}^{**}\text{WASHPO}) * \text{PSHED}$$

where POFF = constituent load washed off at time, t,

PSHED = quantity of constituent available for washoff
at time 't', mg.

RCOEFX = washhoeff coefficient = RCOEF/3600,
(in/hr)**-WASHPO *(1/sec), and

RX = runoff rate, in/hr.

RCOEF = coefficient, includes units conversion

WASHPO = exponent

A rating curve method is included as an alternative to the use of a buildup - washoff formulation. Loads (mass/time) may be generated proportional to flow power

$$\text{POFF} = \text{RCOEF} * (\text{WFLOW}^{**}\text{WASHPO})$$

where:

WFLOW = subcatchment runoff, cfs,
(or cu.m/sec)

RCOEF = coefficient, includes units
conversion,

WASHPO = Exponent

parameters RCOEF and WASHPO are entered for each particular constituent.

Soil erosion from the pervious area is calculated using the universal soil loss equation.

$$L = R.K.LS.C.P.$$

where L = average annual soil loss per unit area

R = rainfall factor

K = soil erodibility factory

LS = the slope length gradient ratio

C = the cropping management factor or cover index factor,

P = the erosion control practice factor

R = E. RAINIT

where E = total rainfall energy for time period of summation, 100 ft.-ton/ac.

$$= (9.16 + 3.31 \log(RNINHR(J))) * RNINHR(J) * DELT$$

RNINHR = rainfall intensity at time interval J, in/hr and

DELT = time interval, hr,

RAINIT = maximum average 30-minute rainfall

intensity for the storm (single event) or

the period of simulation (continuous) in/hr.

Provision has been made to add erosion to other

constituents.

The contribution of pollutants from precipitation is allowed in SWMM by permitting a constant concentration of constituents as an input to the model for a complete catchment.

AREAS FOR IMPROVEMENT

Dust and dirt buildup ideas used in the SWMM do not consider the physics of generation of pollutants from sources such as street pavements, vehicles, atmospheric fallout, scavenging, vegetation, land surfaces, litter, spills, antiskid compounds and chemicals, construction and drainage networks. The model lumps all these sources together in estimating the buildup rates for different land uses. It may be simple to separate some major sources like atmospheric fallout, scavenging, etc. Atmospheric fallout, and the contribution from scavenging, is a local phenomena which mainly depends on the type of city, wind velocity and direction, location of industrial area or major industries and topography of the catchment. Comparison of build-up rates given in SWMM for various land uses with observed atmospheric fallout in Hamilton showed that atmospheric fallout contributes a major portion of dust and dirt (Table 2). The average monthly variations in fallout of 1977-80 is given in Table

TABLE 2
COMPARISON OF CONSTITUENT BUILD UP RATES OF SWMM WITH
ATMOSPHERIC FALLOUT OF HAMILTON

Si No.	Land Use	SWMM dd Rates		Atmos. fall- out of Hamilt. DDlb/acre-day	% Contri- butions from atmos.
		DDlb/100 ft-dryday	DDlb/acre-day		
1	Single Family Residence	0.7	1.54	1.344	86%
2	Multi-Family Residence	2.3	5.06	2.688	54%
3	Commercial	3.3	9.9	2.688	26%
4	Industrial	4.6	5.98	2.688	41%
5	Undeveloped/park Open/Instutional	1.5	2.40	1.344	54%

TABLE 3

Average Monthly Variation of Dustfall, gram/m²-30 days (1977-1980).

Station	Jan	Feb	March	April	May	June	July	Aug	Sept	Oct	Nov	Dec
29001	5.48	6.28	12.65	10.58	9.8	6.88	6.0	5.73	6.75	5.35	5.4	6.68
29006	5.53	6.3	12.08	11.23	8.03	9.83	6.18	7.68	5.93	5.93	5.1	5.75
29008	26.83	17.5	14.75	11.23	9.78	8.37	12.40	11.93	10.45	13.38	13.3	19.60
29009	5.00	5.9	8.4	7.95	6.53	6.65	5.10	5.1	6.03	4.70	4.53	5.05
29010	9.50	13.4	24.68	20.3	18.15	12.77	13.90	16.25	15.57	16.05	19.93	17.33
29011	9.58	15.53	22.4	22.35	19.73	16.33	9.03	12.10	16.23	12.48	13.95	13.6
29012	9.20	7.53	14.47	12.05	14.48	9.93	7.20	7.88	13.28	7.15	8.15	12.3
29017	7.75	7.95	15.93	11.98	10.3	8.93	8.80	8.50	9.00	14.00	8.63	11.22
29019	2.68	3.08	6.58	4.83	6.27	5.35	7.88	3.55	5.80	3.80	3.40	3.53
29025	9.88	7.75	14.28	13.28	14.13	11.60	9.30	9.53	11.20	8.18	8.48	7.00
29026	4.55	5.15	6.70	6.28	6.53	5.95	4.70	4.53	4.83	4.75	4.30	4.93
29030	3.55	4.53	7.40	6.25	8.18	8.75	6.63	6.25	6.00	4.85	4.40	3.75
29031	5.80	7.9	11.25	10.03	8.08	9.35	5.03	6.00	7.83	5.80	6.08	6.25
29036	5.73	9.1	14.98	14.85	12.65	13.88	10.90	9.48	10.45	9.75	8.35	22.20
29037	15.73	14.9	26.83	26.57	18.68	17.50	17.80	21.53	19.95	22.0	24.20	14.75
29044	14.08	12.35	14.78	18.08	10.88	11.35	10.58	9.53	14.95	8.98	9.83	11.10
29046	3.58	3.03	4.93	5.23	14.5	9.25	9.03	3.53	4.03	2.83	3.88	3.40
29067	5.03	5.2	9.68	7.63	8.17	6.00	5.35	4.48	7.08	4.4	3.60	6.80

3. The variation is mainly due to meteorological parameters and location relative to the industrial area. Location of the industrial area, dust sampling stations and subcatchments for runoff calculations are shown in figure 2. Monthly and yearly average wind roses are shown in Figure 3. The yearly average isopleths of atmospheric fallout are shown in Figure 4 (MOE report 1980). Attempts are now underway to correlate the dust concentrations at various stations with wind direction and velocity. General conclusions will be reported in the near future.

Scavenging of pollutants by rain depends on the concentration and source of pollutants, atmospheric stability, intensity of rainfall, wind direction and storm characteristics. Therefore atmospheric fallout and scavenging should be modelled separately. These processes should not be considered build up rates as they are independent of land use. Provision has to be made in the model to generate concentration isopleths for dry periods to obtain a loading rate due to atmospheric fallout and scavenging process for every individual subcatchment, based on source location, atmospheric stability and meteorological condition. Constituents based on land use are added to the above loading rate to obtain total buildup rate for every subcatchment area. This is better than relating build up rates to land use. The authors will attempt to suitably modify SWMM III during summer

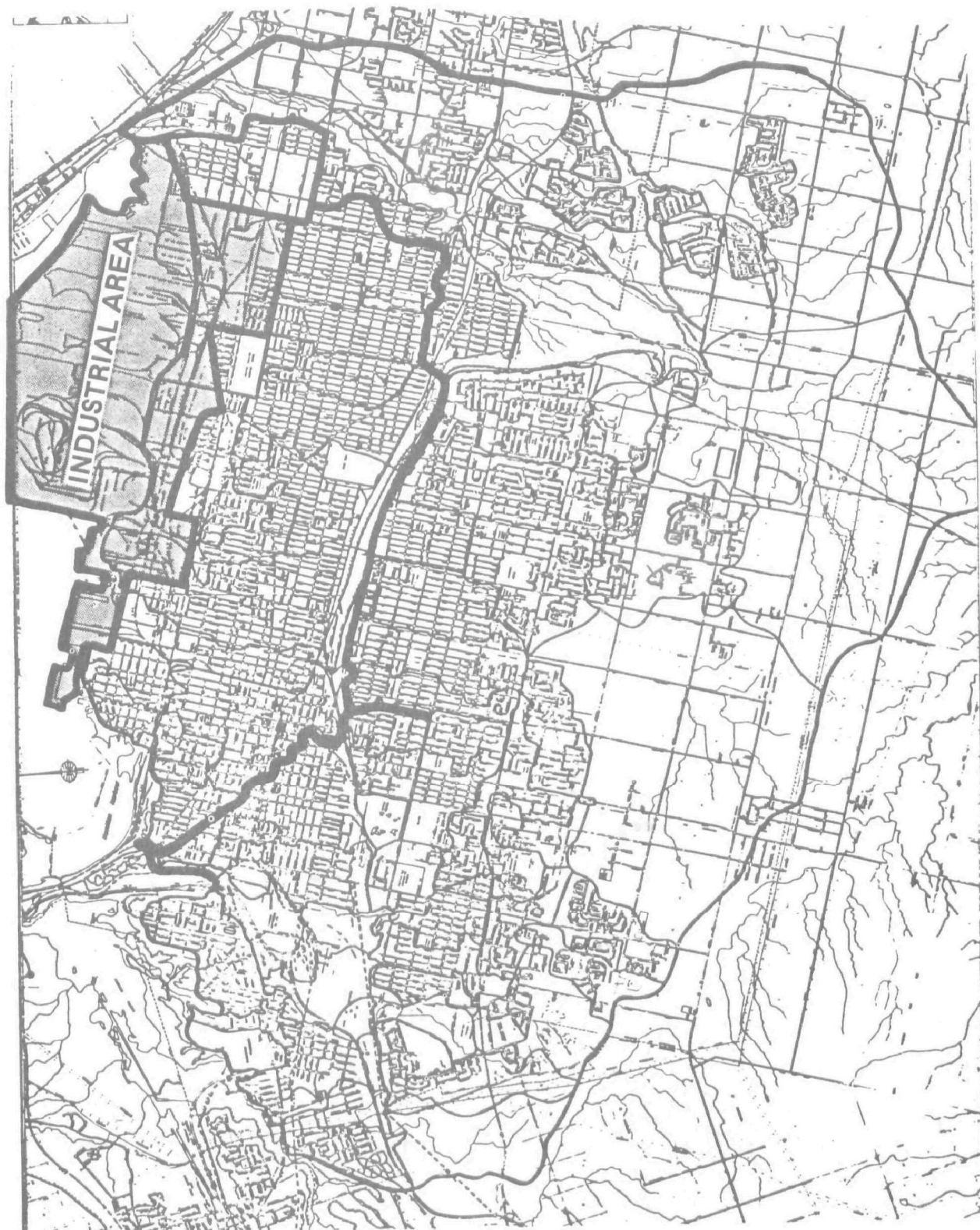
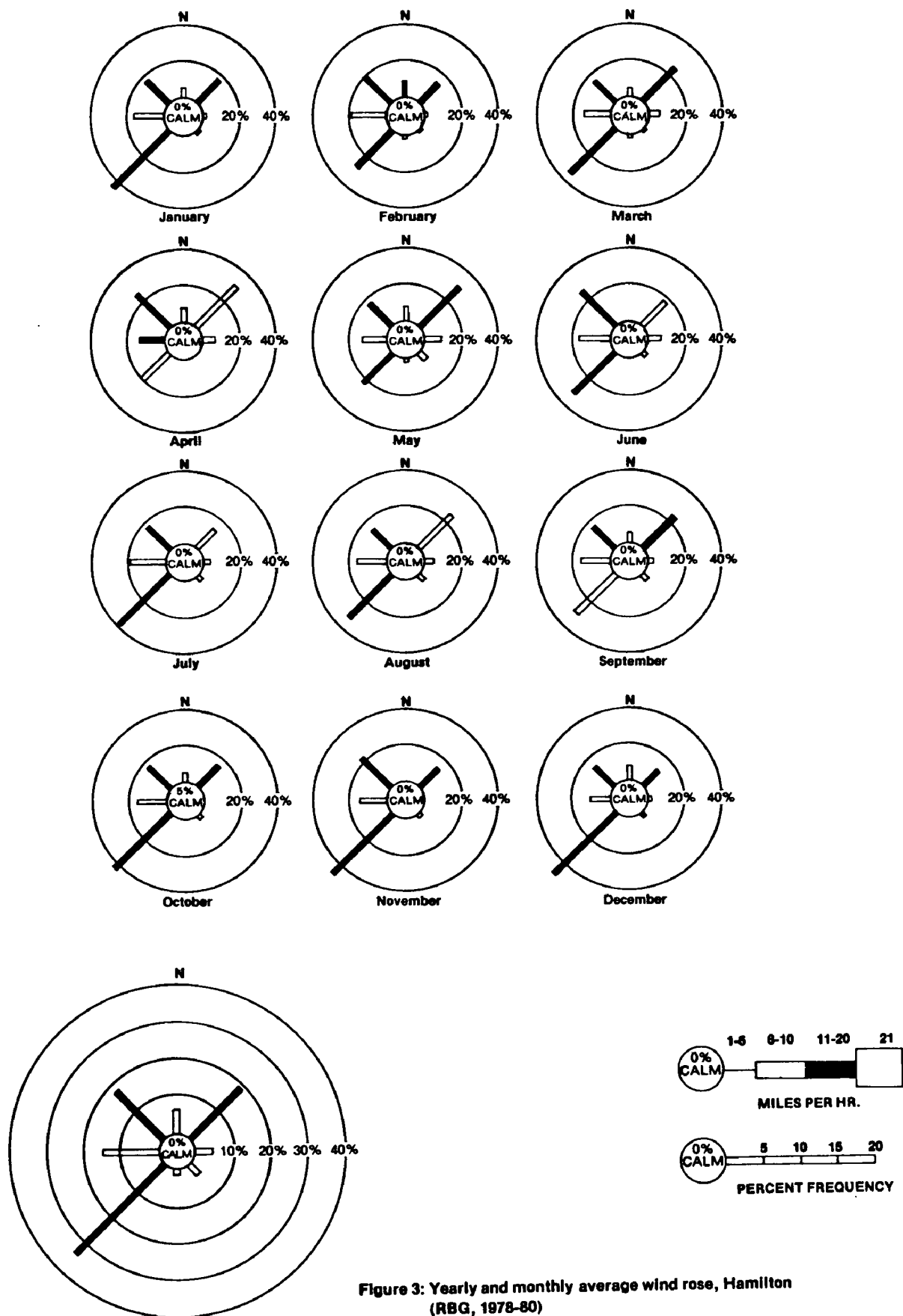


Figure 2: Location of Industrial Area



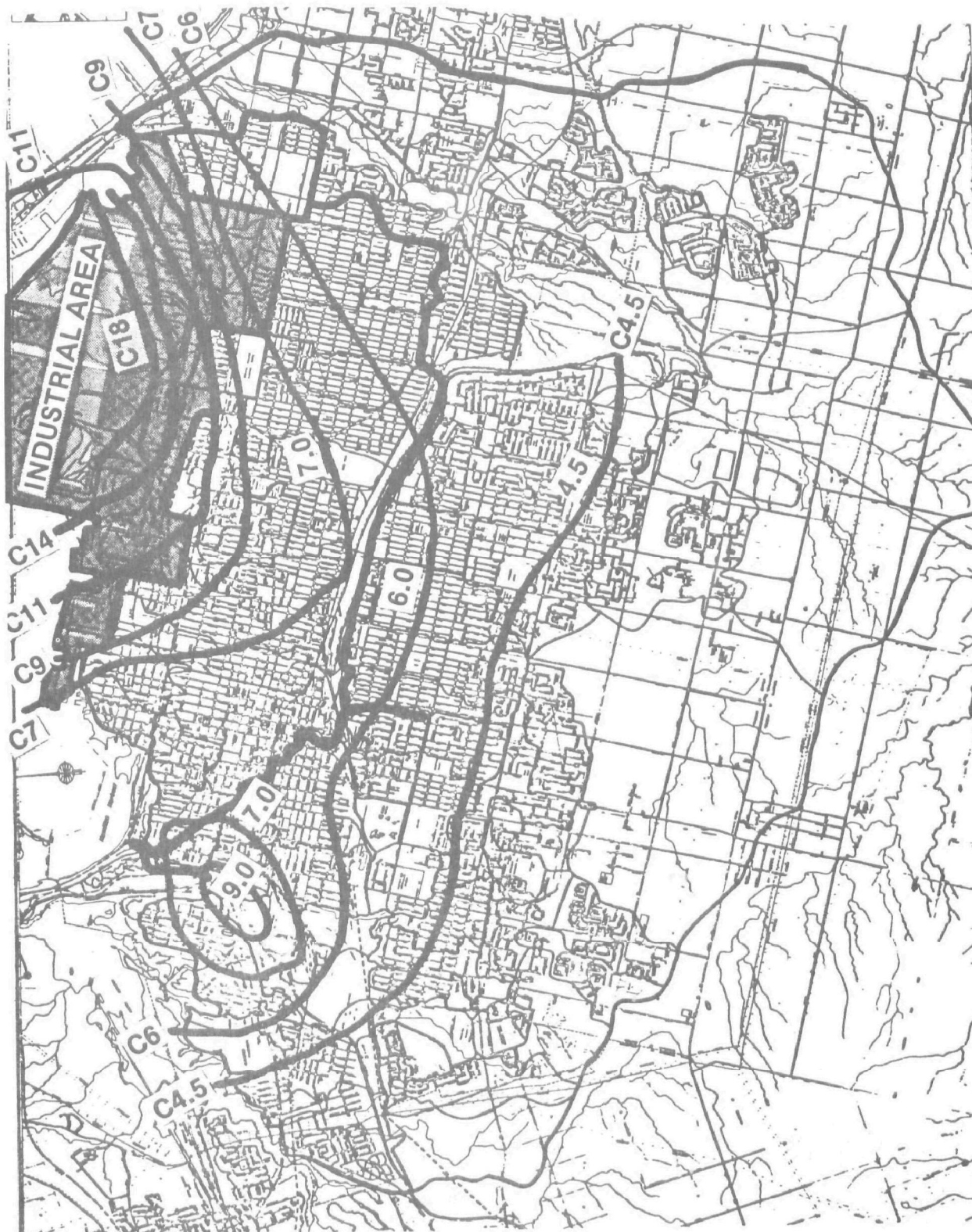


Figure 4: Yearly average isopleths of atmospheric fallout

1982.

The quality of stormwater depends on the concentrations of dust and dirt accumulated on the land surface at the onset of the storm. SWMM assumes a constant cleaning interval for each different land use. There is no control over antecedent conditions, whether or not the street has been swept or not before the storm. Therefore, inclusion of street sweeping data as a time series better simulates the actual dust and dirt accumulation at the beginning of the storm. Support for this modification to SWMM III has been secured for 1982.

SWMM washoff algorithm uses a power exponent of runoff rate and a washoff coefficient. Provision is made to input different values for each constituent in estimating washoff rate. It does not allow for the effect of slope in washoff. In the case of steep roofs, washoff of dust and dirt is much faster and responsive to small rain intensities. Therefore separation of steep sloped roofs in the runoff water quality analysis might yield better results. Not all constituents found on roads and gutters may be expected on roofs or impervious areas, and vice-versa. A modification to SWMM III is currently underway.

SWMM uses a constant time step to integrate over the

period for quantity and quality prediction. The smaller the time step, the greater would be the accuracy in prediction, and higher the computation cost. Introducing a variable time step, allows the user to run the program at smaller time steps during storms and longer time steps in the dry periods for continuous modelling. This modification will be carried out at the same time as the street sweeping input modification.

Thunderstorms are not static, and the intensity of rain varies in each subcatchment (Shtifter and W. James, 1981). Inclusion of storm intensity predictions on a given subcatchment using the storm direction and cell width, age of the storm cell, wind direction and velocity yields better input to the surface runoff calculations. Our SWMM block entitled THOR computes spatially and time averaged hyetographs for kinematic storms.

All of these changes have been or are being implemented in the SWMM package used by the Computational Hydraulics Group at McMaster University as part of our on-going studies. Results obtained for Hamilton have so far shown encouraging improvements (Robinson and James, 1982); (James and Shtifter, 1981).

REFERENCES

- Air Quality Report 1978, Hamilton city, MOE, Ontario.
- Air Quality Report 1979, Hamilton city, MOE, Ontario.
- Air Quality Report 1980, Hamilton city, MOE, Ontario.
- Barton, S. et al (1981), "An Assessment of Street Dust and Other Sources of Airborne Particulate Matter in Hamilton, Ontario", Technology Transfer Seminar, Toronto, November 24, 1981. Sponsored by MOE 11. 11 pp.
- Chamberlain, A.C., (1960), "Aspects of the Deposition of Radioactive and Other Gases and Particles", Inter, J. Air Pollution 3 (1-3).
- Culkowski, W.M., "Deposition and Washout Computations Based on the Generalized Gaussian Plume Model", USAEC Report ORO-599, Weather Bureau, Oak Ridge, Tenn. (1963).
- Stuart, Dean, "Ontario Precipitation Chemistry and Heavy Metal Speciation", Ph.D. Thesis, McMaster University, 1975. pp.1-125.
- Griffiths, V., "The Removal of Iodine from the Atmosphere by Sprays", British Report AHSB(S) R-45 (1963).
- Heidorn, K.C., "Air Pollution Incidents and Wind Variability in Southern Ontario", J. Atmospheric Environment Vol. 12, pp. 2251-2257, 1978.
- Geottle, A. "Atmospheric Contaminants, Fallout and Their Effects on Stormwater Quality", Prog. Wat. Tech., Vol. 10, Nos. 5/6, pp. 455-467, 1978.
- Frizzola, John A., et al, "Contaminants in rainwater and their Relation to Water Quality", Part I, Water and Sewage Works, August, 1975. pp. 72-75.
- Frizzola, John A., et al, "Contaminants in rainwater and their Relation to Water Quality", Part II, Water and Sewage Works, September 1975. pp. 94-95.
- James, W., and Shtifter, Z., "Implications of Storm Dynamics on Design Storm Inputs", proceedings of the Conference on Water Quality and Storm Water Management Modelling, Niagara Falls, Ontario USEPA, October, 1981, pp. 55-78.
- Ledbetter, Joe O., "Air Pollution Part A: Analysis", Marcel Dekker, Inc., New York, 1972.

Junge, C.E., "Air Chemistry and Radioactivity", Academic Press Inc., New York, 1963.

Matheson, D.H., et al, "Air Pollution Survey for Hamilton, Ontario", Atmosphere Environment, Pergamon Press 1969. vol. 3, pp. 11-23. printed in Great Britain.

Ontario Research Foundation Report, "Air Pollution in Hamilton City", Department of Chemistry, December 11, 1957. pp. 1-50.

Malmquist, Per-Arne, (1978), "Atmospheric Fallout and Street Cleaning - Effects on Urban Storm Water and Snow", Prog. Wat. Tech. 1978, vol. 10, nos. 5/6 pp. 495-505.

Randall, C.W., "The Impact of Atmospheric Contaminants on Stormwater Quality in an Urban Area", Prog. Wat. Tech. 1978 Vol. 101, no. 5/6, pp. 417-431.

Randall, C.W., et al, "Comparison of Pollutant Mass Loads in Precipitation and Runoff in Urban Areas", Second International Conference on Urban Storm Drainage, Urbana, Illinois, U.S.A., June 14-19, 1981.

Robinson, M., and James, W., "Continuous SWMM Modelling of Hamilton Summer Stormwater Including Certain Quality Indicators - Preliminary Output Time Series Using Discrete-event Calibration for Non-industrial Areas", published by CHI Publications, March 1982.

Rouse, W.R., and McCutcheon, John G., "The Effect of the Regional Wind on Air Pollution in Hamilton, Ontario", Canadian Geographer, XIV, 4, 1970 pp. 271-285.

Rutherford, G.K. "A Preliminary Study of the Composition of Precipitation in S.E. Ontario", Canadian Journal of Earth Sciences, vol. 4, 1967, pp. 1151-1160.

Stewart I.M., et al, "Methods of Relating High Volume Sampler Particulate Loadings to Wind Direction", Atmospheric Environment, Pergamon Press, 1968, Vol. 2, pp. 181-185.

Novotny, Vladimir, "Acidity of Urban Precipitation and its Buffering during Overland Flow", second International Conference on Urban Storm Drainage, Urbana, Illinois, U.S.A. June 1981.

Huber, Wayne C., et al, "Storm Water Managment Model User's Manual Version III, November 1981.** pp.

The work described in this paper was not funded by the U.S. Environmental Protection Agency. The contents do not necessarily reflect the views of the Agency and no official endorsement should be inferred.

SWMM CONFERENCE - MARCH 25-26, 1982

LIST OF ATTENDEES

Roger K. Wells - HMM Associates, Inc., Raleigh, NC
Curtis H. Dalton - Maryland DHMH, OEP
Stephen L. Luckman - Maryland DHMH, OEP
Joan Lefler - U.S. EPA, Washington, DC
Bastien Jean-N - St. Laurent, Quebec, Immwada
John Roberts - MacLaren Plansearch, Toronto
Steve McKelvie - Gore & Storrie Ltd., Toronto
Bob Walker - Beak Consultants Ltd., Toronto
Gary Woodruff - Tulsa City-County Health Dept.
Joseph L. Norton - Ford Thornton Norton & Assoc., Vicksburg
Fred Morris - S. Florida Water Management District
Robb Startzman - S. Florida Water Management District
Claire Welty - U.S. EPA
Warren Viessman, Jr. - Congressional Research Service
Charles Delos - U.S. EPA
John Weeks - Ketron, Inc., Arlington, VA
Bob Rallison - U.S. Soil Conservation Service, Wash., DC
Gerald Dougherty - Purdum & Jeschke, Balto., MD
Michal D. Norris - Purdum & Jeschke, Balto., MD
Raymond Wright - University of Rhode Island
Wayne Huber - University of Florida
Paul MacLeod - Giffels Associates, Ltd.
Richard Horner - University of Washington
Frank O. Marrazza - GKY Assoc., Springfield, VA
John Barile - GKY Assoc., Springfield, VA
Jack Hartigan - N. Virginia Planning District Comm.
Tom Quasebarth - N. Virginia Planning District Comm.
Betsy Southerland - N. Virginia Planning District Comm.
Dave Gubarry - Woodward-Clyde Consultants
Ellen Petticrew - Canada Centre for Inland Waters
Mark Robinson - McMaster University, Canada
Ron Scheckenberger - McMaster University, Canada

Shivalingaiah. B - McMaster University, Canada
 ? - McMaster University, Canada
 Michael Akerbergs - Woodward-Clyde Consultants
 Raymond Dever - Montgomery County DEP, MD
 Thomas Nesbitt - EPA HQ
 Samuel R. Martin - Regional Planning Council, Balto., MD
 Alan Lamb - U.S. Geological Survey
 Grace Weik - Dames & Moore
 Robert Pasley - USNA Soil Conservation Service
 Padma Datta - EPA - OPP
 A. Charles Rowney - Proctor & Redfern, Ottawa
 Marcella McTaggart - Alcoa
 Phil Rosten - AWARE Corp.
 Lalit Sinha - EPA, IL
 Charles D. Woo - FHWA
 Don Hoang - Portland
 Ray Whittemore - NCASI
 James McKeown - NCASI
 Michael J. Hudson - IEP, Inc.
 Malcolm A. MacGregor - IEP, Inc.
 John Aldrich - CDM, Annandale, VA
 David Schafer - CDM
 H.S. Loijens - Canada
 Peter G. Robertson - MD OEP
 Bernard Ross - USF
 W. Jancs - McMaster University
 Ivan Chou - ESE, Inc.
 Stephen E. Wall - Greeley & Hansen
 Edward R. Ester, III - MMM Design Group
 James E. Scholl - CH₂M Hill
 Roger L. Long - General Software Corp.
 Jan-Tai Kuo - General Software Corp.
 Karl Hemmerich - City of Toronto
 Mike Kangas - Dalton-Dalton-Newport, Cleveland
 Bob Cole - Dalton-Dalton-Newport, Cleveland

Ginger Klingelhoef - Anne Arundel Co., MD
Wan Wong - Ontario Environment
Don Urban - USDA-SES
Charles R. Terrell - USDA-Soil Conservation Service
Bruce Bird - AACC
Jonathan Young - Brown & Caldwell
Larry A. Roesner - Camp Dresser & McKee, Annandale, VA
Prekimi V. Tawari - Engineering & Economics Research, Inc.
Byron Lord - FHWA R&D
John Segna - US EPA
Deborah McCall - Roy F. Weston, Inc.
Marlene Conaway - Anne Arundel Co., MD
Tom Schaffer - MW Council of Gov't.
Jerry Klafter-Snyder - Roy F. Weston, Inc.
Link Haghighaf - Howard County DPW, MD
Arun K. Deb - Roy F. Weston, Inc.
Bob Ambrose - U.S. EPA, Athens, GA
Alan Cavacas - Northern Virginia Planning Dist. Comm.
Tieh Yin - MNCPPC, Upper Marlboro, MD
John A. Friedman - Northern Virginia Planning Dist. Comm.
Donald Groff - Western County State College
Harry Torno - U.S. EPA, SAB
Tom Barnwell - U.S. EPA
Larry Roesner - CDM, Inc., Alexandria, VA